THE UNIVERSITY
of EDINBURGH

B Meson Decays, Conformal Anomalies and Gauge Invariance

Muhammad Saad Nabeebaccus

Doctor of Philosophy
The University of Edinburgh
Mar 2021

Abstract

In this thesis, we discuss the calculation of conformal anomalies using curved spacetime and heat-kernel techniques, and QED corrections to semi-leptonic decays of the pseudoscalar B meson at the full differential level. In the first chapter, the basic ideas of conformal field theory are reviewed, including the importance of the trace of the energy-momentum tensor as a measure of conformal symmetry breaking, and the use of curved spacetime in calculations. In the second chapter, we perform computations of the conformal anomalies for the spin-0, spin-$\frac{1}{2}$ and spin-1 fields in curved spacetime using the De-Witt-Schwinger point splitting method and heat-kernel techniques. Particular focus is given to the spin-1 gauge field, where it is explicitly shown how gauge invariance is obtained, a result that has been overlooked in the literature, and which is also a source of ambiguities in different regularisation schemes. We then proceed to discuss the application of these results on positivity theorems in Chapter 3. It is shown that they could potentially provide tighter bounds on the conformal window in QCD. In chapter 4, a calculation of the QED corrections to the $\bar{B} \to \bar{K}\ell^+\ell^-$ decay process at the double differential rate is introduced, using an effective mesonic Lagrangian. Particular focus is given to the cancellation of infrared soft and collinear divergences between the real and virtual contributions using the phase-space slicing method, which is discussed in Chapter 5. Hard-collinear divergences, appearing in the form of logs of the lepton mass, are shown to cancel depending on the differential variables used and the experimental photon energy cut. Plots and results are given in chapter 6, and some comments on the value of R_K and lepton flavour universality are made.

Lay Summary

In nature, depending at what scale we observe a system, we find that they can be described by different particles and interactions. In most of our everyday life situations, we do not need to know about atomic structure; indeed, excellent predictions about how things evolve (like the flow of water in a river) can be made without their knowledge. However, as soon as one 'zooms in', the microscopic structure is resolved, and one then needs to have a good description of the interactions at the new scale. Particle physicists push the boundary of how much 'zooming in' is done, by smashing tiny sub-atomic particles like protons into each other, and to be able to predict what happens, we need to know exactly how the protons and their constituents (quarks) interact with one another. The renormalisation group describes the changes in the particles and interactions describing a system when the scale changes. In the first part of this thesis, we investigate various aspects of this idea. Then, we discuss the decay of a heavy particle called a B meson (so-called because it contains the heavy b quark) to a specific set of final state particles. We present in detail a calculation that improves the prediction of the probability of its decay, and discuss its consequences, especially in the light of recent experimental results.

Declaration

I declare that this thesis was composed by myself, that the work contained herein is my own except where explicitly stated otherwise in the text, and that this work has not been submitted for any other degree or professional qualification except as specified.

Parts of this work have been published in [1].

(*Muhammad Saad Nabeebaccus, Mar 2021*)

Acknowledgements

First of all, I would like to thank my supervisor Roman Zwicky for his guidance for the last 4 years. I have definitely learnt a lot while working with him. I would also like to thank my second supervisor Jennifer Smillie for her support throughout my PhD.

Many thanks to Einan Gardi and Roger Horsley, who have advised me on my work on various occasions. I would also like to extend my thanks to Gino Isidori, who has been an encouraging collaborator in one of the projects I've participated.

Special thanks to my high school Physics teacher, Jamil Laloo, who has inspired me to do Physics in the first place.

I would also like to thank Fatimah Ramjaun for her amazing support and encouragement. It has definitely made my journey easier and much less stressful.

I am very grateful to my parents, for having been with me every step of the way. It is clear that I would not be where I am today without their support.

Last, but not least, I would like to thank my PPT comrades, who have made the ride more enjoyable: Ben P., Calum, Joël, Ben M., Tommaso, James, Vladimir, Andrew, Niamh, Aris, Fionn, Joseph and Emmet. Special thanks to Calum and Ben P. for so many useful and interesting discussions, and Ben P. for being the best office mate.

Contents

List of Figures

List of Tables

List of Acronyms and shortcuts

CCS	Conformally coupled scalar
CFT	Conformal field theory
DR	Dimensional regularisation
EFT	Effective field theory
EMT	Energy-momentum tensor
EoM	Equation of motion
FCNC	Flavour changing neutral current
IR	Infrared
LFU	Lepton flavour universality
LO	Leading order
NCCS	Non-conformally coupled scalar
NLO	Next to leading order
1PI	One particle irreducible
QCD	Quantum-chromodynamics
QED	Quantum-electrodynamics
QFT	Quantum field theory
RF	Rest frame
RG	Renormalisation group
RNC	Riemann normal coordinates
SM	Standard Model
TEMT	Trace of the energy-momentum tensor
UV	Ultraviolet
VEV	Vacuum expectation value

Chapter 1

Introduction

Symmetries are essential in Physics. To construct a quantum field theory (QFT), we have to ask ourselves two questions: First, how many degrees of freedom (number and type of particles) do we want the theory to have? And second, what symmetries do we want the QFT to obey? It can be argued that the two questions are related, and can only be answered by experiments. However, throughout the advent of the Standard Model, symmetries have time after time lead the way (e.g. in the development of the quark theory [3]).

It is a rather remarkable fact that all of the fundamental interactions in the Standard Model come from symmetries. In fact, many particles have been predicted to exist based solely on symmetry ideas (e.g. the Z boson [4–6] and the Higgs boson [7, 8]).

With the incredible success of Special Relativity, it became clear that any useful QFT able to make predictions about the real world has to be Lorentz invariant. Noether's theorem tells us that continuous symmetries lead to conservation laws, and in this case, Lorentz invariance leads to conservation of angular momentum. Translational symmetry implies conservation of momentum instead, and combined with Lorentz symmetry leads to *Poincaré symmetry*. In this thesis, we discuss different aspects of conformal symmetry which can be understood as an extension of Poincaré symmetry, in which we also have scale invariance. Therefore, it also has a close connection with the Renormalisation Group [9], which describes how a system changes with energy scale.

After discussing several aspects of conformal field theories, we then switch to

B-Physics phenomenology. In particular, we focus on the calculation of the semi-leptonic decay process $\bar{B} \to \bar{K}\ell^+\ell^-$ at the full differential level at $\mathcal{O}(\alpha)$ in QED. As we will see, these calculations are important as the corrections can be relatively large, due to hard-collinear logarithms, $\ln m_\ell$, where m_ℓ is the lepton mass. The results are an important ingredient in the search for new physics in experiments such as LHCb [10–12].

This thesis is structured as follows: In the rest of this chapter, we introduce the basic ideas of conformal field theory, conformal anomalies, and quantum field theories in curved spacetime. An introductory discussion on B-Physics is deferred to Chapter 4, so as not to break the flow of the presentation. In Chapter 2, we calculate conformal anomalies for various quantum field theories (having different spins) using the De-Witt-Schwinger point splitting method [13, 14]. In particular, gauge invariance of the spin-1 gauge field is discussed. Then, in Chapter 3, the conformal anomalies are discussed in the context of flow theorems and their potential consequences on the conformal window in QCD. We transition to B-Physics in Chapter 4, laying the groundwork for the QED corrections to the $\bar{B} \to \bar{K}\ell^+\ell^-$ decay process. The treatment of IR divergences (soft and collinear) is discussed in detail in Chapter 5, where we employ the technique of phase space slicing [15]. Results and plots are presented in Chapter 6, including comments of R_K and lepton flavour universality as well as comparison with the literature.

The sign convention used throughout this thesis is $(---)$ in the convention of Misner, Thorne et al. [16], i.e. the metric has signature $(+---)$, unless other otherwise stated. See App. A.1 for more details on conventions.

1.1 Conformal Field Theory

Conformal symmetry is a higher level of symmetry which includes the Poincaré group as well as invariance under *dilatations* and *special conformal transformations*,

$$x^\mu \to \lambda x^\mu, \qquad \text{Dilatations,} \tag{1.1}$$

$$x^\mu \to \frac{x^\mu - a^\mu x^2}{1 - 2a\cdot x + a^2 x^2}, \qquad \text{Special Conformal Transformations.} \tag{1.2}$$

A special conformal transformation is, in fact, a combination of an inversion,

$$x^\alpha \to \frac{x^\alpha}{x^2}, \tag{1.3}$$

a translation, and an inversion. Therefore, a dilatation is defined by 1 parameter (λ in Eq. (1.1)) while special conformal transformations are defined by 4 parameters (a^μ in Eq. (1.2)). The conformal group extends the Poincaré group by 5 extra generators, in addition to the 4+6 generators corresponding to translations and Lorentz transformations.

Dilatations and special conformal transformations can be understood as transformations that rescale the metric,

$$g_{\mu\nu}(x) \to \Omega^2(x) g_{\mu\nu}(x). \tag{1.4}$$

The transformations of the Poincaré group corresponds to the special case of $\Omega(x) = 1$.

Another equivalent way of defining conformal transformations is that they are those that preserve the surface of the infinitesimal light-cone

$$\mathrm{d}s^2 = g_{\mu\nu}\mathrm{d}x^\mu \mathrm{d}x^\nu = 0. \tag{1.5}$$

These transformations preserve angles but not lengths. A conformal field theory (CFT) is a field theory that is invariant under the *conformal group*. A graphical representation of dilatations and special conformal transformations is given in Fig. 1.1.

1.1.1 Classical trace of the energy-momentum tensor

From Noether's theorem, scale and special conformal invariance correspond to conserved currents j^μ_{D} and $K^{\mu\nu}$ respectively. These are given by [17–19]

$$j^\mu_{\mathrm{D}} = x_\nu T^{\mu\nu} + V^\mu, \tag{1.6}$$

$$K^{\mu\nu} = (x^2 g^{\mu\lambda} - 2x^\mu x^\lambda) T^\nu_\lambda - 2x^\mu V^\nu + 2L^{\mu\nu}, \tag{1.7}$$

where $T^{\mu\nu}$ is the canonical energy-momentum tensor (EMT)[1], V^μ (called the *Virial current* in [20]) is the contribution to j^μ_{D} from intrinsic dilatations, and

[1]The canonical EMT is obtained by directly applying Noether's theorem.

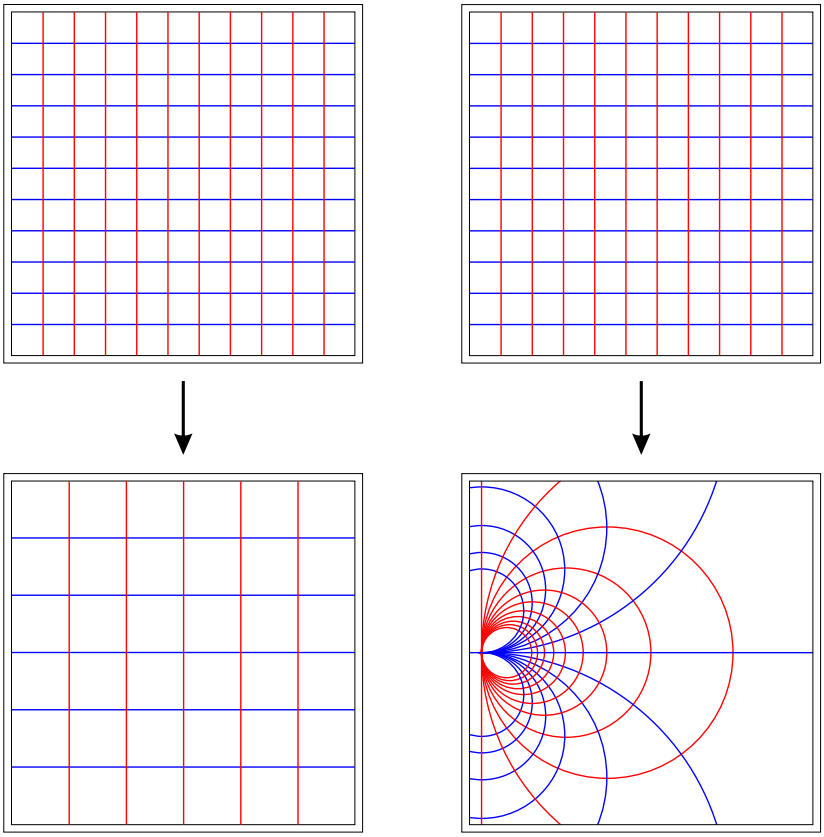

Figure 1.1: Effect of applying a dilatation (left) and special conformal transformations (right) on spacetime, represented by a 2D grid here.

$L^{\mu\nu}$ is a local operator that satisfies $V^\nu = \partial_\mu L^{\mu\nu}$. Scale invariance of a theory, i.e. conservation of the dilatation current j^μ_{D}, implies that

$$T^\mu{}_\mu = -\partial_\mu V^\mu, \tag{1.8}$$

obtained upon using conservation of energy-momentum. Full conformal invariance of a theory then gives the relation [21]

$$T^\mu{}_\mu = -\partial_\mu \partial_\nu L^{\mu\nu}. \tag{1.9}$$

Callan, Coleman and Jackiw showed that such a local term can be removed from the trace of the energy-momentum tensor (TEMT) by adding an *improvement* term to the canonical EMT [22], without changing the four-momentum vectors and Lorentz generators of the canonical EMT, such that we obtain the well-known

result that conformal invariance[2] of a theory implies that the EMT is traceless

$$T^{\mu}{}_{\mu} = 0. \tag{1.10}$$

Free massless scalar field theory

To illustrate an example of where the improvement procedure can be used, let us consider a free massless scalar field theory, given by the Lagrangian

$$\mathcal{L} = \frac{1}{2}\partial_{\mu}\phi\partial^{\mu}\phi. \tag{1.11}$$

The canonical TEMT in 4D is given by

$$T^{\mu}{}_{\mu} = -\frac{1}{2}\Box\phi^2 + \phi\Box\phi. \tag{1.12}$$

The second term vanishes by virtue of the equation of motion ($\Box\phi = 0$). The TEMT then has the form given in Eq. (1.9), with

$$L^{\mu\nu} = \frac{1}{2}g^{\mu\nu}\phi^2, \tag{1.13}$$

meaning it can be improved by the procedure described in [22]. It can be shown explicitly that such a term satisfies the requirement that the four-momentum vectors and Lorentz generators of the canonical EMT are unchanged. Adding the improvement term to the theory makes the TEMT vanishing. Being able to improve the EMT in this way implies that the scalar field is *conformally coupled*. We will come back to this point later in Sec. 2.1.1 when we discuss the scalar field theory in curved spacetime.

Free massive fermion field theory

On the other hand, a non-vanishing TEMT measures the breaking of conformal symmetry; since dilatations rescale distances (and hence energies), it is clear that any theory that has an energy scale breaks scale (and hence conformal) invariance. Indeed, theories that involve massive fields break conformal symmetry *classically* or *softly*. A simple example is the free massive fermion field theory,

[2]Note that we will sometimes assume that scale invariance implies conformal invariance. Whether this is true is still an open question [23].

having Lagrangian

$$\mathcal{L} = \bar{\Psi}\left(i\partial\!\!\!/ - m\right)\Psi. \tag{1.14}$$

The TEMT of this field theory is given by

$$T^{\mu}_{\ \mu} = m\bar{\Psi}\Psi, \tag{1.15}$$

where the Dirac equation $\left(i\partial\!\!\!/ - m\right)\Psi = 0$ has been used. As expected, the TEMT vanishes only if $m \to 0$.

Free massless photon field theory

The canonical EMT in general does not have to be symmetric. However, for a Poincaré invariant theory, conservation of angular momentum implies that it can always be massaged into a symmetric form. The procedure [17, 24] involves adding a total divergence to the canonical EMT, $T^{\mu\nu}$,

$$\theta^{\mu\nu}_{\text{sym}} = T^{\mu\nu} + \partial_\lambda \Sigma^{\mu\nu\lambda}, \tag{1.16}$$

where $\Sigma^{\mu\nu\lambda}$ is antisymmetric under interchange of μ and λ. This redefinition of the EMT leaves it conserved, and does not change the four-momentum vector of the field theory. In what follows, we will use $T^{\mu\nu}$ for the *canonical* EMT and $\theta^{\mu\nu}$ for the *symmetric* EMT.

As a simple example, let us consider a free massless photon field theory, with Lagrangian,

$$\mathcal{L} = -\frac{1}{4}F^{\mu\nu}F_{\mu\nu}. \tag{1.17}$$

The canonical EMT tensor is

$$T^{\mu\nu} = -F^{\mu\lambda}\partial^\nu A_\lambda + \frac{1}{4}g^{\mu\nu}F^2, \tag{1.18}$$

where the indices in $F^2 \equiv F^{\lambda\sigma}F_{\lambda\sigma}$ have been suppressed for convenience. By choosing $\Sigma^{\mu\nu\lambda} = F^{\mu\lambda}A^\nu$, and using the equation of motion $\partial_\lambda F^{\mu\lambda} = 0$, we have that

$$\begin{aligned}\theta^{\mu\nu} &= -F^{\mu\lambda}\left(\partial^\nu A_\lambda - \partial_\lambda A^\nu\right) + \frac{1}{4}g^{\mu\nu}F^2 \\ &= -F^{\mu\lambda}F^{\nu}_{\ \lambda} + \frac{1}{4}g^{\mu\nu}F^2,\end{aligned} \tag{1.19}$$

which is symmetric under interchange of μ and ν. We will later see that using curved space, symmetrising the EMT can be achieved in a quicker way. Taking the trace yields

$$\theta^{\mu}{}_{\mu} = \left(\frac{d}{4} - 1\right) F^2. \tag{1.20}$$

which vanishes in 4D.

1.1.2 Conformal Anomalies

So far, we have only considered classical field theories. In interacting quantum field theories, correlation functions need to be computed, which have a wide range of applications, such as in S-matrix elements used for calculating scattering amplitudes. In general, these correlation functions are UV divergent in perturbation theory due to the presence of loop integrals. However, since the correlation functions are related to physical observables, such as a decay rates, masses and cross-sections, the UV divergences that appear in the calculations are unphysical and have to be treated in some way. Thus, one needs to *regularise* the divergent integrals, and this involves introducing 'extra parameters' in order to separate the UV divergences.

One of the most common regularisation techniques is dimensional regularisation (dim-reg) [25]. This involves working in a general dimension d, which is analytically continued to the complex plane. In this way, poles involving the parameter d appear when one takes d back to its physical value. This will be the main regularisation technique used in Chapter 2.

After regularisation, one still needs to *renormalise* the correlation function. Renormalisation is the process of fixing the value of the correlation function at a particular energy scale. This involves adding local counterterms to the Lagrangian in order to absorb the UV divergences of the theory. This is a classic procedure in quantum field theory, and we refer the reader to [26] for more details.

Regularisation and renormalisation necessarily introduce an energy scale in the interacting theory, no matter which regularisation scheme one picks. The coupling constants, masses and correlation functions all become functions of the energy scale. The evolution of renormalised correlation functions with the energy scale, typically denoted by μ, is given by the *Callan-Symanzik equation* [27, 28]. We discuss this further in the next section.

In fact, renormalisation can be understood in the Wilsonian context, where the dependence on the energy scale comes as a result of separating the (unknown) UV physics from our theory. We refer the reader to [29, 30] for a review on the subject.

Interacting massive scalar field theory

As an example, consider an interacting massive scalar field theory given by the Lagrangian

$$\mathcal{L} = \frac{1}{2}\partial_\mu\phi_0\partial^\mu\phi_0 - \frac{1}{2}m_0^2\phi_0^2 - \frac{\lambda_0}{4!}\phi_0^4, \tag{1.21}$$

where the subscript $'0'$ implies that the quantities are *bare* (not renormalised). As mentioned earlier, renormalisation involves adding local counterterms to the Lagrangian in order to absorb UV divergences in correlation functions. This is conveniently achieved by redefining the fields, masses and coupling constants using Z-factors. The bare field, mass and coupling constant, in terms of the renormalised ones (denoted without a subscript) and Z-factors, are given by

$$\phi_0 = Z_2^{\frac{1}{2}}\phi, \tag{1.22}$$

$$m_0^2 = Z_m Z_2^{-1} m^2, \tag{1.23}$$

$$\lambda_0 = Z_\lambda Z_2^{-2}\lambda, \tag{1.24}$$

The bare quantities are independent of the energy scale μ that appears as a result of renormalisation. Therefore,

$$\frac{d\lambda_0}{d\ln\mu} = 0, \tag{1.25}$$

which implies that

$$\beta_\lambda \equiv \frac{d\lambda}{d\ln\mu} = -\lambda\frac{d}{d\ln\mu}\ln\left(Z_\lambda Z_2^{-2}\right). \tag{1.26}$$

The above equation defines the beta-function β_λ, which characterises the dependence of the (renormalised) coupling constant on the scale μ. Similarly,

the field and mass in the theory also acquire *anomalous dimensions*, defined by

$$\gamma_\phi \equiv -\frac{1}{2}\frac{d}{d\ln\mu}\ln Z_2, \tag{1.27}$$

$$\gamma_m \equiv \frac{d\ln m}{d\ln\mu} = -\frac{1}{2}\frac{d}{d\ln\mu}\ln\left(Z_2^{-1}Z_m\right). \tag{1.28}$$

In general, the scaling dimensions of the renormalised field and mass are given by

$$\Delta_\phi = d_\phi + \gamma_\phi, \tag{1.29}$$

$$\Delta_m = 1 + \gamma_m, \tag{1.30}$$

where d_ϕ is the classical (or engineering) dimension of the field, and is equivalent to the naïve dimension obtained in the classical theory by dimensional analysis. Of course, if the interaction is switched off (i.e. $\lambda \to 0$), then all the anomalous dimensions vanish.

The evolution equation of a general correlation function involving the renormalised scalar fields in momentum space is given by the Callan-Symanzik equation,

$$\left(\frac{\partial}{\partial\ln\mu} + \beta_\lambda\frac{\partial}{\partial\lambda} + \gamma_m\frac{\partial}{\partial\ln m} - n\gamma_\phi\right)\langle\phi(p_1)...\phi(p_n)\rangle = 0. \tag{1.31}$$

This is also sometimes referred to as the *renormalisation group equation*.

Since interacting quantum field theories require regularisation and renormalisation, they acquire an intrinsic energy scale μ, which breaks scale symmetry, and hence conformal symmetry, even if the theory is conformal at the classical level. The breaking of a symmetry due to quantum effects is known as an *anomaly*, and in the case of conformal symmetry, we have a *conformal anomaly*. Due to the connection of conformal symmetry breaking with the TEMT, conformal anomalies are sometimes referred to as *trace anomalies* in the literature.

Quantum Electrodynamics

The Quantum Electrodynamics (QED) Lagrangian is obtained by combining the free fermion field theory in Eq. (1.14) and the free photon field theory in Eq. (1.17), and promoting partial derivatives acting on the fermion field to

covariant derivatives (minimal coupling). By doing this, the symmetry of the Lagrangian under global $U(1)$ transformations is promoted to invariance under *local* $U(1)$ transformations, leading to what is known as *gauge symmetry*. Thus we have, for massless fermions,

$$\mathcal{L} = -\frac{1}{4}F^2 + \bar{\Psi}\left(i\not{D}\right)\Psi, \tag{1.32}$$

where $D_\mu \equiv \partial_\mu + ieA_\mu$ is the covariant derivative.

One can easily find that the TEMT in the classical theory vanishes in 4D (c.f. Eq. (1.15) and Eq. (1.20)), and thus classical QED with massless fermions is conformal in 4D.

However, in the quantum field theory, due to the fermion-photon interaction, the operator $\langle F^2 \rangle$ becomes divergent and contains poles in $(d-4)$ in dimensional regularisation. Therefore, the vacuum expectation value (VEV) of the TEMT for QED becomes [31]

$$\langle T^{\alpha}{}_{\alpha} \rangle = \frac{\beta}{2e^3}\langle F^2 \rangle_{\text{ren}}, \tag{1.33}$$

where $\beta = \frac{\mathrm{d}e}{\mathrm{d}\ln\mu}$ is the QED β-function, and the subscript 'ren' indicates that the operator has been renormalised (and is thus finite).

More generally, anomalies can be understood at the level of the path integral. Correlation functions are defined by

$$\langle \phi_1 ... \phi_n \rangle = \mathcal{N} \int \mathcal{D}\phi \, \phi_1 ... \phi_n \, e^{i\mathcal{S}[\phi]}, \tag{1.34}$$

where $\mathcal{N}$ is a normalisation factor, $\mathcal{S}[\phi]$ is the quantum action, and we have used the shorthand $\phi_1 \equiv \phi(x_1)$. If a theory possesses a continuous symmetry, one can derive *Ward identities* [32, 33], which are essentially the quantum analogue of current conservation in classical field theories. In the path integral picture, anomalies arise as a result of the measure $\mathcal{D}\phi$ not being invariant under the symmetry [34–36]. This happens for exactly the same reasons as described earlier - due to regularisation and renormalisation.

1.1.3 UV and IR fixed points

Consider a quantum field theory with an interaction involving the coupling constant λ. As discussed in the previous section, the variation of λ with the energy scale is given by the beta function,

$$\beta_\lambda \equiv \frac{d\lambda}{d\ln\mu}. \tag{1.35}$$

The exact form of β_λ obviously depends on the field content of the theory, as well as the type of interaction.

An important question that one can ask is whether the QFT is consistent in the far UV and IR. To investigate this, one can integrate Eq. (1.35) to obtain

$$\ln\left(\frac{\Lambda}{\mu}\right) = \int_{\lambda(\mu)}^{\lambda(\Lambda)} \frac{d\lambda}{\beta_\lambda}. \tag{1.36}$$

In the UV limit, $\Lambda \to \infty$, and therefore the integral

$$\int_{\lambda(\mu)}^{\lambda(\infty)} \frac{d\lambda}{\beta_\lambda}, \tag{1.37}$$

has to diverge. This happens only if $\beta_\lambda \to 0$ as $\Lambda \to \infty$, and we thus have a UV *fixed point*. Since the beta function vanishes at the UV fixed point, the theory becomes conformal there[3]. A famous example of a theory with a UV fixed point is QCD. In fact, QCD has *asymptotic freedom*, meaning that the strong coupling constant itself vanishes at the UV fixed point, and the theory becomes non-interacting there [37, 38]. Therefore, this justifies the use of perturbation theory when performing high energy physics calculations. On the other hand, if the coupling constant does not go to zero at the UV fixed point, the theory is said to be *asymptotically safe*.

One can repeat the exact same argument for the IR limit. Again, we find that for the theory to be consistent, the beta function has to vanish when $\Lambda \to 0$, and we have an IR *fixed point*. In QCD, such an IR fixed point is called a *Caswell-Banks–Zaks fixed point* [39, 40] if perturbation theory is valid there (i.e. if the strong coupling constant is less than 1).

Finally, we mention that such fixed points may not exist - This happens if the

[3]Provided there is no soft breaking of conformal symmetry, obviously.

coupling constant blows up at some energy scale, called the *Landau pole* Λ_{LP},

$$\ln\left(\frac{\Lambda_{LP}}{\mu}\right) = \int_{\lambda(\mu)}^{\infty} \frac{d\lambda}{\beta_\lambda}. \tag{1.38}$$

The existence of a Landau pole in the UV merely indicates that the quantum field theory is just an effective field theory, and that there is new physics beyond the scale Λ_{LP}. In fact, QED has this property in the UV, since the β-function is positive and the fine structure constant of QED α continues to grow until it becomes infinite. However, one finds that $\Lambda_{LP} \gg M_P$, the Planck scale, and therefore there are no issues with QED for all relevant purposes. On the other hand, the existence of a Landau pole in the IR (e.g. QCD in the Standard Model) implies that perturbation theory breaks down below a certain scale of the order of Λ_{LP}.

1.1.4 Curved Spacetime

If a quantum field theory is described on a curved background, by coupling the dynamical fields in the theory to the background gravitational field $g_{\mu\nu}(x)$, one can show that $g_{\mu\nu}(x)$ acts as a source for the EMT [41],

$$\theta_{\mu\nu}(x) = \frac{2}{\sqrt{-g}} \frac{\delta \mathcal{S}_M}{\delta g^{\mu\nu}(x)}, \tag{1.39}$$

where $g = \det g_{\mu\nu}$ and

$$\mathcal{S}_M = \int \mathrm{d}^d x \, \sqrt{-g} \, \mathcal{L}_M(x), \tag{1.40}$$

with $\mathcal{L}_M$ being the matter Lagrangian. Note that the variation of this action with $g_{\mu\nu}$, along with the Einstein-Hilbert action, gives the Einstein Field equations by definition.

Coupling a quantum field theory to a background gravitational field generally involves 3 steps:

1. All flat spacetime metric tensors $\eta_{\mu\nu}$ should be changed to $g_{\mu\nu}(x)$.
2. All partial derivatives ∂_μ should be changed to the covariant derivative ∇_μ, which satisfies

$$\nabla_\mu V^\alpha = \partial_\mu V^\alpha + \Gamma^\alpha{}_{\mu\lambda} V^\lambda, \tag{1.41}$$

$$\nabla_\mu V_\alpha = \partial_\mu V_\alpha - \Gamma^\lambda{}_{\mu\alpha} V_\lambda. \tag{1.42}$$

where V is a general vector, and $\Gamma^\alpha{}_{\mu\lambda}$ are the Christoffel symbols. The above equations can be easily generalised to tensors with an arbitrary number of upper and lower Lorentz indices.

3. The invariant volume element $\int d^d x$ goes to $\int \sqrt{-g}\, d^d x$.

In fact, Eq. (1.39) can be used to find the *symmetric* EMT in flat spacetime. This is achieved simply by using Eq. (1.39) and the 3 steps described above, and then setting $g_{\mu\nu}(x) \to \eta_{\mu\nu}$ at the end of the calculation. Metric variations of various gravitational quantities are given in App. B.3.

Tracing Eq. (1.39) gives

$$\theta^\mu{}_\mu(x) = \frac{2}{\sqrt{-g}} g^{\mu\nu} \frac{\delta \mathcal{S}_M}{\delta g^{\mu\nu}(x)}. \tag{1.43}$$

Furthermore, one can directly calculate the TEMT by using *Weyl transformations*. Under a Weyl transformation, the metric tensor transforms as

$$g_{\mu\nu}(x) \to g_{\mu\nu}(x) e^{-2w(x)}, \tag{1.44}$$

$$g^{\mu\nu}(x) \to g^{\mu\nu}(x) e^{2w(x)}. \tag{1.45}$$

The sign of the exponent are opposite for $g_{\mu\nu}$ and $g^{\mu\nu}$, since $g^{\mu\nu} g_{\nu\lambda} = \delta^\mu{}_\lambda$ has to be satisfied (which implies that $g^{\mu\nu}$ is the inverse of $g_{\mu\nu}$). Thus, one deduces that the TEMT is given by

$$\theta^\mu{}_\mu(x) = \frac{1}{\sqrt{-g}} \frac{\delta \mathcal{S}_M}{\delta w(x)}. \tag{1.46}$$

The Weyl variations of various gravitational objects are given in App. B.5. A theory with conformal symmetry is thus invariant under Weyl transformations [42, 43]. Thus, conformal anomalies are also sometimes referred to as *Weyl* anomalies.

QED and vielbeins

In this section, we will apply the above results to QED. The action is given by

$$\mathcal{S} = \int d^d x \sqrt{-g} \left(-\frac{1}{4} F^{\mu\nu} F_{\mu\nu} + \bar{\Psi} \left(\frac{i}{2} \overleftrightarrow{\not{D}} - m \right) \Psi \right), \tag{1.47}$$

where $\overleftrightarrow{\not{D}} \equiv \overrightarrow{\not{D}} - \overleftarrow{\not{D}}$ and $D_\mu \equiv \nabla_\mu + ieA_\mu$ is the covariant derivative wrt the gauge field. To couple fermions to gravity properly however, we will require *vielbeins*. This complication arises due to the gamma matrices in the fermionic action becoming spacetime dependent,

$$\{\gamma^\mu(x), \gamma^\nu(x)\} = 2g^{\mu\nu}(x). \tag{1.48}$$

The following discussion on the vielbein formalism largely follows [44]. The vielbein $e^a{}_\mu(x)$ is connected to the metric tensor $g_{\mu\nu}(x)$ via the equation

$$g_{\mu\nu}(x) = e^a{}_\mu(x) e^b{}_\nu(x) \eta_{ab}, \tag{1.49}$$

where η_{ab} is the flat spacetime local metric. Greek letters represent indices related to the curved spacetime described by the metric $g_{\mu\nu}(x)$, while roman letters represent indices related to the local frame described by the flat spacetime metric η_{ab}. Using the above, one can also define the *inverse* vielbein $E_a{}^\mu$,

$$E_a{}^\mu(x) = \eta_{ab}\, g^{\mu\nu}(x) e^b{}_\nu(x), \tag{1.50}$$

such that

$$e^a{}_\mu E_a{}^\nu = \delta_\mu{}^\nu, \qquad e^a{}_\mu E_b{}^\mu = \delta^a{}_b. \tag{1.51}$$

We also define

$$E^{a\mu}(x) = g^{\mu\nu}(x) e^a{}_\nu(x) = \eta^{ab} E_b{}^\mu(x), \tag{1.52}$$

which is done for notational convenience later. Using[4]

$$\begin{aligned} \delta\left(\sqrt{-g}\right) &= -\frac{\sqrt{-g}}{2} g_{\mu\nu} \delta g^{\mu\nu} \\ &= \frac{\sqrt{-g}}{2} g^{\mu\nu} \delta g_{\mu\nu}. \end{aligned} \tag{1.53}$$

and Eq. (1.49), one can establish that the variation of $e \equiv \det(e^a{}_\mu) = \sqrt{-g}$ is given by

$$\delta e = \frac{e}{2} g^{\mu\nu} \delta g_{\mu\nu} = e E_a{}^\mu \delta e^a{}_\mu, \tag{1.54}$$

[4]Note that the appearance of the negative sign in going to the second equal sign is due to the fact that $g^{\mu\nu}$ is the inverse of $g_{\mu\nu}$, c.f. the discussion below Eq. (1.45)

Furthermore, a variation of Eq. (1.50) gives

$$\delta E_a{}^\mu = -E_a{}^\lambda E_b{}^\mu \delta e^b{}_\lambda. \tag{1.55}$$

Finally, the EMT obtained by varying the vielbein is given by

$$\theta^{\mu\nu} = \frac{1}{2}\left(T^\mu{}_a\, E^{a\nu} + T^\nu{}_a\, E^{a\mu}\right), \tag{1.56}$$

where

$$T^\mu{}_a = -\frac{1}{e}\frac{\delta \mathcal{S}}{\delta e^a{}_\mu}. \tag{1.57}$$

We are now ready to derive the symmetric EMT for QED. Let us first split the action in (1.47) into two parts, the kinetic action for the fermion fields, $\mathcal{S}_K$,

$$\mathcal{S}_K = \int d^d x\, e\, \frac{i}{2}\bar{\Psi}\overleftrightarrow{\not{D}}\Psi, \tag{1.58}$$

which will have to be treated using vielbeins, and the remaining piece $\mathcal{S}_R$,

$$\mathcal{S}_R = \int d^d x \sqrt{-g}\left(-\frac{1}{4}F^{\mu\nu}F_{\mu\nu} - m\bar{\Psi}\Psi\right), \tag{1.59}$$

which can be taken care of by the previously described metric variation technique. The TEMT θ_R corresponding to $\mathcal{S}_R$ is

$$\theta_R = \left(\frac{d-4}{4}\right)F^2 + d\, m\bar{\Psi}\Psi, \tag{1.60}$$

where contracted indices have been suppressed for convenience. We point out that the calculations are significantly simplified by the fact that, in curved spacetime, the Faraday tensor $F_{\mu\nu}$ does not depend on the metric tensor when written with lower indices, since

$$F_{\mu\nu} \equiv \nabla_\mu A_\nu - \nabla_\nu A_\mu = \partial_\mu A_\nu - \partial_\nu A_\mu. \tag{1.61}$$

We now consider $\mathcal{S}_K$ in Eq. (1.58). We write the gamma matrix $\gamma^\mu(x)$ as

$$\gamma^\mu(x) = E_a{}^\mu(x)\gamma^a, \tag{1.62}$$

where γ^a is the gamma matrix in the flat spacetime coordinate representation at

x (also known as normal coordinates), such that

$$\{\gamma^a, \gamma^b\} = 2\eta^{ab}. \tag{1.63}$$

Thus, $\mathcal{S}_K$ becomes

$$\mathcal{S}_K = \int d^d x\, e\, \frac{i}{2}\bar{\Psi} E_a{}^\mu \gamma^a \overleftrightarrow{D}_\mu \Psi. \tag{1.64}$$

Using Eqs. (1.54), (1.55) and (1.57), we have

$$T^\mu{}_a = -\frac{i}{2}\bar{\Psi} E_a{}^\mu \overleftrightarrow{\not{D}} \Psi + \frac{i}{2}\bar{\Psi}\left[E_b{}^\mu E_a{}^\lambda \gamma^b \overleftrightarrow{D}_\lambda\right]\Psi. \tag{1.65}$$

Then, using Eq. (1.56), we arrive at the symmetric EMT $\theta_K^{\mu\nu}$ corresponding to $\mathcal{S}_K$,

$$\theta_K^{\mu\nu} = -\frac{i}{2} g^{\mu\nu}\bar{\Psi}\overleftrightarrow{\not{D}}\Psi + \frac{i}{4}\bar{\Psi}\left[\gamma^\mu \overleftrightarrow{D}^\nu + \gamma^\nu \overleftrightarrow{D}^\mu\right]\Psi. \tag{1.66}$$

Taking the trace of $\theta_K^{\mu\nu}$, and adding with θ_R from (1.60), we obtain the full QED trace,

$$\theta_{\text{QED}} = \left(\frac{d-4}{4}\right) F^2 + d\, m\bar{\Psi}\Psi - \left(\frac{d}{2} - \frac{1}{2}\right)\bar{\Psi}\left(i\overleftrightarrow{\not{D}}\right)\Psi. \tag{1.67}$$

Finally, using the Dirac equation $\left(i\overrightarrow{\not{D}} - m\right)\Psi = \bar{\Psi}\left(i\overleftarrow{\not{D}} + m\right) = 0$, we arrive at the well-known result

$$\theta_{\text{QED}} = \left(\frac{d-4}{4}\right) F^2 + m\bar{\Psi}\Psi. \tag{1.68}$$

In the quantum field theory, since the VEV of the operators are UV divergent, the TEMT receives anomalous contributions, as explained in Sec. 1.1.2. This has been worked out in detail in [31], and the full result (in 4D) is

$$\langle\theta_{\text{QED}}\rangle = \frac{\beta}{4\alpha}\langle F^2\rangle_{\text{ren}} + (1+\gamma_m)\, m\langle\bar{\Psi}\Psi\rangle_{\text{ren}}, \tag{1.69}$$

where the subscript 'ren' denote renormalised correlation functions as before, $\beta \equiv \frac{d\alpha}{d\ln\mu}$ is the QED beta function and $\gamma_m \equiv \frac{d\ln m}{d\ln\mu}$ is the anomalous mass dimension, c.f. Eq. (1.28).

1.1.5 Gravitational Counterterms and Conformal Anomalies

Coupling a quantum field theory with a background gravitational field comes at a cost. As pointed out in [45–47], in general, one needs to add gravitational

counterterms in order to renormalise the theory. The most general form of these local counterterms is

$$\mathcal{L}_g = c_0 R, \qquad d = 2, \tag{1.70}$$

$$\mathcal{L}_g = a_0 E_4 + b_0 H^2 + c_0 W^2, \qquad d = 4, \tag{1.71}$$

where

$$E_4 = R_{\alpha\beta\gamma\delta} R^{\alpha\beta\gamma\delta} - 4 R_{\alpha\beta} R^{\alpha\beta} + R^2, \tag{1.72}$$

$$W^2 = R_{\alpha\beta\gamma\delta} R^{\alpha\beta\gamma\delta} - \frac{4}{d-2} R_{\alpha\beta} R^{\alpha\beta} + \frac{2}{(d-2)(d-1)} R^2, \tag{1.73}$$

$$H = \frac{R}{d-1}. \tag{1.74}$$

E_4 is the Euler density, or Gauss-Bonnet density, and W^2 is the square of Weyl tensor. In the above, $R_{\alpha\beta\gamma\delta}$, $R_{\alpha\beta}$ and R are the usual Riemann tensor, Ricci tensor and Ricci scalar respectively.

For a conformal field theory, the bare coefficients a_0 and c_0 in general have divergent contributions, that are required to renormalise the theory. We note that b_0 is not divergent for a conformal field theory, since the H^2 term is not conformally invariant,

$$\begin{aligned} T^{\mu}{}_{\mu} &= \frac{2}{\sqrt{-g}} g^{\mu\nu} \frac{\delta}{\delta g^{\mu\nu}} \int \mathrm{d}^d x \sqrt{-g} \left(a_0 E_4 + b_0 H^2 + c_0 W^2 \right) \\ &= -\left(d-4\right) a_0 E_4 - \left(d-4\right) b_0 H^2 - 4 b_0 \Box H - \left(d-4\right) c_0 \left[W^2 - \frac{2}{3} \Box R \right]. \end{aligned} \tag{1.75}$$

On the other hand, E_4 and W^2 are conformally invariant in 4D, as can be seen from their coefficient in Eq. (1.75).

Thus, one finds that the TEMT has the general form [42]

$$\langle T^{\mu}{}_{\mu} \rangle = \beta_c R, \qquad d = 2, \tag{1.76}$$

$$\langle T^{\mu}{}_{\mu} \rangle = \beta_a E_4 + \beta_b H^2 + \beta_c W^2 + 4\bar{b} \Box H, \qquad d = 4, \tag{1.77}$$

where the coefficients β_a, β_b, β_c are beta functions in the sense that they arise purely from the divergent components of a_0, b_0 and c_0 respectively, c.f. Eq. (1.75). We note once again that for a CFT, $\beta_b = 0$ since b_0 is not divergent. This also implies that $\bar{b}$ is finite. In fact, the $\bar{b}$ coefficient can be varied by adding a *finite*

local counterterm to $\mathcal{L}_g$ proportional to H^2,

$$\mathcal{L}_g \to \mathcal{L}_g + \omega H^2 \quad \Longrightarrow \quad \bar{b} \to \bar{b} - \omega. \tag{1.78}$$

This apparent ambiguity in the $\bar{b}$ coefficient in explored in Chapter 3, and in particular in Sec. 3.2.

An explicit calculation illustrating the above results is discussed in the next chapter in Sec. 2.1.3 for a scalar field.

Chapter 2

Conformal anomalies in Curved Spacetime

In this chapter, we will calculate the VEV of the TEMT in 4D, using dimensional regularisation (dim reg). We will perform the calculation for various field theories with a scalar, fermion or spin-1 gauge field as the matter field content of the theory.

Note that for notational convenience, we will often use the comma/semicolon notation for expressing derivatives, see App. C.1.1,

$$\nabla_\alpha \nabla_\beta \nabla_\mu A \equiv A_{;\,\mu\beta\alpha} \tag{2.1}$$

$$\partial_\alpha \partial_\beta \partial_\mu A = A_{,\,\mu\beta\alpha} \tag{2.2}$$

Note the order of the indices. Therefore, we will often refrain from punctuating equations, as this may lead to confusion.

There are three ways of computing the VEV of the TEMT in dim reg:

1. $g^{(d)}_{\mu\nu}\langle T^{\mu\nu}\rangle \equiv \langle g^{(d)}_{\mu\nu} T^{\mu\nu}\rangle$
2. $g^{(4)}_{\mu\nu}\langle T^{\mu\nu}\rangle$
3. $\langle g^{(4)}_{\mu\nu} T^{\mu\nu}\rangle$

where the superscript denotes the dimensions. The effect the dimension has on

the metric tensor is evident when it is contracted with itself,

$$g^{(d)}_{\mu\nu} g^{\mu\nu} = d, \tag{2.3}$$

$$g^{(4)}_{\mu\nu} g^{\mu\nu} = 4. \tag{2.4}$$

The three ways of calculating the VEV of the TEMT are, in general, distinct as they each correspond to different ways (and order) of performing the regularisation. The identity

$$g^{(d)}_{\mu\nu} \langle T^{\mu\nu} \rangle \equiv \langle g^{(d)}_{\mu\nu} T^{\mu\nu} \rangle, \tag{2.5}$$

is obvious since every trace that appears on each side is automatically performed in d-dimensions. In this chapter, we will calculate each one of the three ways of obtaining the VEV of the TEMT for the scalar, fermion and spin-1 gauge fields.

Note that we will sometimes use the shorthand

$$\langle T^{\mu}{}_{\mu} \rangle \equiv g^{(d)}_{\mu\nu} \langle T^{\mu\nu} \rangle, \tag{2.6}$$

whereas when the four dimensional metric tensor $g^{(4)}_{\mu\nu}$ is used, we will always write it explicitly.

The focus in this section is dim reg, although we sometimes give the result in Pauli-Villars regularisation [48] where possible.

2.1 Scalar field

To illustrate most of the techniques used in this chapter, we will study the case of the scalar field in detail, as it is a well-known example, which is often discussed in the literature. While we will work in $d = 4 - 2\epsilon$ dimension, it is rather easy to reproduce the results for $d = 2 - 2\epsilon$, since most of the formalism and techniques remain practically the same.

2.1.1 Generalities

The action for a free massive scalar field ϕ is given by

$$\mathcal{S} = \int \mathrm{d}^d x \sqrt{-g} \left[\frac{1}{2} g^{\mu\nu} \nabla_\mu \phi \nabla_\nu \phi - \frac{1}{2} m^2 \phi^2 - \frac{1}{2} \eta R \phi^2 \right]. \tag{2.7}$$

The term $\eta R \phi^2$, with general coupling η, has been added as it is consistent dimensionally and respects all necessary symmetries of the field theory. The equation of motion (EoM) is

$$\phi \Box \phi = -m^2 \phi^2 - \eta R \phi^2. \tag{2.8}$$

A useful identity involving derivatives and the EoM is

$$(\nabla_\mu \phi)^2 = \frac{1}{2} \Box \phi^2 + m^2 \phi^2 + \eta R \phi^2. \tag{2.9}$$

The energy-momentum tensor (EMT) is obtained using

$$T_{\mu\nu} = \frac{2}{\sqrt{-g}} \frac{\delta \mathcal{S}}{\delta g^{\mu\nu}}, \tag{2.10}$$

and for the scalar field theory, it is given by

$$\begin{aligned} T_{\mu\nu} = &-g_{\mu\nu} \left[\frac{1}{2} (\nabla_\mu \phi)^2 - \frac{1}{2} m^2 \phi^2 - \frac{1}{2} \eta R \phi^2 \right] + \nabla_\mu \phi \nabla_\nu \phi \\ &- \eta \Big[R_{\mu\nu} - g_{\mu\nu} \Box + \nabla_\mu \nabla_\nu \Big] \phi^2. \end{aligned} \tag{2.11}$$

After using the EoM, the TEMT becomes

$$T^\mu{}_\mu = m^2 \phi^2 + \left(\eta (d-1) - \frac{d-2}{4} \right) \Box \phi^2. \tag{2.12}$$

In $d = 4 - 2\epsilon$ dimensions,

$$T^\mu{}_\mu = \frac{1}{2} \Big[(6\eta - 1) + \epsilon (1 - 4\eta) \Big] \Box \phi^2 + m^2 \phi^2. \tag{2.13}$$

For the theory to be conformal, we require the TEMT to vanish when $m = 0$.

Therefore, we get the well-known result that

$$\eta \equiv \eta_c = \frac{1}{4}\frac{d-2}{d-1} = \frac{1}{6} - \frac{\epsilon}{18} + \mathcal{O}(\epsilon^2), \tag{2.14}$$

where $d = 4 - 2\epsilon$ has been used in the last equality. The value η_c is known as the conformal coupling, and when $\eta = \eta_c$, the scalar field is said to be *conformally-coupled*. Note that having a conformal coupling is equivalent to adding an improvement term to the EMT, as discussed in Sec. 1.1.1.

To obtain the anomaly, it is clear that one first needs the two point function of the scalar field in curved spacetime, $\langle\phi(x)\phi(x')\rangle$, and derivatives thereof. To this end, we will use the Schwinger-De Witt method [13, 14], described below.

2.1.2 Schwinger-De-Witt method for the scalar field

A powerful technique for evaluating the 2-point Green's function in curved spacetime is discussed here. This revolves around adapting the heat kernel method to deal with a background gravitational field. Note that this method requires keeping a mass for the field, which will be taken to zero in the end when computing the conformal anomalies.

We define the Green's function

$$iG_{\mathrm{F}}(x, x') = \langle\phi(x)\phi(x')\rangle, \tag{2.15}$$

that satisfies the Schwinger-Dyson equation

$$(\Box_x + m^2 + \eta R)\, G_{\mathrm{F}}(x, x') = -\left(-g(x)\right)^{-\frac{1}{2}} \delta^d(x - x'). \tag{2.16}$$

The solution to this equation has been developed by Schwinger [49] in flat space and generalised by De-Witt [14] to curved spacetime. Thus, this technique is often referred to as the De-Witt-Schwinger point splitting method.

We define the states $|x\rangle$ living in a Hilbert space such that

$$\langle x|G|x'\rangle = G_{\mathrm{F}}(x, x'), \tag{2.17}$$

$$\langle x|x'\rangle = \delta^d(x - x'). \tag{2.18}$$

Thus, in operator form, the Schwinger-Dyson equation in (2.16) becomes

$$\left(\pi_\mu \left(-g\right)^{\frac{1}{2}} g^{\mu\nu}\pi_\nu - \left(-g\right)^{\frac{1}{2}} m^2 - \left(-g\right)^{\frac{1}{2}} \eta R\right) G = 1, \tag{2.19}$$

where

$$\pi_\mu |x\rangle = i\nabla_\mu |x\rangle, \tag{2.20}$$

We can rewrite the equation as

$$\left(-g\right)^{-\frac{1}{4}} \left(\pi_\mu \left(-g\right)^{\frac{1}{2}} g^{\mu\nu}\pi_\nu \left(-g\right)^{-\frac{1}{4}} - m^2 \left(-g\right)^{\frac{1}{4}} - \eta R \left(-g\right)^{\frac{1}{4}}\right) \left(-g\right)^{\frac{1}{4}} G \left(-g\right)^{\frac{1}{4}} = 1. \tag{2.21}$$

Next, we define the operator H,

$$H = \left(-g\right)^{-\frac{1}{4}} \pi_\mu \left(-g\right)^{\frac{1}{2}} g^{\mu\nu}\pi_\nu \left(-g\right)^{-\frac{1}{4}} - \eta R. \tag{2.22}$$

Thus, we have that

$$\left(-g\right)^{\frac{1}{4}} G \left(-g\right)^{\frac{1}{4}} = \frac{1}{H - m^2}. \tag{2.23}$$

By giving m^2 a small negative imaginary part, one rewrite the RHS of Eq. (2.23) using the integral representation

$$\left(-g\right)^{\frac{1}{4}} G \left(-g\right)^{\frac{1}{4}} = -i \int_0^\infty \mathrm{d}s \; e^{i\left(H - m^2\right)s}, \tag{2.24}$$

where the parameter s is known as the Schwinger proper time. Introducing the states in the Hilbert space again, and defining

$$\langle x|e^{iHs}|x'\rangle = \langle x, s|x', 0\rangle, \tag{2.25}$$

we obtain the Schrödinger equation

$$\begin{aligned} i\partial_s \langle x, s|x', 0\rangle &= -\langle x, s|H|x', 0\rangle \\ &= \left(\Box_x + \eta R\right) \langle x, s|x', 0\rangle \\ &= \left(\Box_{x'} + \eta R\right) \langle x, s|x', 0\rangle, \end{aligned} \tag{2.26}$$

with the boundary condition

$$\langle x,0|x',0\rangle = \delta\left(x-x'\right). \tag{2.27}$$

To solve Eq. (2.26), we make the Ansatz,

$$\langle x,s|x',0\rangle = \frac{iD^{\frac{1}{2}}\left(x,x'\right)}{\left(4\pi is\right)^{\frac{d}{2}}} e^{\frac{\sigma(x,x')}{2is}} \Omega\left(x,x';is\right). \tag{2.28}$$

In the above, $\sigma\left(x,x'\right)$ is the *geodetic interval*, equal to half of the proper distance between x and x' [14]. It can be expressed as

$$\sigma = \frac{1}{2} g^{\mu\nu}\nabla_{\mu}\sigma\nabla_{\nu}\sigma = \frac{1}{2} g^{\mu'\nu'}\nabla_{\mu'}\sigma\nabla_{\nu'}\sigma. \tag{2.29}$$

We will often suppress the spacetime dependences of $\sigma \equiv \sigma\left(x,x'\right)$. Also, $D\left(x,x'\right)$ is given by

$$D\left(x,x'\right) = \det\left(\nabla_{\nu'}\nabla_{\mu}\sigma\right). \tag{2.30}$$

Substituting the Ansatz into the differential equation, one has

$$\frac{\partial\Omega}{\partial s} = -iD^{-\frac{1}{2}}\left(D^{\frac{1}{2}}\Omega\right)_{;\mu}^{\ \ \mu} - \frac{1}{s}\Omega_{;\mu}\sigma_{;}^{\ \mu} - i\eta R\Omega \tag{2.31}$$

We then perform a power expansion for $\Omega\left(x,x';is\right)$,

$$\Omega\left(x,x';is\right) = \sum_{j=0}^{\infty} a_j\left(x,x'\right)\left(is\right)^j, \tag{2.32}$$

where $a_j\left(x,x'\right)$ are known as the Seeley-De Witt coefficients [13, 14, 50, 51]. This then leads to the recursion relation

$$\nabla_{\lambda}\sigma\nabla^{\lambda}a_0 = 0, \tag{2.33}$$

$$\nabla^{\mu}\sigma\,\nabla_{\mu}a_{n+1} + \left(n+1\right)a_{n+1} = -\Delta^{-\frac{1}{2}}\nabla^{\mu}\nabla_{\mu}\left(\Delta^{\frac{1}{2}}a_n\right) - \eta R a_n, \qquad n \geq 0. \tag{2.34}$$

where

$$\Delta\left(x,x'\right) = \left(-g\right)^{-\frac{1}{2}} D\left(x,x'\right)\left(-g'\right)^{-\frac{1}{2}}, \tag{2.35}$$

is the Van Vleck-Morette determinant [52, 53], and we have used the notation

$g \equiv g(x)$ and $g' \equiv g(x')$.[1]

The final task is to obtain the boundary condition, i.e. $\Omega(x, x'; 0)$. To this end, we consider the flat spacetime limit (denoted by the subscript 'f'), where it is well-known that

$$\langle x(s)'|x(0)''\rangle_{\mathrm{f}} = Cs^{-\frac{d}{2}} e^{\frac{i}{4}\frac{(x'-x'')^2}{s}}, \tag{2.36}$$

with the boundary condition

$$\langle x(0)'|x(0)''\rangle_{\mathrm{f}} = \delta(x'' - x'). \tag{2.37}$$

By integrating both sides over x', one can fix the constant to be

$$C = \frac{i}{(4\pi i)^{\frac{d}{2}}}. \tag{2.38}$$

Thus, in curved spacetime, one concludes that the boundary condition translates to

$$\Omega(x, x'; 0) = 1, \tag{2.39}$$

and this in turn fixes

$$a_0(x, x') = 1. \tag{2.40}$$

Finally, after introducing the states again into Eq. (2.24), we have

$$\begin{aligned} G_{\mathrm{F}}(x, x') &= -i\Delta^{\frac{1}{2}}(x, x')(4\pi)^{-\frac{d}{2}} \int_0^\infty i\,\mathrm{d}s\,(is)^{-\frac{d}{2}} \exp\left[-im^2 s + \frac{\sigma}{2is}\right] \Omega(x, x'; is) \\ &= -i\Delta^{\frac{1}{2}}(x, x')(4\pi)^{-\frac{d}{2}} \sum_{j=0}^\infty \int_0^\infty i\,\mathrm{d}s\,(is)^{j-\frac{d}{2}} \exp\left[-im^2 s + \frac{\sigma}{2is}\right] a_j(x, x'). \end{aligned} \tag{2.41}$$

To obtain coincident limits of $\langle\phi(x)\phi(x')\rangle$ to be used for calculating the VEV of the TEMT, one needs the coincident limits of $\sigma(x, x')$, $\Delta(x, x')$ and $a_j(x, x')$, and their derivatives. The first two are given in App. C.6 and are the same independent of the field content of a theory. The coincident limits of the Seeley-De Witt coefficients $a_j(x, x')$ for the scalar field are given in the next section.

[1] The equation strictly involves D, but we are able to replace D by Δ, since $\nabla_\mu g = 0$ etc.

Coincident limits of $a_j(x,x')$ for a scalar field

The coincident limits will be denoted by

$$a_j(x) = \lim_{x' \to x} a_j(x,x') = [a_j]. \tag{2.42}$$

Using the recursion relations derived in Eqs. (2.33) and (2.34), one can obtain the coincident limits for $a_j(x,x')$. For convenience, we start by defining

$$\begin{aligned} a_{\alpha\beta} = {} & \frac{1}{2}\left(\eta - \frac{1}{6}\right) R_{;\alpha\beta} + \frac{1}{120} R_{;\alpha\beta} - \frac{1}{40} R_{\alpha\beta;\lambda}{}^{\lambda} - \frac{1}{30} R_{\alpha}{}^{\lambda} R_{\lambda\beta} + \frac{1}{60} R^{\mu}{}_{\alpha}{}^{\lambda}{}_{\beta} R_{\mu\lambda} \\ & + \frac{1}{60} R^{\lambda\mu\nu}{}_{\alpha} R_{\lambda\mu\nu\beta} \end{aligned} \tag{2.43}$$

such that

$$a^{\lambda}{}_{\lambda} = \frac{1}{60} R^2_{\alpha\beta\mu\nu} - \frac{1}{60} R^2_{\alpha\beta} - \frac{1}{2}\left(\frac{1}{5} - \eta\right) \Box R. \tag{2.44}$$

We then have that

$$a_0(x) = 1, \tag{2.45}$$

$$a_1(x) = \left(\frac{1}{6} - \eta\right) R, \tag{2.46}$$

$$\begin{aligned} a_2(x) &= \frac{1}{180} R^2_{\mu\nu\alpha\beta} - \frac{1}{180} R^2_{\mu\nu} - \frac{1}{6}\left(\frac{1}{5} - \eta\right) \Box R + \frac{1}{2}\left(\frac{1}{6} - \eta\right)^2 R^2 \\ &= \frac{1}{120} W^2 - \frac{1}{360} E_4 - \frac{1}{6}\left(\frac{1}{5} - \eta\right) \Box R + \frac{1}{2}\left(\frac{1}{6} - \eta\right)^2 R^2 \\ &= \frac{1}{2}\left(\frac{1}{6} - \eta\right)^2 R^2 + \frac{1}{3} a^{\lambda}{}_{\lambda} \end{aligned} \tag{2.47}$$

Since it will be useful in later calculations, we also give the results for coincident limits involving 1 derivative and 2 derivatives. The first set is given by

$$[a_{1;\nu}] = \frac{1}{2}\left(\frac{1}{6} - \eta\right) R_{;\nu} \tag{2.48}$$

$$[a_{1;\nu'}] = \frac{1}{2}\left(\frac{1}{6} - \eta\right) R_{;\nu} \tag{2.49}$$

while the second set is given by

$$\begin{aligned}\left[a_{1;}{}^{\mu\nu}\right] &= \frac{1}{108}R^{\mu\nu}R - \frac{1}{3}\eta R_{;}{}^{\mu\nu} - \frac{1}{3}\left[\Delta^{\frac{1}{2}}{}_{;}{}^{\lambda}{}_{\lambda}{}^{\mu\nu}\right] \\ &= \frac{1}{540}\Bigg[12R^{\mu\lambda}R^{\nu}{}_{\lambda} - 6R^{\alpha\beta}R^{\mu}{}_{\alpha}{}^{\nu}{}_{\beta} - 6R^{\mu\alpha\beta\gamma}R^{\nu}{}_{\alpha\beta\gamma} + 9\Box R^{\mu\nu} \\ &\quad + (27 - 180\eta)\, R_{;}{}^{\mu\nu}\Bigg] \\ &= \frac{1}{2}\left(\frac{1}{6} - \eta\right)R_{;\mu\nu} + \frac{2}{3}a_{\mu\nu} \end{aligned} \tag{2.50}$$

$$\left[a_{1;}{}^{\mu}{}_{\mu}\right] = \frac{1}{3}\left[\frac{1}{30}R^2_{\mu\nu} + \left(\frac{1}{5} - \eta\right)\Box R - \frac{1}{30}R^2_{\mu\nu\alpha\beta}\right] \tag{2.51}$$

$$\begin{aligned}\left[a_{1;\nu\lambda'}\right] &= \frac{1}{90}\left(R_{\nu}{}^{\alpha\beta\gamma}R_{\lambda}{}^{\alpha\beta\gamma} + R^{\alpha\beta}R_{\nu\alpha\lambda\beta} - 2R_{\nu\alpha}R_{\lambda}{}^{\alpha}\right) - \frac{1}{60}\Box R_{\nu\lambda} \\ &\quad + \frac{1}{6}\left(\frac{1}{5} - \eta\right)R_{;\nu\lambda} \end{aligned} \tag{2.52}$$

$$\left[a_{1;}{}^{\mu}{}_{\mu'}\right] = \frac{1}{90}R^2_{\mu\nu\alpha\beta} - \frac{1}{90}R^2_{\mu\nu} + \frac{1}{6}\left(\frac{1}{10} - \eta\right)\Box R \tag{2.53}$$

The explicit coincident limit $\left[\Delta^{\frac{1}{2}}{}_{;}{}^{\lambda}{}_{\lambda}{}^{\mu\nu}\right]$ is given in App. C.6.2. Furthermore, we have used Synge's theorem [54] in working out the coincident limits for those involving derivatives wrt primed indices,

$$\left[A_{;\ldots\alpha'}\right] = -\left[A_{;\ldots\alpha}\right] + \left[A_{;\ldots}\right]_{;\alpha} \tag{2.54}$$

Note that we do not need to go beyond a_2, since we are concerned with calculating the conformal anomaly, and thus focus on terms that survive in the limit of $m \to 0$. This is rather fortunate, as the calculation of coincident limits with higher j gets increasing complicated, due to more complex structures having more derivatives of the metric tensor appearing [55].

Alternative Method using Riemann Normal Coordinates

In this section, we show that the same coincident limits for the $a_j\,(x, x')$ coefficients can be found by introducing *Riemann normal coordinates*[2] y^μ for

[2]Riemann normal coordinates has a lot of similarities with the Fock-Schwinger gauge; this has been pointed out in [55].

the point x, with origin x' [56–58]. One can then expand $g_{\mu\nu}(x)$ about x':

$$g_{\mu\nu}(x) = \eta_{\mu\nu} + \frac{1}{3}R_{\mu\alpha\nu\beta}\,y^\alpha y^\beta - \frac{1}{6}(\nabla_\gamma R_{\mu\alpha\nu\beta})y^\alpha y^\beta y^\gamma + \left[\frac{1}{20}\nabla_\gamma\nabla_\delta R_{\mu\alpha\nu\beta} + \frac{2}{45}R_{\alpha\mu\beta\lambda}R^\lambda{}_{\gamma\nu\delta}\right] y^\alpha y^\beta y^\gamma y^\delta + \dots\,, \tag{2.55}$$

where the coefficients are all evaluated at the origin x'. In this expansion, the metric and its derivative (but not second derivative, hence the appearance of the Riemann tensor) are the same as in flat spacetime.

In Riemann Normal coordinates (RNC),

$$\sigma = \frac{1}{2}y^\alpha y_\alpha. \tag{2.56}$$

Also, the Van Vleck-Morette determinant, $\Delta(x,x')$, becomes

$$\Delta(x,x') = (-g(x))^{-\frac{1}{2}}, \tag{2.57}$$

which goes to 1 in the coincident limit $x \to x'$, as expected.

Non-coincident limits of $a_j\,(x,x')$ in RNC

We start with Eq. (2.16) and define

$$\mathcal{G}_{\rm F}(x,x') = (-g(x))^{\frac{1}{4}}\,G_{\rm F}(x,x'). \tag{2.58}$$

Expressing $\mathcal{G}_{\rm F}(x,x')$ as a Fourier transform, we have

$$\mathcal{G}_{\rm F}(x,x') = \int \frac{d^dk}{(2\pi)^d}\,e^{-iky}\,\mathcal{G}_{\rm F}(k). \tag{2.59}$$

We now perform an adiabatic expansion of $\mathcal{G}_{\rm F}(k)$. To adiabatic order four (i.e. four derivatives of the metric), we have [58]

$$\begin{aligned}\mathcal{G}_{\rm F}(k) \approx\ & (k^2-m^2)^{-1} \\ & - \left(\frac{1}{6}-\eta\right) R\,(k^2-m^2)^{-2} + \frac{1}{2}i\left(\frac{1}{6}-\eta\right)(\nabla_\alpha R)\,\partial^\alpha(k^2-m^2)^{-2} \\ & - \frac{1}{3}a_{\alpha\beta}\,\partial^\alpha\partial^\beta(k^2-m^2)^{-2} + \left[\left(\frac{1}{6}-\eta\right)^2 R^2 + \frac{2}{3}a^\lambda{}_\lambda\right](k^2-m^2)^{-3},\end{aligned} \tag{2.60}$$

where $\partial_\alpha \equiv \frac{\partial}{\partial k^\alpha}$ and $a_{\alpha\beta}$ is given by Eq. (2.43).

Substituting $\mathcal{G}_{\rm F}(k)$ into Eq. (2.59), we get

$$\mathcal{G}_{\rm F}(x,x') \approx \int \frac{d^dk}{(2\pi)^d}\, e^{-iky} \left[a_0(x,x') + a_1(x,x') \left(-\frac{\partial}{\partial m^2}\right) + a_2(x,x') \left(-\frac{\partial}{\partial m^2}\right)^2 \right] (k^2-m^2)^{-1}, \tag{2.61}$$

where the $a_j\,(x,x')$ are given by

$$a_0(x,x') = 1, \tag{2.62}$$

$$a_1(x,x') = \left(\frac{1}{6}-\eta\right) R - \frac{1}{2}\left(\frac{1}{6}-\eta\right) (\nabla_\alpha R)\, y^\alpha - \frac{1}{3} a_{\alpha\beta} y^\alpha y^\beta, \tag{2.63}$$

$$a_2(x,x') = \frac{1}{2}\left(\frac{1}{6}-\eta\right)^2 R^2 + \frac{1}{3} a^\lambda{}_\lambda, \tag{2.64}$$

where all geometric quantities (Riemann tensor, Ricci tensor and Ricci scalar) are evaluated at x', the origin of our RNC system. As can be seen from the above expressions for $a_j\,(x,x')$, in the coincident limit, they all match the results obtained in Eqs. (2.45) to (2.47). It is also not hard to show that the coincident limits of derivatives of $a_j\,(x,x')$ also match.

Furthermore, using the integral representation for $(k^2-m^2)^{-1}$ (giving a small imaginary part to m^2),

$$(k^2-m^2+i\epsilon)^{-1} = -i\int_0^\infty \mathrm{d}s\, e^{is(k^2-m^2+i\epsilon)}, \tag{2.65}$$

we have, after performing the Gaussian integral over k, that

$$\mathcal{G}_{\rm F}(x,x') = -\frac{i}{(4\pi)^{\frac{d}{2}}} \int_0^\infty i\,\mathrm{d}s\, (is)^{-\frac{d}{2}}\, \exp\left[-im^2 s + \frac{\sigma}{2is}\right]\, \Omega(x,x';is), \tag{2.66}$$

which matches Eq. (2.41).

Evaluation of s integral

We present the evaluation of the s-integral[3] in this short section. We take the coincident limit before calculating the integral, and keep the index j generic in what follows.

In dim reg, the result is given by

$$\int_0^\infty i\,\mathrm{d}s\,(is)^{-\frac{d}{2}+j}\,e^{-im^2 s} = \frac{\Gamma(j+1-\frac{d}{2})}{(m^2)^{j+1-\frac{d}{2}}}. \tag{2.67}$$

The integral is evaluated by analytically continuing the variable s to the complex plane.

To incorporate Pauli-Villars regularisation, we use the prescription from [59], which involves multiplying the integrand by the regulator function $\left(1-e^{-i\Lambda^2 s}\right)$, where Λ is the Pauli-Villars mass. Each factor of the regulator function reduces the degree of divergence by 2, so one may have to implement it recursively at different levels to fully regularise an integral (which may involve more than 1 Pauli-Villars mass, as we will illustrate below).

For a logarithmically divergent s integral (i.e. $j=2$),

$$\int_0^\infty i\,\mathrm{d}s\,(is)^{-1}\,e^{-im^2 s}\left(1-e^{-i\Lambda^2 s}\right) = \ln\left(\frac{\Lambda^2}{m^2}\right). \tag{2.68}$$

For a quadratically divergent s integral (i.e. $j=1$),

$$\begin{aligned}&\int_0^\infty i\,\mathrm{d}s\,(is)^{-2}\,e^{-im^2 s}\left(\left(1-e^{-i\Lambda_2^2 s}\right)-e^{-i\Lambda^2 s}\left(1-e^{-i\Lambda_2^2 s}\right)\right)\\ &=\Lambda_2^2\,\ln\left(\frac{\Lambda^2+\Lambda_2^2}{\Lambda_2^2}\right)+\left(m^2+\Lambda^2\right)\,\ln\left(\frac{\Lambda^2+\Lambda_2^2}{\Lambda^2}\right)-m^2\ln\left(\frac{\Lambda_2^2}{m^2}\right).\end{aligned} \tag{2.69}$$

Evaluating condensates

In this section, we provide the results for the condensates of the scalar fields, including those with derivatives. This section will be a useful collection of results for later when computing the conformal anomaly.

[3]Note that it is reminiscent of the Schwinger proper time representation and integration techniques.

By studying the EMT and TEMT in Eq. (2.11) and Eq. (2.12) respectively, we find that we have a total of 5 different condensates to calculate. In what follows, we only keep terms that remain finite when the masses are set to zero.

Also, we wish to fix the mass dimension of the EMT and TEMT to 4 exactly. Therefore, the condensates below will all involve an extra factor of $\mu^{2\epsilon}$, where μ is an arbitrary energy scale. The same has been done in [60].

The simplest condensate is[4]

$$\begin{aligned}\langle\phi^2\rangle &= \frac{\mu^{2\epsilon}}{(4\pi)^{\frac{d}{2}}}\int_0^\infty i\mathrm{d}s\ (is)^{-\frac{d}{2}}\, e^{-im^2 s}\left[a_2(x)\,(is)^2 + a_1(x)\,(is)\right] \\ &= \frac{1}{(4\pi)^2}\left[\frac{a_2(x)}{m^2} + a_1(x)\Gamma(\epsilon)\left(\frac{m^2}{4\pi\mu^2}\right)^{-\epsilon}\right]. \end{aligned} \tag{2.70}$$

For notational convenience, we will define the shorthand

$$\Delta_\epsilon \equiv \Gamma(\epsilon)\left(\frac{m^2}{4\pi\mu^2}\right)^{-\epsilon}. \tag{2.71}$$

Two other condensates are obtained by taking derivatives of the above result

$$\nabla_\mu\nabla_\nu\langle\phi^2\rangle = \frac{1}{(4\pi)^2}\left[\Delta_\epsilon\left(\frac{1}{6}-\eta\right)\nabla_\mu\nabla_\nu R\right], \tag{2.72}$$

$$\Box\langle\phi^2\rangle = \frac{1}{(4\pi)^2}\left[\Delta_\epsilon\left(\frac{1}{6}-\eta\right)\Box R\right], \tag{2.73}$$

where we have substituted the expression for $a_1\,(x)$ from Eq. (2.46), and neglected $a_2\,(x)$.

Now, consider

$$\begin{aligned}\langle\nabla_\mu\phi\nabla_\nu\phi\rangle &= \lim_{x\to x'}\nabla_\mu^{(x)}\nabla_\nu^{(x')}\langle\phi(x)\phi(x')\rangle \\ &= \frac{\mu^{2\epsilon}}{(4\pi)^{\frac{d}{2}}}\int i\mathrm{d}s\, e^{-im^2 s}\,(is)^{1-\frac{d}{2}}\left[\left[\Delta^{\frac{1}{2}}{}_{;\mu\nu'}\right]a_1\,(x) + \frac{[\sigma_{;\mu\nu'}]}{2}a_2\,(x) + [a_{1;\mu\nu'}]\right], \end{aligned} \tag{2.74}$$

where only the relevant terms have been included (by relevant, we mean up to 4 derivatives of the metric).

[4]We keep the term having m^{-2}, since it can be multiplied by m^2 and would thus remain finite in the massless limit, c.f. Eq. (2.12).

Using the results for the coincident limits from App. C.6, we have

$$\langle \nabla_\mu \phi \nabla_\nu \phi \rangle = \frac{\Delta_\epsilon}{(4\pi)^2} \left[\frac{1}{6} \left(\frac{1}{6} - \eta \right) R\, R_{\mu\nu} - \frac{g_{\mu\nu}}{2} a_2(x) + [a_{1;\mu\nu'}] \right]. \tag{2.75}$$

Finally, we have $\langle (\nabla_\mu \phi)^2 \rangle$, which simply corresponds to a metric contraction (in d dimensions) of the previous result. This gives

$$\begin{aligned} \langle (\nabla_\mu \phi)^2 \rangle &= \frac{\mu^{2\epsilon}}{(4\pi)^{\frac{d}{2}}} \int_0^\infty i\mathrm{d}s\ (is)^{1-\frac{d}{2}}\, e^{-im^2 s} \Bigg[-\frac{d}{2} a_2(x) \\ &\quad + \left(\frac{1}{2} \left(\frac{1}{6} - \eta \right) \Box R + \frac{2}{3} a^\lambda{}_\lambda + \frac{1}{6} \left(\frac{1}{6} - \eta \right) R^2 \right) \Bigg] \\ &= \frac{\Delta_\epsilon}{(4\pi)^2} \left[\frac{1}{2} \left(\frac{1}{6} - \eta \right) \Box R + \eta \left(\frac{1}{6} - \eta \right) R^2 + \frac{\epsilon}{2} \left(\frac{1}{6} - \eta \right)^2 R^2 + \frac{\epsilon}{3} a^\lambda{}_\lambda \right]. \end{aligned} \tag{2.76}$$

Effect of using the EoM

In this section, we investigate whether the use of the EoM could potentially change the VEV of the TEMT. More specifically, we investigate whether using Eq. (2.9) changes the result.

From the previous section, we have $\langle (\nabla_\mu \phi)^2 \rangle$ already, which is the LHS of Eq. (2.9). Thus, one suffices to consider the contribution to the RHS,

$$\begin{aligned} \mathrm{RHS} &= \frac{1}{2} \Box \langle \phi^2 \rangle + m^2 \langle \phi^2 \rangle + \eta R \langle \phi^2 \rangle \\ &= \frac{\Delta_\epsilon}{(4\pi)^2} \left[\frac{1}{2} \left(\frac{1}{6} - \eta \right) \Box R + \frac{\epsilon}{2} \left(\frac{1}{6} - \eta \right)^2 R^2 + \frac{\epsilon}{3} a^\lambda{}_\lambda + \eta \left(\frac{1}{6} - \eta \right) R^2 \right]. \end{aligned} \tag{2.77}$$

It matches Eq. (2.76) - Hence, using the EoMs do not affect the calculation of the anomaly.

Conformal anomaly of the Conformally-coupled scalar

We are finally in a position to discuss the conformal anomaly for a conformally coupled scalar (CCS). We return to the discussion of the non-conformally coupled scalar (NCCS) in the next section. From Eq. (2.12)

$$\begin{aligned} g^{(d)}_{\mu\nu}\langle T^{\mu\nu}\rangle = \langle T^{\mu}{}_{\mu}\rangle &= m^2\langle\phi^2\rangle \\ &= \frac{a_2\,(x)}{(4\pi)^2} \\ &= \frac{1}{2880\pi^2}\left(\frac{3}{2}W^2 - \frac{1}{2}E_4 - \Box R\right). \end{aligned} \tag{2.78}$$

Furthermore, we have

$$g^{(4)}_{\mu\nu}\langle T^{\mu\nu}\rangle = 0 \tag{2.79}$$

$$\langle g^{(4)}_{\mu\nu}T^{\mu\nu}\rangle = \frac{1}{2880\pi^2}\left(\frac{3}{2}W^2 - \frac{1}{2}E_4 - \Box R\right) \equiv g^{(d)}_{\mu\nu}\langle T^{\mu\nu}\rangle, \tag{2.80}$$

where the last line indicates that $\langle g^{(4)}_{\mu\nu}T^{\mu\nu}\rangle$ and $g^{(d)}_{\mu\nu}\langle T^{\mu\nu}\rangle$ match for a CCS. The results agree with those in [61–63]. We note, however, that this result will not be true in general, especially when it comes to non-conformal theories.

The above results motivate us to define the *anomalous* part of the TEMT via two possible prescriptions[5]

$$A_1 \equiv g^{(4)}_{\mu\nu}\langle T^{\mu\nu}\rangle - g^{(d)}_{\mu\nu}\langle T^{\mu\nu}\rangle, \tag{2.81}$$

$$A_2 \equiv g^{(4)}_{\mu\nu}\langle T^{\mu\nu}\rangle - \langle g^{(4)}_{\mu\nu}T^{\mu\nu}\rangle. \tag{2.82}$$

In what follows, we will compute both A_1 and A_2, and point out the differences, if any[6]. If one imposes regularisation-independence of the anomaly, the prescription for A_2 makes more sense. For the CCS, the prescription does not make a difference, other than changing the overall sign, which was arbitrary to begin with

$$A_1^{\rm CCS} = A_2^{\rm CCS} = \frac{1}{2880\pi^2}\left(-\frac{3}{2}W^2 + \frac{1}{2}E_4 + \Box R\right). \tag{2.83}$$

[5]The sign convention for the subtraction is arbitrary, but we pick it in a way that facilitates comparison with the results in Chapter 3 in the context of flow theorems.

[6]They would usually happen for the coefficient of the $\Box R$ term, which can be UV divergent without the subtraction.

In the CCS, the first term vanishes in either prescription A_1 or A_2, since the classical theory is conformally invariant, so the prescription is not required per se. Furthermore, in previous calculations, we swept under the rug terms that have negative powers of the mass m. The prescription cancels such infrared divergences, and makes the anomaly well-defined wrt them.[7]

At this point, we would like to mention that while we were working on this prescription, [64] came out, which addressed the issue of isolating the conformal anomaly of a non-conformally coupled scalar (which we discuss in the next section). However, they perform the calculation using linearised gravity in perturbation theory. We will push this prescription further and use it in the context of a spin-1 gauge field in a future section.

Conformal anomaly of the non-conformally coupled scalar

This is where the prescription in Eq. (2.81) and Eq. (2.82) becomes relevant, as it allows the separation of the anomalous part of the TEMT. The results here are important as they model pions.

First, we have, from Eq. (2.12),

$$\langle g^{(d)}_{\mu\nu} T^{\mu\nu} \rangle = \frac{1}{2880\pi^2} \Bigg[\frac{3}{2} W^2 - \frac{1}{2} E_4 + \frac{5}{2} (1-6\eta)^2 R^2 + \left(10 (1-6\eta)^2 - 1 - 15 (1-6\eta)^2 \Delta_\epsilon \right) \Box R \Bigg]. \tag{2.84}$$

Next, we also compute

$$g^{(4)}_{\mu\nu} \langle T^{\mu\nu} \rangle = \frac{1}{2880\pi^2} \Bigg[- 15 (1-6\eta)^2 \Delta_\epsilon \Box R \Bigg]. \tag{2.85}$$

$$\langle g^{(4)}_{\mu\nu} T^{\mu\nu} \rangle = \frac{1}{2880\pi^2} \Bigg[\frac{3}{2} W^2 - \frac{1}{2} E_4 + \frac{5}{2} (1-6\eta)^2 R^2 + \left(30\eta - 6 - 15 (1-6\eta)^2 \Delta_\epsilon \right) \Box R \Bigg], \tag{2.86}$$

[7] We further note that no regularisation is needed for terms that have inverse powers of mass m, c.f. Eq. (2.67), where the s-integral is discussed.

We thus find that $g^{(4)}_{\mu\nu}\langle T^{\mu\nu}\rangle$ only contains the divergent part of the coefficient of $\Box R$. Furthermore, we note that $\langle g^{(d)}_{\mu\nu}T^{\mu\nu}\rangle$ and $\langle g^{(4)}_{\mu\nu}T^{\mu\nu}\rangle$ only differ by a constant factor in the coefficient of $\Box R$.

Isolating the anomaly via the prescriptions in Eq. (2.81) and Eq. (2.82), we have

$$A_1^{\rm NCCS} = \frac{1}{2880\pi^2}\bigg[-\frac{3}{2}W^2+\frac{1}{2}E_4-\frac{5}{2}\left(1-6\eta\right)^2R^2-\left(10\left(1-6\eta\right)^2-1\right)\Box R\bigg], \tag{2.87}$$

$$A_2^{\rm NCCS} = \frac{1}{2880\pi^2}\bigg[-\frac{3}{2}W^2+\frac{1}{2}E_4-\frac{5}{2}\left(1-6\eta\right)^2R^2-\left(30\eta-6\right)\Box R\bigg], \tag{2.88}$$

The 2 prescriptions give the same result except for the coefficient of $\Box R$. $A_2^{\rm NCCS}$ matches the results of Birrell and Davies [60]. We also note that our results match those in [64] calculated using linearised gravity in perturbation theory.

Note that the physicality of the conformal anomaly can be established by showing that it possesses certain properties, such as finiteness, flow-independence and scheme-independence. This is discussed briefly in Chapter 3.

2.1.3 Effective action picture

In this section, we discuss an alternative method for obtaining the conformal anomaly. It relies on the calculation of the effective action, treating curved spacetime as a background gravitational field [65]. We follow largely the method described in [60]. This is not original work per se, and is presented here as it nicely complements and provides insights into the calculation done in the previous section.

We start with some definitions: The effective action $\mathcal{W}$ is obtained from the generating functional $\mathcal{Z}$ via

$$e^{i\mathcal{W}} = \mathcal{Z}[0] = \int \mathcal{D}\phi\, e^{i\mathcal{S}}, \tag{2.89}$$

where the zero in $\mathcal{Z}[0]$ indicates that all sources for the quantum fields are set to zero, and the matter action $\mathcal{S}$ for a massive scalar field is given by

$$\mathcal{S} = \int d^dx(-g(x))^{-\frac{1}{2}}\left[\frac{1}{2}(\nabla_\mu\phi)^2-\frac{1}{2}m^2\phi^2-\frac{1}{2}\eta R\phi^2\right]$$

$$= \int d^d x (-g(x))^{-\frac{1}{2}} \frac{1}{2}\phi \left[-\Box_x - m^2 - \eta R\right] \phi. \tag{2.90}$$

We further define

$$K_{xy} = (\Box_x + m^2 + \eta R)\, \delta^d(x-y), \tag{2.91}$$

$$i\, G_{\rm F}(x,y) = \langle \phi(x)\phi(y)\rangle, \tag{2.92}$$

such that

$$(\Box_x + m^2 + \eta R)\, G_{\rm F}(x,y) = -(-g(y))^{-\frac{1}{2}} \delta^d(x-y). \tag{2.93}$$

Thus, we can write K_{xy} in terms of the Green's function $G_{\rm F}(x,y)$ as

$$K^{-1}_{xy} = -G_{\rm F}(x,y). \tag{2.94}$$

Evaluating the generating functional, we have

$$\begin{aligned} e^{i\mathcal{W}} = \mathcal{Z}[0] &\propto (\det K)^{-\frac{1}{2}} \\ &= (\det(-G_{\rm F}))^{\frac{1}{2}} \\ &= \exp\left[\frac{1}{2}\mathrm{tr}\ln(-G_{\rm F})\right], \end{aligned} \tag{2.95}$$

where the constant of proportionality is metric-independent and can thus be ignored in what follows. So, we have that

$$\mathcal{W} = -\frac{i}{2}\mathrm{tr}\ln(-G_{\rm F}). \tag{2.96}$$

The trace of an operator M is given by

$$\mathrm{tr}\, M = \int d^d x (-g(x))^{\frac{1}{2}} \langle x|M|x\rangle. \tag{2.97}$$

From Eq. (2.94), we deduce that, in operator form,

$$G_{\rm F} = -i\int_0^\infty e^{-iKs}\mathrm{d}s, \tag{2.98}$$

since K has a small negative imaginary part due to $m^2 \to m^2 - i\epsilon$. To get $\ln(-G_{\rm F})$

rather than $G_{\rm F}$ itself, consider

$$\int_{\Lambda}^{\infty} e^{-iKs}(is)^{-1}i\mathrm{d}s = -\mathrm{Ei}(-i\Lambda K)$$
$$= -\gamma - \ln(i\Lambda K) + \mathcal{O}(\Lambda), \tag{2.99}$$

where $\mathrm{Ei}(x)$ is the exponential integral, given by

$$\mathrm{Ei}\,(x) = -\int_{-x}^{\infty} \frac{\mathrm{e}^{-t}}{t}\mathrm{d}t. \tag{2.100}$$

Taking the limit $\Lambda \to 0$, and discarding any terms that are metric-independent, we have

$$-\ln K = \ln(-G_{\rm F}) = \int_{0}^{\infty} e^{-iKs}(is)^{-1}i\mathrm{d}s. \tag{2.101}$$

Using Eq. (2.96), we obtain

$$\mathcal{W} = -\frac{i}{2}\int d^dx(-g(x))^{\frac{1}{2}}\int_0^{\infty} i\,\mathrm{d}s\,(is)^{-1}\langle x|e^{-iKs}|x\rangle. \tag{2.102}$$

Finding the effective Lagrangian $L_{\rm eff}$ defined by

$$\mathcal{W} = \int d^dx(-g(x))^{-\frac{1}{2}}L_{\rm eff}(x), \tag{2.103}$$

now comes down to finding $\langle x|e^{-iKs}|x\rangle$.

Using Eq. (2.98), one has, after introducing the states,

$$G_{\rm F}(x,x') = -i\int_0^{\infty}\langle x|e^{-iKs}|x'\rangle\,\mathrm{d}s, \tag{2.104}$$

which, using Eq. (2.41) in Sec. 2.1.2, identifies

$$\langle x|e^{-iKs}|x'\rangle = \Delta^{\frac{1}{2}}(x,x')\,(4\pi)^{-\frac{d}{2}}\,i\,(is)^{-\frac{d}{2}}\,\exp\left[-im^2s + \frac{\sigma}{2is}\right]\,\Omega(x,x';is). \tag{2.105}$$

Substituting the above into the effective action in Eq. (2.102), we finally get

$$\mathcal{W} = \int d^dx(-g(x))^{-\frac{1}{2}}\,\frac{i}{2}\lim_{x'\to x}\left[\frac{\Delta(x,x')}{(4\pi)^{\frac{d}{2}}}\int_0^{\infty}\mathrm{d}s(is)^{-1-\frac{d}{2}}\right.$$
$$\left.\times\exp\left(-im^2s + \frac{\sigma}{2is}\right)\,\Omega(x,x';is)\right]$$

$$= \int d^d x (-g(x))^{-\frac{1}{2}} L_{\text{eff}}(x), \tag{2.106}$$

which means that

$$L_{\text{eff}}(x) = \frac{1}{2} \lim_{x' \to x} \left[\frac{\Delta(x,x')}{(4\pi)^{\frac{d}{2}}} \sum_{j=0}^{\infty} a_j(x,x') \int_0^{\infty} i\,\mathrm{d}s (is)^{-1-\frac{d}{2}+j} \exp\left(-im^2 s + \frac{\sigma}{2is}\right) \right]. \tag{2.107}$$

We work in $d = 4 - 2\epsilon$ dimensions, and take the limit $x' \to x$, such that

$$L_{\text{eff}}(x) = \frac{1}{2(4\pi)^{\frac{d}{2}}} \sum_{j=0}^{\infty} a_j(x) \int_0^{\infty} i\,\mathrm{d}s\,(is)^{-1-\frac{d}{2}+j}\, e^{-im^2 s}, \tag{2.108}$$

where $a_j(x) \equiv a_j(x,x')$. One can identify the regulator in dim reg to be $\rho_{\text{DR}} = \frac{1}{(4\pi i s)^{-\epsilon}}$ [59]. As done in Sec. 2.1.2, the integral can be evaluated by analytically continuing s to the complex plane. The result is

$$L_{\text{eff}}(x) = \frac{1}{2(4\pi)^{\frac{d}{2}}} \sum_{j=0}^{\infty} a_j(x) \frac{\Gamma(j-\frac{d}{2})}{(m^2)^{j-\frac{d}{2}}}. \tag{2.109}$$

We send $m \to 0$ in Eq. (2.107), and determine any UV divergent contribution that remains. This corresponds to $j = 2$.

Using $d = 4 - 2\epsilon$, we have[8]

$$\mathcal{W}_{\text{div}} = \frac{\Delta_\epsilon}{2(4\pi)^2} \int \mathrm{d}^d x\,(-g(x))^{\frac{1}{2}}\, a_2(x), \tag{2.110}$$

where $\mathcal{W}_{\text{div}}$ corresponds to the UV-divergent part of the effective action $\mathcal{W}$, and the shorthand Δ_ϵ has been defined in Eq. (2.71). Using Eq. (2.47), and the results in App. B.3 and App. B.4, we have

$$\begin{aligned} \langle T^{\mu}{}_{\mu} \rangle_{\text{div}} &= \frac{2}{(-g)^{\frac{1}{2}}} g^{\mu\nu} \frac{\delta \mathcal{W}_{\text{div}}}{\delta g^{\mu\nu}} \\ &= \frac{(-\epsilon)\Delta_\epsilon}{(4\pi)^2} \left[\frac{1}{2} \left(\frac{1}{6} - \eta \right)^2 \left(-R^2 - 4 \frac{(d-1)}{(-2\epsilon)} \Box R \right) \right. \\ &\quad \left. - \frac{1}{120} (W^2 - \frac{2}{3} \Box R) + \frac{1}{360} E_{\text{d}} \right]. \end{aligned} \tag{2.111}$$

[8] We note that we have added the factor $\mu^{2\epsilon}$, as was done in Sec. 2.1.2 and [60], in order to fix the mass dimension of $L_{\text{eff}}(x)$ to be exactly 4.

In [60], the coefficients are expressed using a different basis (Equation (6.124)). Going to that basis (and separating the $\Box R$ term because it is the only divergent term for a general η), we have

$$\begin{aligned}\langle T^{\mu}{}_{\mu}\rangle_{\rm div} =& -\frac{1}{(4\pi)^2}\left[-\frac{1}{180}W^2-\frac{1}{180}\left(R^{\alpha\beta}R_{\alpha\beta}-\frac{1}{3}R^2\right)-\frac{1}{2}\left(\eta-\frac{1}{6}\right)^2R^2\right]\\ &-\frac{1}{(4\pi)^2}\left[\frac{1}{180}+(3-2\epsilon)\,\Delta_\epsilon\left(\eta-\frac{1}{6}\right)^2\right]\Box R. \end{aligned} \tag{2.112}$$

Conformal anomaly for a CCS

For conformal invariance, the *total* TEMT is zero, i.e.

$$\langle T^{\mu}{}_{\mu}\rangle|_{m=0,\,\eta=\frac{1}{6}} \equiv \langle T^{\mu}{}_{\mu}\rangle_{\rm ren}+\langle T^{\mu}{}_{\mu}\rangle_{\rm div}=0, \tag{2.113}$$

where the subscript 'ren' means renormalised. Therefore, for a CCS, we have that

$$\langle T^{\mu}{}_{\mu}\rangle_{\rm ren}=\frac{1}{2880\pi^2}\left[-W^2-\left(R^2_{\alpha\beta}-\frac{1}{3}R^2\right)+\Box R\right], \tag{2.114}$$

which is the result obtained in [60] upon using the conformal coupling.

Furthermore, $\langle T^{\mu}{}_{\mu}\rangle_{\rm ren}$ is equivalent to the conformal anomaly A_1 (and A_2 since they are equal in the conformal limit) calculated using Eq. (2.78).

Conformal anomaly for a NCCS

Here, we no longer have the condition in Eq. (2.113), as the theory is non conformally invariant classically. Instead, we have, using Eq. (2.12),

$$\langle T^{\mu}{}_{\mu}\rangle|_{m=0} \equiv \langle T^{\mu}{}_{\mu}\rangle_{\rm ren}+\langle T^{\mu}{}_{\mu}\rangle_{\rm div}=\left(3\eta-\frac{1}{2}\right)\Box\langle\phi^2\rangle, \tag{2.115}$$

where the last equality is obtained by substituting $d=4$ into Eq. (2.13). This is done as we want to remove the classical violation of the non-vanishing TEMT. Rearranging the above equation, we have

$$\langle T^{\mu}{}_{\mu}\rangle_{\rm ren}=\frac{1}{2880\pi^2}\Bigg[-W^2-\left(R^2_{\alpha\beta}-\frac{1}{3}R^2\right)-90\left(\eta-\frac{1}{6}\right)^2R^2$$

$$+\left(1-10\,(1-6\eta)^2\right)\Box R\Bigg]. \tag{2.116}$$

All the coefficients match those in [60], except the $\Box R$ coefficient. The result also matches the anomaly A_1 calculated in the previous section in Eq. (2.87).

On the other hand, if we use $d = 4 - 2\epsilon$ when calculating the classical violation of the TEMT, we have

$$\langle T^{\mu}{}_{\mu}\rangle|_{m=0} = \frac{1}{2}\Bigg[\,(6\eta-1)+\epsilon\,(1-4\eta)\,\Bigg]\Box\langle\phi^2\rangle, \tag{2.117}$$

which then leads to

$$\begin{aligned}\langle T^{\mu}{}_{\mu}\rangle_{\rm ren} =& \frac{1}{2880\pi^2}\Bigg[-W^2-\left(R^2_{\alpha\beta}-\frac{1}{3}R^2\right)-90\left(\eta-\frac{1}{6}\right)^2R^2\\ &+(6-30\eta)\,\Box R\Bigg],\end{aligned} \tag{2.118}$$

which now matches A_2 in Eq. (2.88) and the result in [60].

In the next sections, we will focus solely on the De-Witt Schwinger technique, and evaluate the VEV of the TEMT directly, since the effective action method might lead to confusion about which value of d to use when there is no conformal invariance at the classical level.

2.2 Spin-1 Gauge field

In this section, we will apply the heat kernel technique to the spin-1 gauge field. We will first focus on the result in the Feynman gauge, and then generalise the results to a general gauge, since the calculations are more involved in that case.

2.2.1 Generalities

Since we need to provide the spin-1 gauge field A_μ with a mass m to be able to use the Schwinger-De Witt technique, we use the Higgs mechanism [7, 8]. Consider a (charged) massive complex scalar field $\phi = \varphi\, e^{i\chi}$ with a quartic potential, coupled

to the gauge field. The Lagrangian is given by[9]

$$\mathcal{L} = -\frac{1}{4}F_{\mu\nu}F^{\mu\nu} + \frac{1}{2}(D_\mu\phi)^\dagger(D^\mu\phi) - \lambda(\phi^\dagger\phi - \Phi_0^2)^2, \tag{2.119}$$

where $D_\mu = \partial_\mu + iQA_\mu$ is the covariant derivative (different from ∇_μ, which couples to the background gravitational field) and Φ_0 is the VEV of the Higgs field φ.

In curved space, assuming a symmetric metric tensor $g_{\mu\nu} = g_{\nu\mu}$, the Maxwell tensor $F_{\mu\nu}$ written with lower indices is equivalent to the one in flat space, i.e.

$$F_{\mu\nu} \equiv \nabla_\mu A_\nu - \nabla_\nu A_\mu = \partial_\mu A_\nu - \partial_\nu A_\mu. \tag{2.120}$$

Note that with upper indices, a similar relation does not hold.

The Lagrangian in Eq. (2.119) is gauge invariant [66] provided the Stückelberg field χ also transforms under a gauge transformation, i.e.

$$\begin{aligned} A_\mu &\to A_\mu - \partial_\mu\alpha, \\ \chi &\to \chi + Q\alpha. \end{aligned} \tag{2.121}$$

In what follows, we will often suppress the explicit indices, and use the following conventions:

$$\begin{aligned} F^{\mu\nu}F_{\mu\nu} &\equiv F^2, \\ A^\mu A_\mu &\equiv A^2, \end{aligned} \tag{2.122}$$

etc.

Expanding the complex scalar ϕ into φ and χ, we have

$$\mathcal{L} = -\frac{1}{4}F^2 + \frac{1}{2}\varphi^2(QA_\mu + \partial_\mu\chi)^2 + \frac{1}{2}(\partial_\mu\varphi)^2 - \lambda(\varphi^2 - \Phi_0^2)^2. \tag{2.123}$$

If we now take the Higgs field φ to be arbitrarily massive, i.e. $\lambda \to \infty$, its dynamics can be neglected and the field can be considered to be frozen at its VEV Φ_0. The

[9] In curved spacetime, all partial derivatives ∂_μ are promoted to covariant derivatives wrt the background gravitational field ∇_μ. However, for scalar fields, $\nabla_\mu\phi \equiv \partial_\mu\phi$.

resulting theory then becomes

$$\mathcal{L} = -\frac{1}{4}F^2 + \frac{1}{2}m^2\left(A_\mu + \frac{\partial_\mu\chi}{m}\right)^2, \tag{2.124}$$

after redefining the Stückelberg field, $\chi \to \frac{\chi}{\Phi_0}$, and using $m \equiv \Phi_0 Q$. The Lagrangian is still gauge invariant, under the transformations in Eq. (2.121).

We now fix the gauge by choosing the gauge-fixing function G to be

$$G = \frac{1}{\sqrt{\xi}}\left(\nabla_\mu A^\mu - \xi m\chi\right). \tag{2.125}$$

Fixing the gauge in this way (R_ξ gauge) is useful because it decouples the gauge field A_μ from the Stückelberg field χ. Following the Faddeev-Popov procedure [67], the full Lagrangian, including ghost fields c and $\bar{c}$ then becomes

$$\begin{aligned}\mathcal{L} =& -\frac{1}{4}F^2 + \frac{1}{2}m^2A^2 - \frac{1}{2\xi}(\nabla\cdot A)^2 \\ &+ \frac{1}{2}(\partial_\mu\chi)^2 - \frac{1}{2}\xi m^2\chi^2 \\ &+ \partial_\mu\bar{c}\partial^\mu c - \xi m^2\bar{c}c.\end{aligned} \tag{2.126}$$

In this section, we will focus on the gauge field part of this action, i.e. the first line of Eq. (2.126). In any case, the rest of the contributions correspond to scalar fields and have already been calculated in the previous section. Note that the mass of the scalar Stückelberg field and the ghost field is ξm^2 if the photon has mass m^2.

Note that while the Stückelberg field and ghost fields are free fields in the sense that they don't couple with the other matter fields, they still couple to the background gravitational field. So, they give non-zero contributions to the VEV of the TEMT, and hence affect the conformal anomalies.

Therefore, the action for a spin-1 massive gauge field (neglecting ghost fields and Stückelberg field) with gauge fixing can be written as

$$\mathcal{S} = \int \mathrm{d}^d x\sqrt{-g}\left[-\frac{1}{4}F_{\mu\nu}F^{\mu\nu} + \frac{1}{2}m^2A^\mu A_\mu - \frac{1}{2\xi}\left(\nabla\cdot A\right)^2\right], \tag{2.127}$$

The equation of motion (EoM) is

$$\nabla_\mu F^{\mu\nu} + m^2 A^\nu + \frac{1}{\xi}\nabla^\nu \left(\nabla \cdot A\right) = 0. \tag{2.128}$$

To obtain the above, we have used the symmetry of the metric tensor $g_{\mu\nu}$.

It is useful to recast the EoM as

$$\Box A^\lambda + m^2 A^\lambda + \left(\frac{1}{\xi} - 1\right)\nabla^\lambda \left(\nabla \cdot A\right) + R^{\lambda\alpha} A_\alpha = 0, \tag{2.129}$$

where $R^{\lambda\alpha}$ is the Ricci tensor, and $\Box \equiv \nabla_\mu \nabla^\mu$.

Taking a covariant derivative of the EoM, it can be shown that

$$\left(\Box + \xi m^2\right)\left(\nabla \cdot A\right) = 0. \tag{2.130}$$

This indicates that $\nabla \cdot A$ acts as a scalar field of mass ξm^2.

The EMT and TEMT for a spin-1 gauge field are given by [68],

$$\begin{aligned} T_{\mu\nu} = {} & \frac{g_{\mu\nu}}{4}F^2 - \frac{g_{\mu\nu}}{2}m^2 A^2 + m^2 A_\mu A_\nu - F_{\alpha\mu}F^\alpha{}_\nu \\ & + \frac{1}{\xi}\Bigg[\frac{g_{\mu\nu}}{2}\left(\nabla \cdot A\right)^2 - \nabla_\mu A_\nu \left(\nabla \cdot A\right) - \nabla_\nu A_\mu \left(\nabla \cdot A\right) + \nabla_\mu \left(A_\nu \nabla \cdot A\right) \\ & + \nabla_\nu \left(A_\mu \nabla \cdot A\right) - g_{\mu\nu}\nabla^\lambda \left(A_\lambda \nabla \cdot A\right)\Bigg], \end{aligned} \tag{2.131}$$

$$T^\mu{}_\mu = \left(\frac{d}{4} - 1\right)F^2 + \left(1 - \frac{d}{2}\right)m^2 A^2 + \frac{2-d}{\xi}\nabla_\lambda \left(A^\lambda \nabla \cdot A\right) + \frac{d-4}{2\xi}\left(\nabla \cdot A\right)^2, \tag{2.132}$$

respectively.

As in the scalar field case, to calculate the VEV of the TEMT, we will require the two-point function of the gauge field, $\langle A_\mu(x) A_{\nu'}(x')\rangle$, and derivatives thereof, and this is discussed in the next section.

2.2.2 De-Witt Schwinger technique in the Feynman gauge $\xi = 1$

We first focus on the calculation of $\langle A_\mu(x) A_{\nu'}(x') \rangle$ in the Feynman gauge $\xi = 1$, as the computation simplifies drastically in this limit. In fact, this is how this calculation is performed in the literature all the time [69–71].

We can express $\langle A_\mu(x) A_{\nu'}(x') \rangle$ in terms of the Green's function $D_{\mathrm{F},\mu\nu'}(x,x')$ of the EoM operator in Eq. (2.129):

$$iD_{\mathrm{F},\mu\nu'}(x,x') = \langle A_\mu(x) A_{\nu'}(x') \rangle, \tag{2.133}$$

$$\left[g_{\mu\rho} \Box_x + R_{\mu\rho} + m^2 g_{\mu\rho} \right] D_{\mathrm{F}}^{\rho\nu'}(x,x') = (-g(x))^{-\frac{1}{2}} g_\mu{}^{\nu'} \, \delta^{(n)}(x-x'). \tag{2.134}$$

In what follows, we will sometimes suppress the spacetime dependence, and it should be clear from context what they are, for example,

$$\langle A_\mu A_{\nu'} \rangle \equiv \langle A_\mu(x) A_{\nu'}(x') \rangle. \tag{2.135}$$

This time, unlike in the scalar field case, we introduce states that have Lorentz indices, in order to move to an operator equation. This becomes necessary due to the $R_{\mu\rho} D_{\mathrm{F}}^{\rho\nu'}(x,x')$ term. We define the states $|x_\mu\rangle$ that satisfy

$$\hat{R}|x_\mu\rangle = R^\alpha{}_\mu |x_\alpha\rangle. \tag{2.136}$$

We can express the Green's function in terms of the heat kernel $\mathcal{G}^{\rho\nu'}(x,x';is)$, using Schwinger-DeWitt point-splitting method as before [14]. We do not present the details here, as it follows through in exactly the same way as in the scalar field in the previous section, which was discussed in great detail.

The result is

$$(-g(x))^{\frac{1}{4}} D_{\mathrm{F}}^{\rho\nu'}(x,x') (-g(x'))^{\frac{1}{4}} = i \int_0^\infty \mathrm{d}s \, \mathrm{e}^{-im^2 s} \, \mathcal{G}^{\rho\nu'}(x,x';is) \,, \tag{2.137}$$

where $\mathcal{G}^{\rho\nu'}(x,x';is)$ satisfies the 'Schrödinger equation'

$$i\partial_s \mathcal{G}^{\rho\nu'}(x,x';is) = (g^\rho{}_\lambda \Box + R^\rho{}_\lambda) \, \mathcal{G}^{\lambda\nu'}(x,x';is) \,, \tag{2.138}$$

with boundary condition

$$\mathcal{G}^{\rho\nu'}(x,x';0) = g^{\rho\nu'}\delta(x-x'). \tag{2.139}$$

We solve the differential equation using the Ansatz

$$\mathcal{G}^{\rho\nu'}(x,x';is) = \frac{i}{(4\pi is)^{\frac{d}{2}}} D^{\frac{1}{2}} \mathrm{e}^{\frac{\sigma}{2is}}\, \Omega^{\rho\nu'}(x,x';is), \tag{2.140}$$

where the quantities σ and D are exactly the same ones that were defined in Eq. (2.29) and Eq. (2.30) respectively. Substituting this into the differential equation, we find that $\Omega^{\rho\nu'}(x,x';is)$ satisfies

$$\partial_s \Omega^{\mu\nu'} = -iR^{\mu}{}_{\lambda}\Omega^{\lambda\nu'} - iD^{-\frac{1}{2}}\nabla^{\lambda}\nabla_{\lambda}\left(D^{\frac{1}{2}}\Omega^{\mu\nu'}\right) - \frac{\nabla_{\lambda}\sigma\,\nabla^{\lambda}\Omega^{\mu\nu'}}{s}. \tag{2.141}$$

with the boundary condition

$$\Omega^{\mu\nu'}(x,x';0) = g^{\mu\nu'}\delta(x-x'). \tag{2.142}$$

At this point, it is useful to replace D by the van Vleck-Morette determinant $\Delta \equiv g^{-\frac{1}{2}} D g'^{-\frac{1}{2}}$. Since $\nabla_{\lambda} g = 0$, we have that

$$\partial_s \Omega^{\mu\nu'} = -iR^{\mu}{}_{\lambda}\Omega^{\lambda\nu'} - i\Delta^{-\frac{1}{2}}\nabla^{\lambda}\nabla_{\lambda}\left(\Delta^{\frac{1}{2}}\Omega^{\mu\nu'}\right) - \frac{\nabla_{\lambda}\sigma\,\nabla^{\lambda}\Omega^{\mu\nu'}}{s}. \tag{2.143}$$

We further express $\Omega^{\rho\nu'}(x,x';is)$ as a power series in (is),

$$\Omega^{\rho\nu'}(x,x';is) = \sum_{j=0}^{\infty} a_j^{\rho\nu'}(x,x')(is)^j. \tag{2.144}$$

From Eq. (2.143) and Eq. (2.144), one can derive the recursion relations on the $a_j^{\mu\nu'}(x,x')$ coefficients in $\Omega^{\rho\nu'}(x,x';is)$ by matching powers of s. They are

$$\nabla_{\lambda} a_0^{\mu\nu'}\,\nabla^{\lambda}\sigma = 0, \tag{2.145}$$

$$\nabla^{\lambda}\sigma\,\nabla_{\lambda} a_{n+1}^{\mu\nu'} + (n+1)\,a_{n+1}^{\mu\nu'} = -\Delta^{-\frac{1}{2}}\nabla^{\lambda}\nabla_{\lambda}\left(\Delta^{\frac{1}{2}} a_n^{\mu\nu'}\right) - R^{\mu}{}_{\lambda} a_n^{\lambda\nu'}, \qquad n \geq 0. \tag{2.146}$$

The boundary condition in Eq. (2.142) translates to

$$a_0^{\mu\nu'}(x,x') = g^{\mu\nu'}. \tag{2.147}$$

Putting all together, we have that

$$D_{\rm F}^{\rho\nu'}(x,x') = i\Delta^{\frac{1}{2}}(x,x')\,(4\pi)^{-\frac{d}{2}}\sum_{j=0}^{\infty}\int_0^\infty i\,{\rm d}s\,(is)^{j-\frac{d}{2}}\,\exp\left[-im^2 s+\frac{\sigma}{2is}\right]\,a_j^{\rho\nu'}(x,x')\,. \tag{2.148}$$

The only ingredient needed now are the coincident limits of $a_j^{\rho\nu'}(x,x')$, which are discussed in the next section.

Coincident limits of $a_j^{\mu\nu'}(x,x')$ for the spin-1 gauge field

We denote the coincident limit of $a_j^{\mu\nu'}(x,x')$ by

$$\lim_{x'\to x} a_j^{\mu\nu'}(x,x') \equiv \left[a_j^{\mu\nu'}(x,x')\right] \equiv a_j^{\mu\nu}(x)\,. \tag{2.149}$$

Using the recursion relations in Eqs. (2.145) and (2.146), and the identities in App. C.6, one can obtain the coincident limits of the $a_j^{\mu\nu}(x)$ coefficients. They are

$$a_0^{\mu\nu}(x) = g^{\mu\nu}, \tag{2.150}$$

$$a_1^{\mu\nu}(x) = \frac{1}{6}R\,g^{\mu\nu} - R^{\mu\nu}, \tag{2.151}$$

$$a_1{}^{\mu}{}_{\mu}(x) = \left(\frac{d}{6}-1\right)R, \tag{2.152}$$

$$\begin{aligned} a_2^{\mu\nu}(x) = &\left[\frac{1}{72}R^2 - \frac{1}{180}R_{\alpha\beta}^2 - \frac{1}{30}\Box R + \frac{1}{180}R_{\alpha\beta\lambda\sigma}^2\right]g^{\mu\nu} \\ &- \frac{1}{12}R^{\mu\alpha\beta\gamma}R^{\nu}{}_{\alpha\beta\gamma} - \frac{1}{6}RR^{\mu\nu} + \frac{1}{2}R^{\mu\lambda}R_{\lambda}{}^{\nu} + \frac{1}{6}\Box R^{\mu\nu}, \end{aligned} \tag{2.153}$$

$$a_2{}^{\mu}{}_{\mu}(x) = \left[\frac{(d-12)}{72}R^2 + \frac{(d-15)}{180}R_{\mu\nu\alpha\beta}^2 - \frac{(d-90)}{180}R_{\alpha\beta}^2 - \frac{(d-5)}{30}\Box R\right]. \tag{2.154}$$

For coincident limits involving 1 derivative, we have[10]

$$\left[a_1{}^{\mu\nu'}{}_{;}{}^{\beta}\right] = \frac{1}{12}R_{;}{}^{\beta}g^{\mu\nu} + \frac{1}{6}R^{\beta\lambda\mu\nu}{}_{;\lambda} - \frac{1}{2}R^{\mu\nu}{}_{;}{}^{\beta} \tag{2.155}$$

[10]From the symmetry of the two-point function, we do not need primed derivatives. We have of course explicitly verified the equivalence of the primed derivative to the unprimed derivative using Synge's theorem.

Taking derivatives of the above, and contracting indices, one has

$$\left[a_1{}^{\mu\nu'}{}_{;\mu}\right]_{;\nu} = -\frac{1}{12}\Box R \tag{2.156}$$

$$\left[a_1{}^{\mu\nu'}{}_{;\nu}\right]_{;\mu} = -\frac{1}{4}\Box R \tag{2.157}$$

$$\left[a_1{}^{\mu}{}_{\mu';}{}^{\nu}\right]_{;\nu} = \frac{(d-6)}{12}\Box R \tag{2.158}$$

For coincident limits involving 2 derivatives, we have

$$\left[a_1{}^{\mu\nu'}{}_{;}{}^{\beta\alpha}\right] = \frac{1}{3}\Bigg[\frac{1}{36}R^{\beta\alpha}g^{\mu\nu}R + \frac{1}{4}RR^{\mu\nu\beta\alpha} - g^{\mu\nu}\left[\Delta^{\frac{1}{2}}{}_{;}{}^{\lambda}{}_{\lambda}{}^{\beta\alpha}\right] - \left[g^{\mu\nu'}{}_{;}{}^{\lambda}{}_{\lambda}{}^{\beta\alpha}\right] - R^{\mu\nu}{}_{;}{}^{\beta\alpha}$$
$$- \frac{1}{2}R^{\mu}{}_{\lambda}R^{\lambda\nu\beta\alpha} + R^{\nu}{}_{\lambda}R^{\mu\lambda\alpha\beta}\Bigg] \tag{2.159}$$

$$\left[a_1{}^{\mu\nu'}{}_{;}{}^{\beta\alpha'}\right] = -\frac{1}{3}\Bigg[\frac{1}{36}R^{\beta\alpha}g^{\mu\nu}R + \frac{1}{4}RR^{\mu\nu\beta\alpha} - g^{\mu\nu}\left[\Delta^{\frac{1}{2}}{}_{;}{}^{\lambda}{}_{\lambda}{}^{\beta\alpha}\right] - \left[g^{\mu\nu'}{}_{;}{}^{\lambda}{}_{\lambda}{}^{\beta\alpha}\right] + \frac{1}{2}R^{\mu\nu}{}_{;}{}^{\beta\alpha}$$
$$- \frac{1}{2}R^{\mu}{}_{\lambda}R^{\lambda\nu\beta\alpha} + R^{\nu}{}_{\lambda}R^{\mu\lambda\alpha\beta} - \frac{1}{4}R_{;}{}^{\beta}g^{\mu\nu} - \frac{1}{2}R^{\beta\lambda\mu\nu}{}_{;\lambda}\Bigg] \tag{2.160}$$

$$\left[a_1{}^{\mu\nu'}{}_{;\mu\nu}\right] = \frac{1}{3}\left[\frac{11}{120}R^2_{\mu\nu\alpha\beta} - \frac{73}{60}R^2_{\mu\nu} - \frac{3}{10}\Box R + \frac{1}{4}R^2\right] \tag{2.161}$$

$$\left[a_1{}^{\mu\nu'}{}_{;\mu\nu'}\right] = -\frac{1}{3}\left[\frac{11}{120}R^2_{\mu\nu\alpha\beta} - \frac{73}{60}R^2_{\mu\nu} - \frac{1}{20}\Box R + \frac{1}{4}R^2\right] \tag{2.162}$$

$$\left[a_1{}^{\mu\nu'}{}_{;\nu\mu}\right] = \frac{11}{360}R^2_{\mu\nu\alpha\beta} + \frac{107}{180}R^2_{\mu\nu} - \frac{1}{10}\Box R - \frac{1}{12}R^2 \tag{2.163}$$

$$\left[a_1{}^{\mu\nu'}{}_{;\nu\mu'}\right] = -\frac{11}{360}R^2_{\mu\nu\alpha\beta} - \frac{107}{180}R^2_{\mu\nu} - \frac{3}{20}\Box R + \frac{1}{12}R^2 \tag{2.164}$$

$$\left[a_1{}^{\mu}{}_{\mu';}{}^{\nu}{}_{\nu}\right] = -\frac{(d-15)}{90}R^2_{\mu\nu\alpha\beta} + \frac{d}{90}R^2_{\mu\nu} + \frac{(d-5)}{15}\Box R \tag{2.165}$$

$$\left[a_1{}^{\mu}{}_{\mu';}{}^{\nu}{}_{\nu'}\right] = \frac{(d-15)}{90}R^2_{\mu\nu\alpha\beta} - \frac{d}{90}R^2_{\mu\nu} + \frac{(d-10)}{60}\Box R \tag{2.166}$$

In the above, we have sometimes kept coincident limits of $\Delta^{\frac{1}{2}}$ and $g^{\mu\nu'}$ involving 4 derivatives explicitly, as they are complicated. They are both given in App. C.6. Also, we have used Synge's theorem to calculate coincident limits involving primed indices.

Evaluation of condensates for the spin-1 gauge field

Since the gauge field carries a Lorentz index, there are more condensates here to evaluate than in the scalar field case. To find out which ones we need to calculate, we consider the EMT and TEMT in Eq. (2.131) and Eq. (2.132) respectively. There are 3 of them, which act as building blocks for others (by contracting with the appropriate metric tensor). They are $\langle A_\mu A_\nu \rangle$, $\langle \nabla_\beta \left((\nabla_\alpha A_\mu) A_\nu \right) \rangle$ and $\langle (\nabla_\alpha A_\mu) (\nabla_\beta A_\nu) \rangle$.[11]

We start with the simplest one, $\langle A^\mu A^\nu \rangle$, which are of course understood to be coincident. Using Eq. (2.133) and Eq. (2.148), we find that[12]

$$\begin{aligned} \langle A^\mu A^\nu \rangle &= -\int_0^\infty \mathrm{d}s\, e^{-im^2 s} \left(\frac{i}{(4\pi i s)^{\frac{d}{2}}} \sum_{j=0}^{\infty} a_j^{\mu\nu}(x) (is)^j \right) \\ &= -\frac{1}{(4\pi)^2} \frac{a_2^{\mu\nu}(x)}{m^2}, \end{aligned} \tag{2.167}$$

where only relevant terms have been kept. The above condensate always comes with a factor of m^2, which is why we have only kept the $j = 2$ term. Next, we have

$$\begin{aligned} \langle \nabla_\beta \left((\nabla_\alpha A^\mu) A^\nu \right) \rangle &= \nabla_\beta \left(\lim_{x' \to x} \nabla_\alpha \left[A^\mu(x) A^{\nu'}(x') \right] \right) \\ &= -\frac{1}{(4\pi)^2} \Delta_\epsilon \left[{a_1}^{\mu\nu'}{}_{;\alpha} \right]_{;\beta} \end{aligned} \tag{2.168}$$

where Δ_ϵ is defined in Eq. (2.71).

Finally, the last 'building block' condensate is given by

$$\begin{aligned} \langle (\nabla_\alpha A^\mu) (\nabla_\beta A^\nu) \rangle &= \lim_{x \to x'} \nabla_\alpha^{(x)} \nabla_\beta^{(x')} \langle A^\mu(x) A^{\nu'}(x') \rangle \\ &= -\frac{1}{(4\pi)^2} \Delta_\epsilon \left[\left[\Delta^{\frac{1}{2}}{}_{;\alpha\beta'} \right] a_1^{\mu\nu}(x) + \frac{\left[\sigma_{;\alpha\beta'}\right]}{2} a_2^{\mu\nu}(x) + \left[{a_1}^{\mu\nu'}{}_{;\alpha\beta'} \right] \right] \end{aligned} \tag{2.169}$$

where the coincident limits for $\Delta^{\frac{1}{2}}$ and σ are given in App. C.6. With all the building blocks in hand, we can start listing the different condensates that appear

[11] Note that instead of $\langle \nabla_\beta \left((\nabla_\alpha A_\mu) A_\nu \right) \rangle$, one could pick $\langle (\nabla_\alpha \nabla_\beta A_\mu) A_\nu \rangle$. Our choice is a little simpler.

[12] We switch to upper indices merely for convenience of writing the condensates.

in the VEV of the TEMT. With d-dimensional traces, we have

$$m^2\langle A_\mu A^\mu\rangle = \frac{1}{2880\pi^2}\left[11R^2_{\mu\nu\alpha\beta} - 86R^2_{\mu\nu} - 6\Box R + 20R^2\right], \tag{2.170}$$

$$\langle\nabla_\nu\left((\nabla\cdot A)\,A^\nu\right)\rangle = \frac{\Delta_\epsilon}{2880\pi^2}15\Box R, \tag{2.171}$$

$$\begin{aligned}\langle\left(\nabla_\mu A_\nu\right)\left(\nabla^\mu A^\nu\right)\rangle = \frac{\Delta_\epsilon}{2880\pi^2}\Bigg[&11\epsilon R^2_{\mu\nu\alpha\beta} + (180-86\epsilon)\,R^2_{\mu\nu} + (30+24\epsilon)\,\Box R\\ &- (30-20\epsilon)\,R^2\Bigg],\end{aligned} \tag{2.172}$$

$$\begin{aligned}\langle\left(\nabla_\mu A_\nu\right)\left(\nabla^\nu A^\mu\right)\rangle = \frac{\Delta_\epsilon}{2880\pi^2}\Bigg[&-\epsilon R^2_{\mu\nu\alpha\beta} + (180+\epsilon)\,R^2_{\mu\nu} + (30+6\epsilon)\,\Box R\\ &- \frac{5}{2}\,(12+\epsilon)\,R^2\Bigg],\end{aligned} \tag{2.173}$$

$$\langle(\nabla\cdot A)^2\rangle = \frac{1}{2880\pi^2}\left[-R^2_{\mu\nu\alpha\beta} + R^2_{\mu\nu} + 6\Box R - \frac{5}{2}R^2\right], \tag{2.174}$$

and for 4-dimensional traces, we have

$$g^{(4)}_{\mu\nu}\langle\nabla^\mu\left((\nabla\cdot A)\,A^\nu\right)\rangle = \frac{\Delta_\epsilon}{2880\pi^2}15\Box R, \tag{2.175}$$

$$g^{(4)}_{\mu\nu}\langle\left(\nabla^\mu A^\nu\right)\left(\nabla\cdot A\right)\rangle = 0, \tag{2.176}$$

$$\begin{aligned}g^{(4)}_{\mu\nu}\langle\left(\nabla^\alpha A^\mu\right)\left(\nabla_\alpha A^\nu\right)\rangle = \frac{\Delta_\epsilon}{2880\pi^2}\Bigg[&11\epsilon\,R^2_{\mu\nu\alpha\beta} + (180-86\epsilon)\,R^2_{\mu\nu} + (30-6\epsilon)\,\Box R\\ &- (30-20\epsilon)\,R^2\Bigg],\end{aligned} \tag{2.177}$$

$$g^{(4)}_{\mu\nu}\langle\left(\nabla^\mu A^\alpha\right)\left(\nabla_\alpha A^\nu\right)\rangle = \frac{\Delta_\epsilon}{2880\pi^2}\left[180R^2_{\mu\nu} + 30\Box R - 30R^2\right], \tag{2.178}$$

$$g^{(4)}_{\mu\nu}\langle\left(\nabla^\mu A^\alpha\right)\left(\nabla^\nu A_\alpha\right)\rangle = \frac{\Delta_\epsilon}{2880\pi^2}\left[180R^2_{\mu\nu} + (30+30\epsilon)\,\Box R - 30R^2\right]. \tag{2.179}$$

This completes the calculation of all the condensate terms required for the calculation of the conformal anomaly for the gauge field.

As in the scalar case, we have verified that using the EoM in Eq. (2.129), which can be recast as

$$\langle\left(\nabla_\lambda\nabla^\lambda A_\mu\right)A^\mu\rangle + R_{\mu\rho}\langle A^\mu A^\rho\rangle + m^2\langle A_\mu A^\mu\rangle = 0, \tag{2.180}$$

has no effect on the calculation. What's more, the result holds independent of

whether the trace is performed over the 4-dimensional metric tensor $g^{(4)}_{\mu\nu}$ or the d-dimensional metric tensor $g^{(d)}_{\mu\nu}$.

Calculation of the conformal anomaly for a spin-1 gauge field in the Feynman gauge

We can now start calculating the VEV of the TEMT, and they are given by

$$\langle g^{(4)}_{\mu\nu} T^{\mu\nu} \rangle_{\rm gf} = \frac{1}{2880\pi^2} \left[-32E_4 + 21W^2 + (6 - 30\Delta_\epsilon)\,\Box R + 5R^2 \right], \tag{2.181}$$

$$\langle g^{(d)}_{\mu\nu} T^{\mu\nu} \rangle_{\rm gf} = \frac{1}{2880\pi^2} \left[-32E_4 + 21W^2 + (36 - 30\Delta_\epsilon)\,\Box R + 5R^2 \right], \tag{2.182}$$

$$g^{(4)}_{\mu\nu} \langle T^{\mu\nu} \rangle_{\rm gf} = \frac{1}{2880\pi^2} (30 - 30\Delta_\epsilon)\,\Box R, \tag{2.183}$$

where we have used the subscript 'gf' to label the gauge field contribution. We can use the prescriptions in Eq. (2.81) and Eq. (2.82) to calculate the conformal anomaly, and they are given by

$$A_1^{\rm gf} = \frac{1}{2880\pi^2} \left[32E_4 - 21W^2 - 6\Box R - 5R^2 \right], \tag{2.184}$$

$$A_2^{\rm gf} = \frac{1}{2880\pi^2} \left[32E_4 - 21W^2 + 24\Box R - 5R^2 \right]. \tag{2.185}$$

Of course, the above results are not physical, since they don't include the other field components that are necessary for gauge invariance. We have the contributions from the ghost fields $c, \bar{c}$ and the Stückelberg field χ to add. We first consider adding only the ghost field contributions, and the corresponding quantities will be labelled with "gf+gh". We note that the contribution from the ghost fields simply correspond to that of NCCS field with $\eta = 0$, multiplied by -2, where the negative sign comes from the anti-commuting nature of ghost fields, and the factor of 2 comes from the fact that the (complex) ghost field can be regarded as two real scalar fields.

Thus, we have

$$\langle g^{(4)}_{\mu\nu} T^{\mu\nu} \rangle_{\rm gf+gh} = \frac{1}{2880\pi^2} \left[-31E_4 + 18W^2 + 18\Box R \right], \tag{2.186}$$

$$\langle g^{(d)}_{\mu\nu} T^{\mu\nu} \rangle_{\rm gf+gh} = \frac{1}{2880\pi^2} \left[-31E_4 + 18W^2 + 18\Box R \right], \tag{2.187}$$

$$g^{(4)}_{\mu\nu} \langle T^{\mu\nu} \rangle_{\rm gf+gh} = \frac{1}{2880\pi^2} 30\Box R. \tag{2.188}$$

We can again use the prescriptions in Eq. (2.81) and Eq. (2.82) to calculate the conformal anomaly, and they are given by

$$A_1^{\text{gf+gh}} = A_2^{\text{gf+gh}} = \frac{1}{2880\pi^2}\left[31E_4 - 18W^2 + 12\Box R\right]. \tag{2.189}$$

Some comments are in order. We first note that while there are no divergences in the coefficients in $\langle g^{(4)}_{\mu\nu}T^{\mu\nu}\rangle_{\text{gf+gh}}$, and hence $\langle g^{(d)}_{\mu\nu}T^{\mu\nu}\rangle_{\text{gf+gh}}$ as they are equal, $g^{(4)}_{\mu\nu}\langle T^{\mu\nu}\rangle_{\text{gf+gh}}$ is *not* zero. This is contrast to the scalar field case treated in the previous section where, whenever the divergences vanished in $\langle g^{(d)}_{\mu\nu}T^{\mu\nu}\rangle$ and $\langle g^{(4)}_{\mu\nu}T^{\mu\nu}\rangle$, so did $g^{(4)}_{\mu\nu}\langle T^{\mu\nu}\rangle$, c.f. Eq. (2.78) to Eq. (2.80).

We further note that Eq. (2.186) matches the result in [60], with an overall negative sign (which we can understand in terms of renormalisation of the effective action, c.f. Sec. 2.1.3). The results also agree with [72] and [73], which specify 2 different prescriptions for how the coefficient of $\Box R$ is obtained, and they correspond to the $\Box R$ coefficient that we have either directly in the TEMT in Eq. (2.186) or in the isolation of the anomaly in Eq. (2.189).

Therefore, the discrepancy regarding the coefficient of $\Box R$ can be traced back to whether the contribution $g^{(4)}_{\mu\nu}\langle T^{\mu\nu}\rangle_{\text{gf+gh}}$ should be included or not when the calculation is performed in the De-Witt-Schwinger point splitting method. We come back to this discussion in the next section in the context of gauge invariance.

For the sake of completeness, we also give the results when the contribution from the Stückelberg field is added. To indicate this, we assign a label "full" to the quantities below. Thus

$$\langle g^{(4)}_{\mu\nu}T^{\mu\nu}\rangle_{\text{full}} = \frac{1}{2880\pi^2}\left[-\frac{63}{2}E_4 + \frac{39}{2}W^2 + (12 - 15\Delta_\epsilon)\Box R + \frac{5}{2}R^2\right], \tag{2.190}$$

$$\langle g^{(d)}_{\mu\nu}T^{\mu\nu}\rangle_{\text{full}} = \frac{1}{2880\pi^2}\left[-\frac{63}{2}E_4 + \frac{39}{2}W^2 + (27 - 15\Delta_\epsilon)\Box R + \frac{5}{2}R^2\right], \tag{2.191}$$

$$g^{(4)}_{\mu\nu}\langle T^{\mu\nu}\rangle_{\text{full}} = \frac{1}{2880\pi^2}(30 - 15\Delta_\epsilon)\Box R. \tag{2.192}$$

We can again use the prescriptions for A_1 and A_2 to calculate the conformal anomaly, and they are given by

$$A_1^{\text{full}} = \frac{1}{2880\pi^2}\left[\frac{63}{2}E_4 - \frac{39}{2}W^2 + 3\Box R - \frac{5}{2}R^2\right], \tag{2.193}$$

$$A_2^{\text{full}} = \frac{1}{2880\pi^2}\left[\frac{63}{2}E_4 - \frac{39}{2}W^2 + 18\Box R - \frac{5}{2}R^2\right]. \tag{2.194}$$

2.2.3 De Witt-Schwinger technique in the general gauge

This section deals with solving for the two-point function of the gauge field with a general gauge parameter in curved spacetime. This generalises a calculation done by Shore for a non-Abelian gauge field [74].

The Schwinger-Dyson equation now becomes

$$iD_{\mathrm{F},\,\mu\nu'}(x,x') = \langle A_\mu(x) A_{\nu'}(x')\rangle, \tag{2.195}$$

$$\left[g_{\mu\rho}\,\Box_x + \left(\frac{1}{\xi} - 1\right)\nabla_\mu\nabla_\rho + R_{\mu\rho} + m^2 g_{\mu\rho}\right] D_{\mathrm{F}}^{\rho\nu'}(x,x') = (-g(x))^{-\frac{1}{2}} g_\mu{}^{\nu'}\,\delta^{(n)}(x-x'). \tag{2.196}$$

Following the same steps as in the previous section, we now have

$$(-g(x))^{\frac{1}{4}}\, D_{\mathrm{F}}^{\rho\nu'}(x,x')\,(-g'(x'))^{\frac{1}{4}} = i\int_0^\infty \mathrm{d}s\; \mathrm{e}^{-im^2 s}\,\mathcal{G}^{\rho\nu'}\,(x,x';is)\,, \tag{2.197}$$

as before, but instead of Eq. (2.138), we have the 'Schrödinger equation'

$$i\partial_s \mathcal{G}^{\rho\nu'}\,(x,x';is) = \left(g^\rho{}_\lambda\Box + R^\rho{}_\lambda + \left(\frac{1}{\xi} - 1\right)\nabla^\rho\nabla_\lambda\right)\mathcal{G}^{\lambda\nu'}\,(x,x';is)\,, \tag{2.198}$$

with boundary condition

$$\mathcal{G}^{\rho\nu'}\,(x,x';0) = g^{\rho\nu'}\,\delta\,(x-x')\,. \tag{2.199}$$

We now make the Ansatz for $\mathcal{G}^{\rho\nu'}\,(x,x';is)$,

$$\mathcal{G}^{\rho\nu'}\,(x,x';is) = \left(g^\rho{}_\lambda\Box + R^\rho{}_\lambda - \nabla^\rho\nabla_\lambda\right)\mathcal{H}^{\lambda\nu'}\,(x,x';is) + \nabla^\rho\nabla_\lambda\mathcal{H}^{\lambda\nu'}\left(x,x';\frac{is}{\xi}\right), \tag{2.200}$$

and define the operators

$$N^{\rho\lambda} \equiv g^{\rho\lambda}\Box + R^{\rho\lambda}, \tag{2.201}$$

$$P^{\rho\lambda} \equiv N^{\rho\lambda} - \nabla^\rho\nabla^\lambda. \tag{2.202}$$

Substituting the Ansatz for $\mathcal{G}^{\rho\nu'}\,(x,x';is)$ into the differential equation (2.198),

we have

$$P^{\mu\alpha}N_{\alpha}{}^{\lambda}\mathcal{H}_{\lambda}{}^{\nu'}(x,x';is)+\frac{1}{\xi}\nabla^{\mu}\nabla^{\lambda}N_{\lambda\alpha}\mathcal{H}^{\alpha\nu'}\left(x,x';\frac{is}{\xi}\right)=i\partial_s\left(P^{\mu\alpha}\,\mathcal{H}_{\alpha}{}^{\nu'}(x,x';is)\right)+i\partial_s\nabla^{\mu}\nabla^{\alpha}\mathcal{H}_{\alpha}{}^{\nu'}\left(x,x';\frac{is}{\xi}\right). \tag{2.203}$$

This equation is satisfied if

$$N^{\alpha\lambda}\mathcal{H}_{\lambda}{}^{\nu'}(x,x';is)=i\partial_s\mathcal{H}^{\alpha\nu'}(x,x';is), \tag{2.204}$$

with the boundary condition

$$N^{\mu\alpha}\mathcal{H}_{\alpha}{}^{\nu'}(x,x',0)=g^{\mu\nu'}\delta(x-x'). \tag{2.205}$$

Next, we define the Green's function $\bar{G}^{\lambda\nu'}$ and heat kernel $\bar{\mathcal{G}}^{\lambda\nu'}$ of the operator $N^{\mu\alpha}$.

$$N^{\mu\lambda}\bar{G}_{\lambda}{}^{\nu'}=g^{\mu\nu'}\delta(x-x'), \tag{2.206}$$

$$\bar{G}_{\lambda}{}^{\nu'}=i\int_0^{\infty}\mathrm{d}s\,\bar{\mathcal{G}}_{\lambda}{}^{\nu'}(x,x';is), \tag{2.207}$$

$$N^{\mu\lambda}\bar{\mathcal{G}}_{\lambda}{}^{\nu'}(x,x';is)=i\partial_s\bar{\mathcal{G}}^{\mu\nu'}(x,x';is). \tag{2.208}$$

From the form of the operator $N^{\mu\lambda}$ in Eq. (2.201), one can deduce the heat kernel $\bar{\mathcal{G}}^{\mu\nu'}(x,x';is)$ is the same as the one calculated in the Feynman gauge in section 2.2.2, cf. Eq. (2.138). The Green's function $\bar{G}^{\mu\nu'}$ is also the same, except that it is strictly massless here.

The solution to Eq. (2.204) is

$$\mathcal{H}_{\mu\nu'}(x,x';is)=\int\mathrm{d}^dz''\,(-g'')^{\frac{1}{2}}\,\bar{G}_{\mu\lambda''}(x,z'')\,\bar{\mathcal{G}}^{\lambda''}{}_{\nu'}(z'',x';is). \tag{2.209}$$

Substituting this into Eq. (2.200), we have that the heat kernel for the Green's function in the general gauge is

$$\mathcal{G}^{\mu\nu'}(x,x';is)=\bar{\mathcal{G}}^{\mu\nu'}(x,x';is)-\nabla^{\mu}\nabla_{\alpha}\left[\mathcal{H}^{\alpha\nu'}(x,x';is)-\mathcal{H}^{\alpha\nu'}\left(x,x';\frac{is}{\xi}\right)\right]. \tag{2.210}$$

It is clear that when $\xi = 1$, we recover the result from section 2.2.2.

Gauge parameter dependence

We will analyse the explicit gauge dependence of the terms that appear in the VEV of the TEMT. First, we will focus on $\langle g^{(d)}_{\mu\nu} T^{\mu\nu} \rangle_{\rm gf}$, see Eq. (2.132). We can list the various terms as

(a) $\frac{1}{2}\langle F^2 \rangle \equiv \lim_{x'\to x} \nabla_{\mu'} \nabla^{\mu} \langle A_\nu A^{\nu'} \rangle - \lim_{x'\to x} \nabla_{\mu'} \nabla_{\nu} \langle A^\mu A^{\nu'} \rangle$

(b) $\langle (\nabla \cdot A)^2 \rangle \equiv \lim_{x'\to x} \nabla_{\nu'} \nabla_{\mu} \langle A^\mu A^{\nu'} \rangle$

(c) $\langle \nabla_\nu \left(A^\nu \nabla_\mu A^\mu \right) \rangle \equiv \nabla_\nu \left(\lim_{x'\to x} \nabla_\mu \langle A^\mu A^{\nu'} \rangle \right)$

(d) $m^2 \langle A^2 \rangle$

We will stick with the convention,

$$\text{unprimed} \equiv x$$
$$\text{primed} \equiv x'$$
$$\text{double primed} \equiv z''$$

We start with (a). Using Eq. (2.197), and focussing only on the gauge-dependent contribution,

$$\begin{aligned}
\langle A^\mu A^{\nu'} \rangle &= -\int_0^\infty \mathrm{d}s \; (-g)^{-\frac{1}{4}} (-g')^{-\frac{1}{4}} \, \mathrm{e}^{-im^2 s} \, \mathcal{G}^{\mu\nu'} (is) \\
&\supset -\int_0^\infty \mathrm{d}s \; (-g)^{-\frac{1}{4}} (-g')^{-\frac{1}{4}} \, \mathrm{e}^{-im^2 s} \, \mathcal{H}^{\alpha\nu'}{}_{;\alpha}{}^{\mu} \left(\frac{is}{\xi} \right) \\
&= -\int_0^\infty \mathrm{d}s \; (-g)^{-\frac{1}{4}} (-g')^{-\frac{1}{4}} \, \mathrm{e}^{-im^2 s} \int \mathrm{d}^d z'' \; (-g'')^{\frac{1}{2}} \, \bar{G}^{\alpha}{}_{\lambda'';\alpha}{}^{\mu} \, \bar{\mathcal{G}}^{\lambda''\nu'} \left(\frac{is}{\xi} \right)
\end{aligned} \tag{2.211}$$

where the '$\supset$' indicates that we neglect terms that are independent of ξ. We then have

$$\begin{aligned}
\text{(a)} &= \lim_{x'\to x} \nabla_{\mu'} \left[\nabla^\mu \langle A_\nu A^{\nu'} \rangle - \nabla_\nu \langle A^\mu A^{\nu'} \rangle \right] \\
&\supset -\lim_{x'\to x} \nabla_{\mu'} \int_0^\infty \mathrm{d}s \; (-g)^{-\frac{1}{4}} (-g')^{-\frac{1}{4}} \, \mathrm{e}^{-im^2 s} \int \mathrm{d}^d z'' \; (-g'')^{\frac{1}{2}} \, \bar{\mathcal{G}}^{\lambda''\nu'} \left(\frac{is}{\xi} \right)
\end{aligned}$$

$$\left[\bar{G}^{\alpha}{}_{\lambda'';\alpha\nu}{}^{\mu} - \bar{G}^{\alpha}{}_{\lambda'';\alpha}{}^{\mu}{}_{\nu}\right]$$
$$= 0 \tag{2.212}$$

where we have used

$$[\nabla_\nu, \nabla^\mu]\, S = 0, \tag{2.213}$$

if S is a scalar. In the above, as far as the unprimed x-variable is concerned, $\bar{G}^{\alpha}{}_{\lambda'';\alpha}$ is a scalar. The result for (a) is reassuring, since we know $\langle F^2 \rangle$ is gauge-invariant by construction.

Next, we consider (b), which has a coefficient proportional to $\frac{1}{\xi}$. So, unlike the case of (a), we will need to consider all the terms that appear in (b).

We start with $\langle A^\mu A^{\nu'} \rangle_{;\mu}$, given by

$$\langle A^\mu A^{\nu'} \rangle_{;\mu} = -\int_0^\infty \mathrm{d}s\ (-g)^{-\frac{1}{4}} (-g')^{-\frac{1}{4}}\, \mathrm{e}^{-im^2 s} \Bigg[\bar{\mathcal{G}}^{\mu\nu'}{}_{;\mu}(is) - \int \mathrm{d}^d z''\ (-g'')^{\frac{1}{2}}\, \bar{G}^{\alpha}{}_{\lambda'';\alpha}{}^{\mu}{}_{\mu} \left(\bar{\mathcal{G}}^{\lambda''\nu'}(is) - \bar{\mathcal{G}}^{\lambda''\nu'}\left(\frac{is}{\xi}\right)\right)\Bigg] \tag{2.214}$$

Next, we focus on $\bar{G}^{\alpha}{}_{\lambda'';\alpha}{}^{\mu}{}_{;\mu}$. We can use identities in App. B.1.6 to move the covariant derivatives; in particular we want to move the α index to the outermost position. Performing these manipulations leads to

$$\begin{aligned} \bar{G}^{\alpha}{}_{\lambda'';\alpha}{}^{\mu}{}_{\mu} &= \left(\left(g^{\mu\alpha}\Box_{(x)} + R^{\mu\alpha} \right) \bar{G}_{\mu\lambda''} \right)_{;\alpha} \\ &= \left(g^{\alpha}{}_{\lambda''}\, \delta\left(x - z''\right) \right)_{;\alpha} \end{aligned} \tag{2.215}$$

where in the second line, we have used the Schwinger-Dyson equation in Eq. (2.206) for the Green's function $\bar{G}_{\mu\lambda''}$. Substituting this result into Eq. (2.214), we have

$$\begin{aligned} \langle A^\mu A^{\nu'} \rangle_{;\mu} &= -\int_0^\infty \mathrm{d}s\ (-g)^{-\frac{1}{4}} (-g')^{-\frac{1}{4}}\, \mathrm{e}^{-im^2 s} \left[\bar{\mathcal{G}}^{\mu\nu'}{}_{;\mu}(is) - \bar{\mathcal{G}}^{\mu\nu'}{}_{;\mu}(is) + \bar{\mathcal{G}}^{\mu\nu'}{}_{;\mu}\left(\frac{is}{\xi}\right) \right] \\ &= -\xi \int_0^\infty \mathrm{d}s\ (-g)^{-\frac{1}{4}} (-g')^{-\frac{1}{4}}\, \mathrm{e}^{-i\xi m^2 s}\, \bar{\mathcal{G}}^{\mu\nu'}{}_{;\mu}(is) \end{aligned} \tag{2.216}$$

where in the second line, we have redefined the variable $s \to \xi s$. Since $\bar{\mathcal{G}}^{\mu\nu'}$ is defined to be the heat kernel in the Feynman gauge, we can now recycle our results from the previous section to evaluate (b) for a general gauge parameter,

keeping in mind that the effective mass here is ξm^2.

$$\begin{aligned}
\text{(b)} &= -\xi \int_0^\infty \mathrm{d}s\ \mathrm{e}^{-i\xi m^2 s}\ \left[(-g)^{-\frac{1}{4}}\ \bar{\mathcal{G}}^{\mu\nu'}{}_{;\mu\nu'}\ (is)\ (-g')^{-\frac{1}{4}}\right] \\
&= -\frac{\xi}{(4\pi)^{\frac{d}{2}}} \int_0^\infty i\,\mathrm{d}s\ \mathrm{e}^{-i\xi m^2 s}\left[\left[\Delta^{\frac{1}{2}}{}_{;\mu\nu'}\right] a_1^{\mu\nu}(x) + \frac{\left[\sigma_{;\mu\nu'}\right]}{2} a_2^{\mu\nu}(x) + \left[a_1{}^{\mu\nu'}{}_{;\mu\nu'}\right]\right] \\
&= \frac{\xi}{2880\pi^2}\left[-R^2_{\mu\nu\alpha\beta} + R^2_{\mu\nu} + 6\Box R - \frac{5}{2}R^2\right] \qquad (2.217)
\end{aligned}$$

Note that for $\xi = 1$, the result for (b) matches Eq. (2.174) exactly, as expected.

We now consider (c). The same trick as above can be applied here. Thus,[13]

$$\begin{aligned}
\text{(c)} &= -\xi\mu^{2\epsilon} \int_0^\infty \mathrm{d}s\ \mathrm{e}^{-i\xi m^2 s}\ (-g)^{-\frac{1}{4}}\left[\bar{\mathcal{G}}^{\mu\nu'}{}_{;\mu}\ (is)\right]_{;\nu} (-g')^{-\frac{1}{4}} \\
&= -\frac{\xi\mu^{2\epsilon}}{(4\pi)^{\frac{d}{2}}} \int_0^\infty i\,\mathrm{d}s\ \mathrm{e}^{-i\xi m^2 s}\left[a_1{}^{\mu\nu'}{}_{;\mu}\right]_{;\nu} \\
&= \frac{\xi}{2880\pi^2}\Gamma(\epsilon)\left(\frac{\xi m^2}{4\pi\mu^2}\right)^{-\epsilon} 15\Box R \qquad (2.218)
\end{aligned}$$

We again note that the result for (c) matches Eq. (2.171) for $\xi = 1$, as expected. We stress that, in contrast to the calculations performed in the Feynman gauge in the previous section, $\Delta_\epsilon \equiv \Gamma(\epsilon)\left(\frac{m^2}{4\pi\mu^2}\right)^{-\epsilon}$ does not appear here.

Finally, we turn to the evaluation of (d). Oddly enough, this is the least straightforward one to evaluate. We will use an indirect method to evaluate it, via the Green's function equation in (2.196). In the coincident limit, the latter can be recast as[14]

$$\left[\langle A_\nu A^{\nu'}\rangle_{;\mu}{}^{\mu}\right] - \left[\langle A^\mu A^{\nu'}\rangle_{;\nu\mu}\right] + m^2\left[\langle A_\nu A^{\nu'}\rangle\right] + \frac{1}{\xi}\left[\langle A^\mu A^{\nu'}\rangle_{;\mu\nu}\right] = 0 \qquad (2.219)$$

where we remind the reader that the square brackets denote the coincident limit. Rearranging the above equation allows us to find (d),

$$m^2\langle A^2\rangle = \left[\langle A^\mu A^{\nu'}\rangle_{;\nu\mu}\right] - \left[\langle A_\nu A^{\nu'}\rangle_{;\mu}{}^{\mu}\right] - \frac{1}{\xi}\left[\langle A_\mu A^{\nu'}\rangle_{;}{}^{\mu}{}_{\nu}\right] \qquad (2.220)$$

[13] We remind the reader that the factor $\mu^{2\epsilon}$ has been introduced to make the mass dimension of the TEMT exactly 4, see the discussion above Eq. (2.70).

[14] We have used the fact that in dim reg, the d-dimensional δ-function evaluated at zero is defined to be equal to zero, i.e. $\delta^{(d)}(0) = 0$.

We can now recycle our previous results to find (d). Considering the first two terms on the RHS, we have that

$$\left[\langle A^{\mu}A^{\nu'}\rangle_{;\nu\mu} - \langle A_{\nu}A^{\nu'}\rangle_{;}{}^{\mu}{}_{\mu}\right]\Big|_{\xi} = \left[\left(\langle A^{\mu}A^{\nu'}\rangle_{;\nu} - \langle A_{\nu}A^{\nu'}\rangle_{;}{}^{\mu}\right)_{;\mu}\right]\Big|_{\xi}$$
$$= 0 \tag{2.221}$$

where we have used the result in Eq. (2.212). The $\Big|_{\xi}$ means that only the gauge dependent part is considered. Turning to the third term of Eq. (2.220), we have, using Eq. (2.216),

$$-\frac{1}{\xi}\left[\langle A^{\mu}A^{\nu'}\rangle_{;\mu\nu}\right] = \mu^{2\epsilon}\int_0^{\infty} \mathrm{d}s\ \mathrm{e}^{-i\xi m^2 s}\ \left[(-g)^{-\frac{1}{4}}\,\bar{\mathcal{G}}^{\mu\nu'}{}_{;\mu\nu}\,(is)\,(-g')^{-\frac{1}{4}}\right]$$
$$= \frac{\mu^{2\epsilon}}{(4\pi)^{\frac{d}{2}}}\int_0^{\infty} i\,\mathrm{d}s\ \mathrm{e}^{-i\xi m^2 s}\Bigg[\left[\Delta^{\frac{1}{2}}{}_{;\mu\nu}\right]a_1^{\mu\nu}(x)$$
$$+\frac{[\sigma_{;\mu\nu}]}{2}a_2^{\mu\nu}(x) + \left[a_1{}^{\mu\nu'}{}_{;\mu\nu}\right]\Bigg]$$
$$= \frac{1}{2880\pi^2}\Gamma(\epsilon)\left(\frac{\xi m^2}{4\pi\mu^2}\right)^{-\epsilon}[-15\Box R + \mathcal{O}(\epsilon)]$$
$$\supset \frac{15\ln\xi}{2880\pi^2}\Box R \tag{2.222}$$

where in the last line, we have focussed only on the gauge dependent part, indicated by the '$\supset$'. Putting all together, we can write the gauge dependent part of (d),

$$(\mathrm{d})\Big|_{\xi} = \frac{15\ln\xi}{2880\pi^2}\Box R. \tag{2.223}$$

We are now finally in a position to write the gauge-dependent part of $\langle g_{\mu\nu}^{(d)}T^{\mu\nu}\rangle_{\mathrm{gf}}$,[15]

$$\langle g_{\mu\nu}^{(d)}T^{\mu\nu}\rangle_{\mathrm{gf}}\Big|_{\xi} = \left(\left(1-\frac{d}{2}\right)\times(\mathrm{d})\right) + \left(\left(\frac{2-d}{\xi}\right)\times(\mathrm{c})\right)$$
$$= \frac{15\ln\xi}{2880\pi^2}\Box R. \tag{2.224}$$

The above result indicates that only the $\Box R$ term is gauge dependent. Further-

[15] We have dropped the term (b) as its coefficient is proportional to ϵ in the TEMT, and it will therefore not contribute to the gauge-dependent part.

more, we note that the appearance of the gauge parameter ξ comes from the ϵ expansion of $\Gamma(\epsilon)\left(\frac{\xi m^2}{4\pi\mu^2}\right)^{-\epsilon}$. Therefore,

$$\langle g^{(4)}_{\mu\nu}T^{\mu\nu}\rangle_{\rm gf}\Big|_{\xi} = \langle g^{(d)}_{\mu\nu}T^{\mu\nu}\rangle_{\rm gf}\Big|_{\xi} = g^{(4)}_{\mu\nu}\langle T^{\mu\nu}\rangle_{\rm gf}\Big|_{\xi} = \frac{15\ln\xi}{2880\pi^2}\Box R, \tag{2.225}$$

since terms proportional to $\epsilon\times\Gamma(\epsilon)\left(\frac{\xi m^2}{4\pi\mu^2}\right)^{-\epsilon}$ will not change the gauge-dependent contribution, and $\langle g^{(4)}_{\mu\nu}T^{\mu\nu}\rangle_{\rm gf}$, $g^{(4)}_{\mu\nu}\langle T^{\mu\nu}\rangle_{\rm gf}$ and $\langle g^{(d)}_{\mu\nu}T^{\mu\nu}\rangle_{\rm gf}$ differ from each other only by such terms.

This is analogous to the fact that the pole term (i.e. $\propto\Gamma(\epsilon)$) in all of the three different ways of calculating the VEV of the TEMT in the Feynman gauge are the same, c.f. Eq. (2.181) to Eq. (2.183),

$$g^{(4)}_{\mu\nu}\langle T^{\mu\nu}\rangle_{\rm gf}\Big|_{\Delta_\epsilon} = \langle g^{(d)}_{\mu\nu}T^{\mu\nu}\rangle_{\rm gf}\Big|_{\Delta_\epsilon} = \langle g^{(4)}_{\mu\nu}T^{\mu\nu}\rangle_{\rm gf}\Big|_{\Delta_\epsilon} = -\frac{30\Delta_\epsilon}{2880\pi^2}\Box R. \tag{2.226}$$

One might wonder why the coefficient for Δ_ϵ is different from that of $\ln\xi$. The crucial difference comes from the $m^2\langle A^2\rangle$ term, which is not UV divergent, and so does not contribute to Δ_ϵ, but which nevertheless is gauge-dependent, as we have calculated in this section.

A further interesting point is that the isolation of the anomaly A_1 and A_2 via the prescriptions in Eq. (2.81) and Eq. (2.82) will be gauge-independent, analogous to the same way that the UV divergences of the $\Box R$ coefficient cancel.

Before concluding this section, we comment on the effects of gauge dependence on the results in Sec. 2.2.2, which was performed in the Feynman gauge. It is clear that the change in a general gauge for the ghost field and Stückelberg field contributions is that one takes $\Delta_\epsilon \equiv \Gamma(\epsilon)\left(\frac{m^2}{4\pi\mu^2}\right)^{-\epsilon} \to \Gamma(\epsilon)\left(\frac{\xi m^2}{4\pi\mu^2}\right)^{-\epsilon}$. Therefore, one has

$$\langle g^{(d)}_{\mu\nu}T^{\mu\nu}\rangle_{\rm gf+gh} = \frac{1}{2880\pi^2}\left[-31E_4 + 18W^2 + (18-15\ln\xi)\,\Box R\right], \tag{2.227}$$

which has a gauge-dependent $\Box R$ term. This allows the resolution of the ambiguity near the end of Sec. 2.2.2 on grounds of gauge invariance - The conformal anomaly has to be calculated by the prescription A_1 and A_2, which means that the result in Eq. (2.189) is correct, and not Eq. (2.186).

Furthermore, if one adds the contribution from the Stückelberg field,

$$\langle g^{(d)}_{\mu\nu} T^{\mu\nu} \rangle_{\text{full}} = \frac{1}{2880\pi^2} \left[-\frac{63}{2} E_4 + \frac{39}{2} W^2 + (27 - 15\Delta_\epsilon) \Box R + \frac{5}{2} R^2 \right], \quad (2.228)$$

the result becomes gauge invariant! This is not surprising, since the theory with the spin-1 gauge field, ghost fields and Stückelberg field was constructed with gauge invariance as the guiding principle. However, it is UV divergent, and therefore, one would still need the prescriptions A_1 or A_2 to isolate the physical conformal anomaly which has to be both gauge invariant and UV finite.

2.3 Fermion field

The calculation of the conformal anomaly for the fermion field is slightly more complicated due to gamma matrices, which become spacetime dependent in curved spacetime. This section does not involve any ambiguities, however, and while the results are well-known in the literature, we provide them here for the sake of completeness.

2.3.1 Generalities

The action for a fermion field is given by

$$\mathcal{S} = \int \mathrm{d}^d x \sqrt{-g} \left[\bar{\Psi} \left(i\gamma^\mu \nabla_\mu - m \right) \Psi \right]. \quad (2.229)$$

The equation of motion (EoM) is the Dirac equation, given by

$$\left(i\gamma^\mu \nabla_\mu - m \right) \Psi = 0. \quad (2.230)$$

Using the results in Sec. 1.1.4, the symmetric energy-momentum tensor is given by

$$T_{\mu\nu} = \frac{i}{2} \bar{\Psi} \left(\gamma_\mu \nabla_\nu + \gamma_\nu \nabla_\mu \right) \Psi. \quad (2.231)$$

Taking the trace and using the EoM, we find that the TEMT is given by

$$T^{\mu}_{\ \mu} = m\bar{\Psi}\Psi. \tag{2.232}$$

As in the scalar field case, to obtain the anomaly, one first needs the two point function of the fermion field in curved spacetime, $\langle\bar{\Psi}(x)\Psi(x')\rangle$ (or equivalently, $\langle\Psi(x)\bar{\Psi}(x')\rangle$). We will focus only on the coincident limit of $\langle\bar{\Psi}(x)\Psi(x')\rangle$, since its trace appears in Eq. (2.232) above. We do this since the fermion case does not involve any ambiguities like the NCCS or spin-1 gauge field discussed in the previous sections.

2.3.2 De-Witt Schwinger Technique for the fermion field

This section is based on results derived from Birrell and Davies [60]. We start by defining

$$iS_{\rm F}(x,x') \equiv \langle\psi(x)\bar{\psi}(x')\rangle. \tag{2.233}$$

The Schwinger-Dyson equation for the two point function of the fermion field is[16]

$$(i\gamma^{\mu}(x)\nabla^{(x)}_{\mu} - m)S_{\rm F}(x,x') = (-g(x))^{-\frac{1}{2}}\delta^{(n)}(x-x'), \tag{2.234}$$

We further define a function $G_{\rm F}(x,x')$ such that[17]

$$S_{\rm F}(x,x') = (i\gamma^{\mu}(x)\nabla^{(x)}_{\mu} + m)G_{\rm F}(x,x'), \tag{2.235}$$

Substituting (2.235) into (2.234) leads to

$$\left[\Box_x + m^2 + \eta R(x)\right] G_{\rm F}(x,x') = -(-g(x))^{-\frac{1}{2}}\delta^{(n)}(x-x')\mathbb{1}, \tag{2.236}$$

with $\eta = \frac{1}{4}$. In the above equation, $\mathbb{1}$ denotes the identity operator in Dirac (spinor) space. We will often suppress it, as it should be obvious from context that it is there.

We thus find that we need to solve exactly the same equation as in Sec. 2.1.2 for

[16]Note that the $\gamma^{\mu}\,(x)$ becomes spacetime dependent here, since they are defined via vielbeins. This has already been described in Chapter 1 in Sec. 1.1.4, and we do not repeat the discussion here.

[17]We note that both $G_{\rm F}(x,x')$ and $S_{\rm F}(x,x')$ are *bi-spinors*, see App. C for a more detailed discussion on such objects.

the scalar field, with $\eta = \frac{1}{4}$, but keeping in mind that we have bi-spinors here. From Eq. (2.41), we have

$$G_{\rm F}(x,x') = -i\Delta^{\frac{1}{2}}(x,x')\,(4\pi)^{-\frac{d}{2}}\sum_{j=0}^{\infty}\int_0^{\infty} i\,{\rm d}s\,(is)^{j-\frac{d}{2}}\,\exp\left[-im^2 s+\frac{\sigma}{2is}\right]\,a_j\,(x,x')\,, \tag{2.237}$$

where the difference from the scalar case is in the Seeley-De Witt coefficients $a_j\,(x,x')$. Proceeding as in the scalar field case, one can show that the recursion relation for the coefficients in the fermion case are

$$\nabla_\lambda\sigma\nabla^\lambda a_0 = 0, \tag{2.238}$$

$$\nabla^\mu\sigma\,\nabla_\mu a_{n+1} + (n+1)\,a_{n+1} = -\Delta^{-\frac{1}{2}}\nabla^\mu\nabla_\mu\left(\Delta^{\frac{1}{2}}a_n\right) - \frac{1}{4}Ra_n, \qquad n\geq 0. \tag{2.239}$$

The boundary condition is now [14]

$$a_0\,(x,x') = I\,(x,x')\,, \tag{2.240}$$

with the bi-spinor $I\,(x,x')$ satisfying

$$\sigma_{;\mu}I_{;}^{\ \mu} = 0 \tag{2.241}$$

$$[I] = \mathbb{1} \tag{2.242}$$

Solving for the coincident limits of the $a_j\,(x,x')$ coefficients, using the identities in App. C.6.3, leads to

$$a_0(x) = \mathbb{1}, \tag{2.243}$$

$$a_1(x) = -\frac{1}{12}R\,\mathbb{1}, \tag{2.244}$$

$$a_2(x) = \left[\frac{1}{288}R^2 - \frac{1}{180}R_{\mu\nu}^2 + \frac{1}{120}\Box R + \frac{1}{180}R_{\mu\nu\alpha\beta}^2 + \frac{1}{48}G_{\alpha\beta}G_{\gamma\delta}R^{\alpha\beta\mu\nu}R^{\gamma\delta}{}_{\mu\nu}\right]\mathbb{1}, \tag{2.245}$$

where, as before, $\mathbb{1}$ corresponds to the identity matrix in spinor space, and $G_{\alpha\beta} = \frac{1}{4}\left[\gamma_\alpha,\gamma_\beta\right]$ is the generator of Lorentz transformations for Dirac fermions.

We want to compute the condensate $m\langle\bar{\psi}\psi\rangle$, which can be obtained from $S_{\rm F}(x,x)$,

and hence $G_{\rm F}(x)$, by

$$\begin{aligned} m\langle\bar{\psi}\psi(x)\rangle &= -m\,\mathrm{tr}\langle\psi\bar{\psi}(x)\rangle \\ &= -im\,\mathrm{tr}\left[S_{\rm F}(x,x)\right] \\ &= -im\lim_{x'\to x}\mathrm{tr}\left[(i\gamma^{\mu}(x)\nabla_{\mu}^{(x)}+m)G_{\rm F}(x,x')\right]. \end{aligned} \tag{2.246}$$

The negative sign in the first line arises due to the anticommuting property of fermions. From Eq. (2.237), we can calculate the relevant contribution (non-vanishing terms as $m\to 0$) to $G_F\,(x)$,

$$G_{\rm F}(x) \supset -\frac{i}{(4\pi)^2}\frac{a_2(x)}{m^2}, \tag{2.247}$$

and hence, in the $m\to 0$ limit, we have that

$$\langle T^{\mu}{}_{\mu}\rangle = -\frac{1}{(4\pi)^2}\mathrm{tr}[a_2(x)]. \tag{2.248}$$

Performing the Dirac space traces, we obtain

$$\begin{aligned} \langle T^{\mu}{}_{\mu}\rangle &= \frac{1}{2880\pi^2}\left[-\frac{5}{2}R^2-6\,\Box R+\frac{7}{2}R^2_{\mu\nu\gamma\delta}+4R^2_{\mu\nu}\right] \\ &= \frac{1}{2880\pi^2}\left[-\frac{11}{2}E_4+9W^2-6\,\Box R\right]. \end{aligned} \tag{2.249}$$

The results match those in [60, 72, 73, 75].

Chapter 3

Calculation of conformal anomalies via moments, flow theorems and the conformal window

The conformal anomalies we calculated in the previous sections have a wide range of applications. In this section, we will discuss their relevance in the context of flow theorems and the conformal window.

3.1 Flow Theorems

For a CFT in 2D flat spacetime, one can construct a function c from the 2-point correlation function of the TEMT ($\langle T^{\alpha}{}_{\alpha}(x) T^{\lambda}{}_{\lambda}(0)\rangle$), which monotonically decreases along an RG flow,[1]

$$\frac{\mathrm{d}c}{\mathrm{d}\ln\mu} \geq 0. \tag{3.1}$$

Furthermore, the function c corresponds to the central charge of the CFT at the conformal fixed points, which measures the number of degrees of freedom in the CFT. In particular, if the central charge has values c^{UV} and c^{IR} at the UV and

[1] Note that an RG flow implies decreasing μ.

IR fixed points respectively, then

$$\Delta c \equiv c^{\mathrm{UV}} - c^{\mathrm{IR}} \geq 0. \tag{3.2}$$

This important result is known as the **c-theorem** [76], and it implies that renormalisation group flows are irreversible in 2D, in the sense that a system necessary loses degrees of freedom along an RG flow. Eq. (3.2) is sometimes referred to as the 'weak' c-theorem.

Such a CFT can be coupled to a background gravitational field (curved spacetime). Like in the previous sections, it can be shown that, in 2D [77],

$$\langle T^{\alpha}{}_{\alpha} \rangle = \frac{c}{24\pi} R. \tag{3.3}$$

It is not a coincidence that this coefficient is also called c; it has been shown that it is equal to the c-function in Eq. (3.1) above, e.g. [78]. Thus, curved spacetime can be used as a tool to determine the flow of c, since one can use it rather than using the 2-point function of the TEMT in flat spacetime.

In 2D, it was also shown that Δc could be calculated via the second moment of the two-point correlation function of TEMT [79, 80],

$$\Delta c = 3\pi \int d^2x \, x^2 \, \langle \Theta(x)\Theta(0) \rangle_{\mathrm{c}} \geq 0, \tag{3.4}$$

where Θ is the TEMT in flat spacetime, and the subscript 'c' stands for the connected component of the two-point correlation function.

In 4D in curved spacetime, we instead have[2]

$$\langle T^{\alpha}{}_{\alpha} \rangle = \beta_a E_4 + \beta_b H^2 + \beta_c W^2 + 4\bar{b} \, \Box H. \tag{3.5}$$

It was long speculated that β_a could play the role of a c-like function in 4D, which monotonically decreases along an RG flow, and this idea goes all the way back to Cardy's conjecture [81]. Jack and Osborn [46] later showed that this was true in theories where perturbation theory was valid. In 2011, Komargodski and Schwimmer produced a proof that the β_a decreases monotonically along an RG flow, by using the analytic structure (and in particular, unitarity) of the S-matrix element of the $2 \to 2$ dilaton scattering [82]. This result is the so-called

[2]We remind the reader that $H = \frac{R}{d-1} = \frac{1}{3}\Box R$ in 4D. Consequently, we will refer to the $\Box H$ term as the $\Box R$ term.

a-theorem. As in 2D, we can also write the weak version of the a-theorem,

$$\Delta\beta_a \equiv \beta_a^{\rm UV} - \beta_a^{\rm IR} \geq 0, \tag{3.6}$$

where $\beta_a^{\rm UV}$ and $\beta_a^{\rm IR}$ correspond to the values of β_a at the UV and IR fixed points respectively.

The conformal anomalies that we were calculating in the previous section correspond to exactly those coefficients. To be more precise, one starts off with a theory with quantum matter fields coupled to a background gravitational field. For simplicity, let us assume that the theory is conformal *classically*. Taking the TEMT then yields

$$T^{\mu}{}_{\mu} = T_{\rm g}{}^{\mu}{}_{\mu} + T_{\rm M}{}^{\mu}{}_{\mu}, \tag{3.7}$$

where

$$T_{\rm g}{}^{\mu}{}_{\mu} = \beta_a^{\rm UV} E_4 + \beta_b^{\rm UV} H^2 + \beta_c^{\rm UV} W^2 + 4\bar{b}^{\rm UV}\,\Box H, \tag{3.8}$$

corresponds to the contribution to the TEMT due to the gravitational action, and $T_{\rm M}{}^{\mu}{}_{\mu}$ corresponds to the contribution due to the matter field content of the theory.

It can be shown that for a conformal field theory, the H^2 counterterm (at the level of the Lagrangian density) is not required [83] since there are no divergences in the theory associated with H^2. Furthermore, the H^2 term itself is not conformally invariant, since[3]

$$\frac{2}{\sqrt{-g}} g_{\mu\nu} \frac{\delta}{\delta g_{\mu\nu}} \int {\rm d}^d x \sqrt{-g}\, H^2 = (d-4)\, H^2 + 4\Box H. \tag{3.9}$$

Thus, $\beta_b^{\rm UV} = 0$ [42, 84], and $\bar{b}^{\rm UV}$ is finite.

The superscript UV implies that the values of the coefficients are taken before including the contribution from the matter fields. By integrating out the matter fields, the coefficients of the gravitational terms in the TEMT change. This is

[3]This equation also indicates the reason why H is defined as $\frac{R}{d-1}$. In Eq. (B.32), we give the same relation in terms of R^2, and one sees that the coefficient of the $\Box R$ term has a prefactor of $(d-1)$ in dimensional regularisation.

equivalent to taking the VEV of the TEMT, and hence one has

$$\langle T^{\mu}{}_{\mu} \rangle = \beta_a^{\rm IR} E_4 + \beta_b^{\rm IR} H^2 + \beta_c^{\rm IR} W^2 + 4\bar{b}^{\rm IR} \Box H, \tag{3.10}$$

Of course, $\langle T^{\mu}{}_{\mu} \rangle$ can also be understood as coming from the *effective action* W,

$$e^{iW} \equiv \int \mathcal{D}\phi \; e^{i\mathcal{S}_M + i\mathcal{S}_g}, \tag{3.11}$$

with

$$\langle T^{\mu}{}_{\mu} \rangle = \frac{2}{\sqrt{-g}} g^{\mu\nu} \frac{\delta W}{\delta g^{\mu\nu}}. \tag{3.12}$$

The superscripts IR then make sense - They correspond to the coefficients of the gravitational terms at the IR fixed point, when all the degrees of freedom of the matter fields have been integrated out.

Thus, one defines the *flow* of the coefficients of the different gravitational terms that appear in the TEMT by the difference between the UV and IR coefficients. For example, the flow of β_a is

$$\Delta\beta_a = \beta_a^{\rm UV} - \beta_a^{\rm IR}. \tag{3.13}$$

In previous sections, we introduced a mass term, which is a relevant operator[4], to perturb the UV conformal theory from its UV fixed point, generating the RG flow.

By combining Eqs. (3.7), (3.8) and (3.10), one can deduce that

$$\langle T_{\rm M}{}^{\mu}{}_{\mu} \rangle = -\Delta\beta_a E_4 - \Delta\beta_b H^2 - \Delta\beta_c W^2 - 4\Delta\bar{b} \Box H \tag{3.14}$$

We indeed find that for the scalar (Eq. (2.78)), fermion (Eq. (2.249)) and spin-1 (Eq. (2.186)) fields, $\Delta\beta_a > 0$.

We refer the reader to the review by Shore [85] for further details on the subject.

[4]A relevant operator is one which is characterised by a coupling constant having positive mass dimensions.

3.2 $\triangle\bar{b}$ calculations via 2-pt function

We use the Euclidean spacetime convention throughout this section, following the convention of [83], unless otherwise stated. See App. A.2 for more details on Minkowski and Euclidean spacetime conventions.

It was recently shown that $\bar{b}$, the coefficient of $\Box R$ might also have the same property as β_a in Eq. (3.6); that is, it decreases monotonically along an RG flow [83], and in particular,

$$\Delta\bar{b} \equiv \bar{b}^{\mathrm{UV}} - \bar{b}^{\mathrm{IR}} \geq 0. \tag{3.15}$$

It can be shown that, analogous to Eq. (3.4), $\Delta\bar{b}$ can be expressed as the fourth moment of the 2-point function of the TEMT in flat spacetime [86, 87],

$$\Delta\bar{b} = \frac{1}{2^9\,3}\int \mathrm{d}^4x\, x^4 \langle\Theta(x)\Theta(0)\rangle_c, \tag{3.16}$$

where Θ is the TEMT in flat spacetime, and the subscript c stands for 'connected'. It was shown in [83] that $\Delta\bar{b}$ is scheme-independent and flow-independent. The proof relies on the UV-finiteness of 2-point functions of the TEMT [88], and uses the positivity of the spectral representation of the RHS of Eq. (3.16). An outline of the positivity of $\Delta\bar{b}$ is given in Sec. 3.2.1.

From our calculations in the previous sections, we find that indeed $\Delta\bar{b} > 0$ for the CCS and fermion fields. For NCCS and spin-1 gauge fields, there are some issues with a proper definition of $\Delta\bar{b}$, since the TEMT is not zero classically in the zero mass limit. This corresponds to having a finite H^2 term in the action, which as we showed in Eq. (3.9), shifts the $\Box R$ term by a corresponding finite amount. Therefore, to isolate the anomalous contributions from those corresponding to the classical breaking of conformal symmetry, we defined the prescriptions A_1 and A_2.

In this section, we will use Eq. (3.16) to calculate $\Delta\bar{b}$, and compare them to the values we obtained using the De-Witt-Schwinger point splitting method in Chapter 2.

3.2.1 Outline of the derivation of the positivity of $\Delta\bar{b}$

We follow the presentation in [83]. The key in the derivation follows from the positivity of the spectral representation of the 2-point function of the TEMT.

We start by defining the Fourier transform of the connected 2-point function of the TEMT,

$$\Gamma_{\theta\theta}(p) = \int d^4x\, e^{ipx}\langle\Theta(x)\Theta(0)\rangle_c = \mathbb{C}^{\mathbb{1}}_{\theta\theta}(p)\, p^4 + c_T\langle\Theta\rangle, \tag{3.17}$$

where $\mathbb{C}^{\mathbb{1}}_{\theta\theta}(p)$ has been shown to be UV-finite in [88]. The contact term $\langle\Theta\rangle$, while present in the above equation, will not be relevant the flow itself. Next we define derivatives of Eq. (3.17),

$$M^{(2)}_{\theta\theta}(p) = \hat{P}_2\Gamma_{\theta\theta}(p) = \frac{1}{2^6 3}\int d^4x\, e^{ipx}x^4\langle\Theta(x)\Theta(0)\rangle_c, \tag{3.18}$$

where

$$\hat{P}_2 = \frac{1}{2^6 3}\left(\partial_{p^\alpha}\partial_{p_\alpha}\right)^2, \tag{3.19}$$

such that

$$\hat{P}_2\, p^4 = 1. \tag{3.20}$$

$\mathbb{C}^{\mathbb{1}}_{\theta\theta}(p)$ and $M^{(2)}_{\theta\theta}(p)$ satisfy the spectral representations (dispersion relations) [89–91],

$$\mathbb{C}^{\mathbb{1}}_{\theta\theta}(p) = \int_0^\infty ds\, \frac{\rho(s)}{(s+p^2)} + \mathbb{C}^{\mathbb{1}}_{\theta\theta}(\infty), \tag{3.21}$$

$$M^{(2)}_{\theta\theta}(p) = \int_0^\infty ds\, \frac{s\,(s-p^2)\,\rho(s)}{(s+p^2)^5} + M^{(2)}_{\theta\theta}(\infty), \tag{3.22}$$

where the spectral function $\rho(s)$ is defined as a sum over a complete set of spin-0 physical states,

$$\rho(s) = (2\pi)^3\sum_n \theta((p_n)^0)\,\delta(p_n^2 - s)\,|\langle n(p_n)|\Theta|0\rangle|^2 \geq 0, \tag{3.23}$$

where the p_n denote momenta in Minkowski space, and $\theta(x)$ is the Heaviside step

function. Thus, using Eqs. (3.16) and (3.18), one finds that

$$\Delta\bar{b} = \frac{1}{8}\left(M^{(2)}_{\theta\theta}(0) - M^{(2)}_{\theta\theta}(\infty)\right) = \frac{1}{8}\int_0^\infty ds\,\frac{\rho(s)}{s^3} \geq 0, \tag{3.24}$$

where positivity follows from Eq. (3.23). The subtraction of $M^{(2)}_{\theta\theta}(\infty)$ becomes relevant when there is a finite contribution at infinity, c.f. Eq. (1.78).

Of course, the results of this section also imply that

$$\mathbb{C}^{\mathbb{1}}_{\theta\theta}(0) = M^{(2)}_{\theta\theta}(0), \tag{3.25}$$

$$\mathbb{C}^{\mathbb{1}}_{\theta\theta}(\infty) = M^{(2)}_{\theta\theta}(\infty), \tag{3.26}$$

which in [83] are then used to prove other properties of the flow of $\Box R$, such as monotonicity and scheme-independence. We refrain from discussing these results here, and we set out to calculate $\Delta\bar{b}$ for various field theories in the next sections.

3.2.2 Scalar Field

The Lagrangian for a scalar field with general coupling η (in Euclidean spacetime) is

$$\mathcal{L} = \frac{1}{2}(\partial_\mu\phi)^2 + \frac{1}{2}m^2\phi^2 + \frac{1}{2}\eta R\phi^2. \tag{3.27}$$

In dimensional regularisation, $d = 4 - 2\epsilon$, the flat spacetime TEMT is given by

$$\Theta = \frac{1}{2}\left[(1-6\eta) + \epsilon\,(-1+4\eta)\right]\Box\phi^2 + m^2\phi^2. \tag{3.28}$$

Performing the calculation for a scalar field with general η, we have that[5]

$$\frac{1}{8}M^{(2)}_{\theta\theta}(0) = \frac{1}{3840\pi^2}\left[15\,\Gamma(\epsilon)\left(\frac{m^2}{4\pi\mu^2}\right)^{-\epsilon}(1-6\eta)^2 - \frac{65}{2}(1-6\eta)^2 + 1\right], \tag{3.29}$$

$$\frac{1}{8}M^{(2)}_{\theta\theta}(\infty) = \frac{1}{3840\pi^2}\lim_{p\to\infty}\left[15\,\Gamma(\epsilon)\left(\frac{p^2}{4\pi\mu^2}\right)^{-\epsilon}(1-6\eta)^2\right.$$

[5]Note that the normalisation $\frac{1}{3840\pi^2}$, instead of $\frac{1}{2880\pi^2}$ which appeared in Chapter 2, is used due to the way the coefficient $\bar{b}$ is defined in Θ (see e.g. Eq. (3.5)), such that $\frac{1}{2880\pi^2} = \frac{4}{3}\frac{1}{3840\pi^2}$, and we can thus compare the coefficients inside the brackets.

$$- \frac{75}{2}(1-6\eta)^2 - 10\,(1-6\eta)\Bigg], \tag{3.30}$$

where the scale μ has been introduced to make the result dimensionless (hence making $\Delta\bar{b}$ dimensionless as well). Taking the difference, we get

$$\Delta\bar{b}_{\mathrm{NCCS}} = \frac{1}{3840\pi^2}\left[15\,(1-6\eta)^2 \lim_{p\to\infty}\left[\ln\left(\frac{p^2}{m^2}\right)\right] + 5(1-6\eta)^2 + 10(1-6\eta) + 1\right]. \tag{3.31}$$

Note that the UV poles and the dependence on the scale μ disappear, but it gets replaced by $\ln\left(\frac{p^2}{m^2}\right)$, which, however, diverges in the limit of $p \to \infty$. We further note that in the limit of conformal coupling (Eq. (2.14)), we have

$$\Delta\bar{b}_{\mathrm{CCS}} = \frac{1}{3840\pi^2}, \tag{3.32}$$

which matches our previous result in Eq. (2.83). From Eq. (3.30), we also find that for the CCS, $M^{(2)}_{\theta\theta}(\infty) = 0$.

On the other hand, the result for $\Delta\bar{b}_{\mathrm{NCCS}}$ does not match our previous calculations in Eqs. (2.84) to (2.88), which indicates that the formula for $\Delta\bar{b}$ somehow breaks down when there are UV divergences. Still, the coefficient of the $\ln m^2$ term matches, and if we treat $\lim_{p\to\infty}[\ln p^2] \leftrightarrow \Gamma(\epsilon)$, we find that these terms match as well.

It is useful to discuss the calculations in the context of another regularisation scheme, and for this, we choose Pauli-Villars (PV) regularisation.

Before showing the results of the calculation, it is useful to express the bubble integral $B_0(p^2, m^2, m^2)$ (which is logarithmically divergent) in PV regularisation, using Feynman parametrisation,

$$\begin{aligned} B_0(p^2, m^2, m^2) &= \frac{1}{\pi^2}\int d^4k \frac{1}{(k^2+m^2)((p+k)^2+m^2)} \\ &= \int_0^1 dz \ln\left(\frac{\Delta_\Lambda}{\Delta}\right), \end{aligned} \tag{3.33}$$

where

$$\Delta_\Lambda = \Lambda^2 + z(m^2-\Lambda^2) + p^2 z(1-z), \tag{3.34}$$

$$\Delta = m^2 + p^2 z(1-z), \tag{3.35}$$

Λ is the PV mass and z is a Feynman parameter. Then, we have

$$\frac{1}{8}M^{(2)}_{\theta\theta}(0) = 30\,\hat{P}_2|_{p^2=0}\left[\left(\frac{p^4}{2}(1-6\eta)^2 - 2m^2p^2(1-6\eta) + 2m^4\right)\int_0^1 dz \ln\left(\frac{\Delta_\Lambda}{\Delta}\right)\right]. \tag{3.36}$$

After performing the differentiation over p and integration over the Feynman parameter z, we get

$$\frac{1}{8}M^{(2)}_{\theta\theta}(0) = \frac{1}{3840\pi^2}\left[15\,(1-6\eta)^2\ln\left(\frac{\Lambda^2}{m^2}\right) - 15(1-6\eta)^2 + 10(1-6\eta) + 1\right]. \tag{3.37}$$

Similarly, we have

$$\frac{1}{8}M^{(2)}_{\theta\theta}(\infty) = \frac{1}{3840\pi^2}\left[(1-6\eta)^2\left(15\lim_{p\to\infty}\left[\ln\left(\frac{\Lambda^2}{p^2}\right)\right] - 20\right)\right]. \tag{3.38}$$

Finally, taking the difference, we get

$$\Delta\bar{b}_{\rm NCCS} = \frac{1}{3840\pi^2}\left[15\,(1-6\eta)^2\lim_{p\to\infty}\left[\ln\left(\frac{p^2}{m^2}\right)\right] + 5(1-6\eta)^2 + 10(1-6\eta) + 1\right]. \tag{3.39}$$

We note that while $\frac{1}{8}M^{(2)}_{\theta\theta}(0)$ and $\frac{1}{8}M^{(2)}_{\theta\theta}(\infty)$ do not match in the two regularisation schemes, the difference $\Delta\bar{b}_{\rm NCCS}$ does, c.f. Eq. (3.31).

3.2.3 Fermion field

The Lagrangian of a (Dirac) fermion field is

$$\mathcal{L} = \bar{\Psi}(\partial\!\!\!/ + m)\Psi, \tag{3.40}$$

and the TEMT in flat spacetime is

$$\Theta = m\bar{\Psi}\Psi. \tag{3.41}$$

The calculation of the fourth moment here gives

$$\Delta\bar{b}_{\rm ferm} = \frac{1}{8}M^{(2)}_{\theta\theta}(0) = \frac{6}{3840\pi^2}, \tag{3.42}$$

and this matches the result in Eq. (2.249).

3.2.4 Massive Gauge Field via Higgs mechanism in R_ξ gauge

As derived in Sec. 2.2.1, the Lagrangian for a massive gauge field (including ghost fields and Stückelberg field) is

$$\mathcal{L} = \frac{1}{4}F^2 + \frac{1}{2}m^2A^2 + \frac{1}{2\xi}(\partial\cdot A)^2 + \frac{1}{2}(\partial_\mu\chi)^2 + \frac{1}{2}\xi m^2\chi^2 + \partial_\mu\bar{c}\partial^\mu c + \xi m^2\bar{c}c. \quad (3.43)$$

In dimensional regularisation, the flat spacetime TEMT in $d = 4-2\epsilon$ is given by

$$\begin{aligned}\Theta = {} & m^2A^2 - \frac{2}{\xi}\partial_\mu\left(A^\mu\partial_\lambda A^\lambda\right) + \epsilon\left(-m^2A^2 - \frac{1}{2}F^2 + \frac{1}{\xi}\left[\partial^\lambda(A_\lambda\partial_\alpha A^\alpha) + A_\lambda\partial^\lambda(\partial_\alpha A^\alpha)\right]\right) \\ & + \frac{(1-\epsilon)}{2}\Box\chi^2 + \xi m^2\chi^2 + (1-\epsilon)\Box(\bar{c}c) + 2\xi m^2\bar{c}c. \end{aligned} \quad (3.44)$$

The results in this section will be given in three lines to show separately the contributions from the gauge field, ghost fields and Stückelberg field respectively. We thus have that

$$\begin{aligned}\frac{1}{8}M^{(2)}_{\theta\theta}(0) = \frac{1}{3840\pi^2}\Bigg[& 15\,\Gamma(\epsilon)\left[\left(\frac{\xi m^2}{4\pi\mu^2}\right)^{-\epsilon} + \left(\frac{m^2}{4\pi\mu^2}\right)^{-\epsilon}\right] - 81 \\ & - 2\left(15\,\Gamma(\epsilon)\left(\frac{\xi m^2}{4\pi\mu^2}\right)^{-\epsilon} - \frac{63}{2}\right) \\ & + 1\left(15\,\Gamma(\epsilon)\left(\frac{\xi m^2}{4\pi\mu^2}\right)^{-\epsilon} - \frac{63}{2}\right)\Bigg], \end{aligned} \quad (3.45)$$

We note that the contribution from the ghost fields and Stückelberg field are simply multiples of the results for the NCCS in Eq. (3.29) with $\eta = 0$ (-2 for ghost fields and $+1$ for the Stückelberg field).

Furthermore, we have

$$\begin{aligned}\frac{1}{8}M^{(2)}_{\theta\theta}(\infty) = \frac{1}{3840\pi^2}\Bigg[& 2\left[15\,\Gamma(\epsilon)\left(\frac{p^2}{4\pi\mu^2}\right)^{-\epsilon} - \frac{95}{2}\right] \\ & - 2\left[15\,\Gamma(\epsilon)\left(\frac{p^2}{4\pi\mu^2}\right)^{-\epsilon} - \frac{95}{2}\right] \\ & + 1\left[15\,\Gamma(\epsilon)\left(\frac{p^2}{4\pi\mu^2}\right)^{-\epsilon} - \frac{95}{2}\right]\Bigg]. \end{aligned} \quad (3.46)$$

The difference then becomes

$$\begin{aligned}\Delta\bar{b}_{\text{full}} = \frac{1}{3840\pi^2}\Bigg[&15\lim_{p\to\infty}\left[\ln\left(\frac{p^2}{m^2}\right)+\ln\left(\frac{p^2}{\xi m^2}\right)\right]+14\\&-30\lim_{p\to\infty}\left[\ln\left(\frac{p^2}{\xi m^2}\right)\right]-32\\&+15\lim_{p\to\infty}\left[\ln\left(\frac{p^2}{\xi m^2}\right)\right]+16\Bigg] \qquad (3.47)\\ = \frac{1}{3840\pi^2}&\left[15\lim_{p\to\infty}\left[\ln\left(\frac{p^2}{m^2}\right)\right]-2\right] \qquad (3.48)\end{aligned}$$

The result is gauge invariant, as well as the individual $\frac{1}{8}M^{(2)}_{\theta\theta}(0)$ and $\frac{1}{8}M^{(2)}_{\theta\theta}(\infty)$ themselves.

In Pauli-Villars regularisation, we instead have

$$\begin{aligned}\frac{1}{8}M^{(2)}_{\theta\theta}(0) = \frac{1}{3840\pi^2}\Bigg[&15\left[\ln\left(\frac{\Lambda^2}{m^2}\right)+\ln\left(\frac{\Lambda^2}{\xi m^2}\right)\right]-26\\&-30\ln\left(\frac{\Lambda^2}{\xi m^2}\right)+8\\&+15\ln\left(\frac{\Lambda^2}{\xi m^2}\right)-4\Bigg] \qquad (3.49)\end{aligned}$$

and

$$\begin{aligned}\frac{1}{8}M^{(2)}_{\theta\theta}(\infty) = \frac{1}{3840\pi^2}\Bigg[&30\ln\left(\frac{\Lambda^2}{p^2}\right)-40\\&-30\ln\left(\frac{\Lambda^2}{p^2}\right)+40\\&+15\ln\left(\frac{\Lambda^2}{p^2}\right)-20\Bigg] \qquad (3.50)\end{aligned}$$

Taking the difference, we get

$$\begin{aligned}\Delta\bar{b}_{\text{full}} = \frac{1}{3840\pi^2}\Bigg[&15\lim_{p\to\infty}\left[\ln\left(\frac{p^2}{m^2}\right)+\ln\left(\frac{p^2}{\xi m^2}\right)\right]+14\\&-30\lim_{p\to\infty}\left[\ln\left(\frac{p^2}{\xi m^2}\right)\right]-32\end{aligned}$$

$$+ 15 \lim_{p\to\infty}\left[\ln\left(\frac{p^2}{\xi m^2}\right)\right] + 16\Bigg] \tag{3.51}$$

$$= \frac{1}{3840\pi^2}\left[15 \lim_{p\to\infty}\left[\ln\left(\frac{p^2}{m^2}\right)\right] - 2\right] \tag{3.52}$$

Thus, we find that, as in the NCCS case, $\Delta\bar{b}_{\text{full}}$ is the same in both dim reg and Pauli-Villars regularisation. Also, the results do not match those obtained in Sec. 2.2.2, which is due to the fact that the formula for $\Delta\bar{b}$ in Eq. (3.16) breaks down when there are UV divergences in the calculation.

3.2.5 Massive Gauge Field with ghosts only

In this section, we consider the situation where only the gauge field and ghost field contributions are considered. We find that

$$\Delta\bar{b}_{\text{gf+gh}} = \frac{1}{8}M^{(2)}_{\theta\theta}(0) = \frac{1}{3840\pi^2}\left[-18 + 15\ln\xi\right], \tag{3.53}$$

where we have used the fact that $M^{(2)}_{\theta\theta}(\infty) = 0$ in the first equality, which has already been established by a direct computation, see Eq. (3.50). The result is not UV divergent, and indeed, the same result is obtained using either dim reg or Pauli-Villars regularisation. We note that the result is gauge-dependent, and it matches exactly those obtained using the heat kernel calculation, in Eq. (2.227), including the gauge-dependent term.

In conclusion, the calculation of $\Delta\bar{b}$ using the prescription in [83] works well when there are no UV divergences, and in such cases, the results agree with those from the heat kernel calculation. The result that $\Delta\bar{b} \geq 0$ derived in [83] could have very important applications, as will be discussed in the next section, provided the issue with UV divergences is properly dealt with. We leave this for future work.

Before concluding this section, we would like to mention that an expression for $\Delta\beta_a$ using moments of the 3-point function of the TEMT was derived in [92]. However, it relies on the formula for $\Delta\bar{b}$, and therefore similar problems arise for the NCCS and spin-1 gauge field. On the other hand, perfect agreement with the results in Chapter 2 was found for the CCS and fermion upon using the expression for $\Delta\beta_a$ in [92]. It is hoped that fixing the formula for $\Delta\bar{b}$ would also fix the one for $\Delta\beta_a$.

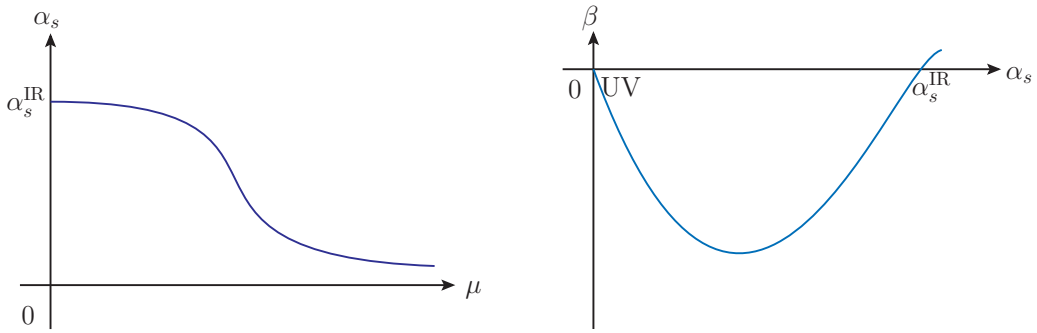

Figure 3.1: Left: Plot showing how the strong coupling constant α_s in QCD varies with the scale μ in the conformal window. There is asymptotic freedom as $\mu \to \infty$ (UV) and $\alpha_s \to 0$, while there is asymptotic safety as $\mu \to 0$ (IR) and $\alpha_s \to \alpha_s^{\mathrm{IR}}$. Right: Plot showing how the β-function changes with α_s. The origin represents the point for asymptotic freedom in the UV, while the other intersection with the α_s-axis represents the IR fixed point for asymptotic safety.

3.3 Comments on QCD in the conformal window

QCD describes the interaction between Dirac fermions having N_f flavours in the fundamental representation, and gluons (spin-1 gauge fields) in the adjoint representation of the gauge group $SU(N_c)$. For certain values of N_f and N_c, the β-function, defined by

$$\beta = \frac{\mathrm{d}g_s}{\mathrm{d}\ln\mu}, \tag{3.54}$$

where g_s is the strong coupling constant in QCD, vanishes both in the UV (very high energies) and the IR (very low energies). Thus, QCD becomes conformal at these fixed points; in the UV, we have *asymptotic freedom*, where the theory become free (non-interacting). In the IR, the coupling of the theory reaches a finite value, and we have *asymptotic safety*. Fig. 3.1 illustrate these points graphically.

The so-called **conformal window** is the range of values of N_f and N_c for which the two fixed points exist. QCD in the Standard Model has $N_f = N_c = 3$ (assuming the u, d and s quarks are light), for which we have asymptotic freedom in the UV, and *confinement* in the IR, since the coupling becomes very large there.

It can be shown quite generally that the condition for asymptotic freedom is

[37, 38]

$$N_f \leq \frac{11}{2} N_c \tag{3.55}$$

which obviously QCD in the Standard Model satisfies.

In the next sections, we will investigate whether the a-theorem or the tentative '$\bar{b}$-theorem' can give us more information on the range of values that N_f can take for QCD in the conformal window.

3.3.1 Conformal Window via the a-theorem

This has been worked out by Cardy in [81]. In the UV, QCD is characterised by $N_c^2 - 1$ spin-1 gauge fields, and $N_c \cdot N_f$ fermions. In the IR, due to spontaneous chiral symmetry breaking [93], we end up with $N_f^2 - 1$ scalar Goldstone bosons (pions). From Eqs. (2.87), (2.189) and (2.249),

$$\Delta\beta_a^{\text{scalar}} = 1, \tag{3.56}$$

$$\Delta\beta_a^{\text{ferm}} = 11, \tag{3.57}$$

$$\Delta\beta_a^{\text{gf+gh}} = 62, \tag{3.58}$$

where we have normalised the units so that the scalar contribution is 1, we have, upon using the a-theorem that

$$62\left(N_c^2 - 1\right) + 11 N_c \cdot N_f \geq \left(N_f^2 - 1\right). \tag{3.59}$$

Solving this equation leads to

$$N_f \leq \frac{11}{2} N_c + \sqrt{\left(\frac{11}{2}\right)^2 N_c^2 + 62\left(N_c^2 - 1\right) + 1}, \tag{3.60}$$

which is consistent with the condition for asymptotic freedom in Eq. (3.55), but is less restrictive.

3.3.2 Conformal Window via the tentative $\bar{b}$-theorem

First of all, we note that this section assumes that $\Delta\bar{b} \geq 0$ even in non-conformal theories (NCCS), and this relies on the derivation provided in [83], which unfortunately has been shown to fail in such cases in Sec. 3.2 by explicit computation. Nevertheless, if the fourth moment formula in Eq. (3.16) could be amended to fix this issue, while preserving the arguments for the proof that $\Delta\bar{b} \geq 0$, one can investigate what the consequence is on the conformal window.

We note that the Goldstone bosons generated by spontaneous chiral symmetry are scalars which are *minimally coupled*, i.e. the coupling $\eta = 0$ in Eq. (2.87). This is due to the fact that chiral symmetry and conformal symmetry are incompatible with each other [94–97]. We further note that the value of the conformal coupling η did not affect the result for $\Delta\beta_a$ in the previous section, but here, η will affect $\Delta\bar{b}$, c.f. Eq. (2.87) and (2.88).

As before, we write the contributions due to the NCCS with $\eta = 0$, fermion and spin-1 gauge field to $\Delta\bar{b}$,

$$\Delta\bar{b}_{\text{NCCS}} = 6, \tag{3.61}$$

$$\Delta\bar{b}_{\text{ferm}} = 6, \tag{3.62}$$

$$\Delta\bar{b}_{\text{gf+gh}} = 12, \tag{3.63}$$

where we have normalised the results in units where the CCS has $\Delta\bar{b}_{\text{CCS}} = 1$. Note that we have used the prescription A_2 (c.f. Eq. (2.82)) for calculating $\Delta\bar{b}$ for the minimally-coupled scalar. We prefer this prescription over A_1 (c.f. Eq. (2.81)) since the latter is not regularisation-independent (it involves an explicit d-dimensional trace). Furthermore, the contribution to $\Delta\bar{b}$ from A_2 is positive, while that from A_1 is negative.

In this case, applying $\Delta\bar{b} \geq 0$ for QCD leads to

$$12\left(N_c^2 - 1\right) + 6N_c \cdot N_f \geq 6\left(N_f^2 - 1\right), \tag{3.64}$$

and the solution to the inequality is

$$N_f \leq \frac{1}{2}N_c + \sqrt{\left(\frac{1}{2}\right)^2 N_c^2 + 2\left(N_c^2 - 1\right) + 1}. \tag{3.65}$$

Therefore, Eq. (3.65) imposes a more strict condition on the upper bound of N_f, compared to the condition obtained upon using the a-theorem (c.f. Eq. (3.60)), and even goes beyond the condition for asymptotic freedom. For $N_c = 3$, we have

$$N_f \leq 16.5, \qquad \text{using asymptotic freedom,} \tag{3.66}$$

$$N_f \leq 44.2, \qquad \text{using } \Delta\beta_a \geq 0, \tag{3.67}$$

$$N_f \leq 5.9, \qquad \text{using } \Delta\bar{b} \geq 0. \tag{3.68}$$

However, the result using the positivity of $\Delta\bar{b}$ contradicts the Banks-Zaks result [40] that the conformal window has to include the region

$$N_f \lesssim \frac{11}{2} N_c, \tag{3.69}$$

i.e. the region close to the upper bound set by asymptotic freedom, c.f. Eq. (3.55). This is not surprising, since the argument relied on unproven assumptions, which may need amendments, as discussed in the outlook section below.

3.4 Outlook

In this section, we highlight some interesting ideas to investigate in the light of the work presented above.

3.4.1 Regularisation-independence of the RG flow of $\Box R$

As explained in Sec. 3.1, the RG flow of the various coefficients is obtained by integrating out the matter fields. The work in Chapter 2 has focussed on the calculation of the coefficients of the gravitational terms (see Eq. (3.14)) in various field theories using *dimensional regularisation* in particular. In gauge theories, this specific regularisation technique somewhat simplifies the identification of gauge dependent terms and irrelevant parts, and this enables the isolation of the conformal anomaly, which was discussed in detail in Sec. 2.2.3. It would be interesting to generalise this to other regularisation schemes, such as differential regularisation [98], and to offer a proof of regularisation-independence if possible.

3.4.2 Fixing the tentative $\bar{b}$-theorem

In Chapter 2, we have presented a detailed calculation where the coefficients of the various gravitational terms in the VEV of the TEMT were calculated. A subtraction scheme, which was defined in Eqs. (2.81) and (2.82), fixes the issues of gauge dependence and UV divergences for $\Delta\bar{b}$, the coefficient of $\Box R$.

Physical meaning can be given to $\Delta\bar{b}$ via the work done in [83], since it was shown to be scheme-independent and flow-independent (and also positive). However, we have shown in Sec. 3.2 that there are some issues with the fourth moment formula for $\Delta\bar{b}$ given in [83] when NCCS and gauge fields (which both have non-vanishing classical TEMT) are involved. $\Delta\bar{b}$ can become gauge dependent, negative or even UV divergent.

First, one would need to revisit the derivation of $\Delta\bar{b}$ in [83], in order to correct for this. It would most likely require a subtraction of some sort. Next, one would need to ensure that the proofs of positivity, scheme-independence and flow-independence still go through after the amendment, which would then qualify $\Delta\bar{b}$ as a physical observable. As a check, the results obtained from the amended formula for $\Delta\bar{b}$ could be compared with those presented in Chapter 2 of this thesis, and the argument in Sec. 3.3.2 could be repeated with the new values.

Finally, it is worth noting that in 4D, there are *four* gravitational terms that appear in the VEV of the TEMT. Therefore, an avenue worth exploring is whether a combination of the different coefficients of the gravitational terms, rather than the coefficients on their own, could be a candidate for a c-theorem in 4D.

Chapter 4

QED corrections to $\bar{B} \to \bar{K}\ell^+\ell^-$: Preliminaries

Rare semileptonic B decays of the type $\bar{B} \to \bar{K}^{(*)}\ell^+\ell^-$ have received significant interest in the last few years because of the hints of Lepton Flavour Universality (LFU) violations reported by the LHCb experiment [10–12], which could be due to physics beyond the Standard Model (SM). In view of higher statistics results on these modes, a detailed study of this phenomenon requires an accurate estimate of all possible sources of LFU violation present within the SM.

Besides trivial kinematic mass effects, the only potential large source of LFU violation present in the SM are hard-collinear singularities in QED. These can induce non-universal corrections of order $\mathcal{O}(\alpha)\ln(m_\ell/m_B)$ to the physical decay rates (depending on the definition of the observables), which can be large for light leptons. These effects are well known and, to a large extent, corrected for in the experimental analyses through Monte Carlo simulations (e.g. PHOTOS [99]). In order to cross-check the reliability of the approximations which are behind this treatment, a detailed analytic analysis of QED corrections is desirable. A first step in this direction was undertaken in [2], where semi-analytic results for the LFU ratios R_K and R_{K^*} have been presented. Here we go one step further: we focus our attention on the process $\bar{B} \to \bar{K}\ell_1\bar{\ell}_2$ (which is a good prototype for a wide class of interesting semi-leptonic decays, including charged-current transitions such as $\bar{B} \to \pi\ell\nu$), and analyse QED corrections at a fully differential level in terms of the "visible" kinematics (i.e. in terms of the two variables that fully specify the kinematics of the non-radiative mode). Moreover, we present a

complete analysis of the problem of evaluating both real and virtual corrections within an effective meson approach which is an improvement over scalar QED. As we demonstrate, this approach is sufficient to trace back the origin of all "dangerous" collinear singularities.

While soft QED singularities cancel out at the differential level in any infrared-safe observable, the cancellation of the collinear singularities, which are actually physical effects regulated by the lepton mass, is more subtle. As we show, the choice of kinematic variables plays a key role in obtaining a differential distribution that is not only infrared-safe, but also free from the sizeable LFU violating terms of order $\mathcal{O}(\alpha)\ln(m_\ell)$. In particular, as far as the invariant mass of the two lepton system is concerned, the following two options can be considered: $q^2_\ell = (\ell_1+\ell_2)^2$ and $q^2_0 = (p_B-p_K)^2$. The first case (q^2_ℓ), which is the natural choice for experiments where the B momentum is not known (such as those performed at hadron colliders), corresponds to defining the invariant mass of the charged lepton system from the measured lepton momenta ($\ell_{1,2}$), i.e. after radiation has occurred. Whereas in the second case (q^2_0), the hadronic momenta ($p_{B,K}$) are used to define the momentum transfer to the lepton system before radiation. These two choices coincide in the non-radiative case, but are different in the presence of radiation. We show that it is only by using q^2_0, as the relevant kinematic variable, that the differential distribution is free from $\mathcal{O}(\alpha)\ln(m_\ell)$-terms. This does not imply that one cannot perform clean tests of LFU at hadron colliders, but rather that in such cases, the collinear singularities are unavoidable and should be properly corrected for.

4.1 Generalities

The two sets of variables we introduce to describe the differential distribution of the $\bar{B}(p_B) \to \bar{K}(p_K)\ell_1(\ell_1)\bar{\ell}_2(\ell_2) + \gamma(k)$ process, assuming that radiation is not detected, are

$$\{q^2_a, c_a\} = \begin{cases} q^2_\ell = (\ell_1+\ell_2)^2, & c_\ell = -\left(\frac{\vec{\ell}_1\cdot\vec{p}_K}{|\vec{\ell}_1||\vec{p}_K|}\right)_{q-\mathrm{RF}} & [\text{“Hadron collider” variables}]\ , \\ q^2_0 = (p_B-p_K)^2\ , & c_0 = -\left(\frac{\vec{\ell}_1\cdot\vec{p}_K}{|\vec{\ell}_1||\vec{p}_K|}\right)_{q_0-\mathrm{RF}} & [\text{“B-factory” variables}]\ , \end{cases} \tag{4.1}$$

where $q-\mathrm{RF}$ and $q_0-\mathrm{RF}$ denote the rest frames of

$$q \equiv \ell_1 + \ell_2 \,, \quad q_0 \equiv p_B - p_K = q + k \,, \tag{4.2}$$

as illustrated in Fig. 4.1 (to conform to standard notations, throughout this thesis, $q_\ell \equiv q$). As indicated, the set $a = \ell$ is the natural choice for a hadron-collider experiment, while the set $a = 0$ can be implemented only in an experiment where the B momentum is known. However, as we shall discuss later on, both sets can be applied to describe appropriate integrated distributions in any kind of experiment.

A further variable that plays a key role in defining infrared-safe observables is

$$\bar{p}_B \equiv p_B - k = \ell_1 + \ell_2 + p_K \,, \tag{4.3}$$

which equals the sum of all visible final-state momenta. The kinematic invariant $\bar{p}_B^2$ is the reconstructed B-meson mass in the hadronic set-up, when p_B is not known, and the variable

$$\delta_{\rm ex} \,>\, 1 - \frac{\bar{p}_B^2}{m_B^2} \,, \tag{4.4}$$

provides the most natural choice for the physical cut-off regulating soft divergences. The complete decomposition of all momenta in the p_B, $\bar{p}_B$, q and q_0 RFs is presented in section 4.3, and the rest frames are denoted as (1), (2), (3) and (4), respectively.

While the cut in Eq. (4.4) is Lorentz invariant, its meaning becomes more transparent when expressed in the p_B-RF,

$$E_\gamma^{(1)} < E_\gamma^{\max(1)} = \delta_{\rm ex} \frac{m_B}{2}, \tag{4.5}$$

where $E_\gamma^{(1)}$ is the energy of the photon in that frame. Therefore, it is clear that $\delta_{\rm ex}$ acts as a cut of the photon energy directly in the p_B-RF. We refer the reader to Sec. 4.8.2 for a more detailed discussion on the experimental cut $\delta_{\rm ex}$.

Schematically, we decompose the double differential rate as

$$d^2\Gamma_{\bar{B}\to\bar{K}\ell_1\bar{\ell}_2}(\delta_{\rm ex}) = \frac{1}{m_B}\left(\rho_a(m_B^2)|\mathcal{A}_V|^2 + \int_{\delta_{\rm ex}} d\Phi_\gamma\, \rho_a(\bar{p}_B^2)\,|\mathcal{A}_R|^2\right) dq_a^2 dc_a \,, \tag{4.6}$$

where $\rho_a(m_B^2)$ and $\rho_a(\bar{p}_B^2)$ denote the 3-body and "effective-3-body" phase space factors respectively, and $d\Phi_\gamma$ indicates the integration over the undetected photon

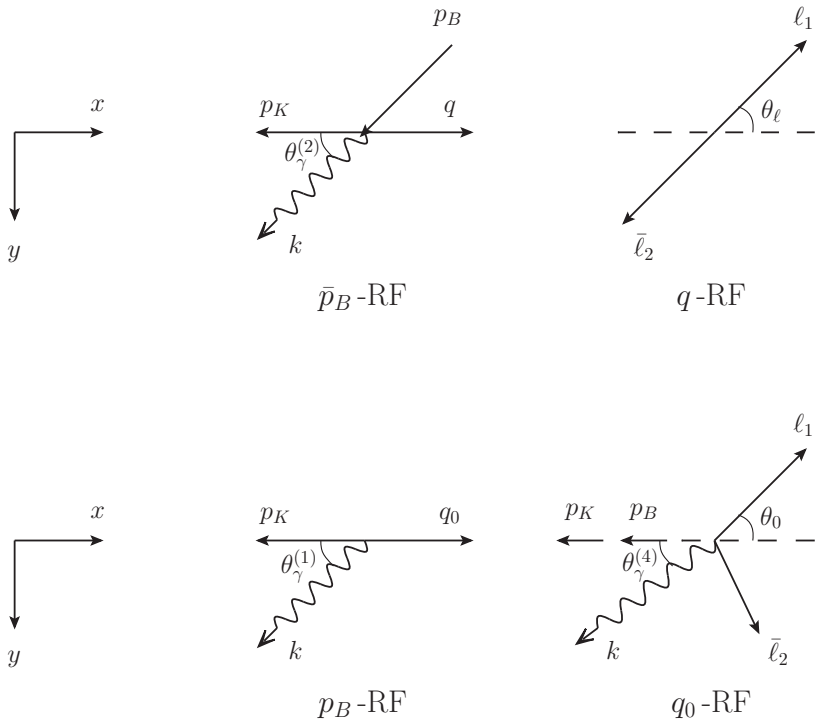

Figure 4.1: Decay kinematics for the different RFs of interest. The dashed line corresponds to what is referred to as the decay axis. For brevity, we drop the frame-label on the lepton angles, $\theta_\ell \equiv \theta_\ell^{(3)}$ and $\theta_0 \equiv \theta_0^{(4)}$, and if no frame-label is indicated on the photon angle, $\theta_\gamma = \theta_\gamma^{(2)}$ is usually understood.

variables over a phase space region specified by the physical cut-off $\delta_{\rm ex}$. In the following, we first introduce the effective Lagrangians used in our analysis, and then present the calculation of the real emission amplitude ($\mathcal{A}_R$) and the one-loop virtual corrections to the tree-level 3-body amplitude ($\mathcal{A}_V$), and finally discuss the corresponding phase space factors. Soft divergences and ultraviolet (UV) divergences are regulated in dimensional regularisation (DR).

Often in QED calculations soft divergences are regulated via an explicit photon mass. For this reason, whenever possible, we will indicate how results change when using this regulator. However, we found that DR is more convenient in performing the soft integrals, and therefore, we adopt it as the default approach.

We use the following conventions throughout: The abbreviation $c_a = \cos\theta_a$ and $s_a = \sin\theta_a$ where the label a stands for either ℓ or 0 and its meaning on the main kinematic variables is depicted in Eq. (4.1). The matrix elements

$$\langle 0|B^\dagger(x)|\bar{B}(p_B)\rangle = e^{-ip_B\cdot x}, \qquad \langle K(p_K)|K^\dagger(x)|0\rangle = e^{ip_K\cdot x}, \tag{4.7}$$

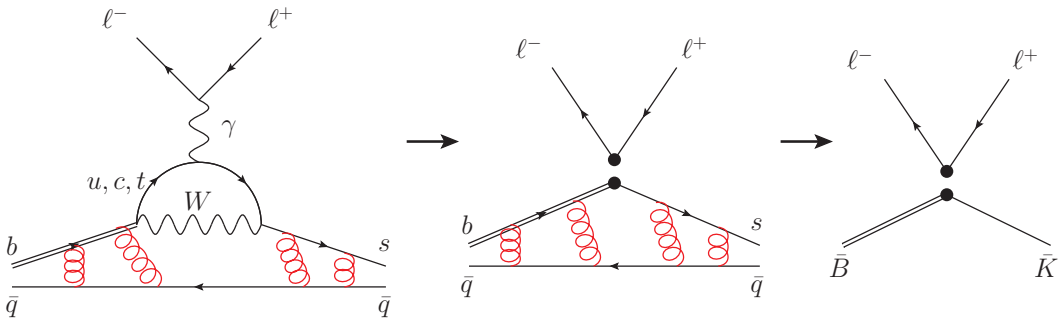

Figure 4.2: Diagrams illustrating the decay process from the full SM to the mesonic effective theory (left to right). The red helices represent gluons which interact non-perturbatively. The leftmost diagram represents a contribution to the decay rate as predicted from the full SM. In the middle diagram, the W boson has been integrated out, and we are left with effective vertices (represented by the black dots), which are given in Eq. (4.8). The rightmost diagram represents the effective mesonic theory (Eq. (4.9)) used in this work, which is obtained by the matching procedure described in Eq. (4.10).

provide the link to the mesonic states $\bar{B}$ and $\bar{K}$ of valence quarks b and s respectively. Whenever there is no ambiguity, we use $p = \sqrt{p^2}$ and hatted quantities are understood to be divided by m_B in order to render them dimensionless e.g. $\hat{q}^2 \equiv q^2/m_B^2$. We use dimensional regularisation with $d = 4 - 2\epsilon$.

4.2 Mesonic effective Lagrangian

Generically, we consider non-radiative processes of the type $M_H \to M_L \ell_1 \bar{\ell}_2$, where $M_{H,L}$ are generic scalar mesons (of either parity). Fig. 4.2 shows the decay process at different scales and levels of approximation, from the full SM to the mesonic effective theory used in this work.

In what follows, we take $M_H = \bar{B}$ and $M_L = \bar{K}$ and the mediation is described by the following effective partonic Lagrangian

$$\mathcal{L}_{\text{int}}^{\text{parton}} = g_{\text{eff}} L_\mu V^\mu + \text{h.c.}\,, \quad L_\mu \equiv \bar{\ell}_1 \Gamma^\mu \ell_2\,, \quad V_\mu \equiv \bar{q}\gamma_\mu(1-\gamma_5)b\,, \quad g_{\text{eff}} \equiv -\frac{G_F}{\sqrt{2}}\lambda_{\text{CKM}}\,, \tag{4.8}$$

where $\Gamma^\mu \equiv \gamma^\mu(C_V + C_A\gamma_5)$. The quark field q, the values of C_V and C_A, and λ_{CKM} can be adapted to describe different processes. Those mediated by the $b \to u(c)\ell\nu$ charged-current interaction correspond to $q = u(c)$, with $(C_V, C_A) = (1, -1)$ and $\lambda_{\text{CKM}} = V_{ub}(V_{cb})$. Processes mediated by the flavour changing neutral

transition $b \to (d,s)\mu^+\mu^-$ are obtained by setting $C_{V(A)} = \alpha C_{9(10)}/(4\pi)$ and $\lambda_{\rm CKM} = V^*_{t(d,s)}V_{tb}$.

The corresponding effective mesonic weak Lagrangian describing the $\bar{B} \to \bar{K}\ell_1\bar{\ell}_2$ process reads

$$\mathcal{L}^{\rm EFT}_{\rm int} = g_{\rm eff}\, L^\mu V^{\rm EFT}_\mu + \text{h.c.}\,, \quad V^{\rm EFT}_\mu = \sum_{n\geq 0} \frac{f^{(n)}_\pm(0)}{n!}(-D^2)^n[(D_\mu B^\dagger)K \mp B^\dagger(D_\mu K)]\,, \tag{4.9}$$

where $D_\mu = (\partial + ieQA)_\mu$ is the covariant derivative and $f^{(n)}_\pm(q^2)$ denotes the $n^{\rm th}$ derivative of the form factor $f_\pm(q^2)$. This Lagrangian maps the q^2-dependence of the non-radiative $B \to K$ form factor into a tower of derivative operators, such that the hadronic matrix element of V_μ is reproduced to LO in the electromagnetic coupling,

$$\begin{aligned} H^\mu_0(q^2_0) \equiv \langle \bar{K}|V_\mu|\bar{B}\rangle &= f_+(q^2_0)(p_B+p_K)^\mu + f_-(q^2_0)(p_B-p_K)^\mu \\ &= \langle \bar{K}|V^{\rm EFT}_\mu|\bar{B}\rangle + \mathcal{O}(e), \end{aligned} \tag{4.10}$$

where $\langle 0|B^\dagger|\bar{B}(p_B)\rangle = e^{-ip_B\cdot x}$ and $\langle \bar{K}(p_K)|K(x)|0\rangle = e^{ip_K\cdot x}$, and $f_0 = f_+ + \frac{q^2}{m^2_B - m^2_K} f_-$ is the scalar part of the form factor.

When performing the numerics, we have included up to first derivative terms in the form factor expansion, as the computation becomes computationally expensive as one goes to higher order. Thus, the corrections induced by such a truncation are of the order of $\left(\frac{q^2}{m^2_B}\right)^2$, and such corrections become larger as one considers larger values of q^2. However, it has been shown in Secs. 5.3 and 5.6 that, as far as hard-collinear logs are concerned, the form factor factorises, such that it is not necessary to perform a form factor expansion in order to obtain the contributions to the hard-collinear logs. Finally, we point out that when considering *relative* QED corrections, as is done in Sec. 6.1.2, such effects may become insignificant, depending on the choice of differential variables. We also refer the reader to Sec. 6.1.3 for a detailed discussion of such effects on the results.

The radiative amplitude is computed at $\mathcal{O}(e)$ by combining the gauge-invariant Lagrangian in (4.9) with the ordinary QED Lagrangian for fermions and mesons,

$$\mathcal{L}_{\rm QED} \equiv \mathcal{L}_\xi(A) + \sum_{\psi=\ell_1,\ell_2} \bar{\psi}(i\not{D} - m_\ell)\psi + \sum_{M=B,K} (D_\mu M)^\dagger D^\mu M - m^2_M M^\dagger M\,, \tag{4.11}$$

where $\mathcal{L}_\xi(A)$ denotes the Maxwell Lagrangian with the covariant gauge-fixing

term,

$$\mathcal{L}_\xi(A) = -\frac{1}{4}F^{\mu\nu}F_{\mu\nu} - \frac{1}{2\xi}\left(\partial\cdot A\right)^2 . \tag{4.12}$$

The propagators of the scalar, fermion and photon are given by

$$\Delta_B(k) = \frac{1}{k^2 - m_B^2} , \tag{4.13}$$

$$S_i(k) = \frac{\not{k} + m_{\ell_i}}{k^2 - m_{\ell_i}^2} , \tag{4.14}$$

$$\Delta_{\mu\nu}(k) = \frac{-1}{k^2 - m_\gamma^2}\left(g_{\mu\nu} - (1-\xi)\frac{k_\mu k_\nu}{k^2}\right) , \tag{4.15}$$

where a photon mass regulator m_γ was added in the last line.

Matters related to going beyond this approximation, at the form factor level, are discussed in Secs. 5.5, 5.6 and 6.2.1. In particular, we have shown that the effective mesonic Lagrangian above captures all the contributions to hard-collinear logs.

The non-radiative amplitude is decomposed as

$$\mathcal{A}_{\bar{B}\to\bar{K}\ell_1\bar{\ell}_2} \equiv \langle \bar{K}\ell_1\bar{\ell}_2|(-\mathcal{L}_{\rm int})|\bar{B}\rangle = \mathcal{A}^{(0)} + \mathcal{A}^{(2)} + \mathcal{O}(e^4) , \tag{4.16}$$

where the superscript indicates the order in the electromagnetic coupling and the phase follows the Particle Data Group (PDG) convention [100]. The lowest-order (LO) amplitude reads

$$\mathcal{A}^{(0)}_{\bar{B}\to\bar{K}\ell_1\bar{\ell}_2} = -g_{\rm eff}\, L_0\cdot H_0 , \tag{4.17}$$

with

$$L_0^\mu \equiv \langle \ell_1\bar{\ell}_2|L^\mu|0\rangle = \bar{u}(\ell_1)\Gamma^\mu v(\ell_2) . \tag{4.18}$$

For flavour changing neutral currents (FCNCs), such as $\bar{B} \to \bar{K}\ell^+\ell^-$, there are additional contributions originating from four-quark operators, dipole and chromomagnetic penguin operators which are apparently not described by the mesonic Lagrangian in (4.9). Some of these effects, in particular the long-distance contribution associated to the charmonium resonances, introduce sizeable distortions of the kinematical distribution in specific regions of q^2. However, in the case of a scalar meson final state, such effects can partially be absorbed for moderate $q^2 \ll m_{J/\Psi}^2$ into a reparametrisation of the $f_\pm$ form

factors.[1] Approaches of this type can be found in the literature in the framework of e.g. QCD factorisation [101] and/or light-cone sum rules [102–104].

4.3 Kinematics

4.3.1 Kinematics in terms of the $\{q^2, \theta_\ell\}$-variables

The main frame is the $\bar{p}_B$-RF, which will serve to define the photon energy cut-off. In this frame, the momenta are parametrised as follows[2]

$$\begin{aligned}
k^{(2)} &= (E_\gamma^{(2)}, -\cos\theta_\gamma |\vec{k}_\gamma^{(2)}|, -\sin\theta_\gamma \cos\phi_\gamma |\vec{k}_\gamma^{(2)}|, -\sin\theta_\gamma \sin\phi_\gamma |\vec{k}_\gamma^{(2)}|) \ , \\
\bar{p}_B^{(2)} &= (\bar{p}_B, 0, 0, 0) \ , \\
q^{(2)} &= (\bar{p}_B - p_K)^{(2)} = (\bar{p}_B - E_K^{(2)}, |\vec{p}_K^{(2)}|, 0, 0) = (E_q^{(2)}, |\vec{p}_K^{(2)}|, 0, 0) \ , \\
p_K^{(2)} &= (E_K^{(2)}, -|\vec{p}_K^{(2)}|, 0, 0) \ ,
\end{aligned} \tag{4.19}$$

where

$$\begin{aligned}
E_K^{(2)} &= \sqrt{|\vec{p}_K^{(2)}|^2 + m_K^2} = \frac{1}{2\bar{p}_B}(\bar{p}_B^2 - q^2 + m_K^2) \ , \qquad |\vec{p}_K^{(2)}| = \frac{\lambda^{1/2}(\bar{p}_B^2, q^2, m_K^2)}{2\bar{p}_B} \ , \\
E_\gamma^{(2)} &= \sqrt{|\vec{k}_\gamma^{(2)}|^2 + m_\gamma^2} = \frac{1}{2\bar{p}_B}\left(m_B^2 - \bar{p}_B^2 - m_\gamma^2\right) \ , \quad |\vec{k}_\gamma^{(2)}| = \frac{\lambda^{1/2}(\bar{p}_B^2, m_B^2, m_\gamma^2)}{2\bar{p}_B} \ , \\
E_q^{(2)} &= \sqrt{|\vec{p}_K^{(2)}|^2 + q^2} = \frac{1}{2\bar{p}_B}(\bar{p}_B^2 + q^2 - m_K^2) \ ,
\end{aligned} \tag{4.20}$$

consistent with $\bar{p}_B - E_K^{(2)} = E_q^{(2)}$. The Källén function,

$$\lambda(s, m_1^2, m_2^2) = (s - (m_1 - m_2)^2)(s - (m_1 + m_2)^2) \ , \tag{4.21}$$

is related to the spatial momentum in the $1 \to 2$ decay [100].

The momenta of the leptons ℓ_1 and ℓ_2, in particular the angle θ_ℓ used by theorists and experimentalists, are defined in the rest frame of q, denoted by the (3)-frame,

[1] Of course, there are additional long-distance effects, such as the photon exchange between a charm-loop and the B-meson which cannot be captured in this way. We expect the simplified procedure outlined above to absorb the main effect at moderate q^2.

[2] All four-momenta are understood to be with upper Lorentz indices e.g. $(k^{(2)})^\mu$. It is understood that $\theta_\gamma \equiv \theta_\gamma^{(2)}, \phi_\gamma \equiv \phi_\gamma^{(2)}$ for brevity. If the angles do not refer to the (2)-frame, then they will be indicated.

for which the momenta are given by

$$
\begin{aligned}
q^{(3)} &= (q,0,0,0)\ , \\
\ell_1^{(3)} &= (E_{\ell_1}, |\vec{\ell}_1|\cos\theta_\ell, -|\vec{\ell}_1|\sin\theta_\ell, 0)\ , \\
\ell_2^{(3)} &= \ell_1^{(3)}|_{\{m_{\ell_1}\to m_{\ell_2}, \theta_\ell\to\theta_\ell+\pi\}} = (E_{\ell_2}, -|\vec{\ell}_1|\cos\theta_\ell, |\vec{\ell}_1|\sin\theta_\ell, 0)\ ,
\end{aligned}
\tag{4.22}
$$

where

$$
\begin{aligned}
E_{\ell_1} \equiv E_{\ell_1}^{(3)} &= \sqrt{|\vec{\ell}_1|^2 + m_{\ell_1}^2} \qquad = \frac{1}{2q}(q^2 + m_{\ell_1}^2 - m_{\ell_2}^2)\ , \\
E_{\ell_2} \equiv E_{\ell_2}^{(3)} &= \sqrt{|\vec{\ell}_1|^2 + m_{\ell_2}^2} \qquad = \frac{1}{2q}(q^2 - m_{\ell_1}^2 + m_{\ell_2}^2)\ , \\
|\vec{\ell}_1| \equiv |\vec{\ell}_1^{(3)}| &= \frac{\lambda^{1/2}(q^2, m_{\ell_1}^2, m_{\ell_2}^2)}{2q},
\end{aligned}
\tag{4.23}
$$

which is consistent with $E_q^{(3)} = E_{\ell_1} + E_{\ell_2} = q$ (and $q = \ell_1 + \ell_2$ of course) and the boost velocity β ,

$$
\beta = \frac{|\vec{p}_q|}{E_q^{(2)}} = \frac{|\vec{p}_K|}{E_q^{(2)}}\ , \quad \gamma = \frac{E_q^{(2)}}{q}\ ,
\tag{4.24}
$$

is obtained by requiring $\vec{q}^{(3)} = 0$.

Thus, in the (2)-frame, the momenta $\ell_{1,2}$ depend on the angle of the lepton ℓ_1 w.r.t to the decay axis in the q-RF and are given by

$$
\begin{aligned}
\ell_1^{(2)} &= (\gamma(E_{\ell_1}^{(3)} + \beta\cos\theta_\ell|\vec{\ell}_1^{(3)}|), \gamma(\beta E_{\ell_1}^{(3)} + \cos\theta_\ell|\vec{\ell}_1^{(3)}|), -|\vec{\ell}_1^{(3)}|\sin\theta_\ell, 0)\ , \\
\ell_2^{(2)} &= (\gamma(E_{\ell_2}^{(3)} - \beta\cos\theta_\ell|\vec{\ell}_1^{(3)}|), \gamma(\beta E_{\ell_2}^{(3)} - \cos\theta_\ell|\vec{\ell}_1^{(3)}|), +|\vec{\ell}_1^{(3)}|\sin\theta_\ell, 0)\ ,
\end{aligned}
\tag{4.25}
$$

and $q \equiv \sqrt{q^2}$, whenever it is clear that q is not a vector, such as in $E_q^{(3)} = E_{\ell_1}^{(3)} + E_{\ell_2}^{(3)} = q$.

4.3.2 Kinematics in terms of the $\{q_0^2, \theta_0\}$-variables

We start by defining kinematic variables in the p_B-RF, denoted by (1). Defining the x-axis along the direction of $\vec{q}_0$, one has

$$
p_B^{(1)} = (m_B, 0, 0, 0)\ , \quad q_0^{(1)} = (E_{q_0}^{(1)}, |\vec{q}_0^{(1)}|, 0, 0)\ , \quad p_K^{(1)} = (E_K^{(1)}, -|\vec{q}_0^{(1)}|, 0, 0)\ .
\tag{4.26}
$$

The momenta ℓ_1, ℓ_2, and k, will be defined in frame (4). Further,

$$E_K^{(1)} = m_B - E_{q_0}^{(1)} \quad = \frac{1}{2m_B}(m_B^2 - q_0^2 + m_K^2) \,,$$
$$E_{q_0}^{(1)} = \sqrt{|\vec{q}_0^{\,(1)}|^2 + q_0^2} = \frac{1}{2m_B}(m_B^2 + q_0^2 - m_K^2) \,, \quad |\vec{q}_0^{\,(1)}| = \frac{\lambda^{1/2}(m_B^2, q_0^2, m_K^2)}{2m_B} \,. \tag{4.27}$$

Frame (1) is useful for imposing the cut-off on the photon energy, c.f. Eq. (4.77). For the phase space integration, we pick the independent variables $|\vec{k}_\gamma^{(4)}|$, $\theta_\gamma^{(4)}$, $\phi_\gamma^{(4)}$, all defined in the q_0-RF, which we denote as the (4)-frame. There, the four-momenta are given by

$$\begin{aligned}
k^{(4)} &= (E_\gamma^{(4)}, -\cos\theta_\gamma^{(4)}|\vec{k}_\gamma^{(4)}|, -\sin\theta_\gamma^{(4)}\cos\phi_\gamma^{(4)}|\vec{k}_\gamma^{(4)}|, -\sin\theta_\gamma^{(4)}\sin\phi_\gamma^{(4)}|\vec{k}_\gamma^{(4)}|) \,, \\
p_B^{(4)} &= \gamma_{q_0} m_B \,(1, -\beta_{q_0}, 0, 0) \;, \\
q_0^{(4)} &= (q_0, 0, 0, 0) \,, \\
p_K^{(4)} &= \gamma_{q_0}\left(\left(E_K^{(1)} + \beta_{q_0}|\vec{q}_0^{\,(1)}|\right), -\left(|\vec{q}_0^{\,(1)}| + \beta_{q_0}E_K^{(1)}\right), 0, 0\right) \;,
\end{aligned} \tag{4.28}$$

where $E_\gamma^{(4)} = \sqrt{|\vec{k}_\gamma^{(4)}|^2 + m_\gamma^2}$ and the boost factors from the p_B-RF to the q_0-RF are given by

$$\beta_{q_0} \;=\; \frac{|\vec{q}_0^{\,(1)}|}{E_{q_0}^{(1)}} \,, \quad \gamma_{q_0} \;=\; \frac{E_{q_0}^{(1)}}{q_0} \,. \tag{4.29}$$

We choose the axes such that $\vec{\ell}_1^{\,(4)}$ lies in the $xy-$plane (see Fig. 4.1). Then

$$\ell_1^{(4)} = \left(E_{\ell_1}^{(4)}, |\vec{\ell}_1^{\,(4)}|c_0, -|\vec{\ell}_1^{\,(4)}|s_0, 0\right), \tag{4.30}$$

where θ_0 is the angle between $\vec{\ell}_1^{\,(4)}$ and the x-axis in the q_0-RF (recall $c_0 \equiv \cos\theta_0$, and $s_0 = \sin\theta_0$), and $E_{\ell_1}^{(4)} = (|\vec{\ell}_1^{\,(4)}|^2 + m_{\ell_1}^2)^{1/2}$. $\ell_2^{(4)}$ is found by momentum conservation via $\ell_2^{(4)} = (q_0 - \ell_1 - k)^{(4)}$. Solving for $|\vec{\ell}_1^{\,(4)}|$ is quite complicated, and the explicit result is given by

$$|\vec{\ell}_1^{\,(4)}| = \frac{AB + \sqrt{D}}{C^2 - B^2} \,, \tag{4.31}$$

where

$$A \equiv q_0^2 - 2q_0E_\gamma^{(4)} + m_{\ell_1}^2 - m_{\ell_2}^2 + m_\gamma^2 \,,$$

$$
\begin{aligned}
B &\equiv 2E_\gamma^{(4)}\beta_\gamma\left(\cos\theta_\gamma^{(4)}\ c_0\ -\ \sin\theta_\gamma^{(4)}\ \cos\phi_\gamma^{(4)}\ s_0\right)\ ,\\
C &\equiv 2q_0 - 2E_\gamma^{(4)}\ ,\\
D &\equiv A^2B^2 + (C^2-B^2)(A^2 - C^2 m_{\ell_1}^2)\ ,
\end{aligned}
\tag{4.32}
$$

where

$$
\beta_\gamma = \sqrt{1 - \frac{m_\gamma^2}{(E_\gamma^{(4)})^2}}.
\tag{4.33}
$$

Using the above, one can also calculate $\omega^2 \equiv 2(|\vec{\ell_1}^{(4)}|E_q^{(4)} + \partial_{|\vec{\ell_1}^{(4)}|}[\vec{k}\cdot\vec{\ell_1}]^{(4)}E_{\ell_1}^{(4)})$, which will be needed in Eq. (4.68). It reads

$$
\omega^2 = 2\left(|\vec{\ell_1}^{(4)}|(q_0 - E_\gamma^{(4)}) + E_{\ell_1}^{(4)}E_\gamma^{(4)}\beta_\gamma(\sin\theta_\gamma^{(4)}\ \cos\phi_\gamma^{(4)}\ s_0\ -\ \cos\theta_\gamma^{(4)}\ c_0)\right)\ .
\tag{4.34}
$$

4.4 Real radiation

The five diagrams relevant to compute real emission amplitude at $\mathcal{O}(e)$ are shown in Fig. 4.3. The result can be expressed as follows.

$$
\begin{aligned}
\mathcal{A}^{(1)} = -eg_{\text{eff}}\Big\{ &\bar{u}(\ell_1)\left[\hat{Q}_{\ell_1}\frac{2\epsilon^*\cdot\ell_1 + \not{\epsilon}^*\not{k}}{2k\cdot\ell_1}\Gamma\cdot H_0(q_0^2) + \hat{Q}_{\bar{\ell}_2}\,\Gamma\cdot H_0(q_0^2)\frac{2\epsilon^*\cdot\ell_2 + \not{k}\not{\epsilon}^*}{2k\cdot\ell_2}\right]v(\ell_2) +\\
&\hat{Q}_{\bar{B}}\,L_0\cdot\bar{H}_0^{(B)}(q^2)\frac{\epsilon^*\cdot(p_B+\bar{p}_B)}{2k\cdot p_B}\ + \hat{Q}_{\bar{K}}\,L_0\cdot\bar{H}_0^{(K)}(q^2)\frac{\epsilon^*\cdot(p_K+\bar{p}_K)}{2k\cdot p_K} +\\
&(\hat{Q}_{\bar{B}} - \hat{Q}_{\bar{K}})\,L_0\cdot\epsilon^*\,f_+(q^2) + (\hat{Q}_{\bar{B}} + \hat{Q}_{\bar{K}})\,L_0\cdot\epsilon^*\,f_-(q^2) +\\
&(\hat{Q}_{\bar{B}} + \hat{Q}_{\bar{K}})L_0\cdot(p_B \pm p_K)(\epsilon^*\cdot(q+q_0))\sum_{n\geq 1}\frac{f_\pm^{(n)}(0)}{n!}P_{n-1}\Big\}\ ,
\end{aligned}
\tag{4.35}
$$

where $P_n = \sum_{m=0}^{n}(q^2)^{(n-m)}(q_0^2)^m$ (with $P_0 = 1$), $\bar{H}_0^{(X)} = H_0|_{p_X\to\bar{p}_X}$ for $X = B, K$ and $\bar{p}_K \equiv p_K + k$ (recall $\bar{p}_B = p_B - k$).

Note that in order to recover the result in photon mass regularisation, the substitution $2k\cdot p \to 2k\cdot p \pm m_\gamma^2$, with plus sign for outgoing and minus sign for incoming momenta, in the denominators is sufficient.

The rules for the hatted charges are: $\hat{Q}^{\text{in}} = -Q^{\text{in}}$ and $\hat{Q}^{\text{out}} = Q^{\text{out}}$. Furthermore we use $Q_{\bar{\ell}_2} = -Q_{\ell_2}$ such that $Q_{\bar{\ell}_2} + Q_{\ell_1} = 0$ in the case where the lepton pair is

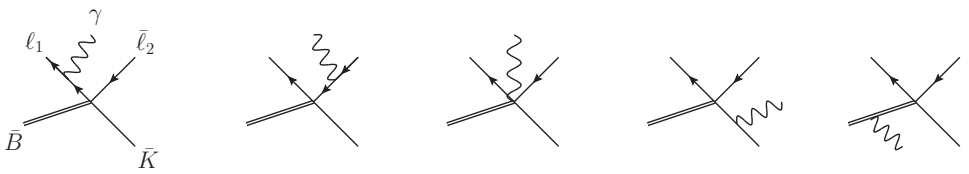

Figure 4.3: $\mathcal{O}(e)$-graphs with nomenclature referring to photon-emission and the P stands for point-like and can also be interpreted as a contact term.

$\bar{B} \to \bar{K}\ell_1\bar{\ell}_2$	$\hat{Q}_{\bar{B}}$	$\hat{Q}_{\bar{K}}$	$\hat{Q}_{\ell_1}$	$\hat{Q}_{\bar{\ell}_2}$
$\bar{B}^- \to \bar{K}^-\mu^-\mu^+$	$+1$	-1	-1	$+1$
$\bar{B}_s \to \bar{K}^-\nu\mu^+$	0	-1	0	$+1$

Table 4.1: Example of charge assignment for FCNC and semileptonic decay which obey (4.36). Note that generally $Q_P = -Q_{\bar{P}}$, rules for the hatted charges are given in the text and by convention $\bar{B}$ and $\bar{K}$ correspond to mesons with a $b\bar{q}$ and $s\bar{q}$ valence quarks.

charge neutral. Charge conservation then implies

$$\sum_{i=\bar{B},\bar{K},\ell_1,\bar{\ell}_2} \hat{Q}_i = 0 \,. \tag{4.36}$$

Hereafter, the $\sum_i$ is defined by the left-hand side (LHS) of the equation above. Keeping the leading terms in the $k \to 0$ limit, i.e. at $\mathcal{O}(1/E_\gamma)$, $\mathcal{A}^{(1)}$ assumes the Low or eikonal form,

$$\mathcal{A}^{(1)}_{\text{Low}} = e\mathcal{A}^{(0)} \sum_i \hat{Q}_i \frac{\epsilon^*\cdot p_i}{k\cdot p_i} \,, \tag{4.37}$$

which is manifestly gauge invariant as a result of Eq. (4.36). The subleading terms of $\mathcal{O}(E_\gamma^0)$ are also universal and are proportional to the angular momentum operator (e.g. $\sigma_{\mu\nu}k^\mu\epsilon^{*\nu}$ terms in the first line of (4.35)).

It is instructive to discuss gauge invariance of the amplitude beyond the $k \to 0$ limit, and we address this in the next section.

4.5 Gauge invariance of the real amplitude $\mathcal{A}^{(1)}_{\bar{B}\to\bar{K}\ell_1\bar{\ell}_2\gamma}$

Gauge invariance follows from the charge conservation (4.36) and inspecting the four terms in (4.35), it is far from obvious how this will work out since

the individual terms depend on the hadronic form factor in a non-uniform way e.g. $\hat{Q}_{\bar{\ell}_2,\ell_1} H_0(q_0^2)$, $\hat{Q}_{B,K} \bar{H}^{(B,K)}(q^2), \ldots$. A special rôle is played by the contact terms arising from diagram P in Fig. 4.3. From the viewpoint of the effective Lagrangian, these terms arise from replacing ordinary derivatives with covariant ones and from the viewpoint of the Ward identity, they are induced by the derivatives acting on the $U(1)$ gauge transformation.

At first, we consider lines two and three of the real amplitude in Eq. (4.35)

$$\begin{aligned}
\mathcal{A}_{23}^{(1)} \quad &\propto \hat{Q}_{\bar{B}}\, L_0{\cdot}\bar{H}_0^{(B)}(q^2)\frac{\epsilon^*{\cdot}p_B}{k{\cdot}p_B} \;+\hat{Q}_{\bar{K}}\, L_0{\cdot}\bar{H}_0^{(K)}(q^2)\frac{\epsilon^*{\cdot}p_K}{k{\cdot}p_K} \\
&\quad + (\hat{Q}_{\bar{B}}{-}\hat{Q}_{\bar{K}})\, L_0{\cdot}\epsilon^*\, f_+(q^2) + (\hat{Q}_{\bar{B}}{+}\hat{Q}_{\bar{K}})\, L_0{\cdot}\epsilon^*\, f_-(q^2) \\
&\overset{\epsilon\to k}{\to} (\hat{Q}_{\bar{B}} + \hat{Q}_{\bar{K}}) L_0{\cdot}H_0(q^2)\;, \qquad (4.38)
\end{aligned}$$

and notice that a gauge transformation combines these two lines into an expression which will combine with the first line

$$\begin{aligned}
\mathcal{A}_1^{(1)} \quad &\propto \bar{u}(\ell_2)\left[\hat{Q}_{\ell_1}\,\frac{2\epsilon^*{\cdot}\ell_1{+}\not{\epsilon}^*\not{k}}{2k{\cdot}\ell_1}\Gamma{\cdot}H_0(q_0^2) + \hat{Q}_{\bar{\ell}_2}\,\Gamma{\cdot}H_0(q_0^2)\frac{2\epsilon^*{\cdot}\ell_2{+}\not{k}\not{\epsilon}^*}{2k{\cdot}\ell_2}\right] v(\ell_1) \\
&\overset{\epsilon\to k}{\to} (\hat{Q}_{\bar{\ell}_2} + \hat{Q}_{\ell_1}) L_0{\cdot}H_0(q_0^2)\;, \qquad (4.39)
\end{aligned}$$

except that the argument of the form factors is q_0^2 in one case and q^2 in the other case. This is remedied, of course, by the fourth line

$$\begin{aligned}
\mathcal{A}_4^{(1)} \quad &\propto (\hat{Q}_{\bar{B}}{+}\hat{Q}_{\bar{K}}) L_0{\cdot}(p_B \pm p_K)(2\epsilon^*{\cdot}q)\sum_{n\geq 1}\frac{f_\pm^{(n)}(0)}{n!}P_{n-1} \\
&\overset{\epsilon\to k}{\to} (\hat{Q}_{\bar{B}}{+}\hat{Q}_{\bar{K}}) L_0{\cdot}(p_B \pm p_K)\sum_{n\geq 1}\frac{f_\pm^{(n)}(0)}{n!}\Delta_q^{2n} \\
&= (\hat{Q}_{\bar{B}}{+}\hat{Q}_{\bar{K}}) L_0{\cdot}(H_0(q_0^2) - H_0(q^2))\;, \qquad (4.40)
\end{aligned}$$

which follows from $\Delta_q^2 = 2q\cdot k$ and $\Delta_q^2 P_{n-1} = \Delta_q^{2n}$ and $\Delta_q^{2n} \equiv (q_0^2)^n - (q^2)^n$. Adding them all together, one obtains

$$\mathcal{A}^{(1)}|_{\epsilon\to k} \propto L_0{\cdot}H_0(q_0^2)\sum_i \hat{Q}_i = 0\;, \qquad (4.41)$$

the explicit gauge invariance of the real amplitude.

4.6 Virtual corrections

The diagrams for the virtual corrections are depicted in Fig. 4.4, and decompose into

$$\mathcal{A}^{(2)} = \mathcal{A}^{(2)}_{1PI} + \frac{1}{2}\frac{\alpha}{\pi}\left[(Q^2_{\ell_1} + Q^2_{\ell_2})\delta Z^{(1)}_2 + (Q^2_B + Q^2_K)\delta Z^{(1)}_S\right]\mathcal{A}^{(0)} \ , \tag{4.42}$$

where 1PI stands for one particle irreducible and δZ correspond to the self-energy corrections. We have computed corrections up to the second derivative of the form factors but show only results up to the first derivative as they are numerically time-consuming.

For the Z-factors, decomposed as

$$Z_i = 1 + Q^2_i\frac{\alpha}{\pi}\delta Z^{(1)}_i + \mathcal{O}(\alpha^2), \tag{4.43}$$

we find, adapting the on-shell scheme,

$$\begin{aligned}
\delta Z^{(1)}_S &= \frac{1}{4}\left((3-\xi)(\frac{1}{\hat{\epsilon}_{\rm UV}} - r_{\rm soft}) + (1-\xi)\right) \ , \\
\delta Z^{(1)}_2 &= \frac{1}{4}\left(-\xi\frac{1}{\hat{\epsilon}_{\rm UV}} - (3-\xi)r_{\rm soft} + 3\ln\left(\frac{m^2}{\mu^2}\right) - (3+\xi)\right) \ ,
\end{aligned} \tag{4.44}$$

with

$$\frac{1}{\hat{\epsilon}} = \frac{1}{\epsilon} - \gamma_E + \ln 4\pi \ . \tag{4.45}$$

The factor $r_{\rm soft}$ reads

$$r_{\rm soft} = \begin{cases} \ln\left(\frac{m^2_\gamma}{\mu^2}\right) & m_\gamma \neq 0 \\ \frac{1}{\hat{\epsilon}_{\rm IR}} & m_\gamma = 0 \end{cases} \ , \tag{4.46}$$

in the case of a photon mass regularisation and DR respectively.

The expressions for the 1PI graphs in Fig. 4.4 are given in Sec. 4.6.1.

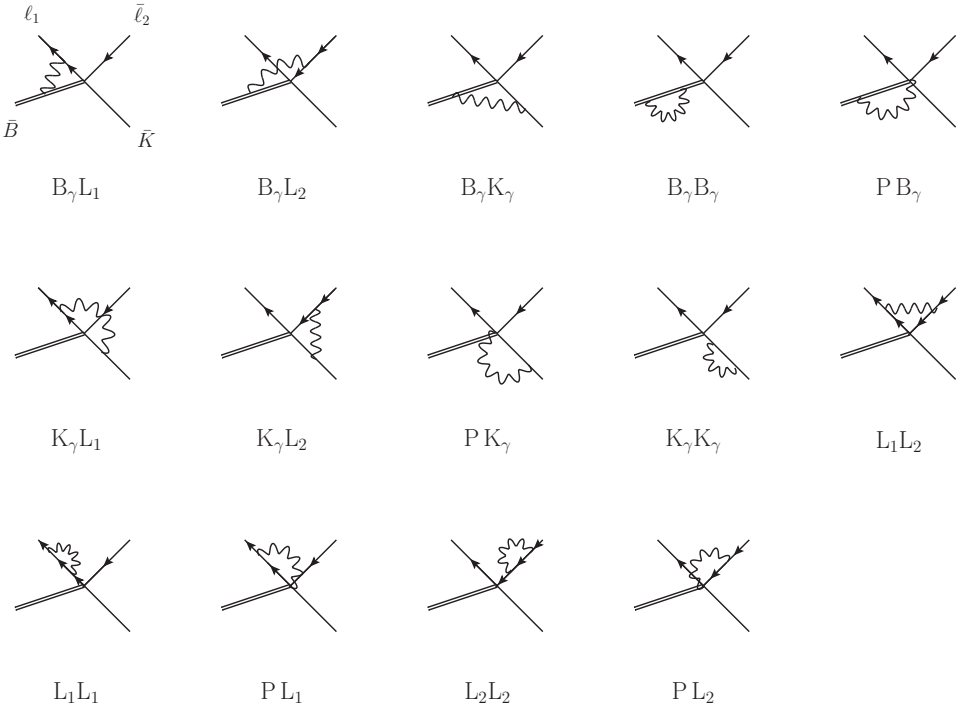

Figure 4.4: $\mathcal{O}(e^2)$-graphs with nomenclature adapted for tracking the cancellation of IR-divergences.

4.6.1 Virtual diagrams

In what follows, we use the notation

$$\int_k \equiv \int \frac{d^d k}{(2\pi)^d}. \tag{4.47}$$

BL_1 and BL_2

$$\begin{aligned} \mathcal{A}^{\bar{B}\to\bar{K}\ell_1\bar{\ell}_2}_{BL_1+BL_2} &= -ig_{\text{eff}}\, Q_B\, e^2 \int_k (2p_B+k)^\nu \Delta_{\nu\rho}(k) F^B_\mu \times \\ &\quad \bar{u}(\ell_1)(Q_{\ell_1}\gamma^\rho S_1(r)\Gamma^\mu + (-Q_{\bar{\ell}_2})\Gamma^\mu S_2(r)\gamma^\rho) v(\ell_2)\ . \end{aligned} \tag{4.48}$$

where

$$F^B_\mu = ((p_B+k)\pm p)_\mu \sum_{n\geq 0} \frac{f^{(n)}_\pm(0)}{n!}(q+k)^{2n}\Delta_B(l)\ , \tag{4.49}$$

and the momentum assignment of the 3 propagators is

$$(r,l) = (\pm[k+\ell_1(\ell_2)], -k-p_B) \ , \tag{4.50}$$

with the first case corresponding to BL_1 and the second to BL_2.

KL_1 and KL_2

$$\begin{aligned}\mathcal{A}^{\bar{B}\to\bar{K}\ell_1\bar{\ell}_2}_{KL_1+KL_2} &= -ig_{\rm eff}\, Q_K\, e^2 \int_k (2p-k)^\nu \Delta_{\nu\rho}(k) F^K_\mu \times \\ &\quad \bar{u}(\ell_1)(Q_{\ell_1}\gamma^\rho S_1(r)\Gamma^\mu + (-Q_{\bar{\ell}_2})\Gamma^\mu S_2(r)\gamma^\rho) v(\ell_2) \ , \end{aligned} \tag{4.51}$$

where

$$F^K_\mu = (p_B \pm (p-k))_\mu \sum_{n\geq 0} \frac{f^{(n)}_\pm(0)}{n!}(q+k)^{2n}\Delta_K(l) \ , \tag{4.52}$$

and the momentum assignment of the 3 propagators is

$$(r,l) = (\pm[k+\ell_1(\ell_2)], k-p) \ , \tag{4.53}$$

with the first case corresponding to KL_1 and the second to KL_2.

PL_1 and PL_2

$$\mathcal{A}^{\bar{B}\to\bar{K}\ell_1\bar{\ell}_2}_{PL_1+PL_2} = ig_{\rm eff}e^2 \int_k F^K_{\mu\rho}\bar{u}(\ell_1)(Q_{\ell_1}\gamma^\rho S_1(r)\Gamma^\mu + (-Q_{\bar{\ell}_2})\Gamma^\mu S_2(r)\gamma^\rho) v(\ell_2) \ , \tag{4.54}$$

with the momentum assignment

$$r = \pm[k+\ell_1(\ell_2)], \tag{4.55}$$

for PL_1 and PL_2 respectively and

$$\begin{aligned} F^K_{\mu\rho} = \big[&(Q_B \pm Q_K)\Delta_{\mu\rho}(k)\sum_{n\geq 0}\frac{f^{(n)}_\pm(0)}{n!}(q+k)^{2n} + \\ &(Q_B - Q_K)(p_B \pm p_K)_\mu (2q+k)^\nu \Delta_{\nu\rho}(k)\sum_{n\geq 1}\frac{f^{(n)}_\pm(0)}{n!}P_{n-1}\big] \ , \end{aligned} \tag{4.56}$$

where sums over $\pm$ are understood and $P_n = \sum_{m=0}^{n} (q^2)^{(n-m)}((q+k)^2)^m$.

PB and PK

$$\begin{aligned}\mathcal{A}^{\bar{B}\to\bar{K}\ell_1\bar{\ell}_2}_{PB+PK} &= -ig_{\rm eff}e^2L_0^\mu \int_k \Big[F^K_{\mu\alpha}Q_B\Delta_B(p_B-k)(2p_B-k)^\alpha + \\ &\quad \tilde{F}^K_{\mu\alpha}Q_K\Delta_K(p+k)(2p+k)^\alpha\Big] \end{aligned} \tag{4.57}$$

where

$$\begin{aligned} F^K_{\mu\alpha} &= (Q_B \pm Q_K)\Delta_{\mu\alpha}(k)f_\pm(q^2) \\ &\quad +(Q_B-Q_K)(2q-k)^\nu\Delta_{\nu\alpha}(k)(p_B-k\pm p)_\mu \sum_{n\geq 1}\frac{f_\pm^{(n)}(0)}{n!}\tilde{P}_{n-1}\,, \end{aligned} \tag{4.58}$$

$$\begin{aligned} \tilde{F}^K_{\mu\alpha} &= (Q_B \pm Q_K)\Delta_{\mu\alpha}(k)f_\pm(q^2) \\ &\quad +(Q_B-Q_K)(2q-k)^\nu\Delta_{\nu\alpha}(k)(p_B\pm(p+k))_\mu \sum_{n\geq 1}\frac{f_\pm^{(n)}(0)}{n!}\tilde{P}_{n-1} \end{aligned} \tag{4.59}$$

and it is understood that $\pm$ is summed and $\tilde{P}_n = \sum_{m=0}^{n}(q^2)^{(n-m)}((q-k)^2)^m$.

BK

The BK-vertex correction graph reads

$$\mathcal{A}^{\bar{B}\to\bar{K}\ell_1\bar{\ell}_2}_{BK} = ig_{\rm eff}Q_BQ_Ke^2L_0^\mu\int_k (2p_B+k)^\beta F^K_{\mu\beta}\Delta_B(l) \tag{4.60}$$

with

$$F^K_{\mu\beta} = \Delta_{\beta\kappa}(k)\Delta_K(r)[(2k+p_B+p)f_+(q^2)+(p_B-p)f_-(q^2)]_\mu(2p+k)^\kappa\,, \tag{4.61}$$

and

$$(l,r) = (-k-p_B,-k-p)\,. \tag{4.62}$$

L_1L_2

For the L_1L_2 graph (lepton vertex correction), the amplitude reads

$$\mathcal{A}^{\bar{B}\to\bar{K}\ell_1\bar{\ell}_2}_{L_1L_2} = ig_{\text{eff}}Q_{\ell_1}(-Q_{\bar{\ell}_2})e^2H_0^\mu(q^2)\int_k \bar{u}(\ell_1)\gamma^\alpha S_1(l)\Gamma_\mu S_2(r)\gamma^\beta v(\ell_2)\Delta_{\alpha\beta}(k)\ , \tag{4.63}$$

with the momentum assignment

$$(l,r) = (\ell_1 - k, -\ell_2 - k). \tag{4.64}$$

PP

They appear in the tower expansion for $n \geq 1$, but are tadpoles. They are proportional to $A_0(m_\gamma^2)$, where the function A_0 is defined in App. E, and vanish in the limit $m_\gamma \to 0$ (and are thus not shown in Fig. 4.4).[3]

4.6.2 Gauge invariance and UV divergences

We explicitly checked that the gauge dependent part of the virtual amplitude vanishes as a consequence of charge conservation,

$$\mathcal{A}^{(2)}|_\xi = \frac{\xi}{2}\frac{\alpha}{4\pi}\mathcal{A}^{(0)}\left(r_{\text{soft}} - \frac{1}{\hat{\epsilon}_{\text{UV}}} - 1\right)(\sum_i \hat{Q}_i)^2 = 0\ . \tag{4.65}$$

Let us turn to the UV divergences. There are no UV divergences in the neutral meson case since the leptonic currents do not renormalise (at our level of approximation). This does not change when the tower of operators $\mathcal{L}_{\text{int}}^{\text{EFT}}$ (4.9) is added as the derivatives acts on the mesons only. As previously mentioned, we restrict ourselves to the first form factor derivative approximation or to dimension-eight operators (the explicit form factors are given in Sec. 6.1). In the case of charged mesons, there are UV divergences associated with operators of dimension six and eight in (4.9) and there is an additional one proportional to $(p_B \cdot \ell_1)\ f_\pm^{(1)}(0)$ which can be interpreted as a t-channel operator.[4] Since $f_\pm$ are

[3]Note that we do not have to even assume cancellation of UV and IR poles if we work in dimensional regularisation, as the individual poles themselves are suppressed by m_γ^2.

[4] The set of operators (4.9) does not close under renormalisation and needs to be completed by the t-channel operator at dimension eight.

to be counted separately this means that there are six counterterms to be fixed at our level of approximation. The appropriate counterterms can be determined by matching to QCD which we hope to address in the future. In the current work presented here, we treat the divergences with minimal subtraction. We comment in Sec. 6.1 on the numerical impact of the undetermined finite counterterms.

4.7 Comments on charge and c_a symmetry

For the process $\bar{B}(p_B) \to \bar{K}(p_K)\ell_1(\ell_1)\bar{\ell}_2(\ell_2) + \gamma(k)$, when $\bar{\ell}_2$ is the anti-particle of ℓ_1 (i.e.), we have a symmetry under[5]

$$\begin{aligned} Q_i &\to -Q_i \quad \text{for} \quad i = \ell_1, \ell_2, \\ c_\ell &\to -c_\ell. \end{aligned} \tag{4.66}$$

We note that this applies only to the variables $\{q^2, c_\ell\}$, as reversing the momenta of the leptons in the (3)-frame corresponds to $c_\ell \to -c_\ell$, while the same is not true for the variables $\{q_0^2, c_0\}$.

One interesting consequence of this is that when the mesons are neutral, the differential rate itself becomes symmetric under $c_\ell \to -c_\ell$. We will also comment on this symmetry further when we discuss hard-collinear divergences in Sec. 5.3.

4.8 Phase space

In this section, we give the 3- and 4-particle phase space measures. For the photon phase space measure, we need a regularised version in order to properly account for finite terms. Here, we find it more instructive to discuss explicitly results obtained using a non-vanishing photon mass. The adaptation to DR is given in App. D.1.

[5]This is of course related to CP invariance of the QED Lagrangian, however, because the particles have different masses, only the leptonic sector has the explicit symmetry in Eq. (4.66), and only when the leptons have the same mass.

4.8.1 Phase space for the radiative and non-radiative decay

The radiative rate $\bar{B} \to \bar{K}\ell_1\bar{\ell}_2\gamma$, without energy cut-off on the photon, is given by

$$d^2\Gamma_{\bar{B}\to\bar{K}\ell_1\bar{\ell}_2\gamma} = \frac{1}{m_B}\left(\int \rho_a \left[|\mathcal{A}^{(1)}|^2 + \mathcal{O}(e^4)\right] d\Phi_\gamma\right) dq_a^2 dc_a \,, \tag{4.67}$$

where

$$\begin{aligned}
\rho_\ell &= \frac{1}{2^6(2\pi)^3}\frac{\lambda^{1/2}(\bar{p}_B^2, q^2, m_K^2)}{\bar{p}_B^2 q^2}\lambda^{1/2}(q^2, m_{\ell_1}^2, m_{\ell_2}^2) \,, \\
\rho_0 &= \frac{1}{2^6(2\pi)^3}\frac{\lambda^{1/2}(m_B^2, q_0^2, m_K^2)}{m_B^2 q_0^2}\frac{1}{\omega^2}\lambda(q_0^2, m_{\ell_1}^2, (k+\ell_2)^2) \,,
\end{aligned} \tag{4.68}$$

where λ is the Källén function (4.21), and ω^2 is given in (4.34). $\frac{\rho_0}{\rho_\ell} = \det\frac{\partial(q^2, c_\ell)}{\partial(q_0^2, c_0)}$ is the Jacobian which can be computed from the defining equation (4.1) and the kinematic parameterisations given in section 4.3. Moreover, the Lorentz-invariant photon phase space integral reads

$$\begin{aligned}
\int_{m_\gamma}^{E_\gamma^{\max}} d\Phi_\gamma &\equiv \frac{1}{(2\pi)^3}\int_{m_\gamma}^{E_\gamma^{\max}} \frac{d^3k}{2E_\gamma} \\
&= \frac{1}{2(2\pi)^3}\int_{m_\gamma}^{(E_\gamma^{(i)})^{\max}} dE_\gamma^{(i)} |\vec{k}^{\,(i)}| \int d\Omega_\gamma^{(i)} \Theta\big[f^{(i)}(E_\gamma^{(i)}, \theta_\gamma^{(i)}, \phi_\gamma^{(i)})\big] \,,
\end{aligned} \tag{4.69}$$

with

$$(E_\gamma^{(1)})^{\max} = \frac{m_B^2 + m_\gamma^2 - (q + m_K)^2}{2m_B} \,, \quad (E_\gamma^{(4)})^{\max} = \frac{q_0^2 + m_\gamma^2 - (m_{\ell_1} + m_{\ell_2})^2}{2q_0} \,, \tag{4.70}$$

where the former and the latter correspond to the $\{q^2, \theta_\ell\}_{a=\ell}$ and $\{q_0^2, \theta_0\}_{a=0}$ variables respectively, and $q_a \equiv \sqrt{q_a^2}$ is understood in this context. The restriction on the angles is

$$\Theta\big[f^{(i)}(E_\gamma^{(i)}, \theta_\gamma^{(i)}, \phi_\gamma^{(i)})\big] = \begin{cases} 1 & i = 1 \\ \Theta[D(E_\gamma^{(4)}, \theta_\gamma^{(4)}, \phi_\gamma^{(4)}, q_0^2, c_0)] & i = 4 \end{cases} \,, \tag{4.71}$$

with the function D defined in (4.32). The reason why the restriction in the (4)-RF, appropriate for the $\{q_0^2, c_0\}$-variables, is non-trivial is that for certain given values of $\{q_0^2, c_0\}$, the true maximum photon energy is a function of the photon angles and is in general below $(E_\gamma^{(4)})^{\max}$. We find it most convenient to implement

the kinematic restrictions via the step-function $\Theta(x)$. Notice, however, that in the limit of $m_{\ell_1} \to 0$, the step-function $\Theta(x)$ becomes redundant, since the function D is then positive for all kinematic configurations, as can be seen from Eq. (4.32).

To obtain $(E_\gamma^{(1)})^{\max}$, consider

$$\begin{aligned}(p_B - k)^2 &= m_B^2 - 2m_B E_\gamma^{(1)} + m_\gamma^2 \\ &= (p_K + q)^2 \,. \end{aligned} \tag{4.72}$$

$E_\gamma^{(1)} = (E_\gamma^{(1)})^{\max}$ when $(p_K + q)^2$ is minimum, and this corresponds to the case when the kaon is also at rest in the rest frame of q. Note that this maximum is completely independent of the lepton angle θ_ℓ.

On the other hand, the way $(E_\gamma^{(4)})^{\max}$ is derived in Eq. (4.70) makes an assumption on the angles in the kinematics. To see this, consider

$$\begin{aligned} q^2 &= (q_0 - k)^2 \\ &= m_\gamma^2 - 2q_0 E_\gamma^{(4)} + q_0^2. \end{aligned} \tag{4.73}$$

As with the derivation of $(E_\gamma^{(1)})^{\max}$, the maximum of $E_\gamma^{(4)}$ happens when q^2 is minimum. However, to say that this happens when $q^2 = (m_{\ell_1} + m_{\ell_2})^2$ implies that in the q_0-RF, the leptons ℓ_1 and ℓ_2 move in the *same* direction, and both move in the opposite direction to the photon. The restriction on the angles is thus evident, and this is why the Heaviside theta had to be introduced in Eq. (4.71). As pointed out earlier, the restriction on the angles becomes obsolete when $m_{\ell_1} \to 0$, as the lepton ℓ_1, wrt which the angle c_0 is defined, can be assigned zero energy for any values of $\{q_0^2, c_0\}$. We have numerically checked that in both RFs, the volume of the phase space is the same.

In the $\{q^2, \theta_\ell\}_{a=\ell}$ case, one can conveniently work with the Lorentz invariant variable $\bar{p}_B^2$, related to $E_\gamma^{(1)}$ through Eq. (4.72). Moreover, since the passage from $E_\gamma^{(1)}$ to $E_\gamma^{(2)}$ is independent of the photon angles, the replacement $d\Omega_\gamma^{(1)} \to d\Omega_\gamma^{(2)}$ is allowed. The photon phase space then assumes the form

$$\int_{m_\gamma}^{E_\gamma^{\max}} d\Phi_\gamma \to \frac{1}{2^3(2\pi)^3} \int_{(q+m_K)^2}^{(m_B - m_\gamma)^2} d\bar{p}_B^2 \frac{\lambda^{1/2}(m_B^2, \bar{p}_B^2, m_\gamma^2)}{m_B^2} \int d\Omega_\gamma^{(1,2)} \,. \tag{4.74}$$

The upper limit on $\bar{p}_B^2$ (corresponding to smallest possible photon energy) is obtained by setting $E_\gamma^{(1)} = m_\gamma$ into Eq. (4.72).

The non-radiative $\bar{B} \to \bar{K}\ell_1\bar{\ell}_2$ rate is given by

$$d^2\Gamma_{\bar{B}\to\bar{K}\ell_1\bar{\ell}_2} = \frac{\rho_\ell|_{\bar{p}_B^2\to m_B^2}}{m_B}\left\{|\mathcal{A}^{(0)}|^2 + 2\mathrm{Re}[\mathcal{A}^{(0)}(\mathcal{A}^{(2)})^*] + \mathcal{O}(e^4)\right\} dq^2 dc_\ell \,. \quad (4.75)$$

Since there is no photon-emission in this case, there is no difference between the $\{q^2, c_\ell\}$- and $\{q_0^2, c_0\}$-variables here.

4.8.2 Introduction of a physical photon energy cut-off

As anticipated, to match experimental observations, we introduce a cut-off on the maximal value of $\bar{p}_B^2$ via the parameter δ_{ex}, defined in (4.4), satisfying

$$0 < \delta_{\mathrm{ex}} < \delta_{\mathrm{ex}}^{\mathrm{inc}} = 1 - \left(\frac{q + m_K}{m_B}\right)^2 \,. \quad (4.76)$$

The value $\delta_{\mathrm{ex}}^{\mathrm{inc}}$ corresponds to the minimal value of $\bar{p}_B^2$ in a fully photon-inclusive decay. This definition translates to the following photon-energy cut-off

$$E_\gamma^{(1)} < E_\gamma^{\max(1)} = \delta_{\mathrm{ex}}\frac{m_B}{2} \,, \quad (4.77)$$

A typical choice for δ_{ex} in realistic experiments is $\delta_{\mathrm{ex}} = \mathcal{O}(0.1)$. When evaluating the photon phase space variable in the (4)-RF, appropriate for the $\{dq_0^2, dc_0\}$-variables, the cut-off can be converted by using

$$E_\gamma^{(1)} = \gamma_{q_0} E_\gamma^{(4)}(1 - \beta_{q_0}\cos\theta_\gamma^{(4)}), \quad (4.78)$$

cf. Eq. (4.30) for the Lorentz boost factors.

With the inclusion of δ_{ex}, the integral (4.69) assumes the form

$$\int_{\delta_{\mathrm{ex}}} d\Phi_\gamma = \frac{1}{2^3(2\pi)^3}\int_{m_B^2(1-\delta_{\mathrm{ex}})}^{(m_B-m_\gamma)^2} d\bar{p}_B^2 \frac{\lambda^{1/2}(m_B^2, \bar{p}_B^2, m_\gamma^2)}{m_B^2}\int d\Omega_\gamma^{(2)} \,. \quad (4.79)$$

4.9 Leading order differential rate $\frac{d^2}{dq^2 dc_\ell}\Gamma^{\rm LO}(q^2, c_\ell)$

The leading order amplitude rate is easily computed from Eq. (4.75) and the amplitude $\mathcal{A}^{(0)}_{\bar{B}\to\bar{K}\ell_1\bar{\ell}_2}$ in Eq. (4.17), and is rather simple

$$\frac{d^2}{dq^2 dc_\ell}\Gamma^{\rm LO}(q^2, c_\ell) \;= \frac{\rho_\ell|_{\bar{p}_B^2\to m_B^2}}{m_B}|\mathcal{A}^{(0)}|^2 = \; 2|g_{\rm eff}|^2\frac{\rho_\ell|_{\bar{p}_B^2\to m_B^2}}{m_B}\times$$
$$\Bigg[|C_V|^2\Big(\lambda_B f_+(q^2)^2(1-(\Delta\bar{m}_\ell)^2-\frac{\lambda_\ell}{q^4}c_\ell^2) \;+(\Delta m_{BK}^2)^2(\Delta\bar{m}_\ell)^2 f_0(q^2)^2(1-\bar{m}_{\ell_1\ell_2}^2)-$$
$$2\Delta\bar{m}_{BK}^2\,\bar{m}_{\ell_1\ell_2}\,\Delta\bar{m}_\ell\, f_0(q^2)f_+(q^2)\lambda_B{}^{1/2}\lambda_\ell^{1/2}c_\ell\Big) + |C_A|^2\Big(\bar{m}_{\ell_1\ell_2}\leftrightarrow\Delta\bar{m}_\ell\Big)\Bigg]\,, \tag{4.80}$$

where $\lambda_\ell = \lambda(q^2, m_{\ell_1}^2, m_{\ell_2}^2)$, $\Delta\bar{m}_\ell = \bar{m}_{\ell_1} - \bar{m}_{\ell_2}$, $\bar{m}_{\ell_1\ell_2} = \bar{m}_{\ell_1} + \bar{m}_{\ell_2}$, $\Delta m_{BK}^2 = m_B^2 - m_K^2$, with ρ_ℓ as in (4.68), and all barred quantities are dimensionless by division with appropriate powers of q. In the limit of equal lepton masses ($m_{\ell_1} = m_{\ell_2} \equiv m_\ell$), the above equation reduces to

$$\frac{d^2}{dq^2 dc_\ell}\Gamma^{\rm LO}(q^2, c_\ell) = 2|g_{\rm eff}|^2\frac{\rho_\ell|_{\bar{p}_B^2\to m_B^2}}{m_B}\Big(|C_V|^2(\lambda_B f_+(q^2)^2(1-\beta_\ell^2 c_\ell^2))+ \tag{4.81}$$
$$|C_A|^2(\lambda_B f_+(q^2)^2(1-c_\ell^2)\beta_\ell^2 + 4f_0(q^2)^2\bar{m}_\ell^2(\Delta m_{BK}^2)^2)\Big)\,,$$

with $\beta_\ell = \sqrt{1-4m_\ell^2/q^2}$ and $\lambda_B = \lambda(m_B^2, q^2, m_K^2)$.

Chapter 5

QED corrections to $\bar{B} \to \bar{K}\ell^+\ell^-$: Treatment of IR divergences

In order to track the IR divergences it is convenient to split the differential rate as follows.

$$\begin{aligned} d^2\Gamma_{\bar{B}\to\bar{K}\ell_1\bar{\ell}_2}(\delta_{\rm ex}) &= d^2\Gamma^{\rm LO} + \frac{\alpha}{\pi}\sum_{i,j}\hat{Q}_i\hat{Q}_j\left(\mathcal{H}_{ij} + \mathcal{F}_{ij}^{(a)}(\delta_{\rm ex})\right)\, dq_a^2 dc_a + \mathcal{O}(e^4)\,, \\ &= d^2\Gamma^{\rm LO}\left[1 + \Delta^{(a)}(q_a^2, c_a; \delta_{\rm ex})\right]\, dq_a^2 dc_a + \mathcal{O}(e^4)\,, \end{aligned} \tag{5.1}$$

where $d^2\Gamma^{\rm LO}$ corresponds to the zeroth order term in (4.80), the sums on the charges is understood as in (4.36), and and $\mathcal{H}$ and $\mathcal{F}$ stand for the virtual and real contributions respectively. More precisely, $\mathcal{H}_{ij}$ and $\mathcal{F}_{ij}$ are related to the amplitudes as follows

$$\begin{aligned} \frac{\alpha}{\pi}\sum_{i,j}\hat{Q}_i\hat{Q}_j\mathcal{H}_{ij} &= \frac{1}{m_B}\rho_\ell|_{\vec{p}_B^{\,2}\to m_B^2}\, 2{\rm Re}[\mathcal{A}^{(2)*}\mathcal{A}^{(0)}]\,, \\ \frac{\alpha}{\pi}\sum_{i,j}\hat{Q}_i\hat{Q}_j\mathcal{F}_{ij}^{(a)} &= \frac{1}{m_B}\int d\Phi_\gamma\, \rho_a\, |\mathcal{A}^{(1)}|^2\,, \end{aligned} \tag{5.2}$$

where $d\Phi_\gamma$ and ρ_a are defined in (4.68) and (4.69) respectively.

In standard fashion, the integrals are split into divergent parts which can be done analytically and a necessarily regular part which is dealt with numerically. We

parameterise this decomposition as follows.

$$\begin{aligned}\mathcal{H}_{ij} &= \frac{d^2\Gamma^{\rm LO}}{dq^2 dc_\ell}\left(\tilde{\mathcal{H}}_{ij}^{(s)} + \tilde{\mathcal{H}}_{ij}^{(hc)}\right) + \Delta\mathcal{H}_{ij}\ , \\ \mathcal{F}_{ij}^{(a)}(\delta_{\rm ex}) &= \frac{d^2\Gamma^{\rm LO}}{dq^2 dc_\ell}\tilde{\mathcal{F}}_{ij}^{(s)}(\omega_s) + \tilde{\mathcal{F}}_{ij}^{(hc)(a)}(\underline{\delta}) + \Delta\mathcal{F}_{ij}^{(a)}(\underline{\delta})\ ,\end{aligned} \tag{5.3}$$

with $\tilde{\mathcal{H}}_{ij}^{(s)}$ ($\tilde{\mathcal{H}}_{ij}^{(hc)}$) and $\tilde{\mathcal{F}}_{ij}^{(s)}$ ($\tilde{\mathcal{F}}_{ij}^{(hc)(a)}$), to be defined further below, containing all soft (hard-collinear) singularities, whereas $\Delta\mathcal{H}$ and $\Delta\mathcal{F}$ are regular (even in the limit $m_{\ell_{1,2}} \to 0$). In order to split the real emission part, besides the previously introduced physical cut-off $\delta_{\rm ex}$, we adopt the phase space slicing method [15], which requires the introduction of two auxiliary (unphysical) soft and hard-collinear cut-offs, ω_s and ω_c respectively,

$$\underline{\delta} \equiv \{\delta_{\rm ex}, \omega_s, \omega_c\}\ , \quad \omega_s \ll 1\ , \quad \frac{\omega_c}{\omega_s} \ll 1\ . \tag{5.4}$$

We remind the reader that $\delta_{\rm ex}$ has been introduced for meaningful comparison with experimental data and mention for clarity that $\tilde{\mathcal{F}}_{ij}^{(hc)(a)}$ is singular in the $m_{\ell_{1,2}} \to 0$ limit but finite for $m_{\ell_{1,2}} \neq 0$.

As already implicit in the decomposition (5.3), soft divergences cancel at the differential level independent of the choice of kinematic variables. This is not the case for hard-collinear singularities, given that the hard-collinear integral ($\tilde{\mathcal{F}}_{ij}^{(hc)(a)}$) is not proportional to the non-radiative kinematics. Without the physical cut-off $\delta_{\rm ex}$, the cancellation of both types of divergences proceeds as in standard in textbooks discussions (see e.g. [89, 105, 106]). However, the choice of a photon energy cut-off, associated with a preferred frame, makes it significantly more involved compared to the semileptonic case [107]. A detailed discussion of the soft singularities and collinear logs follows below, along with the definitions of the $\tilde{\mathcal{F}}$ and $\tilde{\mathcal{H}}$. Particular emphasis is given to single out which observables are IR-safe and not.

5.1 Cancellation of soft divergences at differential level

As far as $\mathcal{A}^{(2)}_{1PI}$ is concerned, soft singularities can be isolated as follows

$$\mathcal{A}^{(2)}_{1PI} = \frac{1}{2}\frac{\alpha}{\pi}\mathcal{A}^{(0)}\sum_{i\neq j}\hat{Q}_i\hat{Q}_j(\hat{p}_i\cdot\hat{p}_j)C_0(m_i^2,m_j^2,(\hat{p}_i+\hat{p}_j)^2,m_i^2,m_\gamma^2,m_j^2) + \text{non-soft}\ , \tag{5.5}$$

where the explicit expression of the C_0 function can be found in App. E, including its various limits. Here, $\hat{p}^{\text{in}} = -p^{\text{in}}$, $\hat{p}^{\text{out}} = p^{\text{out}}$ in analogy with the hatted charges (and $p_{\ell_{1,2}} \equiv \ell_{1,2}$). Note that (5.5) is consistent with the crossing rule of reversing momenta and charge when passing from in(out)- to out(in)-state.

The soft singularities in the virtual corrections are encoded in the triangle functions C_0 in (5.5) and the self energy contributions in (4.44). Combining them, we define[1]

$$\begin{aligned}\tilde{\mathcal{H}}^{(s)}_{ij} &\overset{\text{def}}{=} (1-\delta_{ij})(\hat{p}_i\cdot\hat{p}_j)\text{Re}[C_0(m_i^2,m_j^2,(\hat{p}_i+\hat{p}_j)^2,m_i^2,m_\gamma^2,m_j^2)] + \delta_{ij}\times\delta Z_i^{(1)} \\ &= -r_{\text{soft}}\left\{(1-\delta_{ij})\frac{\hat{p}_i\cdot\hat{p}_j}{m_im_j}\frac{x_{ij}}{(1-x_{ij}^2)}\ln|x_{ij}| + \delta_{ij}\frac{1}{2}\right\} + \mathcal{O}(f_{\mathcal{R}})\ ,\end{aligned} \tag{5.6}$$

where $f_{\mathcal{R}}$ stands for IR finite terms, including regularisation-dependent ones. The x_{ij}-variables are given by

$$x_{ij} \equiv \frac{\sqrt{y_{ij}}-1}{\sqrt{y_{ij}}+1}\ , \quad y_{ij} \equiv \frac{(\hat{p}_i+\hat{p}_j)^2-(m_i+m_j)^2+i0}{(\hat{p}_i+\hat{p}_j)^2-(m_i-m_j)^2+i0}\ . \tag{5.7}$$

Considering the soft part of the real emission amplitude, namely the Low part of the amplitude in (4.37), we define[2]

$$\tilde{\mathcal{F}}^{(s)}_{ij}(\omega_s) \overset{\text{def}}{=} (2\pi)^2\int_{\omega_s}\frac{-p_i\cdot p_j}{(k\cdot p_i)(k\cdot p_j)}d\Phi_\gamma = (2\pi)^2\int_{\omega_s}\frac{-\hat{p}_i\cdot\hat{p}_j}{(k\cdot\hat{p}_i)(k\cdot\hat{p}_j)}d\Phi_\gamma$$

[1] In reality, the $\ln|x_{ij}|$ that appears in the C_0 function really is $\ln(x_{ij})$, see App. E. Taking the real part then corresponds to taking the modulus of the argument. Note that while x_{ij} appears to be negative from Eq. (5.7), it can be positive when it involves an initial state particle, the B-meson in this case.

[2] The argument of the log comes with a modulus here by construction. When the integral is evaluated, it naturally comes with a $\ln\left[\left(\frac{1+\beta_{ij}}{1-\beta_{ij}}\right)^2\right] \equiv \ln x_{ij}^2 = 2\ln|x_{ij}|$. See Eq. (5.10) and Eq. (5.11) for more details.

$$
\begin{aligned}
&= -K_{\mathcal{R}}(\omega_s) I_{ij}^{(0)} + \mathcal{O}(f_{\mathcal{R}}) \\
&= [r_{\text{soft}} - 2\ln(\omega_s)] \left\{ (1-\delta_{ij}) \frac{\hat{p}_i \cdot \hat{p}_j}{m_i m_j} \frac{x_{ij}}{(1-x_{ij}^2)} \ln|x_{ij}| + \delta_{ij} \frac{1}{2} \right\} + \mathcal{O}(f_{\mathcal{R}}) \ , \quad (5.8)
\end{aligned}
$$

where the $\mathcal{O}(f_{\mathcal{R}})$ terms can be found in App. D.2. In the first line, changing the 4-momenta from unhatted to hatted leaves the integral invariant, as there are an even number of each 4-momentum in the expression. As can be checked, the sum $\tilde{\mathcal{H}}_{ij}^{(s)} + \tilde{\mathcal{F}}_{ij}^{(s)}(\omega_s)$ is free from soft divergences and this ensures their cancellation at the differential level. Moreover, the individual $\mathcal{F}_{ij}$ are gauge dependent (the result is presented for $\xi = 1$), whereas in the sum over all charges, gauge dependence disappears. This includes $\ln^2 m_{\ell_{1,2}}$-terms which cancel when the real and virtual terms are summed up: these are genuine soft-collinear terms, which cancel as a result of the cancellation of the soft divergences.

In order to track the $\ln m_\ell$ terms, note that

$$
x_{ij} \to -\frac{m_i m_j}{(\hat{p}_i + \hat{p}_j)^2}, \tag{5.9}
$$

for $(\hat{p}_i + \hat{p}_j)^2 \gg m_{i,j}^2$. Moreover it is worth pointing out that one can write $I_{ij}^{(0)}$ in terms of physically transparent variables,

$$
I_{ij}^{(0)} = \frac{1}{2\beta_{ij}} \ln\left(\frac{1+\beta_{ij}}{1-\beta_{ij}} \right), \tag{5.10}
$$

with

$$
\beta_{ij} = \frac{\beta_i + \beta_j}{1 + \beta_i \beta_j}, \tag{5.11}
$$

being the relativistic addition of the velocities of the two particles $\beta_i \equiv |\vec{p}_i|/E_i$ in the ij-RF.

We note that as a result of these cancellations, scheme dependent terms due to IR regularisation disappear as well.

The crucial step in evaluating (5.8) is that, neglecting finite terms, the integral over the photon energy and the photon angles factorises: the angular integral $I_{ij}^{(0)}$ alone becomes separately Lorentz invariant (i.e. frame independent) and can be performed in the RF of the radiating pair, where it is particularly simple (see

App. D for more details). The energy and angular integral evaluate to

$$K_{\mathcal{R}}(\omega_s) \quad = \quad -\frac{1}{2} r_{\text{soft}} + \ln\left(\frac{m_B}{\mu}\right) + \ln(\omega_s) + \mathcal{O}(\omega_s) \;, \tag{5.12}$$

and

$$I_{ij}^{(0)} = \begin{cases} 1 & i = j \;, \\ 2\frac{\hat{p}_i \cdot \hat{p}_j}{m_i m_j} \frac{x_{ij}}{1-x_{ij}^2} \ln|x_{ij}| & i \neq j \;. \end{cases} \tag{5.13}$$

We wish to emphasise that there are single collinear logs, $\ln m_{\ell_{1,2}}$, in $\tilde{\mathcal{H}}_{ij}^{(s)} + \tilde{\mathcal{F}}_{ij}^{(s)}(\omega_s)$ which match up with corresponding terms in $\tilde{\mathcal{H}}_{ij}^{(hc)} + \tilde{\mathcal{F}}_{ij}^{(hc)}(\underline{\delta})$. The procedure is therefore well set-up for tracking analytically after what phase space integration IR sensitive terms cancel against each other.

However, since there remain $\ln \omega_s$-terms in the analytic expression one might wonder whether this leads to a numerically stable integral. We have found that the phase space integral is stable when using a Monte Carlo integration on the photon variables for suitably chosen values of ω_s, see Sec. 6.1. Alternatively, one might use the dipole subtraction method [108] as applied to QED [109–111].

5.2 Hard-collinear virtual contribution $\tilde{\mathcal{H}}^{(hc)}$

The hard-collinear virtual contribution, after summing over charges, is given by

$$\begin{aligned} \tilde{\mathcal{H}}^{(hc)} &\stackrel{\text{def}}{=} \sum_{i,j} \hat{Q}_i \hat{Q}_j \tilde{\mathcal{H}}_{ij}^{(hc)} \\ &= -\hat{Q}_{\ell_1} \left(\hat{Q}_{\bar{\ell}_2} + \hat{Q}_{\bar{B}} + \hat{Q}_{\bar{K}}\right) \left(\frac{\mu^2}{4\pi}\right)^{\epsilon_{\text{UV}}} B_0(m_{\ell_1}^2, 0, m_{\ell_1}^2)\Big|_{\ln m_{\ell_1}} + \{1 \leftrightarrow 2\} \\ &= 2\hat{Q}_{\ell_1} \left(\hat{Q}_{\bar{\ell}_2} + \hat{Q}_{\bar{B}} + \hat{Q}_{\bar{K}}\right) \ln\left(\frac{m_{\ell_1}}{\mu}\right) + \{1 \leftrightarrow 2\} \\ &= -2\hat{Q}_{\ell_1}^2 \ln\left(\frac{m_{\ell_1}}{\mu}\right) + \{1 \leftrightarrow 2\}, \end{aligned} \tag{5.14}$$

where only terms proportional to $\ln m_{\ell_{1,2}}$ were kept. In the simplification, $\left(\frac{\mu^2}{4\pi}\right)^{\epsilon_{\text{UV}}} B_0(m^2, 0, m^2) = \frac{1}{\hat{\epsilon}_{\text{UV}}} - 2\ln(m/\mu) + 2 + \mathcal{O}(\epsilon)$ and charge conservation were used. The bubble integral B_0 is given in App. E.

5.3 The hard-collinear integral $\tilde{\mathcal{F}}^{(hc,a)}$

We evaluate the hard-collinear integral using the phase space slicing method [15] following the specific recipe in [112]. The integral is given by

$$\begin{aligned}\frac{\alpha}{\pi}\tilde{\mathcal{F}}^{(hc,a)}(\underline{\delta}) &= \frac{\alpha}{\pi}\sum_{i,j}\hat{Q}_i\hat{Q}_j\tilde{\mathcal{F}}_{ij}^{(hc,a)}(\underline{\delta}) \\ &= \frac{1}{m_B}\int_{\omega_s}^{\delta_{\rm ex}}\rho_a^{\ell_1||\gamma}(\omega_c)\,|\mathcal{A}^{(1)}_{\ell_1||\gamma}|^2 d\Phi_\gamma \;+\; \{1\leftrightarrow 2\}\;, \qquad (5.15)\end{aligned}$$

where $|\mathcal{A}^{(1)}_{\ell_1||\gamma}|^2$ is the part of $|\mathcal{A}^{(1)}|^2$ proportional to $1/(k\cdot\ell_1)$ when $m_{\ell_1}\to 0$ which includes contributions beyond the Low term. Note that the photon-energy integral runs from ω_s till $\delta_{\rm ex}$, consistent with (5.3) where the soft modes have already been absorbed into $\tilde{\mathcal{F}}_{ij}^{(s)}(\omega_s)$. The phase space factor $\rho_a^{\ell_1||\gamma}(\omega_c)$ is defined as

$$\rho_a^{\ell_1||\gamma}(\omega_c) = \rho_a\,\Theta(\omega_c m_B^2 - k\cdot\ell_1)\;, \qquad (5.16)$$

where ρ_a is defined in (4.68) , the meaning of the integration boundaries can be inferred from (4.79), and the step-function encodes the phase space slicing. The quantity $\omega_c \ll 1$ then implies that k and ℓ_1 are nearly collinear.

5.3.1 Phase space slicing of the hard-collinear integral

In the phase space slicing method, the photon and the light particle it is emitted from, are effectively treated as a single particle. This follows up on the intuitive picture that a particle and its collinear photon are hard to disentangle. Below, we give the explicit expressions for $\ell_1||\gamma$, and the $\ell_2||\gamma$ case is obtained in a completely analogous fashion. Formally, one decomposes the phase space as follows.

$$d\Phi_{\bar{B}\to\bar{K}\ell_1\bar{\ell}_2\gamma} = d\Phi_{\bar{B}\to\bar{K}\ell_{1\gamma}\bar{\ell}_2}d\Phi_\gamma\frac{E_{\ell_{1\gamma}}}{E_{\ell_1}}\;. \qquad (5.17)$$

The collinear region is parameterised by $\ell_1 = z\ell_{1\gamma}$, where $\ell_{1\gamma}\equiv\ell_1+k$, assuming that the transverse part can be neglected in order to extract the collinear logs. The two parts in (5.17) then assume the form

$$d\Phi_\gamma\frac{E_{\ell_{1\gamma}}}{E_{\ell_1}} \quad\to \frac{1}{16\pi^2}dz\;d\ell_{1\gamma}^2\;,$$

$$d\Phi_{\bar{B}\to\bar{K}\ell_{1\gamma}\bar{\ell}_2} \to \frac{1}{2^5(2\pi)^3}\frac{\lambda^{1/2}(m_B^2,q_0^2,m_K^2)}{m_B^2}dq_0^2dc_0\ . \tag{5.18}$$

In those variables, the amplitude squared assumes the form (in the $\xi = 1$ gauge)

$$\begin{aligned}|\mathcal{A}^{(1)}_{\ell_1\|\gamma}|^2 &= \frac{e^2}{(k\cdot\ell_1)}\hat{Q}_{\ell_1}\Bigg[\hat{Q}_{\ell_1}(1-z) - \frac{2z}{1-z}\left(\hat{Q}_{\bar{\ell}_2}+\hat{Q}_{\bar{B}}+\hat{Q}_{\bar{K}}\right)\\ &\quad - \hat{Q}_{\ell_1}\frac{m_{\ell_1}^2}{k\cdot\ell_1}\Bigg]|\mathcal{A}^{(0)}_{\ell_1\|\gamma}|^2 + \mathcal{O}(m_{\ell_1}^2)\\ &= \frac{e^2}{(k\cdot\ell_1)}\hat{Q}_{\ell_1}^2\left(\tilde{P}_{f\to f\gamma}(z) - \frac{m_{\ell_1}^2}{k\cdot\ell_1}\right)|\mathcal{A}^{(0)}_{\ell_1\|\gamma}(q_0^2,c_0)|^2\Big|_{\bar{B}\to\bar{K}\ell_{1\gamma}\bar{\ell}_2} + \mathcal{O}(m_{\ell_1}^2)\ ,\end{aligned} \tag{5.19}$$

where $|\mathcal{A}^{(0)}_{\ell_1\|\gamma}|^2 = |\mathcal{A}^{(0)}_{\bar{B}\to\bar{K}\ell_{1\gamma}\bar{\ell}_2}|^2$ and $\tilde{P}_{f\to f\gamma}(z)$ is the collinear emission part of the splitting function for a fermion to a photon[3]

$$\tilde{P}_{f\to f\gamma}(z) \equiv \left(\frac{1+z^2}{1-z}\right)\ , \tag{5.20}$$

and the $m_{\ell_1}^2/(k\cdot\ell_1)$ term is immaterial for the hard-collinear logs per se but of importance for the numerics as it captures relevant $\ln\omega_s$ terms (which have to cancel when all contributions are added). The LO order matrix element squared in (5.19), was given in section 4.9. The first line in (5.19) is gauge dependent whereas the second is not since charge conservation has been applied. This is further manifested by the appearance of the splitting function which is a universal object.

5.3.2 $\tilde{\mathcal{F}}^{(hc,0)}$, structure of collinear singularities in $dq_0^2dc_0$

Taking (5.15) and using the integration measure $d\Phi_\gamma$ in (5.18) one arrives at

$$\begin{aligned}\tilde{\mathcal{F}}^{(hc,0)}(\underline{\delta}) = \frac{1}{2^{10}\pi^3 m_B^3}\Bigg(&\hat{Q}_{\ell_1}^2\int_{\max(z(\delta_{\rm ex}),0)}^{z(\omega_s)}\tilde{f}^{(hc)}(c_0,m_{\ell_1},\omega_c)dz\ +\\ &\hat{Q}_{\bar{\ell}_2}^2\int_{\max(z'(\delta_{\rm ex}),0)}^{z'(\omega_s)}\tilde{f}^{(hc)}(-c_0,m_{\ell_2},\omega_c)dz\Bigg)\ ,\end{aligned} \tag{5.21}$$

[3] No prescription is required when $z\to 1$, in our case, as this soft region has been treated in another section and is cut off by ω_s. c.f. section 6.1.4 for a discussion involving the full splitting function.

where the boundaries on z are determined by the phase space slicing cut-off ω_s and the real photon energy cut-off $\delta_{\rm ex}$ (4.4),

$$z(\delta) = z(\delta, q_0^2, c_0) = 1 - \frac{\delta}{1 - \hat{s}_{K\ell_2}(q_0^2, c_0)} \,, \tag{5.22}$$

with

$$\hat{s}_{K\ell_2} \equiv (\hat{p} + \hat{\ell}_2)^2 = \frac{1}{2}\left(1 - \hat{q}_0^2 + \hat{m}_K^2 - c_0\,\lambda^{1/2}\left(1, \hat{q}_0^2, \hat{m}_K^2\right)\right), \tag{5.23}$$

and $z' = z|_{c_0 \to -c_0}$.

Note that in the (4)-frame, the collinear limit forces the pair of particles (either $\ell_{1\gamma}$ and ℓ_2, or $\ell_{2\gamma}$ and ℓ_1) to move in opposite directions. Since c_0 is defined w.r.t. ℓ_1, this explains the $c_0 \to -c_0$ procedure to obtain the corresponding formulae for $\ell_2||\gamma$.

Hard-collinear logs are proportional to Q_i^2, where $i = \ell_1, \bar{\ell}_2$. Furthermore, we note that in the collinear limit, $c_0 \to -c_0$ reverses the momenta $\ell_{1\gamma}$ and ℓ_2 (or correspondingly, ℓ_1 and $\ell_{2\gamma}$). This implies that the symmetry discussed in Sec. 4.7 extends to the (4)-frame for the hard-collinear logs, and hence, Eq. (5.21) possesses this symmetry as well.

The integrand in (5.21) reads

$$\tilde{f}^{(hc)}(c_0, m_\ell, \omega_c) = \lambda^{1/2}(m_B^2, q_0^2, m_K^2)|\mathcal{A}^{(0)}_{m_\ell \to 0}(q_0^2, c_0)|^2 \left(\tilde{P}_{q\to q\gamma}(z)\, j^{hc} - j^{hc}_{(m_{\ell_1})}\right) \,, \tag{5.24}$$

with the LO amplitude squared given in section 4.9 (in terms of q^2, c_ℓ though) and the j^{hc}'s are functions of z, m_{ℓ_1} and the collinear scale ω_c,

$$\begin{aligned} j^{hc}(z, \omega_c, m_{\ell_1}) &= \int_{\frac{1-z}{2z} m_{\ell_1}^2}^{\omega_c m_B^2} \frac{d(k\cdot\ell_1)}{k\cdot\ell_1} = \ln\frac{2\omega_c z}{\hat{m}_{\ell_1}^2(1-z)} \,, \\ j^{hc}_{(m_{\ell_1})}(z, \omega_c, m_{\ell_1}) &= \int_{\frac{1-z}{2z} m_{\ell_1}^2}^{\omega_c m_B^2} \frac{m_{\ell_1}^2\, d(k\cdot\ell_1)}{(k\cdot\ell_1)^2} = \frac{2z}{1-z} - \frac{\hat{m}_{\ell_1}^2}{\omega_c} \,. \end{aligned} \tag{5.25}$$

Here and below, hatted quantities are normalised w.r.t. the m_B mass, i.e. $\hat{m}_K = m_K/m_B$. The upper integration boundary on $d\ell_{1\gamma}^2$ correspond to (5.16). For the lower integration boundary, we first note that in dim reg, it would be simply zero, and the IR regulator would appear in the integrand instead (as a power involving ϵ). Since we are performing the calculation in mass regularisation, we expect the

lower limit to be of $\mathcal{O}\left(m_{\ell_1}^2\right)$. To understand the lower boundary, consider

$$\begin{aligned} k{\cdot}\ell_1 &= E_1 E_\gamma \left(1-\beta_{\ell_1}\cos\theta_{\ell_1\gamma}\right) \\ &\approx E_1 E_\gamma \left(1-\beta_{\ell_1}\right) \\ &\approx E_1 E_\gamma \left(\frac{m_{\ell_1}^2}{2E_1^2}\right) \\ &\approx \frac{m_{\ell_1}^2\left(1-z\right)}{2z}, \end{aligned} \tag{5.26}$$

where we have used the collinear limit $\cos\theta_{\ell_1\gamma} \to 1$ in going from the first to second line, and $\beta_{\ell_1} = \sqrt{1-\frac{m_{\ell_1}^2}{E_1^2}} \approx 1-\frac{m_{\ell_1}^2}{2E_1^2}$ in going to the third line, and then finally used the parametrisation $\ell_1 = z\ell_{1\gamma}$ and $k = (1-z)\,\ell_{1\gamma}$, valid in the collinear limit.

As can be seen from Eq. (5.25), only $j^{hc}(z,\omega_c,m_{\ell_1})$ contains collinear divergences, appearing in the form of $\ln m_{\ell_1}$. However, as mentioned earlier, $j^{hc}_{(m_{\ell_1})}(z,\omega_c,m_{\ell_1})$ is needed since, when integrated over z, it produces a $\ln\omega_s$ term, due to the factor of $(1-z)$ in the denominator. We finally point out that the situation is much simpler in dim reg, since such a term simply vanishes.[4]

The boundary for z in Eq. (5.22) is derived as follows. We consider the $m_K \to 0$ limit here for simplicity (for the numerics, we kept $m_K \neq 0$ of course). We know that with photon energy cuts, the range of $\bar{p}_B^2$ is

$$m_B^2\left(1-\delta_{\rm ex}\right) \leq \bar{p}_B^2 \leq m_B^2\left(1-\omega_s\right). \tag{5.27}$$

But

$$\begin{aligned} \bar{p}_B^2 &= \left(p_K+\ell_1+\ell_2\right)^2 \\ &= 2\ell_1{\cdot}\left(p_K+\ell_2\right)+\left(p_K+\ell_2\right)^2 \\ &= z\left(2\ell_{1\gamma}{\cdot}p_K+2\ell_{1\gamma}{\cdot}\ell_2\right)+s_{K\ell_2} \\ &= z\left(m_B^2-s_{K\ell_2}\right)+s_{K\ell_2}, \end{aligned} \tag{5.28}$$

[4]One might wonder how independence of the result on ω_s is maintained in the dim reg case. The answer is that the corresponding soft integral (in this case, $\mathcal{F}^{(s)}_{\ell_1\ell_1}$), which has exactly the opposite sign as the term arising here in the hard-collinear integral, also vanishes in dim reg.

where in the last line, we have used

$$m_B^2 = p_B^2 = (\ell_{1\gamma} + \ell_2 + p_K)^2 = 2\ell_{1\gamma}\cdot p_K + 2\ell_{1\gamma}\cdot\ell_2 + s_{K\ell_2}. \tag{5.29}$$

Solving the inequality in Eq. (5.27) using $\bar{p}_B^2$ in Eq. (5.28) gives the z integral boundary in Eq. (5.22). We note that while the presentation assumes $m_K \to 0$, the final result in Eq. (5.22) is the same. Furthermore, the derivation for the same limit for $\ell_2||k$ follows through in exactly the same way, with $\ell_1 \leftrightarrow \ell_2$.

We stress that the fully inclusive limit does *not* simply imply $\delta_{\rm ex} \to 1$; rather, it merely means that there are no phase space cuts on the photon energy. In this case, this corresponds to $z = 0$. This is precisely the reason why the max. condition has been used on the integration boundaries in Eq. (5.21), as a specific $\delta_{\rm ex}$ can make the z-boundary negative for some regions of the phase space, characterised by $\{q_0^2, c_0\}$.

In the case of the $\{q_0^2, c_0\}$-variables, as adapted in this section, (5.21) can be simplified considerably

$$\tilde{\mathcal{F}}^{(hc,0)}(\underline{\delta}) = \frac{\lambda^{1/2}(m_B^2, q_0^2, m_K^2)}{2^{10}\pi^3 m_B^3}\left(|\mathcal{A}^{(0)}(q_0^2, c_0)|^2\, \hat{Q}_{\ell_1}^2\, J^{(hc,0)}(\underline{\delta}) + \ \{1, c_0 \leftrightarrow 2, -c_0\}\right)\ , \tag{5.30}$$

and the remaining hard-collinear integral $J^{(hc,0)}$ is easily evaluated [5]

$$\begin{aligned} J^{(hc,0)}(\underline{\delta}) &= \int_{z(\delta_{\rm ex})}^{z(\omega_s)} dz\left(\tilde{P}_{q\to q\gamma}(z)\, j^{hc} - j^{hc}_{(m_{\ell_1})}\right) \\ &= A(\delta_{\rm ex}, \omega_s)\ln\frac{m_{\ell_1}^2}{2\omega_c m_B^2} + B(\delta_{\rm ex}, \omega_s, m_{\ell_1})\ , \end{aligned} \tag{5.31}$$

where

$$\begin{aligned} A(\delta_{\rm ex}, \omega_s) &= \frac{1}{2}(z(\omega_s) - z(\delta_{\rm ex}))(2 + z(\omega_s) + z(\delta_{\rm ex})) + 2\ln\frac{\bar{z}(\omega_s)}{\bar{z}(\delta_{\rm ex})} \\ &\overset{z(\omega_s)\to 1}{\to} \frac{1}{2}\bar{z}(\delta_{\rm ex})(3 + z(\delta_{\rm ex})) + 2\ln\frac{\bar{z}(\omega_s)}{\bar{z}(\delta_{\rm ex})} \overset{z(\delta_{\rm ex})\to 0}{\to} \frac{3}{2} + 2\ln\bar{z}(\omega_s)\ , \\ B(\delta_{\rm ex}, \omega_s, m_\ell) &= \frac{1}{2}\Big[\left(z(\delta_{\rm ex})^2 + 2z(\delta_{\rm ex})\right)\ln\frac{z(\delta_{\rm ex})}{\bar{z}(\delta_{\rm ex})} - \ln\bar{z}(\delta_{\rm ex}) - 4\,{\rm Li}_2\,\bar{z}(\delta_{\rm ex}) \\ &\quad - 2\ln^2\bar{z}(\delta_{\rm ex}) - \left(3 + 2\frac{\hat{m}_\ell^2}{\omega_c}\right)z(\delta_{\rm ex}) - \{\delta_{\rm ex} \leftrightarrow \omega_s\}\Big] \end{aligned} \tag{5.32}$$

[5] Note that the lower z-integration strictly speaking involves max conditions, c.f. (5.21), and this is how we have performed the integral. However for $\delta_{\rm ex} \ll 1$, $z(\delta_{\rm ex})$ is always greater than zero, hence the simplification.

$$\overset{z(\omega_s)\to 1}{\to} \frac{1}{2}\Big[\big(z(\delta_{\rm ex})^2+2z(\delta_{\rm ex})\big)\ln\frac{z(\delta_{\rm ex})}{\bar z(\delta_{\rm ex})}-\ln\bar z(\delta_{\rm ex})-4\,{\rm Li}_2\,\bar z(\delta_{\rm ex})$$
$$+\left(3+2\frac{\hat m_\ell^2}{\omega_c}\right)\bar z(\delta_{\rm ex})-2\ln^2\bar z(\delta_{\rm ex})\;+2\ln^2\bar z(\omega_s)+4\ln\bar z(\omega_s)\Big]\,, \tag{5.33}$$

with $\bar z\equiv 1-z$ and the $z(\omega_s)\to 1$ limit has been used since $\omega_s\ll 1$. Moreover, A is the coefficient of the collinear log, for which we have also indicated the result for the photon-inclusive limit (i.e. $z(\delta_{\rm ex})\to 0$).

The hard-collinear logs from $\tilde{\mathcal{F}}^{(hc,0)}$ in the fully photon inclusive limit becomes

$$d^2\Gamma^{(0)}\Big|^{(hc)}_{\ell_1||\gamma,\,\ln m_{\ell_1}} = d^2\Gamma^{\rm LO}_{\bar B\to\bar K\ell_{1\gamma}\bar\ell_2}\left(\frac{\alpha}{\pi}\right)\hat Q_{\ell_1}^2\left[\frac{3}{2}+2\ln\bar z(\omega_s)\right]\ln m_{\ell_1}+\text{reg. terms}\,, \tag{5.34}$$

where "reg. terms" stands for terms which are finite in the $m_{\ell_1}\to 0$ limit.

We are now ready to show the cancellations of the $\ln m_{\ell_1}$-terms by assembling all pieces. Defining

$$\frac{d^2\Gamma}{dq_0^2dc_0}\bigg|_{\ln m_{\ell_1}} = \frac{d^2\Gamma^{\rm LO}}{dq_0^2dc_0}\left(\frac{\alpha}{\pi}\right)\hat Q_{\ell_1}^2\ln m_{\ell_1}\times C_{\ell_1}^{(0)}\,, \tag{5.35}$$

we find

$$C_{\ell_1}^{(0)}=\left[\frac{3}{2}+2\ln\bar z(\omega_s)\right]_{\tilde{\mathcal{F}}^{(hc)}}+\left[-1-2\ln\bar z(\omega_s)\right]_{\tilde{\mathcal{F}}^{(s)}}+\left[\frac{3}{2}-2\right]_{\tilde{\mathcal{H}}}=0\,, \tag{5.36}$$

complete cancellation. As explicitly indicated, the first term in square brackets comes from the hard-collinear integral, (5.34), the second term from the soft integral in Eq. (D.23) of App. D.2, and the last term from the virtual corrections (here the $\frac{3}{2}$ originates from the Z-factors in Sec. 4.6 and the -2 from the B_0-functions in (5.14)). Note that the passage from $\bar B\to\bar K\ell_{1\gamma}\bar\ell_2$ in (5.34) to $\bar B\to\bar K\ell_1\bar\ell_2$ in (5.35) is justified since the lepton and the photon are collinear and can thus be treated as a single particle. The cancellation for the lepton $\bar\ell_2$ is of course completely analogous. It is worthwhile to point out that the hard-collinear logs, as well as the soft divergences, do cancel charge by charge as explicitly shown in section 5.4. Note that, in general, the cancellation at the differential level is spoiled by non photon-inclusiveness ($\delta_{\rm ex}<\delta_{\rm ex}^{\rm inc}$) and/or going over to the $\{q^2,c_\ell\}$-variables, which we discuss in the next section.

5.3.3 $\tilde{\mathcal{F}}^{(hc,\ell)}$, structure of collinear singularities in $dq^2 dc_\ell$

We now proceed to analyse the analogous question for the $\{q^2, c_\ell\}$-variables. Setting $m_K \to 0$ again for simplicity in the presentation, and focussing on the case $\ell_1||\gamma$, we have[6]

$$q_0^2 = \frac{q^2}{z} \,, \quad c_0|_{m_K\to 0} = \frac{c_\ell(1+z)+1-z}{c_\ell(1-z)+1+z} \,. \tag{5.37}$$

The first equation follows from using $\ell_1 = z\ell_{1\gamma}$ in the expressions for q^2 and q_0^2. The second can be derived by considering the following ratio of scalar products in the massless kaon limit,

$$\frac{p_K\cdot\ell_{1\gamma}}{p_K\cdot\ell_2} = z\left(\frac{p_K\cdot\ell_1}{p_K\cdot\ell_2}\right) = z\left(\frac{1+c_\ell}{1-c_\ell}\right), \tag{5.38}$$

but

$$\frac{p_K\cdot\ell_{1\gamma}}{p_K\cdot\ell_2} = \left(\frac{1+c_0}{1-c_0}\right). \tag{5.39}$$

Equating the two expressions for $\frac{p_K\ell_{1\gamma}}{p_K\ell_2}$, and solving for c_0 leads to Eq. (5.37).

The Jacobian of the change of variables from $\{q_0^2, c_0\}$ to $\{q^2, c_\ell\}$ is given by

$$dq_0^2 dc_0 \;=\; 4(c_\ell(1-z)+1+z)^{-2} dq^2 dc_\ell \,. \tag{5.40}$$

The analogue of (5.21) then becomes

$$\begin{aligned}\tilde{\mathcal{F}}^{(hc,\ell)}(\underline{\delta}) = \frac{\hat{Q}_{\ell_1}^2}{2^8\pi^3 m_B^3}\int_{\max(z_{\rm inc}(c_\ell),z_{\delta_{\rm ex}}(c_\ell))}^{z_{\omega_s}(c_\ell)} dz\,[\,\frac{|\mathcal{A}^{(0)}(q_0^2,c_0)|^2\lambda^{1/2}(q_0^2,m_B^2,0)}{(c_\ell(1-z)+1+z)^2}\times \\ \left(\tilde{P}_{q\to q\gamma}(z)\,j^{hc} - j^{hc}_{(m_{\ell_1})}\right)\,] \;+\; \{1, c_\ell \leftrightarrow 2, -c_\ell\}\,,\end{aligned} \tag{5.41}$$

where $c_0 = c_0(c_\ell)$ with regard to the symmetrisation over c_ℓ, $z_{\delta_{\rm ex}}(c_\ell)$ implements the photon energy cut (4.4) and the arguments have to be substituted by (5.37). The boundaries for the z-integral are given by

$$z_{\rm inc}(c_\ell)|_{m_K\to 0} = \hat{q}^2 \,, \quad z_\delta(c_\ell)|_{m_K\to 0} = \frac{1+\hat{q}^2-\delta+c_\ell(1-\hat{q}^2-\delta)}{1+\hat{q}^2+\delta+c_\ell(1-\hat{q}^2-\delta)} \,. \tag{5.42}$$

[6]For $\ell_2||\gamma$, the prescription $c_\ell \to -c_\ell$ works as before.

To obtain $z_{\rm inc}(c_\ell)|_{m_K\to 0}$, we first note that the photon-inclusive case, $\delta_{\rm ex}^{\rm inc}$, corresponds to the minimum value of z, for a given q^2. In the limit of $m_K \to 0$, one can deduce, from (5.37), that this corresponds to $q_0^2 = m_B^2$, which then leads to $z_{\rm inc}(c_\ell)|_{m_K\to 0}$ in (5.42).

On the other hand, $z_\delta(c_\ell)|_{m_K\to 0}$ is obtained by solving (5.22) for $\delta = \omega_s, \delta_{\rm ex}$ as appropriate, with (5.37) in place.

Note that the phase space slicing condition is implemented via $z_{\omega_s}(c_\ell)$, which is less than 1.

The new aspect is that the $|\mathcal{A}^{(0)}(q_0^2, c_0)|^2$ cannot be factored out since it depends on z implicitly through q_0^2 and c_0. However, in the limit of $m_K \to 0$ and $m_{\ell_{1,2}} \to 0$, the amplitude squared (4.17) is simple enough,

$$|\mathcal{A}^{(0)}(q_0^2, c_0)|^2 = g_{\rm eff}^2(|C_V|^2 + |C_A|^2)\, 2(1-c_0^2)(1-\hat{q}_0^2)^2\, f_+^2(q_0^2)\ , \tag{5.43}$$

and the integral can be done analytically. Note that $\{q_0^2, c_0\}$ are to be substituted as in (5.37).

Adding all the contributions, real and virtual, that contribute to the hard-collinear logs, one finds

$$\frac{d^2\Gamma}{dq^2 dc_\ell}\Big|_{\ln m_{\ell_{1,2}}} = \frac{\alpha}{\pi}(\hat{Q}_{\ell_1}^2 K_{\rm hc}(q^2, c_\ell)\ln m_{\ell_1} + \hat{Q}_{\ell_2}^2 K_{\rm hc}(q^2, -c_\ell)\ln m_{\ell_2})\ , \tag{5.44}$$

where $K_{\rm hc}(q^2, c_\ell)$ is a non-vanishing function. Plots of this quantity are shown in Sec. 6.1.4 for $(\ell_1, \bar{\ell}_2 = \ell^-, \ell^+)$, with $\ell = e, \mu$.

At last, we would like to mention that for $q^2 \to (m_{\ell_1} + m_{\ell_2})^2$ and $c_\ell \to -1$ the assumption that $k \cdot \ell_1$ is small compared to other scalar products starts to break down and this leads to artificial enhancements. For example, the Jacobian factor in (5.41) becomes too large when q^2 is small and $c_\ell \to -1$. However, for a binned rate this effect is negligible and moreover, for the $\{q_0^2, c_0\}$-variables there are no such issues at all.

We have made the $m_K \to 0$ approximation for simplicity in presentation. However, to obtain the final numerical results, which are shown in Chapter 6, the full expressions have been used.

5.3.4 Cancellation of hard-collinear logs for the total differential rate

It is well-known that all IR divergences and IR sensitive terms ought to cancel at the level of the total, photon-inclusive, rate [113]. It is the aim of this section to verify this for the case at hand. The hard-collinear part of the total rate is given by

$$\begin{aligned}\tilde{\Gamma}^{(hc,\ell)}(\omega_s)\Big|_{\ln m_{\ell_1}} &\equiv \frac{\alpha}{\pi}\int_0^1 d\hat{q}^2 \int_{-1}^1 dc_\ell\ \tilde{\mathcal{F}}^{(hc,\ell)}\ ,\\ \tilde{\Gamma}^{(hc,0)}(\omega_s)\Big|_{\ln m_{\ell_1}} &\equiv \frac{\alpha}{\pi}\int_0^1 d\hat{q}_0^2 \int_{-1}^1 dc_0\ \tilde{\mathcal{F}}^{(hc,0)}\ ,\end{aligned} \tag{5.45}$$

where we have assumed the $m_K \to 0$ limit.

In accordance with the general expectation, we find

$$\tilde{\Gamma}^{(hc)}\Big|_{\ln m_{\ell_1}} \equiv \tilde{\Gamma}^{(hc,0)}\Big|_{\ln m_{\ell_1}} = \tilde{\Gamma}^{(hc,\ell)}\Big|_{\ln m_{\ell_1}}\ , \tag{5.46}$$

equality at the level of the hard-collinear logs originating from the real radiation

$$\tilde{\Gamma}^{(hc)}(\omega_s)\Big|_{\ln m_{\ell_1}} = \frac{m_B \hat{Q}_{\ell_1}^2}{2^9\,(9\pi^3)} f_+^2 g_{\rm eff}^2 (|C_V|^2+|C_A|^2)\,[8+6\ln\omega_s+\mathcal{O}(\omega_s)]\ln m_{\ell_1}\ . \tag{5.47}$$

Since we have explicitly shown the cancellation for $\frac{d^2\Gamma}{dq_0^2 dc_0}$, this implies that the hard-collinear logs cancel for the integrated $\int \frac{d^2\Gamma}{dq^2 dc_\ell} dq^2 dc_\ell$. The $\mathcal{O}(\omega_s)$-terms can be safely neglected, since $\omega_s \ll 1$, and in any case the same approximation has been used when evaluating the soft integrals, c.f. App. D.2.

5.4 Cancellation of hard-collinear logs charge by charge

Whereas for the cancellation of soft divergences, charge conservation was not assumed, the presentation for the hard-collinear logs $\ln m_\ell$ in Sec. 5.3.2 makes use of it. The aim of this section is to show that this assumption is unnecessary, i.e. that hard-collinear logs cancel charge by charge. Charge conservation is

though necessary for gauge invariance or conversely imposing gauge invariance implies charge conservation. Using charge conservation can still be convenient such as for the photon-inclusive hard-collinear log formula (6.14).

First, we focus on the soft contribution $\mathcal{F}^{(s)}(\omega_s)|_{\ln m_{\ell_1}} \equiv \sum_{i,j} \hat{Q}_i \hat{Q}_j \mathcal{F}^{(s)}_{ij}(\omega_s)|_{\ln m_{\ell_1}}$ to the hard-collinear log. In the limit of $m_{\ell_1} \to 0$, using Eqs. (D.10), (D.11), (D.12), (D.21) and (D.23), one gets

$$\mathcal{F}^{(s)}(\omega_s)|_{\ln m_{\ell_1}} = \ln m_{\ell_1} \left[-\hat{Q}^2_{\ell_1} + 2\hat{Q}_{\ell_1} \left(\hat{Q}_{\bar{\ell}_2} + \hat{Q}_{\bar{B}} + \hat{Q}_{\bar{K}} \right) \ln \bar{z}(\omega_s) \right] . \tag{5.48}$$

where we have used $\bar{z}(\omega_s) = \frac{\omega_s m_B}{2E_{\ell_1}}$, as explained below Eq. (D.23). Next, the virtual contribution, $\tilde{\mathcal{H}}|_{\ln m_{\ell_1}} \equiv \sum_{i,j} \hat{Q}_i \hat{Q}_j \left(\tilde{\mathcal{H}}^{(s)}_{ij} + \tilde{\mathcal{H}}^{(hc)}_{ij} \right) \Big|_{\ln m_{\ell_1}}$, using Eqs. (4.44), (5.6) and (5.14), is given by

$$\tilde{\mathcal{H}}|_{\ln m_{\ell_1}} = \ln m_{\ell_1} \left[\frac{3}{2} \hat{Q}^2_{\ell_1} + 2\hat{Q}_{\ell_1} \left(\hat{Q}_{\bar{\ell}_2} + \hat{Q}_{\bar{B}} + \hat{Q}_{\bar{K}} \right) \right] . \tag{5.49}$$

Finally, $\mathcal{F}^{(hc)}(\underline{\delta})|_{\ln m_{\ell_1}} \equiv \sum_{i,j} \hat{Q}_i \hat{Q}_j \mathcal{F}^{(hc)}_{ij}(\underline{\delta})|_{\ln m_{\ell_1}}$ is given by

$$\mathcal{F}^{(hc)}(\underline{\delta})|_{\ln m_{\ell_1}} = \ln m_{\ell_1} \left[-\frac{1}{2} \hat{Q}^2_{\ell_1} - 2\hat{Q}_{\ell_1} \left(\hat{Q}_{\bar{\ell}_2} + \hat{Q}_{\bar{B}} + \hat{Q}_{\bar{K}} \right) (1 + \ln \bar{z}(\omega_s)) \right] . \tag{5.50}$$

In obtaining (5.50), we followed the procedure in Sec. 5.3.2 without using charge conservation in Eq. (5.19).

Adding the three contributions, one finds (with ordering as above)

$$\begin{aligned} \left[\mathcal{F}^{(s)}(\omega_s) + \tilde{\mathcal{H}} + \mathcal{F}^{(hc)}(\underline{\delta}) \right] \Big|_{\ln m_{\ell_1}} = & \left[2 \ln \bar{z}(\omega_s) + 2 - 2(1 + \ln \bar{z}(\omega_s)) \right] \times \\ & \hat{Q}_{\ell_1} (\hat{Q}_{\bar{\ell}_2} + \hat{Q}_{\bar{B}} + \hat{Q}_{\bar{K}}) + \left[-1 + \frac{3}{2} - \frac{1}{2} \right] \hat{Q}^2_{\ell_1} = 0 , \end{aligned} \tag{5.51}$$

that the hard-collinear cancel charge by charge (without the need for charge conservation).

5.5 On hard-collinear logs and structure-dependent terms

We turn to the important question as to whether further hard-collinear logs could be missing due to omitted structure-dependent corrections. Using gauge invariance, we are able to show that this is not the case. In doing so, we will further establish why the hard-collinear logs can be written as a sum of terms proportional to $\hat{Q}^2_{\ell_1,\bar{\ell}_2}$. At the end of the section, we give a physical argument of the previously established result that hard-collinear logs cancel at differential rate $\frac{d^2}{dq_0^2 dc_0}\Gamma$, that is when expressed in $\{q_0^2, c_0\}$-variables.

The starting point is to realise that hard-collinear logs $\ln m_{\ell_{1,2}}$ are generated by interference of

$$\frac{1}{k\cdot\ell_{1,2}} \tag{5.52}$$

denominators with other terms. Without loss of generality, we may focus our attention to lepton ℓ_1. The real amplitude can be decomposed,

$$\mathcal{A}^{(1)} = \hat{Q}_{\ell_1}\mathcal{A}^{(1)}_{\ell_1} + \delta\mathcal{A}^{(1)} \ , \tag{5.53}$$

into a term $\hat{Q}_{\ell_1}\mathcal{A}^{(1)}_{\ell_1}$ with all terms proportional to $\hat{Q}_{\ell_1}$, and the remainder $\delta\mathcal{A}^{(1)}$. Note that at this point, we have not yet made use of charge conservation. From (4.35),

$$\mathcal{A}^{(1)}_{\ell_1} = -eg_{\rm eff}\bar{u}(\ell_1)\left[\frac{2\epsilon^*\cdot\ell_1 + \not{\epsilon}^*\not{k}}{2k\cdot\ell_1}\Gamma\cdot H_0(q_0^2)\right]v(\ell_2) \ , \tag{5.54}$$

which contains all $1/(k\cdot\ell_1)$-terms. It is seen that the structure-dependence of this term is encoded in the form factor H_0 (defined in (4.10)) only. For our purposes it is convenient to write the amplitude square, using (5.53), in terms of three terms

$$\sum_{\rm pol}|\mathcal{A}^{(1)}|^2 = \sum_{\rm pol}|\delta\mathcal{A}^{(1)}|^2 - \hat{Q}^2_{\ell_1}\sum_{\rm pol}|\mathcal{A}^{(1)}_{\ell_1}|^2 + 2\hat{Q}_{\ell_1}{\rm Re}[\sum_{\rm pol}\mathcal{A}^{(1)}\mathcal{A}^{(1)*}_{\ell_1}] \ , \tag{5.55}$$

where it will be important that $\mathcal{A}^{(1)}$ is gauge invariant. By construction, the first term is manifestly free from hard-collinear logs $\ln m_{\ell_1}$. To simplify the discussion, we may use gauge invariance and set $\xi = 1$ in this section under which the polarisation sum,

$$\sum_{\rm pol}\epsilon^*_\mu\epsilon_\nu = (-g_{\mu\nu} + (1-\xi)k_\mu k_\nu/k^2) \to -g_{\mu\nu} \tag{5.56}$$

collapses to the metric term only. In this case, the second term evaluates to

$$\int d\Phi_\gamma \, \hat{Q}_{\ell_1}^2 \sum_{\text{pol}} |\mathcal{A}_{\ell_1}^{(1)}|^2 = \int d\Phi_\gamma \, \hat{Q}_{\ell_1}^2 \frac{\mathcal{O}(m_{\ell_1}^2) + \mathcal{O}(k\cdot\ell_1)}{(k\cdot\ell_1)^2} = \mathcal{O}(1)\, \hat{Q}_{\ell_1}^2 \ln m_{\ell_1} \ , \quad (5.57)$$

where we used $k - \ell_1 = \mathcal{O}(m_{\ell_1}^2)$, valid in the collinear region. Note that the form factor part $H_0(q_0^2)$ does not participate in the photon phase space integration, and factorises when working with dq_0^2. We now turn to the third term. Noting that $\mathcal{A}^{(1)} \equiv \epsilon^{*\mu}\mathcal{A}_\mu^{(1)}$, the crucial step in use is that gauge invariance $k^\mu \mathcal{A}_\mu^{(1)} = 0$ implies $\ell_1^\mu \mathcal{A}_\mu^{(1)} = \mathcal{O}(m_{\ell_1}^2)$ in the collinear region and thus the third term assumes the form

$$\hat{Q}_{\ell_1} \sum_{\text{pol}} \mathcal{A}^{(1)} \mathcal{A}_{\ell_1}^{(1)*} = c_1 \, \hat{Q}_{\ell_1}^2 \frac{\mathcal{O}(m_{\ell_1}^2) + \mathcal{O}(k\cdot\ell_1)}{(k\cdot\ell_1)^2} + c_2 \, \hat{Q}_{\ell_1}\hat{Q}_X \frac{\mathcal{O}(m_{\ell_1})}{(k\cdot\ell_1)} + \dots \ , \quad (5.58)$$

where $X \in \{\bar{B}, \bar{K}, \bar{\ell}_2\}$ and the ellipses stand for less singular contributions. The c_1-term has the same origin as the one in (5.57). The c_2-term comes from interfering the spin dependent term in (5.54) with the $\hat{Q}_{\ell_1}$-independent part of $\mathcal{A}^{(1)}$ and it is by the use of the equation of motion, that one arrives at the $\mathcal{O}(m_{\ell_1})$-suppression[7]

$$\int d\Phi_\gamma \frac{\mathcal{O}(m_{\ell_1})}{(k\cdot\ell_1)} = \mathcal{O}(m_{\ell_1}) \ln m_{\ell_1} \ , \quad (5.59)$$

as compared to (5.57). Hence we have established that all hard-collinear terms $\ln m_{\ell_1}$ can be written as a sum of terms proportional to $\hat{Q}_{\ell_1}^2$. It should be added that in making this statement, charge conservation was used since gauge invariance was assumed. All statements hold irrespective of any photon phase space restrictions such as an energy cut-off δ_{ex} or a photon angle cut (cf. Sec. 6.1.3). Thus, any gauge invariant addition to the amplitude, due to structure-dependent terms, will not give rise to any additional $\ln m_{\ell_1}$-terms.

So far, our analysis has been concerned with the real amplitude only. Assuming that hard-collinear logs cancel charge by charge combination at the differential level in the $\{q_0^2, c_0\}$-variables, irrespective of the microscopic approach, the same conclusion applies to each virtual diagram.[8] For virtual diagrams, there is no

[7] In fact, this result is true more generally since the spin dependent part is proportional to the Lorentz-generator which, by contraction, is a boost into the direction of the photon. Let us assume that $m_{\ell_1} = 0$. Since in the collinear limit, the photon and the lepton are parallel, the massless lepton is boosted in direction of movement. Since the helicity of a massless particle cannot be changed, the generator has to vanish. If the lepton mass is reinstalled, then there are terms of the form $m_{\ell_1} \ln m_{\ell_1}$ which are however safe.

[8] A physical argument of the correctness of this assumption is given in the last of paragraph

distinction between $\{q_0^2, c_0\}$- and $\{q^2, c_\ell\}$-variables and thus the conclusion holds irrespective of the differential variables. As the reader might suspect, the same conclusion holds for lepton ℓ_2 by symmetry. Let us summarise these findings:

- Additional structure-dependent corrections, which are of course gauge invariant, will not give rise to any additional hard-collinear logs $\ln m_{\ell_{1,2}}$.[9]
- At the double-differential level, hard-collinear logs $\ln m_{\ell_{1,2}}$, real and virtual, can be written as a sum of terms proportional to $\hat{Q}^2_{\ell_{1,2}}$ consistent with our explicit evaluation using the phase space slicing method in Eq. (5.34).

To this end, let us give a physical explanation as to why hard-collinear logs $\ln m_{\ell_{1,2}}$ are to cancel at the differential level in $\{q_0^2, \theta_0\}$. In those variables, the decay corresponds to the disintegration of a scalar particle of mass q_0^2 which is an infrared-safe observable. Now, the angle θ_0 has no meaning when the decay axis, cf. Fig. 4.1, is decoupled and the $\bar{B}$ and the $\bar{K}$ are interpreted as a single particle of mass q_0^2. This observation is backed up by our explicit formal verification in Eq. (5.35).

5.6 Structure-dependence of hard collinear logs in the virtual diagrams

The main result of this section is that in the virtual diagrams, the form-factors $f_\pm(q^2)$ are independent of the loop momentum for the hard collinear logs. This is important, as this means that truncating the form-factor expansion in Eq. (4.9) does not lead to significant errors in the result. Furthermore, this implies that the cancellation of hard-collinear logs happens at all orders in the form-factor expansion, as mentioned in footnote (8). This is in contrast to what happens in Sec. 6.1.3, where there is migration of radiation. This means that even at fixed q^2, the energy scale in the form-factors actually explore all of the kinematic region allowed by the phase space. This is explained in detail in Sec. 6.1.3 for the radiative process. Therefore, the results in this section do not definitively

of this section. In particular, we have verified this explicitly up to the second derivative of the form factor in our approach and produced a formal derivation that holds to all orders. This is shown in section 5.6.

[9] This applies to either, approaches resolving the mesons by partons or an evaluation of the $B(K)_\gamma L_{1,2}$-diagrams, cf. Fig. 4.4, including higher terms in the expansion (4.9).

prove the absence of structure-dependent collinear logs in the virtual diagrams per se, but they do provide some protection, especially in the case of form factor expansion.

Without loss of generality, we will consider the charged semi-leptonic case ($Q_K = Q_{\ell_2} = 0$), since the algebra is simpler in that case.

We will focus on collecting all single collinear logs, as all double logs are captured by the C_0 functions in Eq. (5.5). We start by considering the virtual amplitudes of the relevant diagrams. They are PL_1 and BL_1 (see Sec. 4.6), since they are the only ones having a Feynman propagator involving the light lepton.

Before writing the sum, we first show how the amplitude PL_1 can be simplified. We focus on the term from Eq. (4.56), which contains

$$\sum_{n\geq 1} \frac{f_\pm^{(n)}(0)}{n!} P_{n-1}, \qquad \text{where} \qquad P_n = \sum_{m=0}^{n} (q^2)^{(n-m)} ((q+k)^2)^m. \tag{5.60}$$

Now, defining $q_0^2 \equiv (q+k)^2$, consider

$$\begin{aligned}
\left(q_0^2 - q^2\right) P_n &= \sum_{m=0}^{n} (q^2)^{(n-m)} (q_0^2)^{m+1} - \sum_{m=0}^{n} (q^2)^{(n-m+1)} (q_0^2)^m \\
&= \sum_{m=1}^{n+1} (q^2)^{(n-m+1)} (q_0^2)^m - \sum_{m=0}^{n} (q^2)^{(n-m+1)} (q_0^2)^m \\
&= \left(q_0^2\right)^{n+1} - \left(q^2\right)^{n+1},
\end{aligned} \tag{5.61}$$

where we have redefined the index in the first sum in going to the second line. A similar trick has been used in Eq. (4.40) when discussing gauge invariance of the real amplitude. Using this result, one readily finds that

$$\sum_{n\geq 1} \frac{f_\pm^{(n)}(0)}{n!} P_{n-1} = \frac{f_\pm(q_0^2) - f_\pm(q^2)}{q_0^2 - q^2}. \tag{5.62}$$

We are now in a position to write the sum of the relevant amplitudes. It reads

$$\begin{aligned}
\mathcal{A}_{BL_1+PL_1} = i g_{\text{eff}} e^2 Q_{\ell_1} Q_B \int_k & \frac{\bar{u}\left(2\not{p}_B - \not{k}\right)\left(\not{\ell}_1 - \not{k} + m_{\ell_1}\right) f_\pm\left(q^2\right) \Gamma\cdot(p_B - k \pm p_K)\, v}{\left(k^2 - m_\gamma^2\right)\left(k^2 - 2k\cdot\ell_1\right)\left(k^2 - 2k\cdot p_B\right)} \\
- \int_k & \frac{i g_{\text{eff}} e^2 Q_{\ell_1} Q_B}{\left(k^2 - m_\gamma^2\right)\left(k^2 - 2k\cdot\ell_1\right)} \Bigg[\bar{u}\gamma^\mu \left(\not{\ell}_1 - \not{k} + m_{\ell_1}\right) f_\pm\left(q^2\right) \Gamma_\mu v
\end{aligned}$$

$$+\frac{\bar{u}\left(2\left(\not{p}_B-\not{p}_K\right)-\not{k}\right)\left(\not{\ell}_1-\not{k}+m_{\ell_1}\right)\left[f_\pm\left(q_0^2\right)-f_\pm\left(q^2\right)\right]\Gamma\cdot\left(p_B\pm p_K\right)v}{2k\cdot\left(p_B-p_K\right)-k^2}\Bigg],$$

(5.63)

where the spinors are understood to be $\bar{u}\equiv\bar{u}\left(\ell_1\right)$ and $v\equiv v\left(\ell_2\right)$, and

$$q=p_B-p_K-k, \tag{5.64}$$

and thus, in this notation, q^2 depends on the loop momentum k. We define

$$N\equiv\frac{ig_{\text{eff}}e^2Q_{\ell_1}Q_B}{\left(k^2-m_\gamma^2\right)\left(k^2-2k\cdot\ell_1\right)}, \tag{5.65}$$

as a common prefactor. Then, dropping the integral over k for simplicity,

$$\begin{aligned}\mathcal{A}_{BL_1+PL_1}=N\Bigg[&-\bar{u}\gamma^\mu\left(\not{\ell}_1-\not{k}+m_{\ell_1}\right)f_\pm\left(q^2\right)\Gamma_\mu v\\&+\frac{\bar{u}\left(2\not{p}_B-\not{k}\right)\left(\not{\ell}_1-\not{k}+m_{\ell_1}\right)f_\pm\left(q^2\right)\Gamma\cdot\left(p_B-k\pm p_K\right)v}{\left(k^2-2k\cdot p_B\right)}\\&+\frac{\bar{u}\left(2\left(\not{p}_B-\not{p}_K\right)-\not{k}\right)\left(\not{\ell}_1-\not{k}+m_{\ell_1}\right)\left[f_\pm\left(q_0^2\right)-f_\pm\left(q^2\right)\right]\Gamma\cdot\left(p_B\pm p_K\right)v}{k^2-2k\cdot\left(p_B-p_K\right)}\Bigg].\end{aligned}$$

(5.66)

Given the prefactor in Eq. (5.65), in the collinear limit ($k\to\ell_1$), any term of $\mathcal{O}\left(m_{\ell_1}\right)$ in the square bracket in Eq. (5.66) will be suppressed and would thus not contribute to the hard-collinear logs. Thus, one concludes that the first term in the square bracket of Eq. (5.66) is not collinear divergent. To simplify the rest, consider the Dirac structure

$$\begin{aligned}\bar{u}\left[\frac{\left(2\not{p}-\not{k}\right)\left(\not{\ell}_1-\not{k}+m_{\ell_1}\right)}{\left(k^2-2k\cdot p\right)}\right]&=\bar{u}\left[2\frac{\left(2p\cdot\ell_1-k\cdot\ell_1\right)}{\left(k^2-2k\cdot p\right)}+\frac{\left(\not{k}-2\not{p}\right)\not{k}}{\left(k^2-2k\cdot p\right)}\right]\\&=\bar{u}\left[2\frac{\left(2p\cdot\ell_1-k\cdot\ell_1\right)}{\left(k^2-2k\cdot p\right)}+2-\frac{k^2-2\not{k}\not{p}}{\left(k^2-2k\cdot p\right)}\right]\\&\to\bar{u}\left[\frac{4p\cdot\ell_1}{\left(k^2-2k\cdot p\right)}+2\right],\end{aligned} \tag{5.67}$$

where the Dirac equation and anti-commutation relations were used in the simplification. In the last line, we have kept terms that are not suppressed by

$\mathcal{O}(m_{\ell_1})$ in the collinear limit. This allows us to write

$$\begin{aligned}\mathcal{A}_{BL_1+PL_1}\Big|_{\text{coll}} &= N\Bigg[\bar{u}\left(\frac{4p_B\cdot\ell_1}{k^2-2k\cdot p_B}+2\right)f_\pm\left(q^2\right)\Gamma\cdot(p_B-k\pm p_K)\,v \\ &\quad+\bar{u}\left(\frac{4\,(p_B-p_K)\cdot\ell_1}{k^2-2k\cdot(p_B-p_K)}+2\right)\left[f_\pm\left(q_0^2\right)-f_\pm\left(q^2\right)\right]\Gamma\cdot(p_B\pm p_K)\,v\Bigg] \\ &= N\,\bar{u}\,\Gamma\cdot(p_B\pm p_K)\,v\Bigg[2f_\pm\left(q_0^2\right) \\ &\quad+f_\pm\left(q^2\right)\left(\frac{4p_B\cdot\ell_1}{k^2-2k\cdot p_B}-\frac{4\,(p_B-p_K)\cdot\ell_1}{k^2-2k\cdot(p_B-p_K)}\right)\Bigg],\end{aligned} \tag{5.68}$$

where we have neglected the $\Gamma\cdot k\propto \not{k}$ term in going to the second line as it is suppressed by m_{ℓ_1} upon using the Dirac equation. We have also dropped the term

$$N\left(\frac{4\,(p_B-p_K)\cdot\ell_1}{k^2-2k\cdot(p_B-p_K)}\right)f_\pm\left(q_0^2\right)\bar{u}\,\Gamma\cdot(p_B\pm p_K)\,v, \tag{5.69}$$

which, while being collinear divergent, leads to a C_0 function. We have already collected them in Eq. (5.5), and we know from App. E that they do not contribute to single collinear logs.

We now consider the second term in the square bracket in the last line of Eq. (5.68). We can show that it is not collinear divergent since

$$\begin{aligned}\frac{4p_B\cdot\ell_1}{k^2-2k\cdot p_B}-\frac{4\,(p_B-p_K)\cdot\ell_1}{k^2-2k\cdot(p_B-p_K)} &= \frac{4p_B\cdot\ell_1-2k^2+2k^2}{k^2-2k\cdot p_B}-\frac{4\,(p_B-p_K)\cdot\ell_1-2k^2+2k^2}{k^2-2k\cdot(p_B-p_K)} \\ &\to \frac{2k^2}{k^2-2k\cdot p_B}-\frac{2k^2}{k^2-2k\cdot(p_B-p_K)} \\ &\to 0,\end{aligned} \tag{5.70}$$

where we have added and subtracted appropriate factors of k on the first line, and performed cancellations valid in the collinear limit on the second line.

Finally, we have the hard-collinear contributions to single logs from the virtual diagrams,

$$\mathcal{A}_{BL_1+PL_1}\Big|_{\text{coll}} = \int_k \frac{2ig_{\text{eff}}e^2Q_{\ell_1}Q_B}{\left(k^2-m_\gamma^2\right)\left(k^2-2k\cdot\ell_1\right)}\,f_\pm\left(q_0^2\right)\bar{u}\,\Gamma\cdot(p_B\pm p_K)\,v$$

$$= -\mathcal{A}^{(0)}_{\bar{B}\to\bar{K}\ell_1\bar{\ell}_2} \int_k \frac{2ie^2 Q_{\ell_1} Q_B}{\left(k^2 - m_\gamma^2\right)\left(k^2 - 2k\cdot\ell_1\right)}, \tag{5.71}$$

where we have substituted the expression for the tree level amplitude in the second line. The crucial point of Eq. (5.71) is that the form factor dependent part, contained in $\mathcal{A}^{(0)}_{\bar{B}\to\bar{K}\ell_1\bar{\ell}_2}$, factorises from the loop integration. It is easy to check that Eq. (5.71), which leads to a B_0 function, is consistent with the results for the hard-collinear logs from the virtual diagrams derived in Eq. (5.14).

This completes our discussion since only $f_\pm\left(q_0^2\right)$ survive, and these completely factorise from the loop integral since $q_0 = p_B - p_K$.

Chapter 6

QED corrections to $\bar{B} \to \bar{K}\ell^+\ell^-$: Results and Outlook

6.1 Results for $\bar{B} \to \bar{K}e^+e^-$ and $\bar{B} \to \bar{K}\mu^+\mu^-$

The results for the tree level differential rate is presented in Sec. 6.1.1. The total radiative corrections are presented in Sec. 6.1.2, followed by a discussion of the distortion of the spectrum due to γ-radiation in Sec. 6.1.3. The size of the hard collinear logs and some comparison with older work is discussed in sections 6.1.4 and 6.1.5 respectively. In Sec. 6.1.6, we present the results at full differential rate in the form of heat maps. The effect of the hard-collinear slicing parameter ω_c is discussed in Sec. 6.1.7. Finally, in Sec. 6.1.8, plots for the moments of the differential distribution are shown. Before proceeding thereto, we summarise the input to the numerics below.

For the particles participating in the decay, the following masses are assumed: $m_e = 0.511\,\text{MeV}$, $m_\mu = 0.10565\,\text{GeV}$, $m_B = 5.28\,\text{GeV}$ and $m_K = 0.495\,\text{GeV}$. Other parameters are the Wilson coefficients, $C_9 = 4.035$ and $C_{10} = -4.25$ at $\mu_{\text{UV}} = 4.7\,\text{GeV}$ (the b-quark pole mass) and the fine structure constant, $1/\alpha = 137.036$. For the $B \to K$ form factors (4.10), the light-cone sum rules computation [114], including radiative correction up to twist-3, was used with

updated Kaon distribution amplitude parameters[1]

$$\{f_+, f_-\}^{B\to K}(0) = \{0.271, -0.206\}$$
$$\frac{d}{dq^2}\{f_+, f_-\}^{B\to K}(0) = \{0.0151, -0.0109\}\,\mathrm{GeV}^{-2}\,, \tag{6.1}$$

where the uncertainty is roughly 15% if one additionally takes into account the error on the Kaon distribution amplitude. For the auxiliary cut-offs of the phase space slicing method, $\omega_s(e) = 2.5\cdot 10^{-3}$, $\omega_s(\mu) = 4\cdot 10^{-3}$, $\omega_c(e) = 1\cdot 10^{-2}\omega_s(e)$ and $\omega_c(\mu) = 2\cdot 10^{-2}\omega_s(\mu)$, where the argument denotes the type of lepton, lead to stable results. The hierarchy $\omega_c/\omega_s \ll 1$ is important since terms of this order are neglected.[2] Here, we refrain from a complete uncertainty analysis. Let us nevertheless mention the sources. There are the form factor uncertainties which can be largely reduced by considering correlations amongst the four numbers (6.1) entering the computations. Besides a more complete structure-dependent approach, cf. Sec. 6.2.1, there are missing finite counterterms in the charged meson case, which we set to zero and refer the reader to the discussion in Sec. 4.6.2. Concerning the latter, one might get a naive dimensional analysis estimate by varying the constant the renormalisation scale μ by a factor of 2. Adding these effects in quadrature results in an $\mathcal{O}(1\%)$-variation.

6.1.1 Leading Order Results

We present the leading order differential rate in Fig. 6.1 as a function of q^2 and c_ℓ. The quantities plotted are

$$\frac{d\Gamma_{\mathrm{LO}}}{dq^2} = \int_{-1}^{1} dc_\ell \frac{d^2\Gamma_{\mathrm{LO}}}{dq^2 dc_\ell},$$
$$\frac{d\Gamma_{\mathrm{LO}}[q^2_{\mathrm{min}}, q^2_{\mathrm{max}}]}{dc_\ell} = \int_{q^2_{\mathrm{min}}}^{q^2_{\mathrm{max}}} dq^2 \frac{d^2\Gamma_{\mathrm{LO}}}{dq^2 dc_\ell}. \tag{6.2}$$

These are trivial results per se, but are shown here for reference.

[1] For the Kaon distribution amplitude, the values $a_1^K(1\,\mathrm{GeV}) = 0.115(34)$ and $a_2^K(1\,\mathrm{GeV}) = 0.090(20)$ taken from the $N_f = 2+1$ lattice computation [115] (uncertainties were added in quadrature) were used. These values are consistent with earlier QCD sum rule computations [116–119].

[2] We refer the reader to [112] for an uncertainty analysis involving the auxiliary cut-offs.

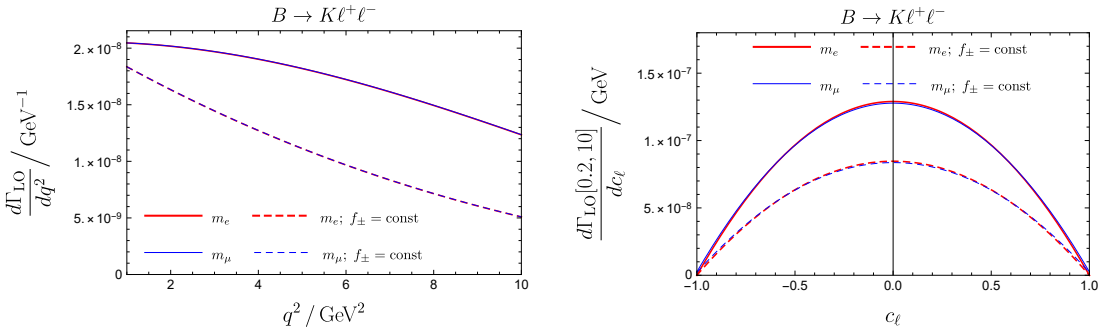

Figure 6.1: Plots showing the variation of the LO differential rate with respect to q^2 (left) and c_ℓ (right). The different lepton masses (electron in red and muon in blue) have very little effect on the rate. The solid line includes the contribution from the first derivative expansion of the form factors, while the dotted includes only the leading term. See comments in the main text regarding the discprecancy between the dotted and solid lines.

It should be noted that there is a rather significant discrepancy between the LO result with and without the first derivative term of the form factors, and it becomes larger as q^2 increases (see plot on the left in Fig. 6.1). However, when one considers *relative* QED corrections, which are discussed in Sec. 6.1.2, the effects become insignificant (depending on the choice of differential variables). The reader is particularly encouraged to read Sec. 6.1.3 for an interesting discussion on such effects wrt to the choice of differential variables.

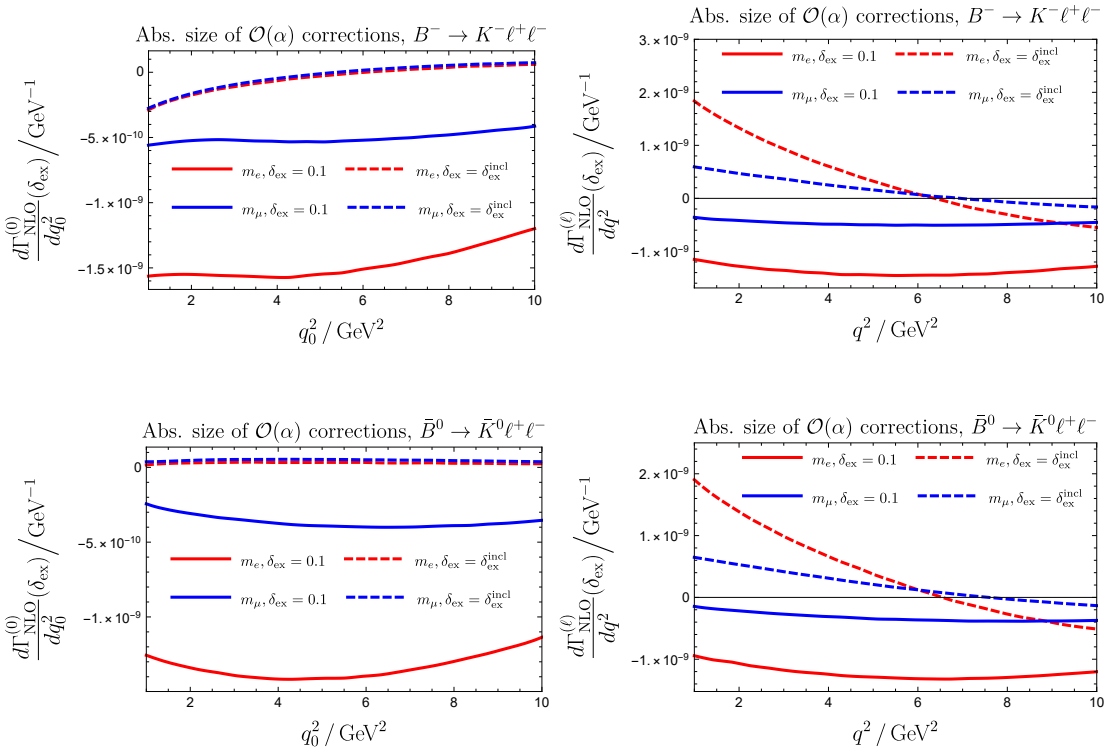

Figure 6.2: Absolute QED-corrections, cf. (6.3) for the definition, including finite terms. The upper and lower figures correspond to the charged and neutral modes in the q_0^2- and q^2-variables on the left and right respectively. In the photon-inclusive case ($\delta_{\rm ex} = \delta_{\rm ex}^{\rm inc}$, dashed lines), all IR sensitive terms cancel in the q_0^2 variable locally and in the q^2-variable when integrated which is nicely visible in both cases (electrons and muons). An important aspect is the (approximate) lepton universality on the plots on the left. As is well-known, effects due to the photon energy cuts are sizeable since hard-collinear logs do not cancel in that case.

6.1.2 QED corrections as a function of q_0^2, c_0 and q^2, c_ℓ

We define absolute (unnormalised) QED corrections, given by

$$\frac{d\Gamma^{(a)}_{\rm NLO}}{dq_a^2}(\delta_{\rm ex}) = \int_{-1}^{1} dc_a \frac{d^2\Gamma^{(a)}_{\rm NLO}}{dq_a^2 dc_a}(\delta_{\rm ex}),$$

$$\frac{d\Gamma^{(a)}_{\rm NLO}}{dc_a}([q^2_{\rm min}, q^2_{\rm max}], \delta_{\rm ex}) = \int_{q^2_{\rm min}}^{q^2_{\rm max}} dq_a^2 \frac{d^2\Gamma^{(a)}_{\rm NLO}}{dq_a^2 dc_a}(\delta_{\rm ex}). \tag{6.3}$$

The plots of the unnormalised differential rates as a function of q_a^2 and c_a are given in Fig. 6.2 and Fig. 6.4 respectively. While the relative corrections are more instructive as they correspond to the experimental situation, we give the unnormalised plots here for reference.

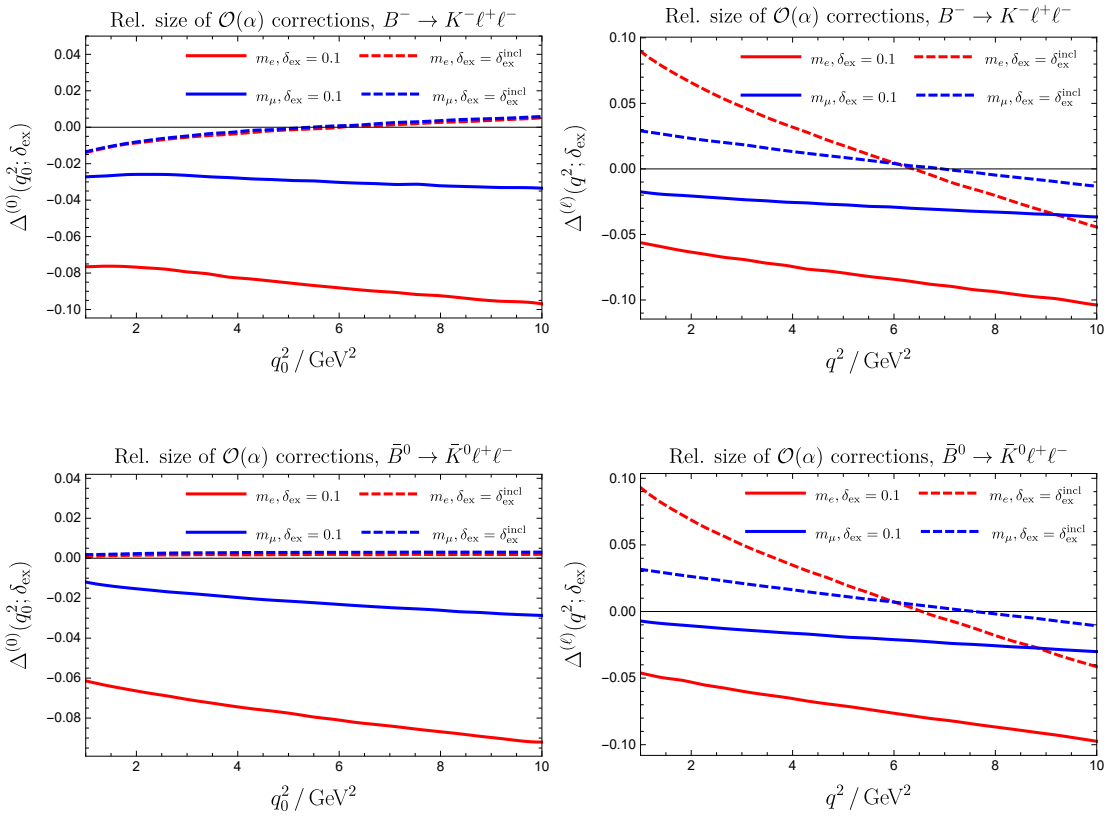

Figure 6.3: Total relative QED-corrections, cf. (6.5) for the definition, including finite terms. The upper and lower figures correspond to the charged and neutral modes in the q_0^2- and q^2-variables on the left and right respectively. In the photon-inclusive case ($\delta_{\rm ex} = \delta_{\rm ex}^{\rm inc}$, dashed lines), all IR sensitive terms cancel in the q_0^2 variable locally. In the charged case, however, we see finite effects of the $\mathcal{O}(2\%)$ due to $\ln \hat{m}_K$ "collinear logs" which do not cancel. An important aspect is the (approximate) lepton universality on the plots on the left. As is well-known, effects due to the photon energy cuts are sizeable since hard-collinear logs do not cancel in that case. This is more pronounced for electrons.

We define relative QED corrections, see Eq. (5.1),

$$\Delta^{(a)}(q_a^2, c_a; \delta_{\rm ex}) = \left(\frac{d^2\Gamma^{\rm LO}}{dq_a^2 dc_a}\right)^{-1} \frac{d^2\Gamma(\delta_{\rm ex})}{dq_a^2 dc_a}\bigg|_\alpha \,. \tag{6.4}$$

Above $|_\alpha$ stands for the inclusion of the $\mathcal{O}(\alpha)$-corrections only. The LO rate is given Eq. (4.80). We further consider the relative single differential in $\frac{d}{dq_a^2}$

$$\Delta^{(a)}(q_a^2; \delta_{\rm ex}) = \left(\frac{d\Gamma^{\rm LO}}{dq_a^2}\right)^{-1} \frac{d\Gamma(\delta_{\rm ex})}{dq_a^2}\bigg|_\alpha \,, \tag{6.5}$$

where the numerator and denominator are integrated separately over $\int_{-1}^{1} dc_a$

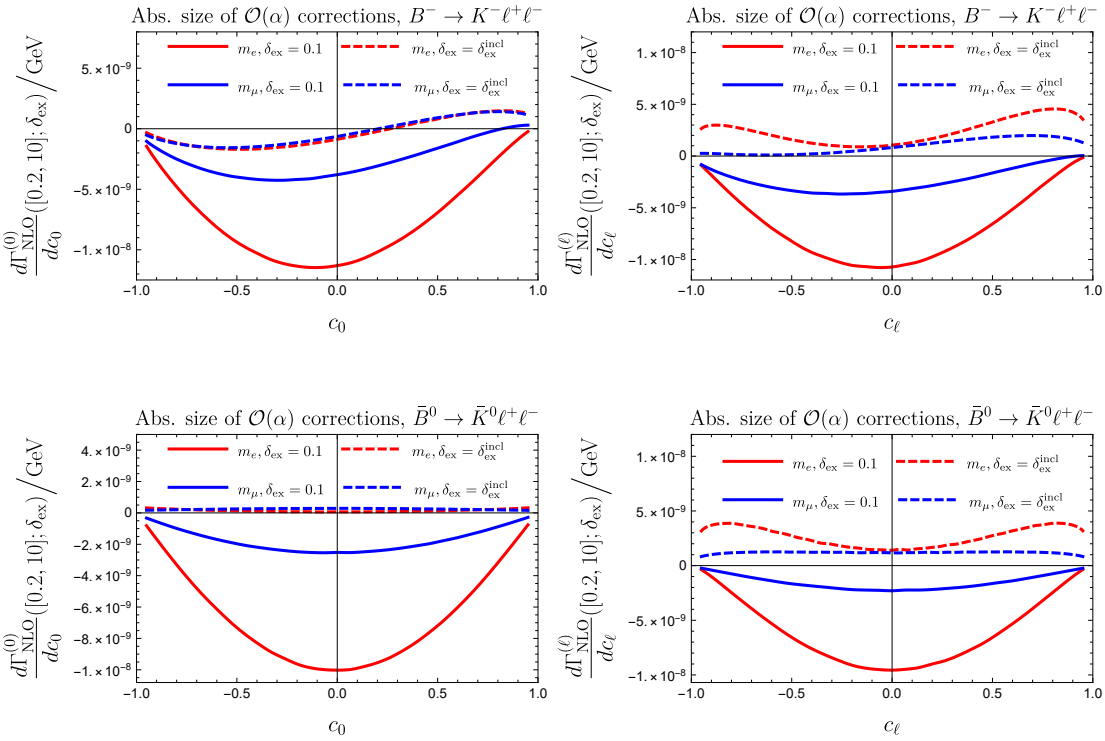

Figure 6.4: Total absolute QED-corrections (6.3) in terms of $c_0 = \cos(\theta_0)$ $c_\ell = \cos(\theta_\ell)$ respectively for the charged hadron case (top) and the neutral hadron case (bottom). In the c_0-variable effects are small for $\delta_{\rm ex} = \delta_{\rm ex}^{\rm inc}$, cf. comments in text and previous figures.

respectively. In addition, we define the single differential in $\frac{d}{dc_a}$

$$\Delta^{(a)}(c_a, [q_1^2, q_2^2]; \delta_{\rm ex}) = \left(\int_{q_1^2}^{q_2^2} \frac{d^2\Gamma^{\rm LO}}{dq_a^2 dc_a} dq_a^2 \right)^{-1} \int_{q_1^2}^{q_2^2} \frac{d^2\Gamma(\delta_{\rm ex})}{dq_a^2 dc_a} dq_a^2 \Big|_\alpha \,, \tag{6.6}$$

where the non-angular variable is binned. We would like to stress that it is important to integrate the QED correction and the LO separately as this corresponds to the experimental situation.

Results for $\Delta^{(a)}(q_a^2; \delta_{\rm ex})$ and $\Delta^{(a)}(c_a, [q_1^2, q_2^2]; \delta_{\rm ex})$ are shown in Figs. 6.3 and 6.5 respectively. Let us first focus on Fig. 6.3 where in the photon-inclusive case ($\delta_{\rm ex} = \delta_{\rm ex}^{\rm inc}$, dashed line), one observes two important features: Approximate lepton-universality and the cancellation of the hard-collinear logs. In the q_0^2-variable, this happens at the differential level whereas for the q^2-variable, integration over the entire range is needed (the tendency thereto is visible in the plot on the RHS). To be clear, the cancellation in the latter case only occurs upon integration over the full q^2-range. We further remind the reader that in all cases the soft divergences cancel locally as explicitly shown in Sec. 5.1. It is noticeable that for the charged

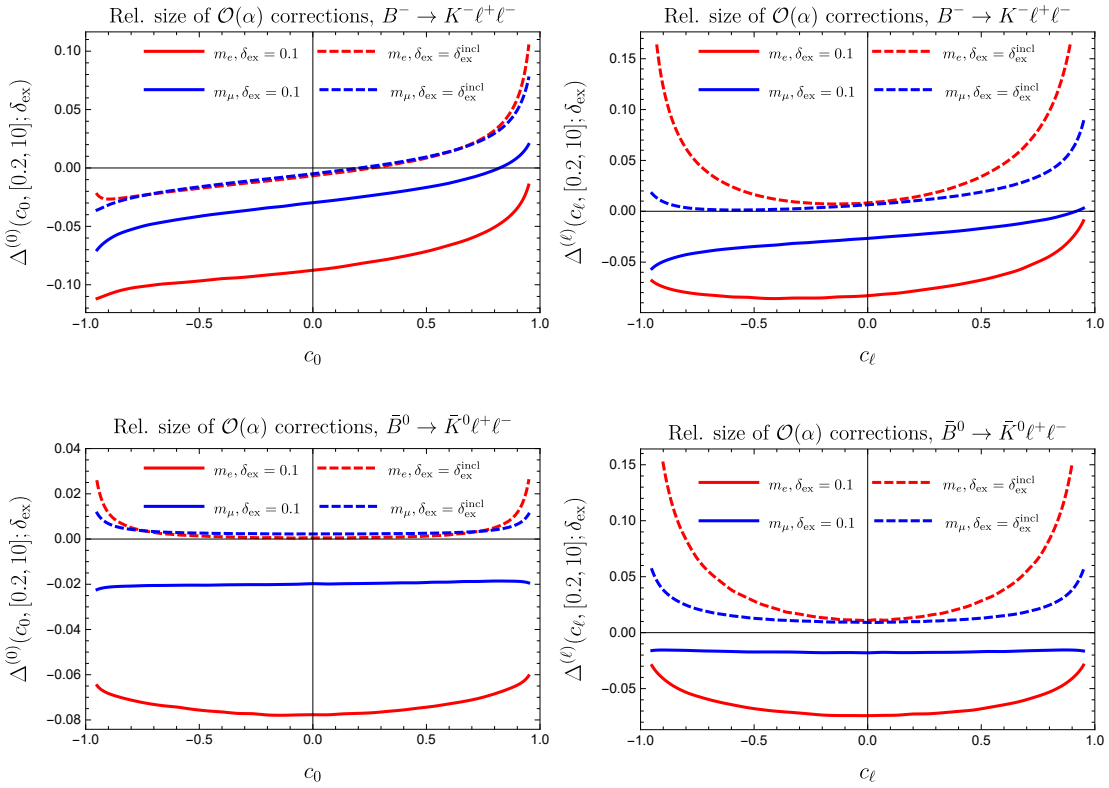

Figure 6.5: Total relative QED-corrections (6.6) in terms of $c_0 = \cos(\theta_0)$ $c_\ell = \cos(\theta_\ell)$ respectively for the charged hadron case (top) and the neutral hadron case (bottom). In the c_0-variable effects are small for $\delta_{\rm ex} = \delta_{\rm ex}^{\rm inc}$ cf. comments in text and previous figures. The enhanced effect towards the endpoints $\{-1, 1\}$ in the electron case is, partly, due to the special behaviour of the LO expression (4.81) which behaves like $\propto (1-c_\ell^2)+\mathcal{O}(m_\ell^2)$ and explains why the effect is less pronounced for muons. It can be seen from Fig. 6.4 that there is no peculiar behaviour at the endpoints.

case, there are $\mathcal{O}(2\%)$-effects in the q_0^2-variable due to "collinear logs", $\ln \hat{m}_K \simeq -2.36$. These logs, of course, cancel upon integration over all differential variables. The impact of the photon energy cuts are large, cf. section 6.1.4, and care needs to be taken when considering quantities like R_K for example. An important physical effect, visible in the plots on the right in Figs. 6.3, is the distortion of the q^2 distribution w.r.t. the non-radiative case (q_0^2). This is particularly prominent in the photon-inclusive limit as discussed in the next section.

The angular differential $\Delta^{(a)}(c_a, [q_1^2, q_2^2]; \delta_{\rm ex})$ in Fig. 6.5 shows similar patterns in the photon-inclusive case ($\delta_{\rm ex} = \delta_{\rm ex}^{\rm inc}$, dashed lines), e.g. lepton universality and small effects in the c_0-variable due to the cancellation of hard-collinear logs. In the electron case, there is a significant enhancement towards the endpoints $\{-1, 1\}$ which is due to the peculiar behaviour of the LO rate $d\Gamma^{\rm LO} \propto (1 - c_\ell^2) + \mathcal{O}(m_\ell^2)$ (4.81). This is the same effect as the helicity suppression in a $\pi^- \to \ell^-\bar{\nu}$ decay

and further explains why the effect is less prominent in the muon case. Note that without the normalisation, the plots in Fig. 6.4 show indeed that there is no strange behaviour at the endpoints. Cuts on the photon energy are again sizeable and the same remarks as before apply.

Plots of the hard-collinear logs $\ln m_\ell$ are discussed in section 6.1.4. Moreover in section 6.1.5, our results are compared to the earlier work [2] where virtual corrections were indirectly inferred and radiative corrections have been evaluated in terms of a radiator function depending on q^2 and q_0^2 only, and not on the photon-emission angle.

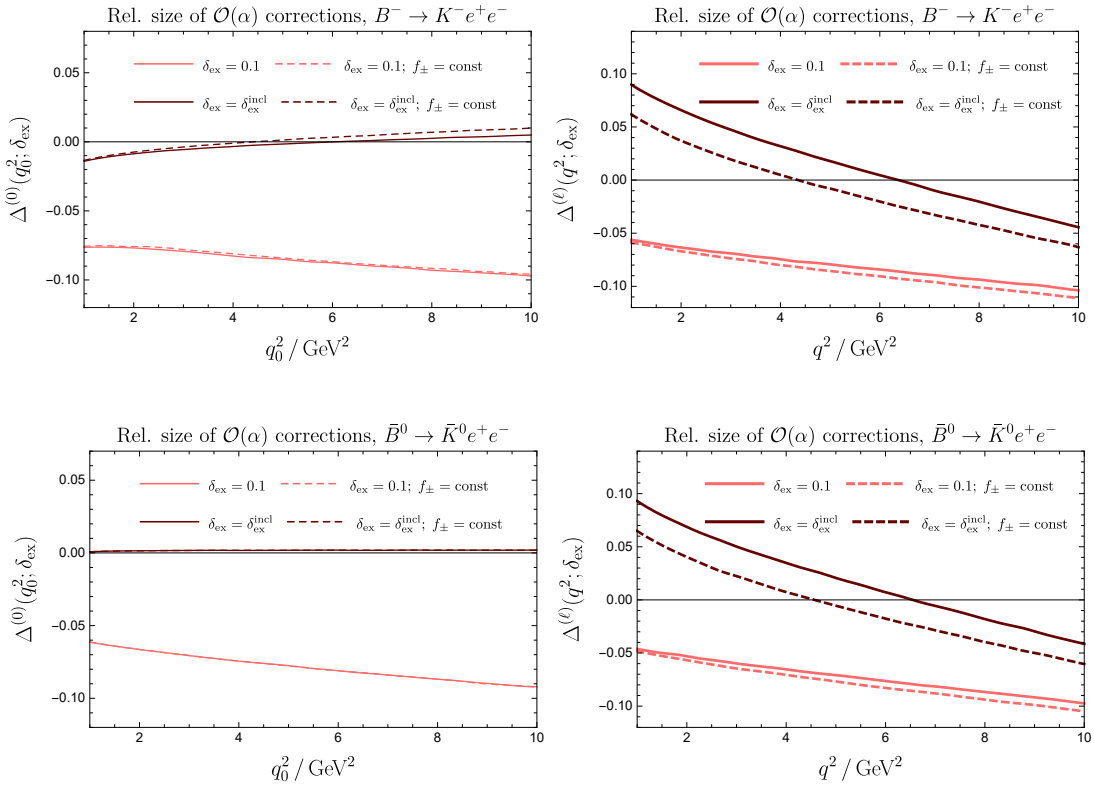

Figure 6.6: Plots of total relative QED corrections (6.4) for $B^- \to K^-\ell^+\ell^-$ (top) and $\bar{B}^0 \to \bar{K}^0\ell^+\ell^-$ (bottom) comparing the constant form factor case versus taking one derivative correction into account with values given in (6.1) (cf. below (4.18) for further comments). Effects are more prominent in the photon-inclusive case ($\delta_{\rm ex} = \delta_{\rm ex}^{\rm inc}$) since there is more phase space for the q^2- and q_0^2-variables to differ. In the neutral case, the effects are similar albeit slightly smaller.

6.1.3 Distortion of the $\bar{B} \to \bar{K}\ell^+\ell^-$ spectrum due to γ-radiation

As discussed in Chapter 5, the $\{q_0^2, \theta_0\}$-variables are safer than the $\{q^2, \theta_\ell\}$-variables because of the cancellation of the hard-collinear divergences at the differential level. In this section, we wish to emphasise yet another reason why it is preferable to use the $\{q_0^2, \theta_0\}$-variables. This is sometimes called the migration of radiation or the distortion of the spectrum: at fixed q^2, effectively the radiative process is probed at a different $q_0^2 = (q+k)^2$ as a result of the photon carrying away momentum. If the spectrum has significant variations in q_0^2, this implies a significant distortion in the kinematical distribution. This effect is indeed well-known from the determination of the J/Ψ-pole in $e^+e^- \to$ hadrons [120]. Generically, the more inclusive one gets in the photon energy and angle, the more pronounced it is, as in this case the radiative topologies (4-body) can be

very different from the virtual ones (3-body).

Let us illustrate the effect by considering the hard-collinear radiation, $\tilde{\mathcal{F}}^{(hc,\ell)}(\underline{\delta})$ given in Eq. (5.41). Assuming the $m_K = 0$ limit, for simplicity, the dz-integrand contains $|\mathcal{A}^{(0)}(q_0^2, c_0)|^2 \propto f_+(q_0^2)^2 = f_+(q^2/z)^2$ (c.f. Eq. (4.81) with $m_\ell = 0$) and $q_0^2 = q^2/z$ from Eq. (5.37). Since $z < 1$ in general, it is clear that momentum transfers of a higher range are probed. For $c_\ell = -1$, maximising the effect, one gets

$$z_{\delta_{\rm ex}}(q^2)\Big|_{c_\ell=-1} = \frac{q^2}{q^2 + \delta_{\rm ex} m_B^2} \,, \quad (q_0^2)_{\rm max} = q^2 + \delta_{\rm ex} m_B^2 \,, \tag{6.7}$$

upon using (5.42). Thus for $\delta_{\rm ex} = 0.15$ and $q^2 = 6\,\text{GeV}^2$ one finds $(q_0^2)_{\rm max} = 10.18\,\text{GeV}^2$ which is of course problematic when one wants to probe R_K in the $q^2 \in [1, 6]\,\text{GeV}^2$ range, given that the charmonia start to impact more severely well below $10\,\text{GeV}^2$. In the photon-inclusive case, the lower boundary becomes $z_{\rm inc}(c_\ell)|_{m_K \to 0} = \hat{q}^2$ by Eq. (5.42) and $(q_0^2)_{\rm max} = m_B^2$. Hence, in that case the entire spectrum is probed for any fixed value of q^2 which confirms the earlier statement. This would be rather problematic in $\bar{B} \to \bar{K}\ell^+\ell^-$ decays due to the large charmonia contributions (cf. comments below (4.18)), that would "contaminate" all the q^2 region below their masses. This is why in experimental analyses, stringent cuts on the photon energy (or the reconstructed B-meson mass) and its emission angle are implemented.

The effects described above are visible in all of the plots in Fig. 6.6. We stress that they are underestimated since a) we kept only one power in the derivative expansion and b) one would need to incorporate long-distance effects in addition. Note that for the virtual contributions, it is only when both hadrons are neutral that the derivative expansion can be avoided. If this is not the case, it is important to take into account higher derivative corrections and perform the matching of the finite counterterms from QCD.

As alluded to above, besides the cut on the reconstructed B-meson mass, in order to reduce the migration of radiation (or better the distortion of the q^2 spectrum) one can further restrict the photon's phase space in the photon's emission angle. From $q = q_0 - k$, taking into account (4.26), one gets

$$q^2 = q_0^2 - 2E_\gamma^{(1)}(E_{q_0}^{(1)} + |\vec{q}_0^{\,(1)}|\cos\theta_\gamma^{(1)}). \tag{6.8}$$

Then, using the expression of the maximum photon energy in (4.77), one arrives

at

$$(q_0^2)_{\max} = q^2 + \delta_{\rm ex} m_B (E_{q_0}^{(1)} + |\vec{q}_0^{\,(1)}| \cos\theta_\gamma^{(1)}) \; . \tag{6.9}$$

Assuming again for simplicity the $m_K = 0$ limit where $E_{q_0}^{(1)} = (m_B^2 + q_0^2)/(2m_B)$ and $|\vec{q}_0^{\,(1)}| = (m_B^2 - q_0^2)/(2m_B)$, one finds

$$(q_0^2)_{\max} = \begin{cases} q^2 + \delta_{\rm ex} q_0^2 & \cos\theta_\gamma^{(1)} = -1 \quad \text{tight-angle cut} \\ q^2 + \delta_{\rm ex} m_B^2 & \cos\theta_\gamma^{(1)} = +1 \quad \text{max-angle} \end{cases} \; . \tag{6.10}$$

This means that for fixed q^2, and a cut of $\delta_{\rm ex} = 0.15$, the radiative process probes values of $(q_0^2)_{\max} = q^2/(1-\delta_{\rm ex}) \simeq 1.18\, q^2$ (tight-angle cut) and $(q_0^2)_{\max} \simeq q^2 + 4.18\,\text{GeV}^2$ (max-angle) respectively. Note that the maximum angle cut in the photon-emission gives the same result as the maximum lepton angle, c.f. Eq. (6.7). This is because in the collinear limit ($\vec{\ell}_1 \propto \vec{k}$), the maximum lepton angle aligns $\vec{\ell}_1$ and $\vec{k}$ with the decay axis (x-axis, see Fig. 4.1), and this coincides with the maximum angle cut.

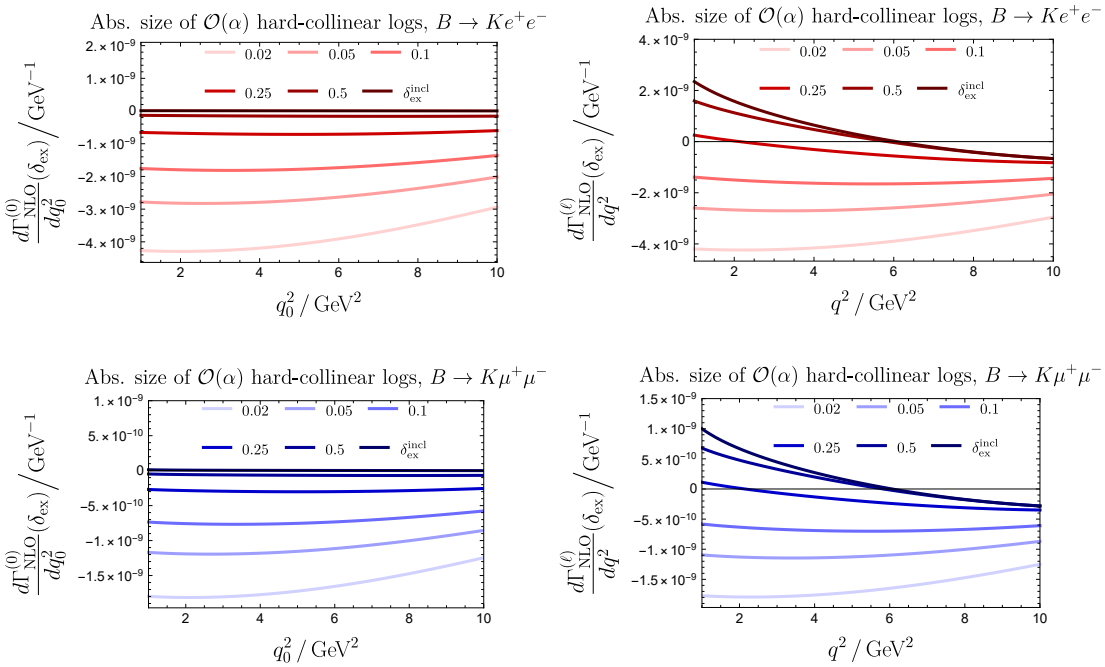

Figure 6.7: Absolute size of hard-collinear logs as a function of q_a^2 for the electron and muon (top) and (bottom) respectively. The quantity is shown for various photon cut-offs $\delta_{\rm ex}$ (4.4). It is noted that for $\delta_{\rm ex} = \delta_{\rm ex}^{\rm inc}$, the cancellation of the logs can be seen in the q_0^2 variable. When integrated over q^2, the cancellation of hard-collinear happens, although it is not fully visible from the plot as we show a restricted region for q^2. Bottom and top figures are similar by a scaling factor, cf. (6.12) and the explanation above it.

6.1.4 The size of hard-collinear logarithms as a function of $\delta_{\rm ex}$ and q^2

It is of interest to investigate the size of the collinear logs. We do this by normalising against the non-radiative LO differential rate, as done previously in Sec. 6.1.2,

$$\Delta^{(a)}_{\rm hc}(q_a^2, c_a; \delta_{\rm ex}) = \Delta^{(a)}(q_a^2, c_a; \delta_{\rm ex})\Big|_{\ln \hat{m}_{\ell_{1,2}}} = \left(\frac{d^2\Gamma^{\rm LO}}{dq_a^2 dc_a}\right)^{-1} \frac{d^2\Gamma(\delta_{\rm ex})}{dq_a^2 dc_a}\Big|_{\ln \hat{m}_{\ell_{1,2}}}, \quad (6.11)$$

where the terms on the RHS can be found in Eqs. (4.80) and (5.44) respectively. Charged and neutral meson modes are not distinguished as they contain the same collinear divergences as the latter are strictly proportional to the lepton charges, i.e. independent of the hadron charges. Thus, there is only one basic mode of interest for the hard-collinear logs per lepton pair final state. The integrated quantities $\Delta^{(a)}_{\rm hc}(q^2; \delta_{\rm ex})$ and $\Delta^{(a)}_{\rm hc}(c_\ell, [q_1^2, q_2^2]; \delta_{\rm ex})$ are defined in complete analogy to Eqs. (6.5) and (6.6) respectively.

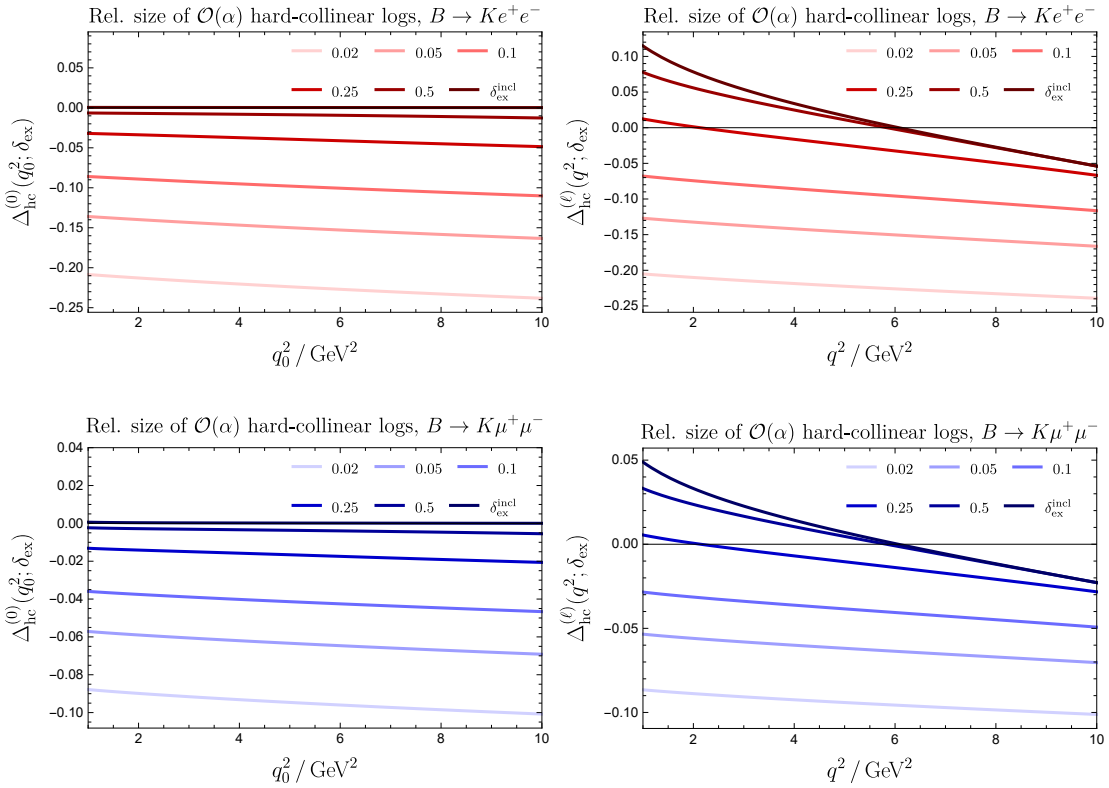

Figure 6.8: Relative size of hard-collinear logs $\Delta^{(a)}_{\rm hc}(q_a^2;\delta_{\rm ex})$ as a function of q_a^2 for the electron and muon (top) and (bottom) respectively. The quantity is shown for various soft-photon cut-offs $\delta_{\rm ex}$ (4.4). As in Fig. 6.7, the cancellation of the hard collinear logs can be seen for the q_0^2 variable for $\delta_{\rm ex} = \delta_{\rm ex}^{\rm inc}$. Bottom and top figures are similar by a scaling factor cf. (6.12).

Plots of absolute (unnormalised) hard-collinear QED corrections are shown in Fig. 6.7 as a function of q_a^2 and in Fig. 6.9 as a function of c_a. Plots of $\Delta^{(a)}_{\rm hc}(q_a^2;\delta_{\rm ex})$ and $\Delta^{(a)}_{\rm hc}(c_a,[q_1^2,q_2^2];\delta_{\rm ex})$, in complete analogy to those in Sec. 6.1.2, are shown in Fig. 6.8 and Fig. 6.10 respectively for different photon energy cuts $\delta_{\rm ex}$ (4.4) for electrons and muons. The effects are larger for the electrons because of the size of $\ln \hat{m}_e$ versus $\ln \hat{m}_\mu$ logs. In the photon-inclusive case, the cancellation of the hard-collinear logs is visible at the differential level in the q_0^2-variable. For the q^2-variable, the hard-collinear logs cancel when integrated over the entire q^2-interval, the tendency of which can be inferred from the plots on the reduced interval $q^2_{\rm max} < 10\,{\rm GeV}^2$. The reader is reminded that hatted quantities are normalised w.r.t. to the B-mass, $\hat{m}_{\ell_{1,2}} = m_{\ell_{1,2}}/m_B$. Hence one expects

$$R_{\rm hc} = \frac{\Delta^{(a)}_{\rm hc}(q_a^2;\delta_{\rm ex})|_{\bar{B}\to\bar{K}e^+e^-}}{\Delta^{(a)}_{\rm hc}(q_a^2;\delta_{\rm ex})|_{\bar{B}\to\bar{K}\mu^+\mu^-}} \simeq \frac{\ln(\hat{m}_e)}{\ln(\hat{m}_\mu)} \simeq 2.363\,, \tag{6.12}$$

with corrections of the order of $\mathcal{O}(m_e^2\ln(\hat{m}_e) - m_\mu^2\ln(\hat{m}_\mu))$.

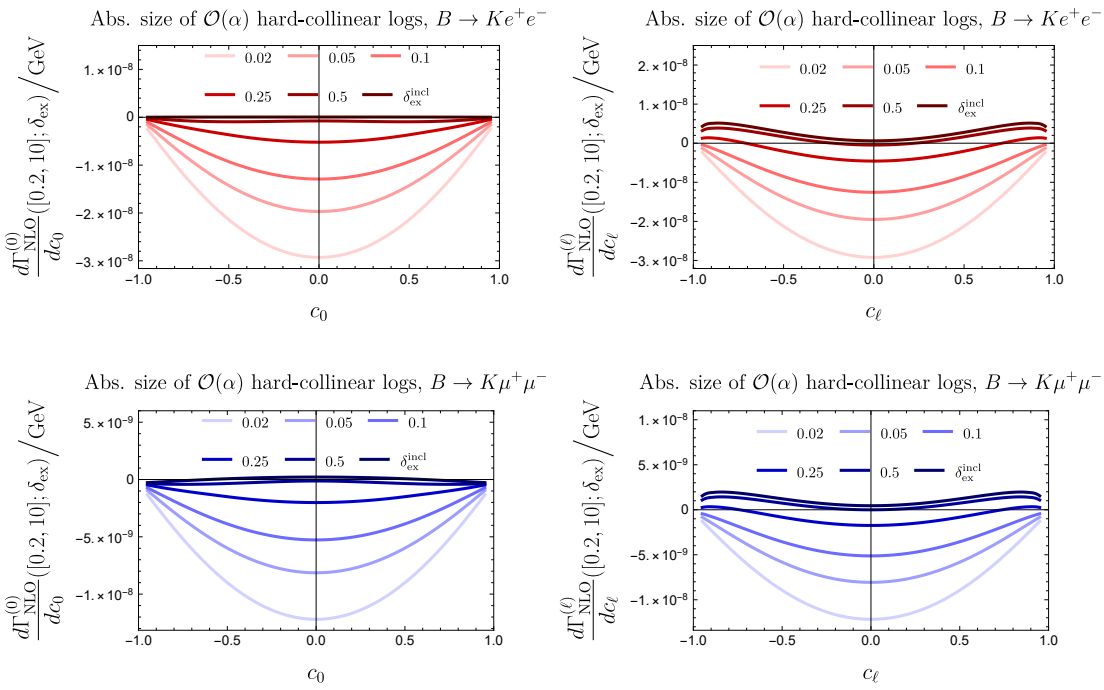

Figure 6.9: Absolute size of hard-collinear logs as a function of c_a for the electron and muon (top) and (bottom) respectively. The quantity is shown for various photon cut-offs $\delta_{\rm ex}$ (4.4). It is noted that for $\delta_{\rm ex} = \delta_{\rm ex}^{\rm inc}$, the cancellation of the logs can be seen in the q_0^2 variable. When integrated over c_ℓ, the cancellation does not fully happen, and this is due to the binning of q^2. As with the plots against q_a^2 in Fig. 6.8, bottom and top figures are similar by a scaling factor cf. (6.12).

Inspection of the plots shows that this is indeed the case. We would like to stress that extracting the hard-collinear logs on their own is slightly ambiguous as one needs to normalise them (hatted notation). The unambiguous way to show them is through the full plots in the main text. Nevertheless, they illustrate nicely the effect of the photon energy cut.

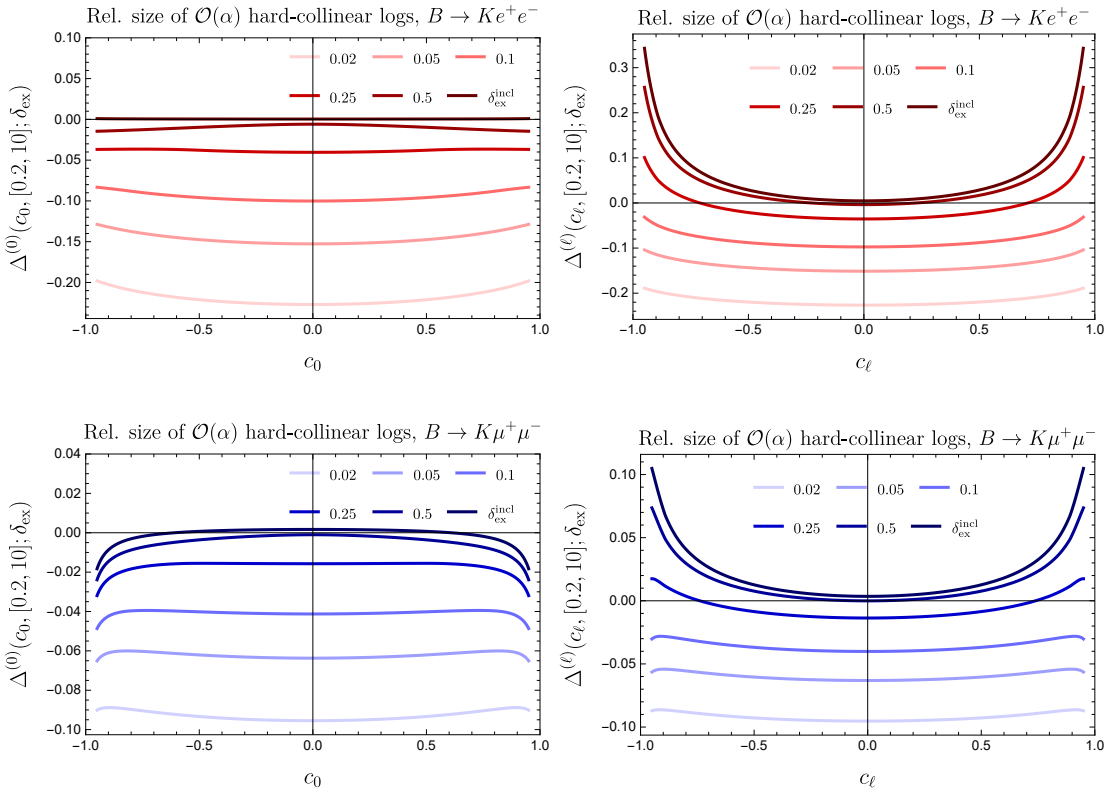

Figure 6.10: Relative size of hard-collinear logs as a function of c_a for the electron and muon (top) and (bottom) respectively. The quantity is shown for various photon cut-offs $\delta_{\rm ex}$ (4.4). It is noted that for $\delta_{\rm ex} = \delta_{\rm ex}^{\rm inc}$, the cancellation of the logs can be seen in the q_0^2 variable. As with the plots against q_a^2 in Fig. 6.8, bottom and top figures are similar by a scaling factor cf. (6.12). Note that the enhancing towards the end-points happens due to the leading order rate being $\propto (1 - c_\ell^2) + \mathcal{O}(m_\ell^2)$, as was the case in Fig. 6.5.

Comparison of $\bar{B} \to \bar{K}\ell^+\ell^-$ to the inclusive case $b \to s\ell^+\ell^-$

It is interesting to compare our results to the inclusive rate in [121] with regard to the hard-collinear logs. Let us define

$$\Delta_{\rm hc}^{(\ell)}(\hat{q}^2) = \frac{2\alpha\,\hat{Q}_{\ell_1}^2}{\pi}\left(\frac{1}{\Gamma^{\rm LO}}\frac{d\Gamma^{\rm LO}(\hat{q}^2)}{d\hat{q}^2}\right)^{-1}\tilde{\Delta}_{\rm hc}^{(\ell)}(\hat{q}^2)\,, \tag{6.13}$$

where $\hat{Q}_{\ell_1}^2 = \hat{Q}_{\bar{\ell}_2}^2$ and $m_{\ell_1} = m_{\ell_2} \equiv m_\ell$ have been assumed. Then, it is known that the collinear logs of the electron can be extracted from (e.g. chapter 17 in

[122])[3]

$$\tilde{\Delta}^{(\ell)}_{\rm hc}(\hat{q}^2) = \frac{1}{\Gamma^{\rm LO}}\left(\int_{\hat{q}^2}^1 \frac{dz}{z} P_{f\to f\gamma}(z) \frac{d\Gamma^{\rm LO}(\hat{q}^2/z)}{d\hat{q}^2/z}\right) \ln\frac{\Lambda_b}{m_\ell}\,, \tag{6.14}$$

where $\Lambda_b = \mathcal{O}(m_b)$ is some reference scale, $P_{f\to f\gamma}(z)$ is the full leading order splitting function,

$$P_{f\to f\gamma}(z) = \frac{1+z^2}{(1-z)_+} + \frac{3}{2}\delta(1-z)\,, \tag{6.15}$$

and $1/(1-z)_+$ is the plus distribution,

$$\int_0^1 dz f(z)/(1-z)_+ = \int_0^1 dz (f(z)-f(1))/(1-z). \tag{6.16}$$

Note that by construction, the hard-collinear logs cancel in the total rate. This can be seen by reversing the order of integration and adopting the change of variable $\hat{q}^2/z = \hat{q}_0^2$ to arrive at $\int_0^1 d\hat{q}^2 \tilde{\Delta}^{(\ell)}_{\rm hc}(\hat{q}^2) \propto \int_0^1 dz P_{f\to f\gamma}(z) = 0$. Now, the zeroth moment of the splitting function vanishes since it corresponds to the anomalous dimension of the (conserved) electromagnetic current. Conversely, (6.14) can be deduced from Eq. (5.19) by integrating over dc_0, substituting $q_0^2 = q^2/z$ and then integrating over z. From (5.20), the full splitting function is then easily deduced by adding a delta function ansatz $A\delta(1-z)$ and regularising the $1/(1-z)$ such that the soft divergences cancel (which leads to the plus distribution).

The leading order differential rates are given by

$$\frac{1}{\Gamma^{\rm LO}}\frac{d\Gamma^{\rm LO}(\hat{q}^2)}{d\hat{q}^2} = \begin{cases} 2(1-\hat{q}^2)^2(2\hat{q}^2+1) & b\to s\ell^+\ell^- \\ 4(1-\hat{q}^2)^3 & \bar{B}\to \bar{K}\ell^+\ell^- \end{cases}\,, \tag{6.17}$$

where the $m_s \to 0$ limit is implied in [121] and for simplicity we have assumed the $m_K \to 0$ limit and a constant form factor. Note that the factor $\hat{\lambda}_B^{1/2} = \lambda^{1/2}(1, \hat{m}_K^2, \hat{q}^2)|_{m_K\to 0} = 1-\hat{q}^2$ is the square root of the Källén-function and as such, is related to the three velocity of the strange particle in the B-meson's RF.

[3] From section 5 in [121], one can extract a similar formula for the collinear logs

$$\tilde{\Delta}^{(\ell)}_{\rm hc}(\hat{q}^2) = \frac{1}{\Gamma^{\rm LO}}\left(\int_{\hat{q}^2}^1 \frac{dz}{z}\tilde{P}_{f\to f\gamma}(z)\frac{d\Gamma^{\rm LO}(\hat{q}^2/z)}{d\hat{q}^2/z} - \int_0^1 dz \tilde{P}_{f\to f\gamma}(z)\frac{d\Gamma^{\rm LO}(\hat{q}^2)}{d\hat{q}^2}\right)\ln\frac{\Lambda_b}{m_\ell}\,,$$

where $\tilde{P}_{f\to f\gamma}(z)$ (given by (5.20)) is the collinear emission part of the splitting function. Soft divergences at $z\to 1$ cancel between the two integrals. Translating into our notation from [121] demands $x = 1-z$, $\hat{s} = \hat{q}^2$ and $\tilde{P}_{f\to f\gamma}(z)$ is the the part collinear in $f_\gamma^{(m)}$ up to factors of proportionality properly accounted for. Our formula (6.14) can be recovered upon using that $\int dz P_{f\to f\gamma}(z) = 0$.

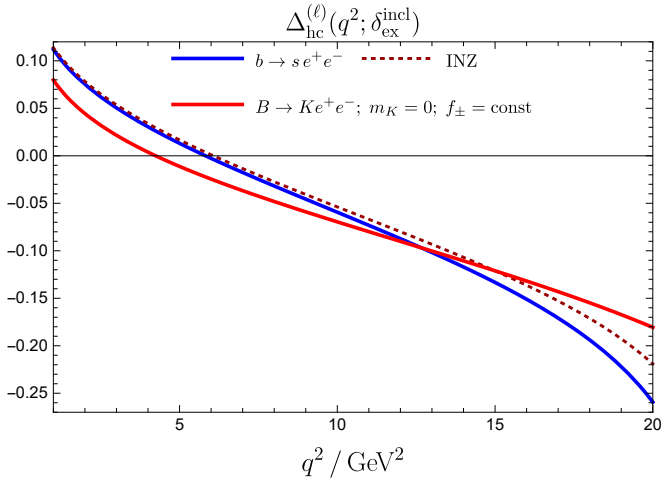

Figure 6.11: Comparison of hard-collinear logs in $b \to s e^+ e^-$ (solid blue line) versus $\bar{B} \to \bar{K} e^+ e^- (\gamma)$ with no photon energy cut, constant form factors and $m_K \to 0$ (solid red line) corresponding to Eqs. (6.18). This illustrates the spin-dependence of the hard-collinear which can be traced back to the LO differential rates in the case at hand cf. (6.17). For further comparison, we have added the full result in the dotted red line for our work with no photon energy cut either. The agreement at low q^2 of the latter with the $b \to s e^+ e^-$ is somewhat accidental.

Its power in the rate is determined by the interaction and the spin of the particle (e.g. if it were $\bar{B} \to \bar{K}^* \ell^+ \ell^-$ then $d\Gamma^{\rm LO} \propto (1 - \hat{q}^2)$ [123]). The factor $2\hat{q}^2 + 1$ originates from the s-quark's spin summation. One finds

$$\begin{aligned}
\tilde{\Delta}_{\rm hc}^{b\to s\ell^+\ell^-}(\hat{q}^2) \;&=2\left((6\hat{q}^4-4\hat{q}^6-1)\ln\hat{q}^2+2(1-\hat{q}^2)^2(2\hat{q}^2+1)\ln(1-\hat{q}^2)+\frac{12\hat{q}^4-8\hat{q}^6-3\hat{q}^2-1}{3}\right),\\
\tilde{\Delta}_{\rm hc}^{\bar{B}\to\bar{K}\ell^+\ell^-}(\hat{q}^2)&=4\left(\left(2\hat{q}^6-6\hat{q}^4+3\hat{q}^2-1\right)\ln\hat{q}^2+2(1-\hat{q}^2)^3\ln(1-\hat{q}^2)+\frac{4\hat{q}^6-6\hat{q}^4+6\hat{q}^2-6}{3})\right).
\end{aligned} \tag{6.18}$$

The basic form is similar in both cases and we observe the $\ln q^2$-term leading to enhanced collinear emission at low q^2 which can be interpreted as a migration of the photon radiation cf. Sec. 6.1.3. We wish to stress again that $\tilde{\Delta}_{\rm hc}^{\bar{B}\to\bar{K}\ell^+\ell^-}$ receives corrections due to finite m_K and non-constant form factor and that $\delta_{\rm ex} = \delta_{\rm ex}^{\rm inc}$ was assumed. Both of these features are included in the comparison plot Fig. 6.11. We have checked that integrating (5.44) over $\int_{-1}^{1} dc_\ell$ reproduces the $\tilde{\Delta}_{\rm hc}^{\bar{B}\to\bar{K}\ell^+\ell^-}$-expression in (6.18). This comparison provides another non-trivial cross-check of our analysis.

6.1.5 Comparison with earlier work on $\bar{B} \to \bar{K}\ell^+\ell^-$ and comments on R_K

In this section, we compare our results to those presented in [2]. The analysis of [2], which first investigated the impact of LFU breaking in $\bar{B} \to \bar{K}\ell^+\ell^-$ induced by QED corrections, is a simplified analysis based on the following three principles/assumptions:

i. indirect determination of virtual corrections by imposing the absence of log-enhanced terms in the photon-inclusive $d\Gamma/dq_0^2$ spectrum (for any value of q_0^2);

ii. constructing a radiator function depending on q^2 and q_0^2 only, which describes the probability of a dilepton pair (of invariant mass q^2) to originate from momentum transfer q_0^2, after photon-emission;

iii. neglecting lepton-flavour universal radiative corrections, such as those induced by the emissions from meson legs only.

As proved in general terms in this work, assumption i. is correct and provides an efficient way to determine the radiator function. Our analysis shows that the non-log enhanced terms are small in the neutral-meson case (as shown in Fig. 6.3). They do exceed the 1% level in the charged-meson case, but this is a lepton-flavour universal effect.

On the other hand, while assumption ii. is a legitimate choice, it is incompatible with the goal of estimating radiative corrections by implementing only a cut on the reconstructed B-meson mass:[4] the radiator in [2] is obtained by integrating over all photon angles; however, as already discussed in Sec. 6.1.3, in the B-RF the relation connecting q_0^2 and q^2 does not only depend on $m_B^{\rm rec}$ but also on the photon's emission angle. To overcome this problem, in [2] the maximal q_0^2 value affecting the spectrum at a given q^2 value has been determined by imposing the tight cut defined in (6.10). This choice corresponds to the *minimal* value of $(q_0^2)_{\rm max}$ obtainable with an experimental cut on photons not emitted forward with respect to $\vec{q}$ (in the B-RF). Incidentally, we note that a cut of this type is implemented in the experimental analysis to avoid a large migration effect (e.g. charmonium

[4] We note that a radiator function depending on q^2 and q_0^2 only is sufficient to estimate the distortion of the q^2 spectrum in the absence of a photon-energy cut, as is for instance done in Higgs-collider physics [124].

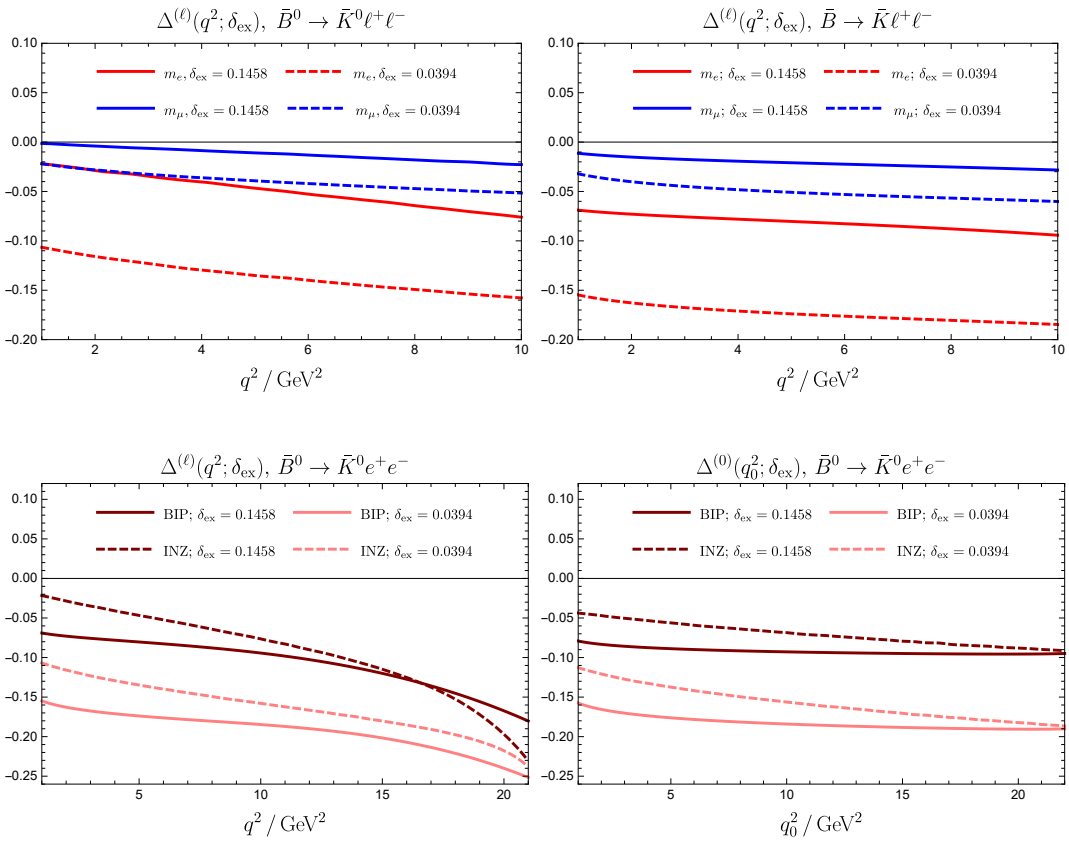

Figure 6.12: Relative effects of relative corrections as a function of q^2, in the neutral case, with the cuts on $m_B^{\rm rec}$ used in [2] computed in this work (top left) vs. those presented in [2] (top right). The bottom left and bottom right plots compare our results with those in [2] for the q^2 and q_0^2-spectrum respectively. The translation between the notation of this reference and ours is $\delta_{\rm ex} = 1-(m_B^{\rm rec}/m_B)^2$ with $(\bar{p}_B = m_B^{\rm rec})$ and $\{0.1458, 0.1, 0.0394\} \leftrightarrow m_B^{\rm rec} = \{4.88, 5.009, 5.175\}$ GeV.

resonances at low q^2, cf. Sec. 6.1.3). This is the most important difference among the two approaches. As illustrated in Fig. 6.12, the net effect is quite sizeable, especially for the electrons at low values of q^2.

In practice, the implicit cut applied in [2] on the photon-emission angle removes some hard-collinear logs. We may track the difference on the collinear logs analytically. We demonstrate this for the q_0^2-spectrum since the expression (5.30) is much simpler than the corresponding one for q^2 in (5.41). Let us consider

$$\frac{d\Gamma}{dq_0^2} = \frac{\alpha}{\pi}\left[\frac{d\Gamma}{dq_0^2}\right]^{\rm LO}\left(A_0 \ln\delta_{\rm ex} + C_0\right)\ln m_\ell + \text{non-collinear}\,. \tag{6.19}$$

The coefficients A_0 and C_0 are obtained by integrating Eq. (9) –using the boundary conditions implied by Eq. (10) of [2]– w.r.t. to x (which is our z and moreover, $1-\delta^2 = \delta_{\rm ex}$), and the expression in (5.30) with $z(\omega_s) \to 1$ but

finite $\delta_{\rm ex}$. Not surprisingly, we find

$$A_0 = A_0^{\rm INZ} = A_0^{\rm BIP} = -4\ . \tag{6.20}$$

This is the universal coefficient of the soft–collinear singularity (double log), which is independent of the boundary conditions. Incidentally, we note that this coefficient is also the same for the $\frac{d\Gamma}{dq^2}$-distribution. Low's theorem guarantees that the single $\ln\delta_{\rm ex}$-term is identical. For the C_0 term, however, there are differences

$$\begin{aligned} C_0^{\rm INZ} =& -\frac{25}{3} + 2\ln\hat{q}_0^2 + 2\frac{(1-\hat{m}_K^2+\hat{q}_0^2)^2}{\hat{\lambda}} - R\ln\left[\frac{1-\hat{m}_K^2+\hat{q}_0^2-\hat{\lambda}^{1/2}}{1-\hat{m}_K^2+\hat{q}_0^2+\hat{\lambda}^{1/2}}\right] + \mathcal{O}(\delta_{\rm ex}), \\ C_0^{\rm BIP} =& \left(-3-4\ln\left[1+\frac{\hat{m}_K^2}{1-\hat{q}_0^2}\right]\right) + \mathcal{O}(\delta_{\rm ex})\ , \end{aligned} \tag{6.21}$$

where $\hat{\lambda} \equiv \lambda(1,\hat{m}_K^2,\hat{q}_0^2)$ and

$$R = 2(1+\hat{q}_0^2-\hat{m}_K^2)\left(\frac{1}{\hat{\lambda}^{1/2}} - \frac{2\hat{q}_0^2}{\hat{\lambda}^{3/2}}\right)\ . \tag{6.22}$$

Note that in [2], only the leading term in m_K^2 was kept in $(q_0^2)_{\rm max}$ and thus, for meaningful comparison, one has to assume the $m_K \to 0$ limit

$$\begin{aligned} C_0^{\rm INZ} &= -\frac{19}{3} + 8\frac{\hat{q}_0^2}{(1-\hat{q}_0^2)^2} + 4\frac{(3-\hat{q}_0^2)}{(1-\hat{q}_0^2)^3}\hat{q}_0^4\ln\hat{q}_0^2 + \mathcal{O}(\delta_{\rm ex}) \\ &\overset{\hat{q}_0^2\to 1}{\longrightarrow} -3 + \mathcal{O}(\delta_{\rm ex}) + \mathcal{O}(\hat{q}_0^2-1), \\ C_0^{\rm BIP} &= -3 + \mathcal{O}(\delta_{\rm ex})\ . \end{aligned} \tag{6.23}$$

Agreement is found at the kinematic endpoint $\hat{q}_0^2 \to 1$ (including $\mathcal{O}(\delta_{\rm ex})$-terms). This is to be expected since the cut on $(q_0^2)_{\rm max}$ is independent of the photon-emission angle, whereas differences are maximal at low q_0^2 values, consistent with the numerical findings in Fig. 6.12 (bottom-right).

To better understand the agreement at large $\hat{q}_0^2$ illustrated in (6.23), consider (5.22), with $\delta = \delta_{\rm ex}$, which corresponds to the case where the photon becomes collinear with ℓ_1. With a non-zero Kaon mass, $(\hat{q}_0^2)_{\rm max} = (1-\hat{m}_K)^2$, and thus the lower limit for the $z-$integration becomes

$$z_{\rm INZ}(\delta_{\rm ex},(\hat{q}_0^2)_{\rm max},c_0) = 1 - \frac{\delta_{\rm ex}}{1-\hat{m}_K}\ , \tag{6.24}$$

where the c_0-dependence drops (and thus the same z limit applies for ℓ_2). Now, consider $q_0^2 = q^2 + m_B\delta_{\rm ex}(E_{q_0}^{(1)} + |\vec{q}_0^{\,(1)}|\cos\theta_\gamma^{(1)})$, which is the defining principle behind Eq. (10) of [2], where $E_{q_0}^{(1)}$ and $|\vec{q}_0^{\,(1)}|$ are given in (4.27). Substituting $q^2 = zq_0^2$, one gets

$$z_{\rm BIP} = 1 - \frac{m_B\,\delta_{\rm ex}}{q_0^2}(E_{q_0}^{(1)} + |\vec{q}_0^{\,(1)}|\cos\theta_\gamma^{(1)}) \stackrel{\hat{q}_0^2\to(\hat{q}_0^2)_{\rm max}}{\longrightarrow} 1 - \frac{\delta_{\rm ex}}{1-\hat{m}_K}, \tag{6.25}$$

which matches (6.24). This explains the agreement at large $\hat{q}_0^2$ in (6.23) and in Fig. 6.12. Note that the $\theta_\gamma^{(1)}$ dependence drops in the limit of $\hat{q}_0^2 \to (\hat{q}_0^2)_{\rm max}$, analogous to the c_0 dependence in (6.24). The c_0-independence (or equivalently $\theta_\gamma^{(1)}$) at $(\hat{q}_0^2)_{\rm max}$ happens since the Kaon's three-momentum vanishes and the (1)- and (4)-RF become equivalent and thus, there cannot be any non-trivial angular dependence.

On the other hand, the same argument does not apply to the differential rate in q^2. As $q^2 \to q^2_{\rm max}$, the range of allowed photon energies becomes more and more restricted. The cut $\bar{p}_B^2 > m_B^2(1-\delta_{\rm ex})$ on its own is independent of q^2, and it is for this reason that one needs the maximum condition imposed on the lower limit of the z-integration in (5.41). For larger q^2, the kinematic restriction on z, denoted by $z_{\rm inc}$, becomes more important than the restriction on z due to the photon energy cut $\delta_{\rm ex}$. This is why the two INZ-curves in the bottom left plot in Fig. 6.12 approach each other for large q^2.

In summary, from the comparison of our work with [2] we may deduce the following two lessons or insights.

a) The indirect determination of virtual logs in the photon-inclusive $d\Gamma/dq_0^2$-spectrum, which is the key assumption behind both the approach of Ref. [2] and PHOTOS [99], is correct.

b) A meaningful comparison between theory and experiment (in a collider environment) cannot be done by only considering the two non-radiative variables ($\{q_a^2, c_a\}$) and the cut on the reconstructed B-meson mass, but it requires a detailed information on the (inevitable) photon-emission angle cut as their impact is sizeable.

Point a) is reassuring in view of the current treatment of radiative corrections in R_K-measurements with PHOTOS. Incidentally, we note that considering only the cuts on reconstructed B-meson mass in [10], the net QED correction that

should be applied to R_K according to our analysis amounts to

$$\Delta_{\rm QED} R_K \approx \left.\frac{\Delta\Gamma_{K\mu\mu}}{\Gamma_{K\mu\mu}}\right|^{m_B^{\rm rec}=5.175\,{\rm GeV}}_{q_0^2\in[1,6]\,{\rm GeV}^2} - \left.\frac{\Delta\Gamma_{Kee}}{\Gamma_{Kee}}\right|^{m_B^{\rm rec}=4.88\,{\rm GeV}}_{q_0^2\in[1,6]\,{\rm GeV}^2} \approx +1.7\% \ , \qquad (6.26)$$

where in the SM

$$R_K\big|_{q_0^2\in[q_1^2,q_2^2]\,{\rm GeV}^2} = \frac{\Gamma[\bar{B}\to\bar{K}\mu^+\mu^-]}{\Gamma[\bar{B}\to\bar{K}e^+e^-]}\Big|_{q_0^2\in[q_1^2,q_2^2]\,{\rm GeV}^2} \approx 1+\Delta_{\rm QED}R_K \ , \qquad (6.27)$$

and the binning is understood as previously. The correction has to be compared with the $\Delta_{\rm QED}R_K \approx +3\%$ quoted in [2] that, as explained above, takes into account an additional implicit tight cut on the photon-emission angle. Note that the different photon energy cuts for muons ($m_B^{\rm rec} = 5.175\,{\rm GeV} \leftrightarrow \delta_{\rm ex} = 0.0394$) and electrons ($m_B^{\rm rec} = 4.88\,{\rm GeV} \leftrightarrow \delta_{\rm ex} = 0.1458$) reduce the effect of QED corrections to R_K. In addition, $|\Delta_{\rm QED}R_K^{\rm BIP}| > |\Delta_{\rm QED}R_K^{\rm INZ}|$ has to be expected since the BIP computation is more exclusive, in view of the tight photon-angle cut, than the explicit computation presented here. However, in both cases the overall impact of QED corrections in the LFU ratios (currently estimated by the experiment using PHOTOS) is not exceedingly large and below the current experimental error $R_K = 0.846^{+0.060+0.016}_{-0.054-0.014}$ [12].

On the other hand, point b) indicates the necessity to build a Monte Carlo program with a complete differential treatment of radiative corrections and an accurate parameterisation of the hadronic form factors (with the effective inclusion of long-distance effects, which we recall are *not* included in PHOTOS), in order to check the impact of the QED corrections on the kinematical distributions at the %-level, with the explicit cuts applied in experiments.

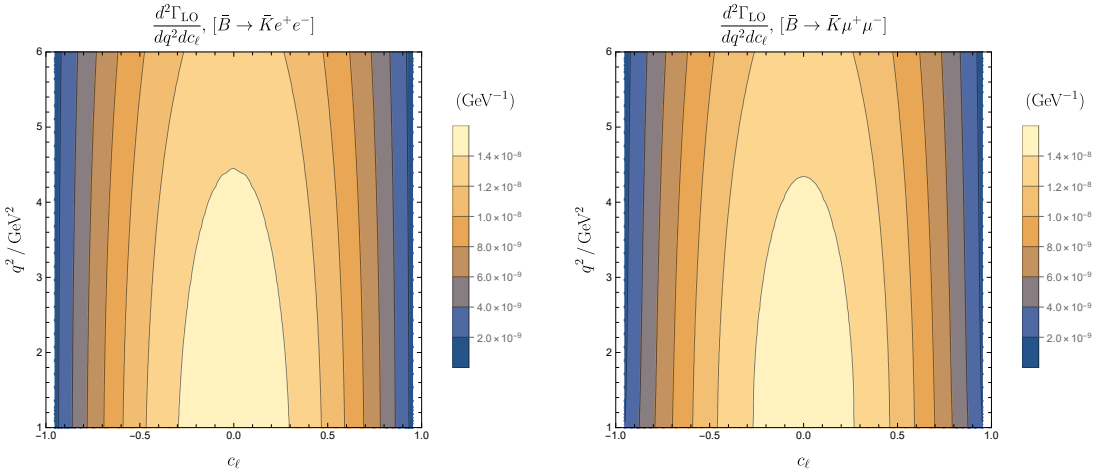

Figure 6.13: LO differential rate for electrons (right) and muons (left). They seem inverted compared to the NLO results in the figures below, since the LO contribution is positive while the corrections are generally negative. Also, the smallness of the lepton masses in both cases makes the heat maps look very similar.

6.1.6 Radiative corrections as a function of q_0^2, c_0 and q^2, c_ℓ at full differential level

In previous sections, the size of the corrections were shown as a 1D plot, i.e. after integrating one of the differential variables. Here, we present the results as a function of both differential variables, in the form of heat maps.

First, we show the LO result in Fig. 6.13, which is given as reference. Note that while the LO result is positive, all the NLO QED corrections are negative, and this causes the LO heat maps to appear inverted compared to the NLO ones. Furthermore, the LO differential rate for the muons very closely matches that for the electrons, and this is due to the smallness of the lepton masses compared to the other scales, such as q^2 and m_B^2.

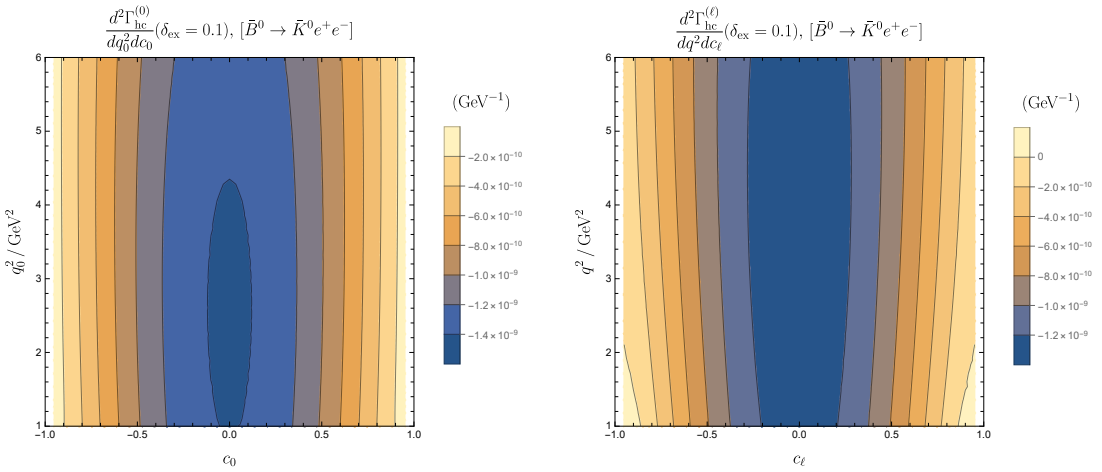

Figure 6.14: Absolute size of QED corrections as a function of $\{q_0^2, c_0\}$ (left) and $\{q^2, c_\ell\}$ (right). As expected, the heatmaps are symmetric with respect to $c_{\ell,0} \to -c_{\ell,0}$. A value of $\delta_{\rm ex} = 0.1$ was used for the experimental cut-off on the photon energy.

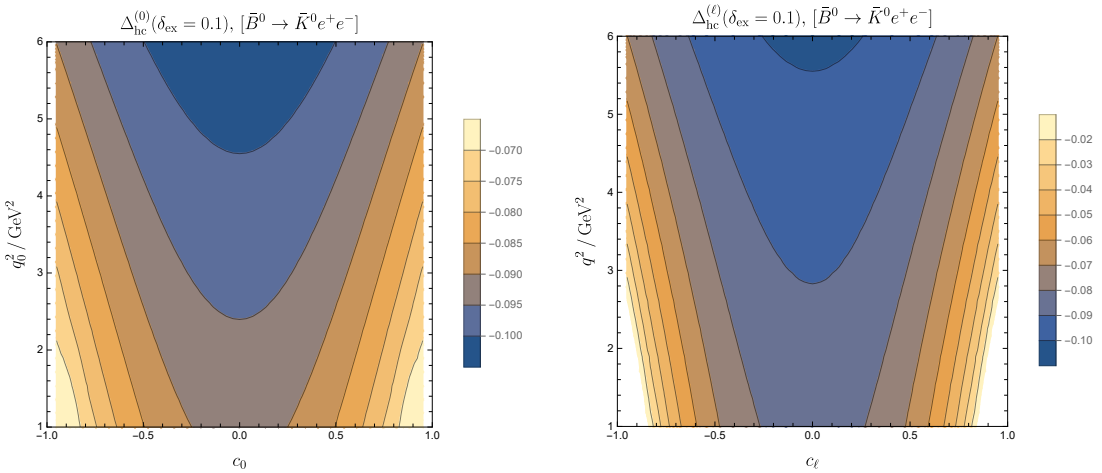

Figure 6.15: Relative QED corrections as a function of $\{q_0^2, c_0\}$ (left) and $\{q^2, c_\ell\}$ (right). As in Fig. 6.14, the heatmaps are symmetric with respect to $c_{\ell,0} \to -c_{\ell,0}$. A value of $\delta_{\rm ex} = 0.1$ was used for the experimental cut-off on the photon energy.

Next, we present the contributions coming from hard-collinear logs, defined by

$$\frac{d^2\Gamma_{\rm hc}^{(a)}(\delta_{\rm ex})}{dq_a^2 dc_a} \equiv \frac{d^2\Gamma(\delta_{\rm ex})}{dq_a^2 dc_a}\bigg|_{\ln \hat{m}_{\ell_{1,2}}}, \tag{6.28}$$

and Eq. (6.11) for the unnormalised and normalised QED corrections respectively. These are shown in Fig. 6.14 and 6.15 respectively. One thus finds that the differential rate can receive corrections of up to $\sim 10\%$. The heat maps for the muon case are simply a rescaling of the ones for the electrons, as is discussed in and around Eq. (6.12), and we omit the same discussion here. The charge of the

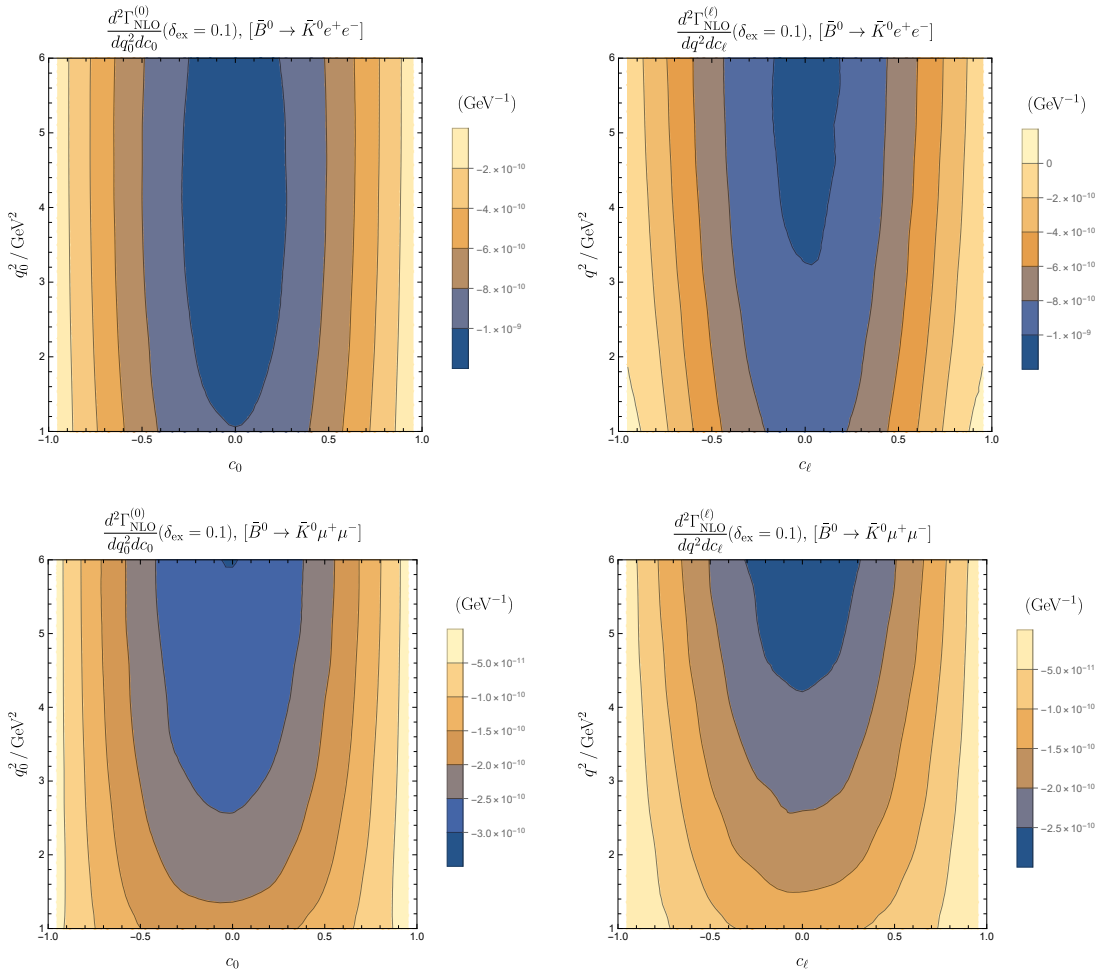

Figure 6.16: Absolute size of QED corrections as a function of $\{q_0^2, c_0\}$ (left) and $\{q^2, c_\ell\}$ (right) for electrons (top) and muons (bottom) in the neutral meson case. The corrections are larger for the electrons, as expected, due to the bigger size of the hard-collinear logs.

hadrons do not affect the heat maps for the hard-collinear corrections.

We use an experimental photon energy cut-off of $\delta_{\rm ex} = 0.1$ for all the heat maps in this section.

We also show the heat maps for total QED corrections for the unnormalised and normalised differential rate, c.f. Eq. (6.4). The total unnormalised and normalised QED corrections for the neutral meson cases are shown in Fig. 6.16 and 6.17 respectively for the muon and electron cases in the differential variables $\{q_0^2, c_0\}$ and $\{q^2, c_\ell\}$.

In both the electron and muon cases, there is perfect $c_\ell \to -c_\ell$ symmetry, as expected. There is a slight asymmetry for the heat maps in the c_0 variable, and this is due to the non-hard collinear contributions not being even in the c_0

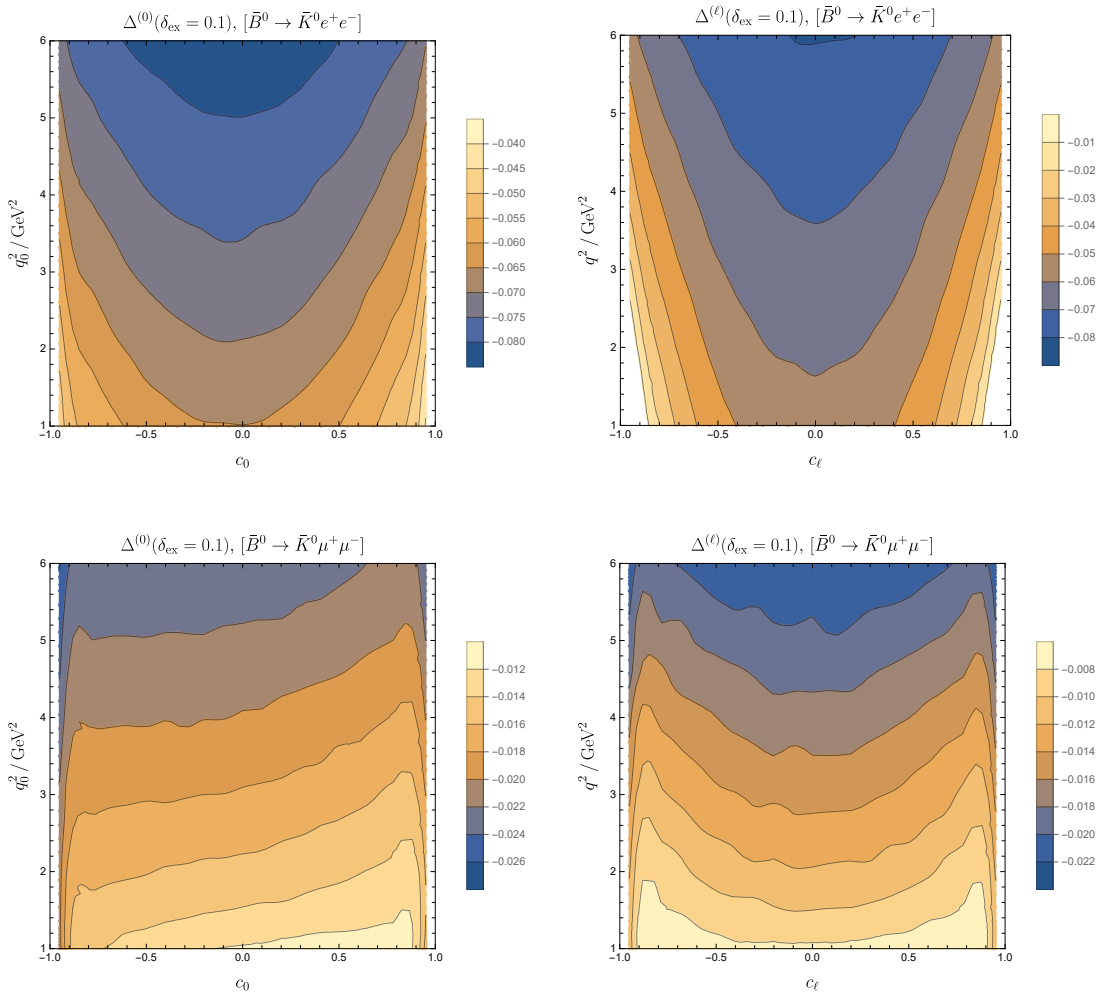

Figure 6.17: Relative size of QED corrections as a function of $\{q_0^2, c_0\}$ (left) and $\{q^2, c_\ell\}$ (right), with the top two heatmaps corresponding to $\bar{B}^0 \to \bar{K}^0 e^+ e^-$ and the bottom two to $\bar{B}^0 \to \bar{K}^0 \mu^+ \mu^-$. The heatmaps are symmetric only with respect to $c_\ell \to -c_\ell$; the non-hard-collinear corrections in the $\{q_0^2, c_0\}$ variables do not possess this symmetry, and this explains the slight asymmetry in the heat maps on the left.

variable.

The charged meson results for the unnormalised and normalised QED corrections are presented in Fig. 6.18 and 6.19 respectively. The heat maps are no longer symmetric in $c_\ell, c_0 \to -c_\ell, c_0$, due to the $\ln m_K$ contributions, which are odd in c_ℓ, c_0, and are sizeable. Furthermore, the same peculiar behaviour towards the endpoints ($c_\ell, c_0 \to \pm 1$) happens in Fig. 6.19 as in the 1D plots, due to the LO differential rate $\propto (1 - c_\ell^2) + \mathcal{O}(m_\ell^2)$, c.f. Eq. (4.81).

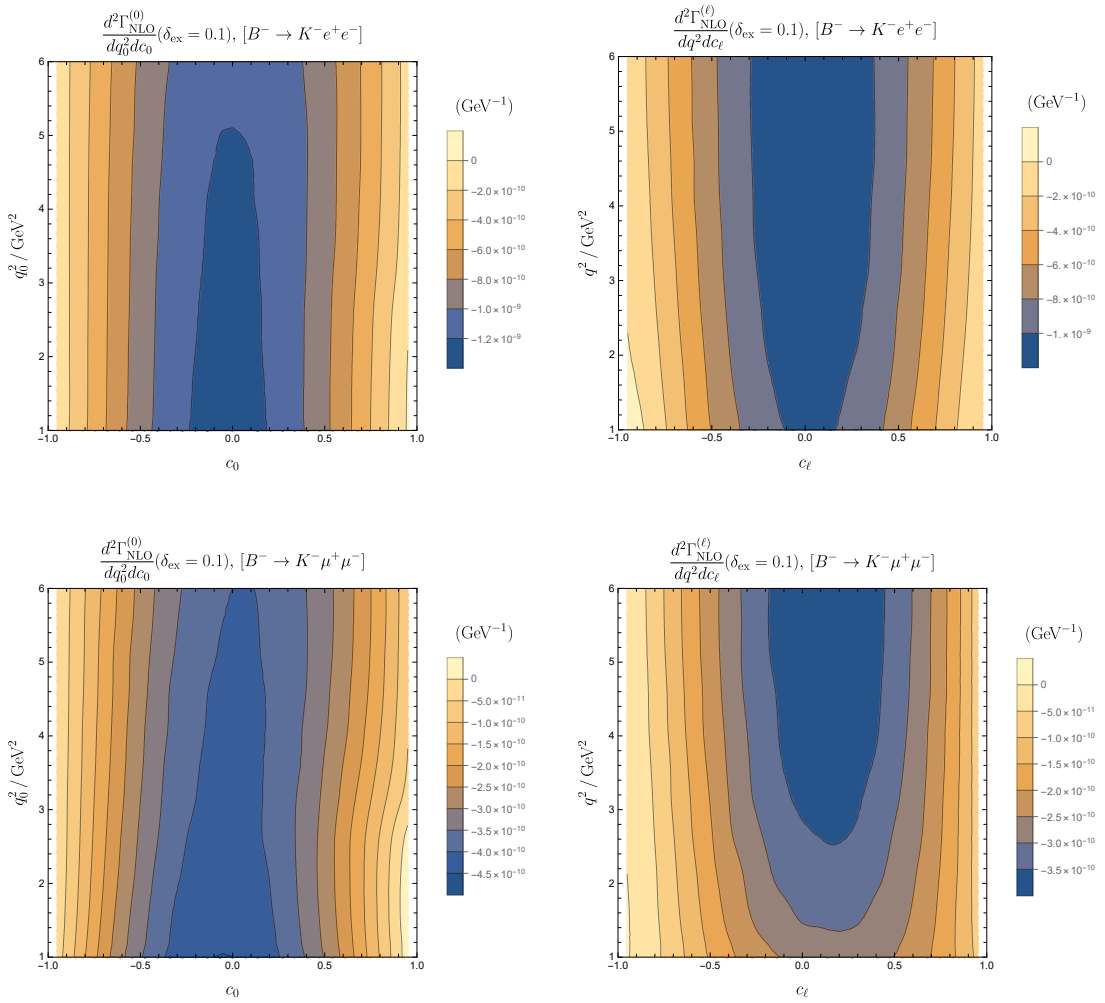

Figure 6.18: Absolute size of QED corrections as a function of $\{q_0^2, c_0\}$ (left) and $\{q^2, c_\ell\}$ (right) for electrons (top) and muons (bottom) in the charged meson case. The corrections are larger for the electrons, as expected, due to the hard-collinear logs being larger.

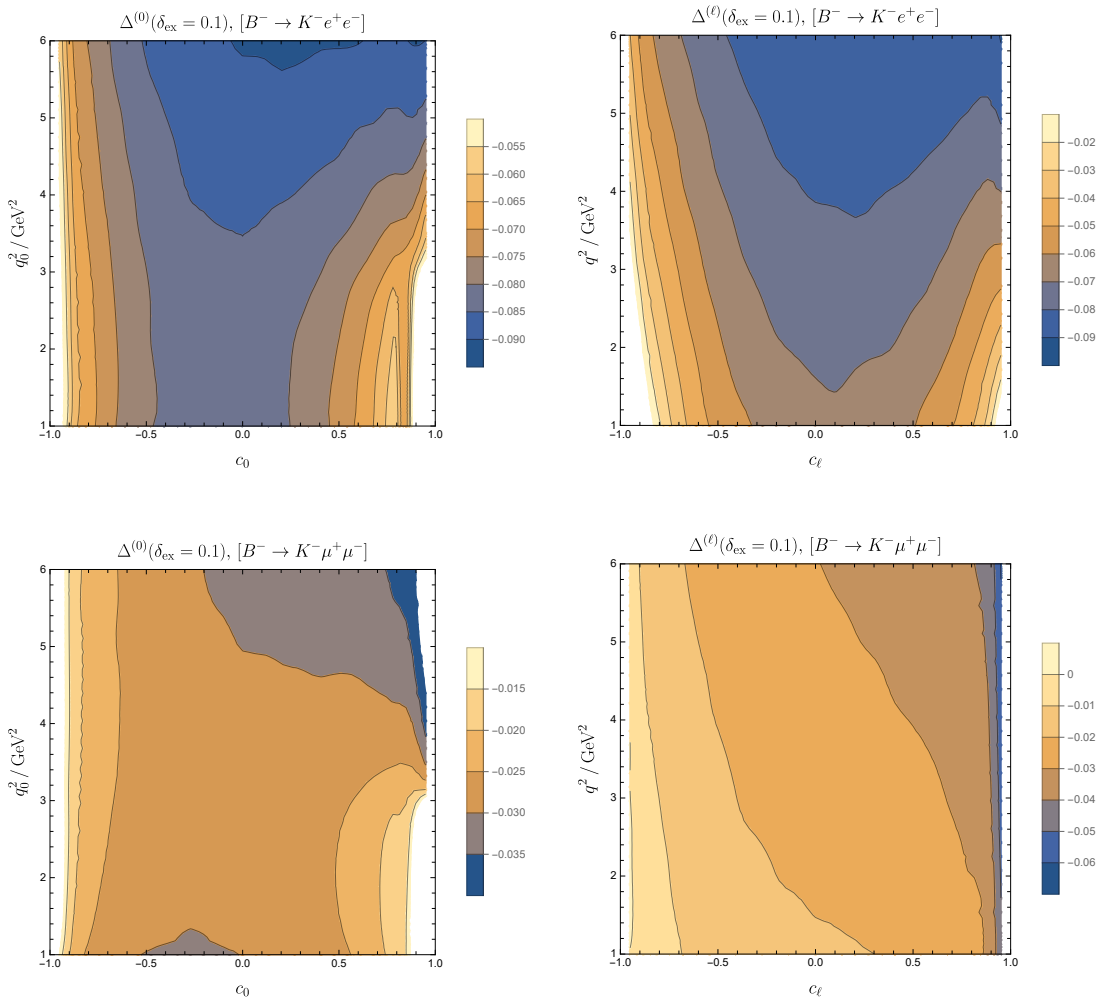

Figure 6.19: Relative size of QED corrections as a function of $\{q_0^2, c_0\}$ (left) and $\{q^2, c_\ell\}$ (right), with the top two heatmaps corresponding to $B^- \to K^- e^+ e^-$ and the bottom two to $B^- \to K^- \mu^+ \mu^-$. There is no symmetry with respect to c_ℓ, c_0 this time, and this is due to the $\ln m_K$ contributions, which is linear in c_ℓ, c_0.

6.1.7 Effect of the collinear slicing parameter

To separate the hard collinear logs for numerical stability, we introduced the auxiliary parameter ω_c. It is interesting to investigate how big the error is due to this parameter. To this end, we have performed the numerical integration for the $\bar{B}^0 \to \bar{K}^0 \mu^+ \mu^-$ with no cut ($\omega_c = 0$), and compared it to the case with $\omega_c = 8{\cdot}10^{-5}$, which was used in all previous sections for the muon case. This is possible as the muon mass is not too small. Simply using more points (roughly 10 times more) for our numerical Monte Carlo integration gave relatively stable results. On the other hand, the same calculation could not be performed with the electron, since increasing computing time reasonably did not lead to better

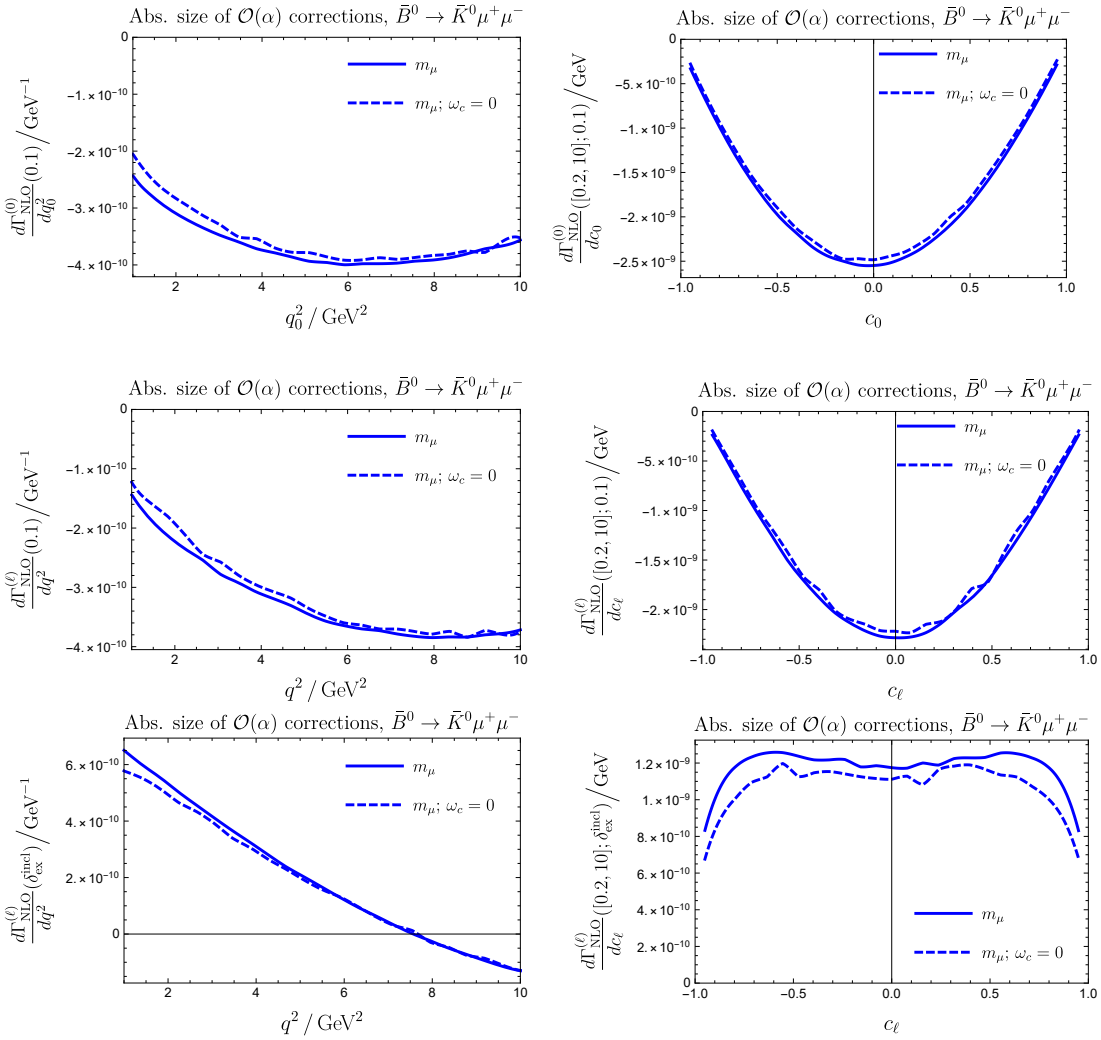

Figure 6.20: Effects of the auxiliary cut ω_c on the size of the absolute QED corrections. The dotted line corresponds to the case with no cut ($\omega_c = 0$), and the solid line to $\omega_c = 8{\cdot}10^{-5}$. The left and right plots are differential in q_a^2 and c_a respectively. The top two plots are in the $\{q_0^2, c_0\}$ variables, with the rest in the $\{q^2, c_\ell\}$ variables. A photon energy cut-off of $\delta_{\rm ex} = 0.1$ has been used for the top four plots, while the bottom two corresponds to the fully inclusive photon. In all cases, there is good agreement between the plots with and without the hard-collinear cut ω_c.

results.

The unnormalised and normalised plots showing the effect of the cut ω_c are shown in Fig. 6.20 and 6.21 respectively. As can be seen in all of the plots, the agreement between them is very good. This is an excellent check of the phase-space slicing procedure, as well as for the implementation of the analytical results in chapter 5. This also gives us confidence that the results involving the electron case must also be correct.

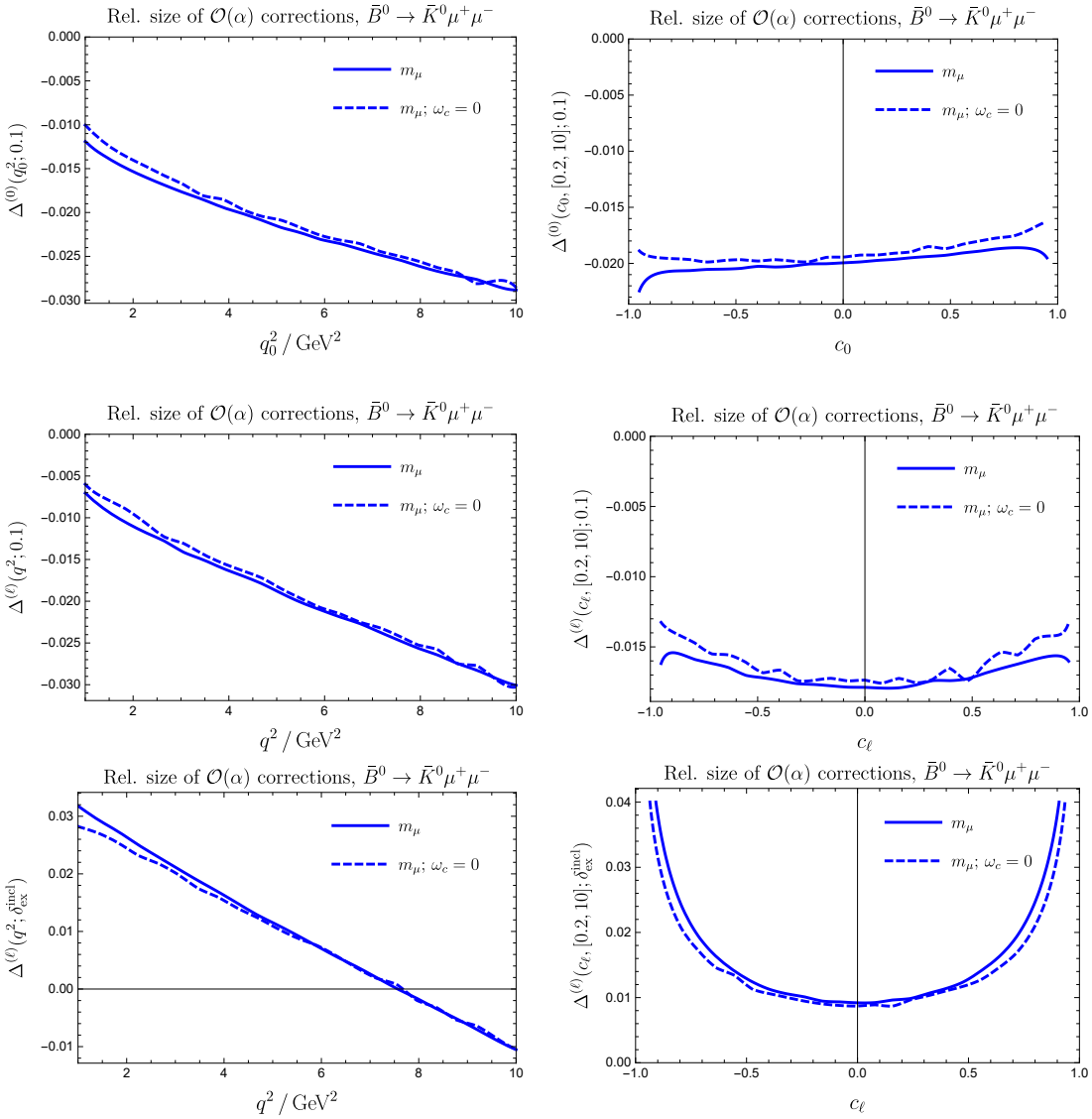

Figure 6.21: Effects of the auxiliary cut ω_c on the size of the relative QED corrections. The dotted line corresponds to the case with no cut ($\omega_c = 0$), and the solid line to $\omega_c = 8{\cdot}10^{-5}$. The left and right plots are differential in q_a^2 and c_a respectively. The top two plots are in the $\{q_0^2, c_0\}$ variables, with the rest in the $\{q^2, c_\ell\}$ variables. A photon energy cut-off of $\delta_{\rm ex} = 0.1$ has been used for the top four plots, while the bottom two corresponds to the fully inclusive photon.

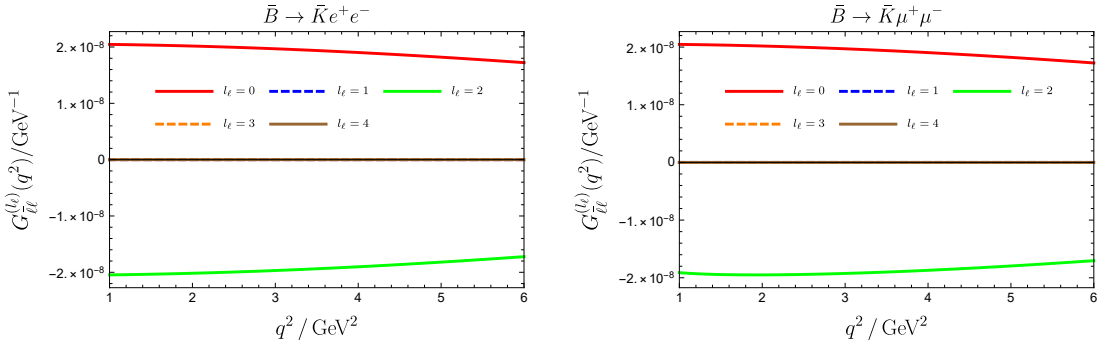

Figure 6.22: Moments of the LO distribution. All moments (except the zeroth and second ones) are highly suppressed, due to the smallness of the lepton masses, see Eq. (4.81).

6.1.8 Moments of the differential distribution

A special feature of QED corrections is that they have genuine infrared effects when compared to the weak interaction with natural scale $m_W \gg m_B$. As pointed out in [125], this changes the angular distribution in that there is not a specific hierarchy of moments in the angles (cf. section 5 in [125]). Without QED corrections, it is the dimension of the effective Hamiltonian that limits the partial waves to its lowest numbers. Higher moments (in the partial wave expansion) are therefore absent or suppressed by further powers of m_b/m_W. Hence, measuring higher moments allows us to measure QED effects. It is therefore interesting to scrutinise the size of these corrections from the theory side in order to identify the most sensitive moments and give further motivation to an experimental investigation.

To this end, we express the differential rate as an expansion in terms of Legendre polynomials $P_{l_a}(c_a)$,

$$\frac{d^2\Gamma_{\bar{B}\to\bar{K}\ell_1\bar{\ell}_2}(q_a^2, c_a; \delta_{\mathrm{ex}})}{dq_a^2\, dc_a} = \sum_{l_a \geq 0} G^{(l_a)}_{\bar{\ell}\ell}\left(q_a^2; \delta_{\mathrm{ex}}\right) P_{l_a}(c_a)\,. \tag{6.29}$$

The $\bar{B} \to \bar{K}\bar{\ell}\ell$ moments are then simply given by

$$M^{(l_a)}_{\bar{\ell}\ell}\left(q_a^2; \delta_{\mathrm{ex}}\right) = \int_{-1}^{1} dc_a P_{l_a}(c_a) \frac{d^2\Gamma_{\bar{B}\to\bar{K}\ell_1\bar{\ell}_2}(q_a^2, c_a; \delta_{\mathrm{ex}})}{dq_a^2\, dc_a} = \frac{1}{2l_a+1} G^{(l_a)}_{\bar{\ell}\ell}\left(q_a^2; \delta_{\mathrm{ex}}\right) \tag{6.30}$$

where we have introduced a lepton-subscript for further reference, and the subscript a denotes the two sets of variables $\{q_0^2, c_0\}$ and $\{q^2, c_\ell\}$ as before.

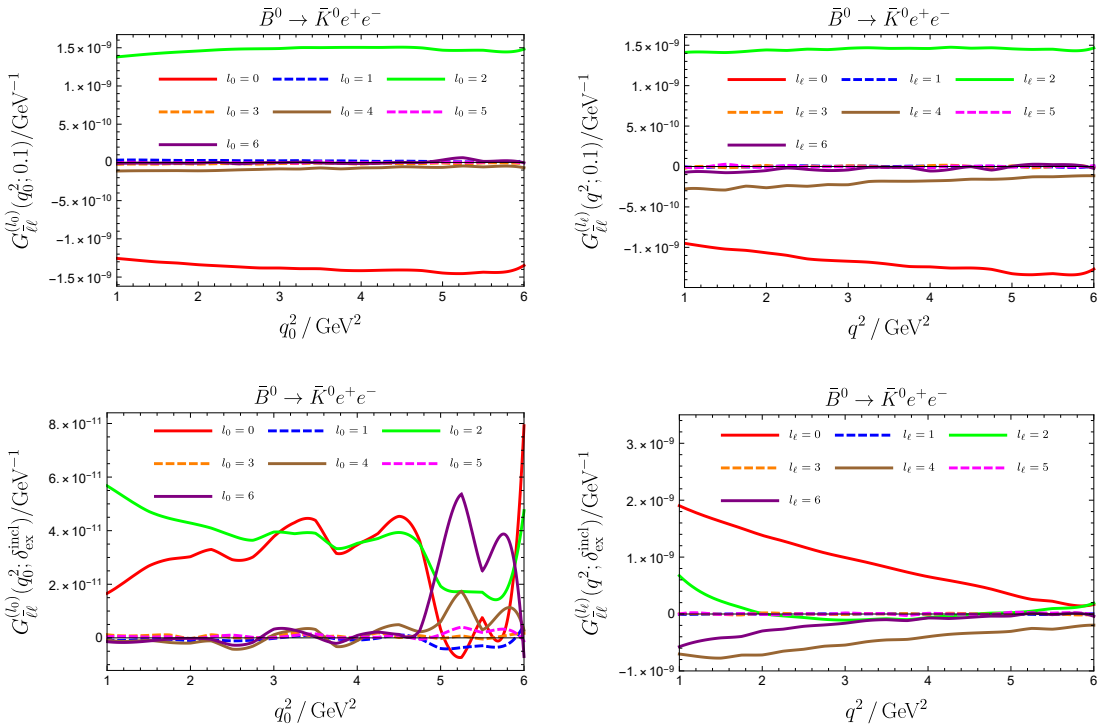

Figure 6.23: Moments of the NLO distribution for $\bar{B}^0 \to \bar{K}^0 e^+ e^-$ in the $\{q_0^2, c_0\}$ variables (left) and the $\{q^2, c_\ell\}$ variables (right) with a cut-off $\delta_{\text{ex}} = 0.1$ (top) and no cut-off (bottom). When fully inclusive, the moments in the $\{q_0^2, c_0\}$ variables are rather unstable (note that they are very small though, see y-axis values). The even moments (solid lines) decrease as l_ℓ increases, but remain sizeable nevertheless.

Fig. 6.22 shows the moments of the LO distribution. Due to the smallness of the lepton masses, all moments except the zeroth and second are highly suppressed, since the LO differential rate $\propto (1 - c_\ell^2) + \mathcal{O}(m_\ell^2)$. Therefore, in what follows, we refrain from calculating the ratio of NLO corrections to LO values. The even and odd moments are represented by solid and dashed lines respectively to distinguish between them easily.

Figs. 6.23 and 6.24 show the moments of the NLO distribution for the $\bar{B}^0 \to \bar{K}^0 e^+ e^-$ and $\bar{B}^0 \to \bar{K}^0 \mu^+ \mu^-$ processes respectively. When fully inclusive, the moments in the $\{q_0^2, c_0\}$ variables are rather unstable, especially in the electron case (bottom left plot in Fig. 6.23); note, however, that they are very small, see the values on the y-axis, due to the absence of hard-collinear logs in this set of differential variables. The even moments decrease as l_ℓ increases, but remain sizeable nevertheless, while the odd moments are relatively small. We note that the higher order moments are larger in the electron case.

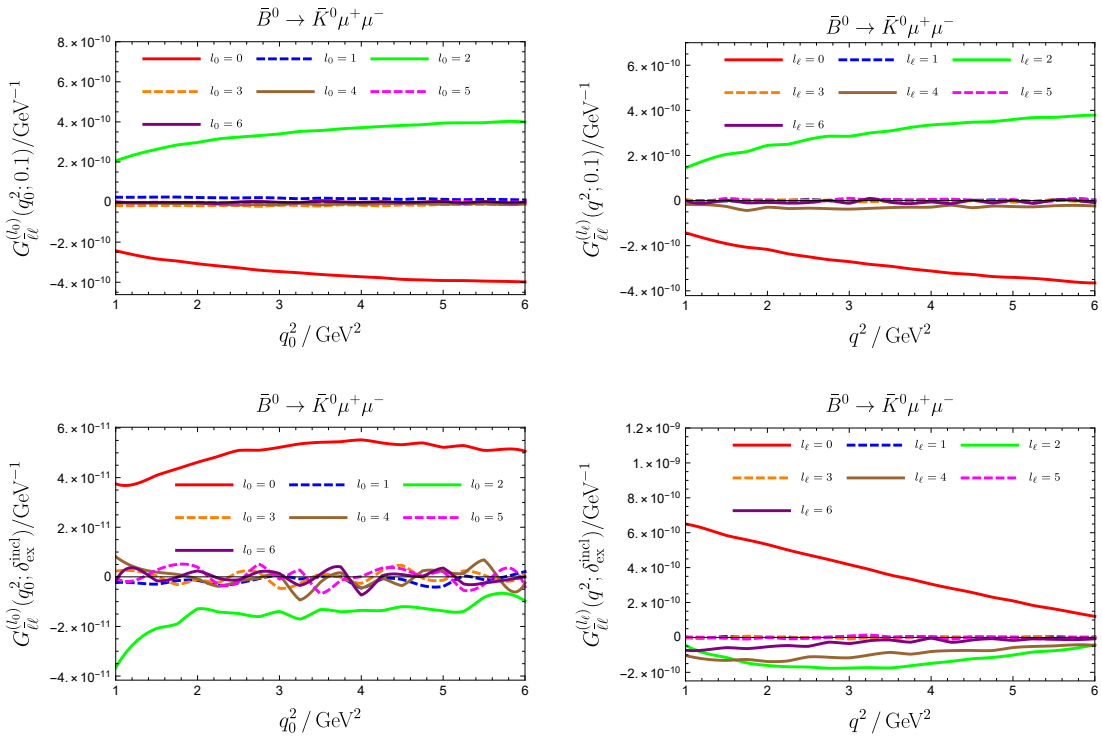

Figure 6.24: Moments of the NLO distribution for $\bar{B}^0 \to \bar{K}^0\mu^+\mu^-$ in the $\{q_0^2, c_0\}$ variables (left) and the $\{q^2, c_\ell\}$ variables (right) with a cut-off $\delta_{\rm ex} = 0.1$ (top) and no cut-off (bottom). As in the electron case, the even moments (solid lines) decrease as l_ℓ increases, but remain sizeable.

Finally, Fig. 6.25 and 6.26 show the moments of the NLO distribution for the $B^- \to K^- e^+ e^-$ and $B^- \to K^- \mu^+ \mu^-$ processes respectively. The odd moments are no longer small in the charged meson case, and this is due to the $\ln m_K$ contributions which are odd in c_ℓ, c_0 and are sizeable.

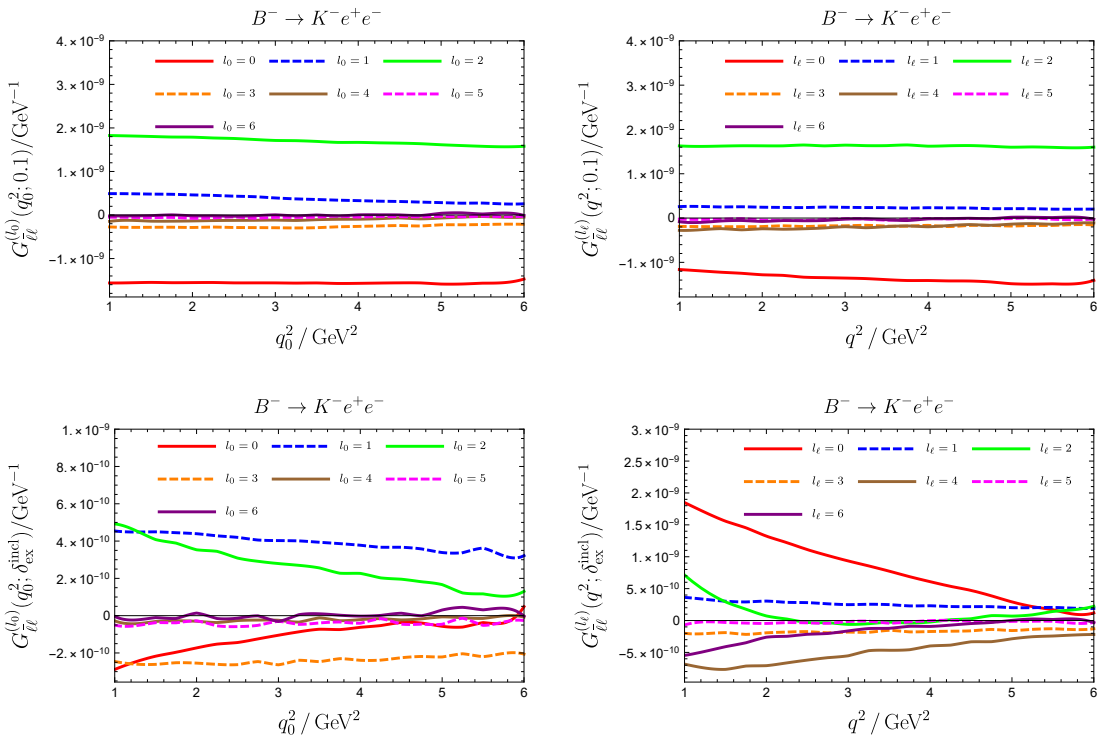

Figure 6.25: Moments of the NLO distribution for $B^- \to K^- e^+ e^-$ in the $\{q_0^2, c_0\}$ variables (left) and the $\{q^2, c_\ell\}$ variables (right) with a cut-off $\delta_{\text{ex}} = 0.1$ (top) and no cut-off (bottom). The odd moments (dashed lines) are no longer small in the charged meson case, and this is due to the $\ln m_K$ contributions which are odd in c_ℓ, c_0 and are sizeable.

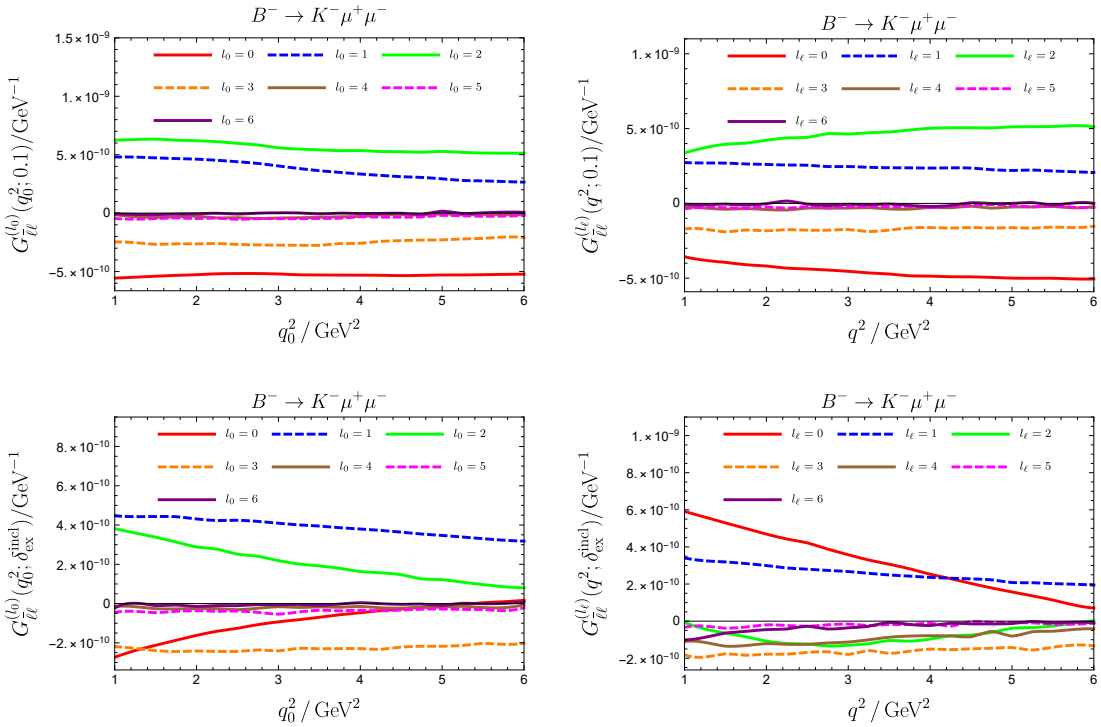

Figure 6.26: Moments of the NLO distribution for $B^- \to K^- \mu^+ \mu^-$ in the $\{q_0^2, c_0\}$ variables (left) and the $\{q^2, c_\ell\}$ variables (right) with a cut-off $\delta_{\text{ex}} = 0.1$ (top) and no cut-off (bottom). As in the electron case, the odd moments (dashed lines) are no longer small in the charged meson case, and this is due to the $\ln m_K$ contributions which are odd in c_ℓ, c_0 and are sizeable.

6.2 Outlook

In this section, we briefly address various topics which go beyond the scope of this work and are worthwhile to be pursued in future investigations.

6.2.1 Structure-dependent terms

In this work, we have treated the mesons as fundamental fields. The effective Lagrangian employed is able to perfectly describe their internal structure up to $\mathcal{O}(e^0)$. However, the electromagnetic probe sees the mesons as a structureless particle. Hence our effective Lagrangian corresponds to approximating a multipole expansion by the monopole term.

In the language of meson fields, one would need to build a systematic effective field theory with gauge invariant operators out of covariant derivatives and meson

fields. This would include, amongst others, terms beyond minimal coupling of the form $(D^\mu B)^\dagger F_{\mu\nu} D^\nu K$. It is beyond doubt that in full QCD, the meson's partons give rise to such higher multipole emissions, which we referred to as structure-dependent terms.[5] The question is whether they are sizeable. For light-light systems, such as $K \to \pi$ decays, these terms are known to be small e.g. [126, 127] (unless the leading amplitude is accidentally suppressed). For heavy-light systems, this might change since the masses of the valence quarks introduce a sizeable asymmetry that will eventually be resolved.

A result established in this work provides some protection. It was shown in Sec. 5.5 and 5.6 that structure-dependent corrections do not lead to any additional hard-collinear logs. Since soft divergences cancel at the differential level, this means that the employed approximation captures all IR sensitive terms. However, it cannot be precluded that new and interesting hadronic effects, not directly related to infrared effects, could come into play. An example of which is provided by $B_s \to \mu^+\mu^-$, where it was found that the chirality suppression of the non radiative decay m_μ/m_b is lifted to $m_\mu/\Lambda_{\rm QCD}$ ("enhanced power corrections") when QED corrections are taken into account [128]. These authors develop QED corrections to B decays within the soft collinear effective theory (SCET) framework. It allows for the the resummation of different types of logarithms [129] but does not capture all $1/m_b$ effects. To what extent $1/m_b$-corrections are important in QED corrections to B-mesons decays is an interesting and open question. Another approach is lattice QCD, where the precision in Kaon physics per se demands the inclusion of QED corrections [130, 131] with first results in leptonic decays [132–134]. For B decays, in the region of fast recoiling particles, more work is needed because of too many exponentially growing modes that have to be captured by a fit or dealt with in some other way.

6.2.2 The $\bar{B} \to \bar{K}\ell^+\ell^-$ differential distribution through Monte Carlo

Our results can be used to estimate the radiative corrections to the $\bar{B} \to \bar{K}\ell^+\ell^-(\gamma)$ differential distribution semi-analytically.[6] As demonstrated, the choice of differential variables (which might be dictated by their accessibility

[5] The full theory, including QCD and QED, is needed to compute the corresponding Wilson coefficients and counterterms when involving loops.

[6] The integration over the photon variables is done numerically and this is why we refer to them as semi-analytic.

in a given experiment) that we have introduced (4.1) directly impacts in what way hard-collinear logs cancel. An alternative approach, more in line with current analysis techniques, is to build a Monte Carlo program for the numerical simulation of the radiative and the non-radiative processes, and evaluate the impact of the radiative corrections entirely numerically. This happens at an even more differential level by taking into account the photon kinematics on an event-by-event basis. Given the sizeable contributions from hard-collinear logs, it will be an important task to cross-check the purpose-built Monte Carlo against standard tools used in experimental analysis. In this case, our virtual corrections are essential in that they provide the normalisation of the Monte Carlo code.[7] Within this approach, we are free to adopt the $\{q_0^2, c_0\}$ or the $\{q^2, c_\ell\}$-variables, since these are used to describe the simulated events and the experiment can produce a distribution in either of the variables by using local corrections factors. The final comparison with experiment is performed in a subsequent step after taking into account experimental efficiencies, resolutions, and cuts to reduce the background. Given our results in Chapter 5, it is clear that the choice of $\{q_0^2, c_0\}$ is more convenient, since for each value of q_0^2 and c_0, the corresponding photon-inclusive rate is free from hard-collinear singularities.

It is worth stressing that most of the considerations presented in this work, and particularly the strategy outlined above to build a Monte Carlo code, apply if the final-state hadron is a narrow vector resonance (such as the $\bar{K}^*$), rather than a stable scalar meson. In the narrow-width approximation, we can neglect the interference of the radiation emitted by the final-state mesons, produced by the vector-meson decay, with the radiation from the B decay products (i.e. the radiation described in this work). In this limit (which is a rather good approximation in the $\bar{K}^*$ case, given that $\Gamma_{\bar{K}^*}/m_{\bar{K}^*} \approx 5\%$) the formalism is essentially identical, up to a richer form factor structure.

[7] The Monte Carlo code requires the introduction of an (unphysical) soft cut-off Λ_s, below which the mode is treated as a three-body decay. The rate (5.1) is then split into, $d^2\Gamma(\delta_{\rm ex}) = [d^2\Gamma(\Lambda_s)]_{\rm MC_3} + \left[\frac{\alpha}{\pi}\sum_{i,j}\hat{Q}_i\hat{Q}_j(\mathcal{F}_{ij}^{(a)}(\delta_{\rm ex}) - \mathcal{F}_{ij}^{(a)}(\Lambda_s))\right]_{\rm MC_4} dq_a^2 dc_a$, a first term which is done semi-analytically with our computation and simulated with three-body kinematics, and a second term which is obtained through the simulation of the full four-body kinematics. Note that both terms are free from soft divergences and Λ_s is analogous to phase space slicing cut-off ω_s introduced in Chapter 5.

6.2.3 Remarks on charged-current semileptonic decays

In the main section, charges and masses were kept completely general, so that any semileptonic decay can be covered, including charged-current processes such as $\bar{B} \to D\ell\nu$. A significant difference to $\bar{B} \to \bar{K}\ell^+\ell^-$ is that the variable $\bar{p}_B^2$, defined as in (4.3), is not observable (because of the unidentified neutrino). Whereas this does not pose a problem for the Monte Carlo simulation discussed above, this is an issue for the semi-analytical determination of an $\mathcal{O}(\alpha)$ infrared-safe distribution of $\bar{B} \to D\ell\nu$.

One possibility to overcome this problem is to consider $\hat{p}_B^2 \equiv (p_B - p_\nu)^2$ as the effective photon energy variable. A photon energy cut-off, similar to (4.4), can be introduced as follows. $\delta_{\rm SL}^{\rm ex} = (1 - p_{D\ell}^2/\hat{p}_B^2)$ which translates to $E_\gamma^* < \delta_{\rm SL}^{\rm ex}(p_{D\ell}/2)$ (E_γ^* is the photon energy in the D-lepton RF). The new aspect with regards to the FCNC case is that the lower cut-off on the energy variable, $(\hat{p}_B^2)_{\rm min} = p_{D\ell}^2/(1 - \delta_{\rm SL}^{\rm ex})$, is dependent on a differential variable.[8]

Another strategy is to impose the minimal kinematic limits on $\bar{p}_{\rm vis}^2 \equiv (p_B - k - p_\nu)^2$ and accept all events with E_D and E_ν which lie within the non-radiative Dalitz-plot. This is the "traditional" approach adopted in Refs. [107, 135, 136]. This can work in a clean environment, in K-factories, but would not be a feasible approach for the LHC collider environment. Incidentally, we note that the variables (E_D, E_ν) are an alternative choice to our $\{q^2, c_\ell\}$-variables. We finally stress that the approach followed in [137], where an effective cut on the photon energy is implemented irrespective of the photon-emission angle, might lead to a miss-estimate of the hard collinear logs.

[8] Alternatively, one could trade $\bar{p}_B$ with $\bar{p}_{\rm vis} \equiv p_B - k - p_\nu$. The upper cut-off on $\bar{p}_B^2$ is then to be replaced by a lower cut-off on $\bar{p}_{\rm vis}^2$ and the adaptation of our formalism requires working with a finite neutrino mass. It is understood that this approach might be challenging on the numerical side.

Chapter 7

Conclusion

After a general discussion on conformal field theories and curved spacetime in the Introduction (Chapter 1), we presented a detailed discussion of conformal anomalies in curved spacetime in Chapter 2. We have calculated them for a scalar field, spin-1 gauge field, and fermion field in Secs. 2.1, 2.2 and 2.3 respectively, using the Schwinger-De-Witt point splitting method, employing heat-kernel techniques. We have focussed our calculation mainly in dimensional regularisation. For the case of the non-conformally coupled scalar (NCCS) field, we argued how the anomaly could be extracted from the calculation by employing a subtraction, described by Eq. (2.81) and Eq. (2.82). This follows the calculation in [64] performed in perturbation theory of linearised gravity, which appeared while we were working on this. This makes the result for the $\Box R$ coefficient of the conformal anomaly of the NCCS finite. We also looked at the issue of gauge invariance for the spin-1 gauge field theory in Sec. 2.2.3, where we showed when and how gauge invariance occurs. In a general gauge, the calculations were more involved and we built up on the work done by Shore [74], which addressed the case of a non-Abelian gauge theory in flat spacetime, to perform them. We were able to show that gauge invariance is recovered upon employing the subtraction, and hence that the conformal anomaly is gauge invariant, while the VEV of the TEMT itself might not be. Furthermore, we showed how introducing a Stückelberg scalar field makes the vacuum expectation value (VEV) of the trace of the energy-momentum tensor (TEMT) gauge invariant, without the need for subtraction.

The connection of conformal anomalies to renormalisation group flows was

explained in Chapter 3. The c- and a-theorems, in 2 and 4 dimensions respectively [46, 76, 82], were also discussed in this context, as well as the possibility of an alternative $\bar{b}$-theorem in 4D. The latter relies on the work done in [83], and uses the fourth moment of the two-point correlation function of the TEMT, given in Eq. (3.16). We discussed its derivation briefly in Sec. 3.2.1, and applied it to the same quantum field theories we considered in Chapter 2. Using the results, we discussed some of its shortcomings, and proceeded to investigate its possible impact on QCD in the conformal window in Sec. 3.3. We found that it gives a smaller upper bound on the number of fermion flavours N_f compared to using the a-theorem and asymptotic freedom (Eqs. (3.66) to (3.68)). On the other hand, we noted that it eliminates a region of N_f expected to be within the conformal window, according to the Banks-Zaks argument. We plan on finding a resolution of the issues for the tentative $\bar{b}$-theorem in the future.

Then, in Chapters 4-6, we analysed the $\mathcal{O}(\alpha)$ corrections to a generic $M_H \to M_L \ell_1 \bar{\ell}_2$ decay, where $M_{H,L}$ are scalar mesons (of either parity). We have performed a complete calculation of these corrections within improved scalar QED, employing a mesonic effective Lagrangian (with a tower of effective operators) which provides an accurate description of the non-radiative hadronic form factors. We have shown by means of explicit computation that all soft divergences cancel at the double differential level (Sec. 5.1), irrespective of the choice of the variables used to describe the "visible" kinematics. On the other hand, we have demonstrated that the hard-collinear logs can survive, even in the photon-inclusive limit, depending on the variables employed to describe the photon-inclusive distribution. More precisely, they cancel in the case of the $\{q_0^2, c_0\}$- but not the $\{q^2, c_\ell\}$-variables defined in Eq. (4.1).

Our analysis goes well beyond, in terms of accuracy and generality, w.r.t. previous analytical treatments of radiative effects in $M_H \to M_L \ell_1 \bar{\ell}_2$ decays. Still, some open issues remain, as discussed in Sec. 6.2.1. In particular, the matching of the residual UV ambiguities with QCD and resolving the photon interaction with the quarks themselves. As we have shown, gauge invariance ensures that such ambiguities cannot induce $\ln m_\ell$-enhanced corrections (Sec. 5.5). This implies, in particular, that these corrections have a negligible impact on the experimental determination of the LFU ratios. At the time of writing of this thesis, we were working on the resolution of the UV ambiguities via a matching to a QCD sum rules calculation, and we hope that the results will be published soon.

Our analysis indicates that great care must be taken when comparing theoretical

with experimental data, given that radiative corrections for the electron modes can easily exceed the 10%-level (as already indicated by previous analyses). As discussed in section 6.1.5, the overall impact of QED corrections on (integrated) LFU ratios, such as R_K, is not too large, especially given the current cuts applied on the reconstructed invariant mass for electron and muon modes [12]. On the other hand, differential observables are subject to potentially larger effects. In particular, as we have shown in Sec. 6.1.3, a sizeable lepton-non-universal distortion of the dilepton invariant mass spectrum occurs if the latter is expressed in term of the $\{q^2, c_\ell\}$-variables. To overcome this problem the best way to report data is in terms of the of the $\{q_0^2, c_0\}$ distribution (as currently done by most experiments), where the "dangerous" hard-collinear logs ($\ln m_\ell$) cancel at the differential level. In the case of the LHCb experiment, where q_0^2 is not directly measurable, this is done after comparing the results with a Monte Carlo code and correcting for the effect of the QED radiation. In this context, we note that our analysis provides the theoretical groundwork to build a Monte Carlo program with a complete differential treatment of radiative corrections and an accurate parameterisation of the hadronic form-factors (possibly including also long-distance contributions), which represents a key ingredient for a precise comparison between data and theoretical predictions in the future.

Appendix A

Conventions

A.1 Sign Conventions in Curved Spacetime

The two relevant sign conventions are $(---)$ and $(+++)$ in the notation of Misner et al. [16].

In $(---)$,

1. The metric has signature $(+---)$.
2. $R^{\alpha}{}_{\beta\gamma\delta} = \partial_{\delta}\Gamma^{\alpha}{}_{\beta\gamma} - ....$
3. $R_{\mu\nu} = R^{\alpha}{}_{\mu\alpha\nu}$.

Birrell and Davies [60] have a prescription to go from $(---)$ to $(+++)$. The steps are as follows:

1. Change signs of $g_{\mu\nu}$, $\Box$, $R^{\alpha}{}_{\beta\gamma\delta}$, $R_{\mu\nu}$, $T^{\mu}{}_{\nu}$, ∇^{α}.
2. Leave signs unchanged for $R_{\alpha\beta\gamma\delta}$, $R^{\mu}{}_{\nu}$, R, $T_{\mu\nu}$.

In fact, the 3 signs in the brackets, (s_1, s_2, s_3) mean

$$\eta_{\mu\nu} = s_1 \times \mathrm{diag}\,(-,+,+,+)\,, \tag{A.1}$$

$$R^{\lambda}{}_{\tau\mu\nu} = s_2 \times \left(\partial_{\mu}\Gamma^{\lambda}{}_{\tau\nu} - \partial_{\nu}\Gamma^{\lambda}{}_{\tau\mu} + \Gamma^{\lambda}{}_{\mu\sigma}\Gamma^{\sigma}{}_{\tau\nu} - \Gamma^{\lambda}{}_{\nu\sigma}\Gamma^{\sigma}{}_{\tau\mu}\right), \tag{A.2}$$

$$G_{\mu\nu} = s_3 \times 8\pi G\, T_{\mu\nu}, \tag{A.3}$$

where

$$G_{\mu\nu} = R_{\mu\nu} - \frac{1}{2} R g_{\mu\nu} + \Lambda g_{\mu\nu}, \tag{A.4}$$

is the Einstein tensor.

The default convention used through this thesis is $(---)$, unless otherwise stated.

A.2 Minkowski and Euclidean Coordinates

In the following, 'M' and 'E' denote Minkowski coordinates and Euclidean coordinates respectively.

A.2.1 Metric Tensor

In a Minkowski coordinate system, the flat spacetime metric tensor, in 4 dimensions, conventionally used (in particle physics) is given by

$$\eta^{\mathrm{M}}_{\mu\nu} = \mathrm{diag}(+---). \tag{A.5}$$

The metric in Euclidean coordinates is

$$\eta^{\mathrm{E}}_{\mu\nu} = \mathrm{diag}(++++). \tag{A.6}$$

A.2.2 4-vectors

The scalar product $x_{\mathrm{M}} \cdot x_{\mathrm{M}}$ between two 4-vectors in Minkowski space is

$$x_{\mathrm{M}} \cdot x_{\mathrm{M}} = (x^0_{\mathrm{M}})^2 - (x^i_{\mathrm{M}})^2. \tag{A.7}$$

The transformation between Minkowski and Euclidean coordinates is given by

$$x^0_{\mathrm{M}} = -i x^4_{\mathrm{E}}, \tag{A.8}$$

$$x^k_{\mathrm{M}} = x^k_{\mathrm{E}}, \tag{A.9}$$

$$\partial^0_{\mathrm{M}} = i\partial^4_{\mathrm{E}}, \tag{A.10}$$
$$\partial^k_{\mathrm{M}} = -\partial^k_{\mathrm{E}}. \tag{A.11}$$

The scalar product in the 2 different coordinates is then related by

$$x_{\mathrm{M}} \cdot x_{\mathrm{M}} = -x_{\mathrm{E}} \cdot x_{\mathrm{E}}. \tag{A.12}$$

Note that the momentum 4-vector p^μ also has the same transformation properties as x^μ. This means that

$$p_{\mathrm{M}} \cdot p_{\mathrm{M}} = -p_{\mathrm{E}} \cdot p_{\mathrm{E}}, \tag{A.13}$$
$$p_{\mathrm{M}} \cdot x_{\mathrm{M}} = -p_{\mathrm{E}} \cdot x_{\mathrm{E}}. \tag{A.14}$$

However, they have different behaviours in the complex plane due to the position of poles, see section A.2.4 for how they should be understood inside integrals.

Gauge fields A^μ transform as

$$A^0_{\mathrm{M}} = iA^4_{\mathrm{E}}, \tag{A.15}$$
$$A^k_{\mathrm{M}} = -A^k_{\mathrm{E}}. \tag{A.16}$$

Note that in Euclidean coordinates, upper and lower indices do not matter.

A.2.3 Gamma Matrices

Gamma matrices have different transformation properties. We stick to the following convention:

$$\gamma^0_{\mathrm{M}} = \gamma^4_{\mathrm{E}}, \tag{A.17}$$
$$\gamma^k_{\mathrm{M}} = i\gamma^k_{\mathrm{E}}. \tag{A.18}$$

This then means that slashed vectors and derivatives have the following transformations:

$$\not{\partial}_{\mathrm{M}} = i\not{\partial}_{\mathrm{E}}, \tag{A.19}$$
$$\not{k}_{\mathrm{M}} = -i\not{k}_{\mathrm{E}}. \tag{A.20}$$

Lagrangians are redefined with a negative sign, i.e.

$$\mathcal{L}_{\mathrm{M}} = -\mathcal{L}_{\mathrm{E}}, \tag{A.21}$$

For example, the Dirac Lagrangian becomes

$$\bar{\Psi}(i\partial\!\!\!/_{\mathrm{M}} - m)\Psi = -\bar{\Psi}(\partial\!\!\!/_{\mathrm{E}} + m)\Psi. \tag{A.22}$$

A.2.4 Integrals

In Minkowski space, in momentum integrals, the position of the poles in momentum space in the $+i\epsilon$ prescription are

$$p_0 = -\omega + i\epsilon, \quad p_0 = \omega - i\epsilon, \tag{A.23}$$

where $\omega = \sqrt{\mathbf{p}^2 + m^2}$.

From the way the contour is closed (i.e. top-right and lower-left planes), one finds that

$$\int_{-\infty}^{\infty} \mathrm{d}p_0 = i \int_{-\infty}^{\infty} \mathrm{d}p_4. \tag{A.24}$$

On the other hand, in position space, the poles are on opposite sides of the real x_0 axis. This time, closing the contour appropriately to ensure convergence implies that

$$\int_{-\infty}^{\infty} \mathrm{d}x_0 = -i \int_{-\infty}^{\infty} \mathrm{d}x_4. \tag{A.25}$$

This explains why we define the Lagrangians as in Eq. (A.21).

The generating functional then has the form

$$\begin{aligned} \mathcal{Z} &= \int [\mathcal{D}\phi_{\mathrm{M}}]\, e^{i\mathcal{S}_{\mathrm{M}}} \\ &= \int [\mathcal{D}\phi_{\mathrm{E}}]\, e^{-\mathcal{S}_{\mathrm{E}}}, \end{aligned} \tag{A.26}$$

where

$$\mathcal{S}_{\mathrm{M}} = \int \mathrm{d}^4 x_{\mathrm{M}}\ \mathcal{L}_{\mathrm{M}}, \tag{A.27}$$

$$\mathcal{S}_{\mathrm{E}} = \int \mathrm{d}^4 x_{\mathrm{E}}\ \mathcal{L}_{\mathrm{E}}. \tag{A.28}$$

A.2.5 Propagators

Free Massive Scalar Field

A massive scalar field ϕ having Lagrangian

$$\mathcal{L}_{\mathrm{M}} = \frac{1}{2}(\partial_\mu \phi)^2 - \frac{1}{2}m^2\phi^2, \tag{A.29}$$

$$\mathcal{L}_{\mathrm{E}} = \frac{1}{2}(\partial_\mu \phi)^2 + \frac{1}{2}m^2\phi^2, \tag{A.30}$$

has the momentum space propagator

$$\frac{i}{p_{\mathrm{M}}^2 - m^2} \qquad \text{in Minkowski space,} \tag{A.31}$$

$$\frac{1}{p_{\mathrm{E}}^2 + m^2} \qquad \text{in Euclidean space.} \tag{A.32}$$

Note that massive ghosts have the same propagator as the massive scalar field.

Free Massive Fermion Field

A free massive Dirac field Ψ has Lagrangian

$$\mathcal{L}_{\mathrm{M}} = \bar{\Psi}(i\not{\partial} - m)\Psi, \tag{A.33}$$

$$\mathcal{L}_{\mathrm{E}} = \bar{\Psi}(\not{\partial} + m)\Psi. \tag{A.34}$$

We define the position space propagator in Minkowski space as

$$S(x-y) \equiv \langle 0|T\Psi(x)\bar{\Psi}(y)|0\rangle. \tag{A.35}$$

Then, expressing it as the Fourier transform of the momentum space propagator, we have

$$S(x) = \int \frac{\mathrm{d}^4k}{(2\pi)^4} \frac{i(\not{k} + m)e^{-ik\cdot x}}{k^2 - m^2} \qquad \text{in Minkowski space,} \tag{A.36}$$

$$S(x) = \int \frac{\mathrm{d}^4k}{(2\pi)^4} \frac{(i\not{k} + m)e^{-ik\cdot x}}{k^2 + m^2} \qquad \text{in Euclidean space.} \tag{A.37}$$

Note that the sign of the Fourier transform is very important in this case (as opposed to the scalar field case).

Free Massive U(1) Gauge Field

A massive U(1) gauge field A^μ with R_ξ gauge has the Lagrangian

$$\mathcal{L}_{\rm M} = -\frac{1}{4}F_{\mu\nu}F^{\mu\nu} + \frac{1}{2}m^2 A_\mu A^\mu - \frac{1}{2\xi}(\partial\cdot A)^2, \tag{A.38}$$

$$\mathcal{L}_{\rm E} = \frac{1}{4}F_{\mu\nu}F^{\mu\nu} + \frac{1}{2}m^2 A_\mu A^\mu + \frac{1}{2\xi}(\partial\cdot A)^2, \tag{A.39}$$

The momentum space propagators are

$$-\frac{i}{k^2-m^2}\left(g_{\mu\nu} - (1-\xi)\frac{k_\mu k_\nu}{k^2-\xi m^2}\right) \qquad \text{in Minkowski space,} \tag{A.40}$$

$$\frac{1}{k^2+m^2}\left(g_{\mu\nu} - (1-\xi)\frac{k_\mu k_\nu}{k^2+\xi m^2}\right) \qquad \text{in Euclidean space.} \tag{A.41}$$

A.2.6 Energy-Momentum Tensors

The energy-momentum tensor $T_{\mu\nu}$ in Euclidean space is given by

$$T_{\mu\nu} = \frac{2}{\sqrt{-g}}\frac{\delta\mathcal{S}_M}{\delta g^{\mu\nu}}, \qquad T^{\mu\nu} = -\frac{2}{\sqrt{-g}}\frac{\delta\mathcal{S}_M}{\delta g_{\mu\nu}}, \qquad \text{in Minkowski space,} \tag{A.42}$$

$$T_{\mu\nu} = \frac{2}{\sqrt{g}}\frac{\delta\mathcal{S}_E}{\delta g^{\mu\nu}}, \qquad T^{\mu\nu} = -\frac{2}{\sqrt{g}}\frac{\delta\mathcal{S}_E}{\delta g_{\mu\nu}}, \qquad \text{in Euclidean space.} \tag{A.43}$$

In terms of the Weyl variation, $g_{\mu\nu} \to e^{-2w}g_{\mu\nu}$, c.f. App. B.5, we have

$$T^\mu{}_\mu = \frac{1}{\sqrt{-g}}\frac{\delta\mathcal{S}_M}{\delta w} \qquad \text{in Minkowski space,} \tag{A.44}$$

$$T^\mu{}_\mu = \frac{1}{\sqrt{g}}\frac{\delta\mathcal{S}_E}{\delta w} \qquad \text{in Euclidean space.} \tag{A.45}$$

Appendix B

Curved Spacetime Identities

B.1 General

B.1.1 Invariant Volume Element

In curved spacetime, the invariant volume element is given by

$$|\det(g_{\mu\nu})|^{\frac{1}{2}}\,\mathrm{d}^d x. \tag{B.1}$$

Often, $|\det(g_{\mu\nu})|^{\frac{1}{2}}$ is written as $\sqrt{-g}$.

B.1.2 Christoffel Symbol

The Christoffel symbol is given by

$$\Gamma^{\lambda}{}_{\mu\nu} = \Gamma^{\lambda}{}_{\nu\mu} = \frac{1}{2} g^{\lambda\sigma}\left(\partial_\mu g_{\sigma\nu} + \partial_\nu g_{\mu\sigma} - \partial_\sigma g_{\mu\nu}\right). \tag{B.2}$$

B.1.3 Riemann Tensor

The Riemann tensor is given by

$$R^{\lambda}{}_{\tau\mu\nu} = \partial_\nu \Gamma^{\lambda}{}_{\tau\mu} - \partial_\mu \Gamma^{\lambda}{}_{\tau\nu} + \Gamma^{\lambda}{}_{\nu\sigma}\Gamma^{\sigma}{}_{\tau\mu} - \Gamma^{\lambda}{}_{\mu\sigma}\Gamma^{\sigma}{}_{\tau\nu}. \tag{B.3}$$

Note that it changes sign when one goes to the other convention, see Sec. A.1.

B.1.4 Symmetries of Riemann Tensor

In this section, we discuss some of the properties and symmetries of the Riemann tensor.

$$R_{\alpha\beta\mu\nu} = R_{\mu\nu\alpha\beta} = -R_{\beta\alpha\mu\nu} = -R_{\alpha\beta\nu\mu}. \tag{B.4}$$

$$R_{\alpha\beta\mu\nu} + R_{\alpha\mu\nu\beta} + R_{\alpha\nu\beta\mu} = 0, \qquad \text{1st Bianchi Identity} \tag{B.5}$$

$$\nabla_\lambda R_{\alpha\beta\mu\nu} + \nabla_\mu R_{\alpha\beta\nu\lambda} + \nabla_\nu R_{\alpha\beta\lambda\mu} = 0, \qquad \text{2nd Bianchi Identity} \tag{B.6}$$

$$R_{\mu\nu\alpha\beta}\, R^{\mu\alpha\nu\beta} = \frac{1}{2} R^2_{\mu\nu\alpha\beta}. \tag{B.7}$$

$$\frac{1}{2} R^{\mu\alpha\beta\gamma} R^{\nu}{}_{\alpha\beta\gamma} = R^{\mu\alpha\beta\gamma} R^{\nu}{}_{\beta\alpha\gamma}. \tag{B.8}$$

$$\nabla_\mu \nabla_\nu R^{\alpha\beta\mu\nu} = 0. \tag{B.9}$$

The identity in Eq. (B.9) has been derived in [138], Eq. (2.7).

B.1.5 Ricci Tensor

The Ricci tensor is given by contracting two indices in the Riemann tensor,

$$R_{\mu\nu} = R^{\lambda}{}_{\mu\lambda\nu}. \tag{B.10}$$

B.1.6 Covariant Derivatives

Covariant derivatives of contravariant and covariant vectors are given by

$$\nabla_\mu V^\alpha = \partial_\mu V^\alpha + \Gamma^\alpha{}_{\mu\lambda} V^\lambda, \tag{B.11}$$

$$\nabla_\mu V_\alpha = \partial_\mu V_\alpha - \Gamma^\lambda{}_{\mu\alpha} V_\lambda. \tag{B.12}$$

The commutation of covariant derivatives generate the Riemann tensor and is given by

$$[\nabla_\mu, \nabla_\nu] V_\lambda = R^\alpha{}_{\lambda\mu\nu} V_\alpha, \tag{B.13}$$

$$[\nabla_\mu, \nabla_\nu] V^\alpha = -R^\alpha{}_{\lambda\mu\nu} V^\lambda, \tag{B.14}$$

for covariant and contravariant vectors respectively. The two equations are, of course, related by symmetries of the Riemann tensor. Note that this is easily generalisable to tensors of arbitrary lower and upper indices.

B.2 Topological Objects

B.2.1 Gauss-Bonnet Density/Euler Density (4D)

The Gauss-Bonnet Density (or Euler Density) in 4D (in dimensional regularisation) is given by [46],

$$G = E_d = \frac{2}{(d-3)(d-2)} \left(R^2_{\mu\nu\alpha\beta} - 4R^2_{\mu\nu} + R^2 \right). \tag{B.15}$$

B.2.2 Weyl Tensor

The Weyl tensor is defined as

$$C_{\rho\sigma\mu\nu} = R_{\rho\sigma\mu\nu} - \frac{2}{d-2} \left(g_{\rho[\mu} R_{\nu]\sigma} - g_{\sigma[\mu} R_{\nu]\rho} \right) + \frac{2}{(d-1)(d-2)} g_{\rho[\mu} g_{\nu]\sigma} R, \tag{B.16}$$

where the square brackets implies anti-symmetrisation over the indices,

$$g_{\rho[\mu} R_{\nu]\sigma} = \frac{1}{2} \left(g_{\rho\mu} R_{\nu\sigma} - g_{\rho\nu} R_{\mu\sigma} \right). \tag{B.17}$$

Further, the square of the Weyl tensor, W^2, is given by

$$W^2 = C^2_{\rho\sigma\mu\nu} = R^2_{\mu\nu\alpha\beta} - \frac{4}{d-2} R^2_{\mu\nu} + \frac{2}{(d-2)(d-1)} R^2. \tag{B.18}$$

B.2.3 H, modified Ricci scalar

For convenience, we sometimes define the object H such that

$$H = \frac{R}{d-1}. \tag{B.19}$$

This is done in order to cancel prefactors of R, which often comes with $d-1$.

B.3 General Metric Variations

Note that varying the metric tensor with upper or lower indices is different by a sign, i.e.

$$g_{\mu\lambda}\, g_{\nu\sigma} \frac{\delta}{\delta g_{\lambda\sigma}} = -\frac{\delta}{\delta g^{\mu\nu}}, \tag{B.20}$$

This is due to the fact that the inverse of the metric tensor $g_{\mu\nu}$ is simply $g^{\mu\nu}$, i.e. the metric tensor itself but with upper indices,

$$g_{\mu\nu} g^{\nu\alpha} = \delta_\mu{}^\alpha \qquad \Longrightarrow \qquad g^{\nu\alpha}\delta g_{\mu\nu} = -\delta g^{\nu\alpha} g_{\mu\nu}. \tag{B.21}$$

This means that a variation of $\delta g_{\mu\nu}$ and $\delta g^{\mu\nu}$ are *not* independent, and the consequence of this is the negative sign in Eq. (B.20) and Eq. (B.21).

B.3.1 $\sqrt{-g}$

The variation of $\sqrt{-g} \equiv \sqrt{-\det(g_{\mu\nu})}$ is given by

$$\begin{aligned} \delta\left(\sqrt{-g}\right) &= -\frac{\sqrt{-g}}{2} g_{\mu\nu}\delta g^{\mu\nu} \\ &= \frac{\sqrt{-g}}{2} g^{\mu\nu}\delta g_{\mu\nu}. \end{aligned} \tag{B.22}$$

B.3.2 $\Gamma^{\lambda}{}_{\mu\nu}$

The variation of the Christoffel symbol is given by

$$\begin{aligned}\delta\Gamma^{\lambda}{}_{\mu\nu} &= \frac{1}{2}g^{\lambda\alpha}\left[\partial_\mu\delta g_{\alpha\nu} + \partial_\nu\delta g_{\mu\alpha} - \partial_\alpha\delta g_{\mu\nu} - 2\Gamma^{\beta}{}_{\mu\nu}\delta g_{\alpha\beta}\right] \\ &= \frac{1}{2}g^{\lambda\alpha}\left[\nabla_\mu\delta g_{\alpha\nu} + \nabla_\nu\delta g_{\mu\alpha} - \nabla_\alpha\delta g_{\mu\nu}\right] \\ &= -\frac{1}{2}g_{\mu\alpha}\, g_{\nu\beta}\left[\nabla^\alpha\delta g^{\lambda\beta} + \nabla^\beta\delta g^{\alpha\lambda} - \nabla^\lambda\delta g^{\alpha\beta}\right]. \end{aligned} \tag{B.23}$$

B.3.3 $R^{\alpha}{}_{\beta\mu\nu}$

The variation of the Riemann tensor is given by

$$\begin{aligned}\delta R^{\lambda}{}_{\tau\mu\nu} &= \nabla_\nu\delta\Gamma^{\lambda}{}_{\tau\mu} - \nabla_\mu\delta\Gamma^{\lambda}{}_{\tau\nu} \\ &= \frac{1}{2}g^{\lambda\alpha}\Big[\nabla_\nu\nabla_\tau\delta g_{\alpha\mu} - \nabla_\nu\nabla_\alpha\delta g_{\tau\mu} - \nabla_\mu\nabla_\tau\delta g_{\alpha\nu} + \nabla_\mu\nabla_\alpha\delta g_{\tau\nu} \\ &\quad + R^{\beta}{}_{\tau\nu\mu}\delta g_{\beta\alpha} + R^{\beta}{}_{\alpha\nu\mu}\delta g_{\tau\beta}\Big] \\ &= -\frac{1}{2}g_{\gamma\nu}\, g_{\sigma\tau}\, g_{\rho\mu}\Big[\nabla^\gamma\nabla^\sigma\delta g^{\lambda\rho} - \nabla^\gamma\nabla^\lambda\delta g^{\sigma\rho} - \nabla^\rho\nabla^\sigma\delta g^{\lambda\gamma} + \nabla^\rho\nabla^\lambda\delta g^{\sigma\gamma} \\ &\quad + R_\beta{}^{\sigma\gamma\rho}\delta g^{\beta\lambda} + R_\beta{}^{\lambda\gamma\rho}\delta g^{\sigma\beta}\Big]. \end{aligned} \tag{B.24}$$

B.3.4 $R_{\mu\nu}$

This involves just setting $\lambda = \mu$ in $\delta R^{\lambda}{}_{\tau\mu\nu}$, but we give the result anyway for the sake of completeness.

$$\begin{aligned}\delta R_{\tau\nu} &= \nabla_\nu\delta\Gamma^{\lambda}{}_{\tau\lambda} - \nabla_\lambda\delta\Gamma^{\lambda}{}_{\tau\nu} \\ &= \frac{1}{2}g^{\lambda\alpha}\Big[\nabla_\nu\nabla_\tau\delta g_{\alpha\lambda} - \nabla_\nu\nabla_\alpha\delta g_{\tau\lambda} - \nabla_\lambda\nabla_\tau\delta g_{\alpha\nu} + \nabla_\lambda\nabla_\alpha\delta g_{\tau\nu}\end{aligned}$$

$$+ R^{\beta}{}_{\tau\nu\lambda}\delta g_{\beta\alpha} + R^{\beta}{}_{\alpha\nu\lambda}\delta g_{\tau\beta}\Big]$$

$$= -\frac{1}{2}g_{\gamma\nu}\, g_{\sigma\tau}\, g_{\rho\lambda}\Big[\nabla^{\gamma}\nabla^{\sigma}\delta g^{\lambda\rho} - \nabla^{\gamma}\nabla^{\lambda}\delta g^{\sigma\rho} - \nabla^{\rho}\nabla^{\sigma}\delta g^{\lambda\gamma} + \nabla^{\rho}\nabla^{\lambda}\delta g^{\sigma\gamma}$$

$$+ R_{\beta}{}^{\sigma\gamma\rho}\delta g^{\beta\lambda} + R_{\beta}{}^{\lambda\gamma\rho}\delta g^{\sigma\beta}\Big]. \tag{B.25}$$

A better version of the above (i.e. removing the Riemann tensors) is

$$\delta R_{\tau\nu} = \frac{1}{2}g^{\lambda\alpha}\left[\nabla_{\nu}\nabla_{\tau}\delta g_{\alpha\lambda} + \nabla_{\lambda}\nabla_{\alpha}\delta g_{\tau\nu} - \nabla_{\lambda}\nabla_{\tau}\delta g_{\alpha\nu} - \nabla_{\alpha}\nabla_{\nu}\delta g_{\tau\lambda}\right]$$

$$= -\frac{1}{2}g_{\lambda\alpha}\, g_{\delta\nu}\, g_{\sigma\tau}\left[\nabla^{\delta}\nabla^{\sigma}\delta g^{\alpha\lambda} + \nabla^{\lambda}\nabla^{\alpha}\delta g^{\sigma\delta} - \nabla^{\lambda}\nabla^{\sigma}\delta g^{\alpha\delta} - \nabla^{\alpha}\nabla^{\delta}\delta g^{\sigma\lambda}\right]. \tag{B.26}$$

B.3.5 R

The variation of the Ricci scalar is given by

$$\delta R = -R^{\tau\nu}\delta g_{\tau\nu} + g^{\tau\nu}\Box\delta g_{\tau\nu} - \nabla^{\tau}\nabla^{\nu}\delta g_{\tau\nu}$$

$$= R_{\tau\nu}\delta g^{\tau\nu} - g_{\tau\nu}\Box\delta g^{\tau\nu} + \nabla_{\tau}\nabla_{\nu}\delta g^{\tau\nu}. \tag{B.27}$$

B.3.6 $R^2_{\mu\nu\alpha\beta}$

The variation of the square of the Riemann tensor is given by

$$\delta\left(R^2_{\mu\nu\alpha\beta}\right) = R^{\gamma\nu\alpha\beta}\left[\nabla_{\beta}\nabla_{\nu}\delta g_{\gamma\alpha} - \nabla_{\beta}\nabla_{\gamma}\delta g_{\nu\alpha} - \nabla_{\alpha}\nabla_{\nu}\delta g_{\gamma\beta} + \nabla_{\alpha}\nabla_{\gamma}\delta g_{\nu\beta}\right]$$

$$- 2R^{\alpha}{}_{\beta\mu\nu}R^{\delta\beta\mu\nu}\delta g_{\alpha\delta}$$

$$= -R_{\gamma\nu\alpha\beta}\left[\nabla^{\beta}\nabla^{\nu}\delta g^{\gamma\alpha} - \nabla^{\beta}\nabla^{\gamma}\delta g^{\nu\alpha} - \nabla^{\alpha}\nabla^{\nu}\delta g^{\gamma\beta} + \nabla^{\alpha}\nabla^{\gamma}\delta g^{\nu\beta}\right]$$

$$+ 2R_{\alpha\beta\mu\nu}R_{\delta}{}^{\beta\mu\nu}\delta g^{\alpha\delta}. \tag{B.28}$$

B.3.7 $R^2_{\mu\nu}$

The variation of the square of the Ricci tensor is given by

$$\begin{aligned}\delta\left(R^2_{\mu\nu}\right) = & -2R^{\beta\mu}R^{\alpha}{}_{\beta}\delta g_{\mu\alpha} + R^{\mu\nu}g^{\lambda\alpha}\Big[\nabla_\nu\nabla_\mu\delta g_{\alpha\lambda} - \nabla_\nu\nabla_\alpha\delta g_{\mu\lambda} - \nabla_\lambda\nabla_\mu\delta g_{\alpha\nu} \\ & + \nabla_\lambda\nabla_\alpha\delta g_{\mu\nu} + R^{\beta}{}_{\mu\nu\lambda}\delta g_{\beta\alpha} + R^{\beta}{}_{\alpha\nu\lambda}\delta g_{\mu\beta}\Big] \\ = & \, 2R_{\alpha\beta}R^{\beta}{}_{\mu}\delta g^{\mu\alpha} - R^{\mu\nu}g^{\lambda\alpha}g_{\mu\delta}g_{\nu\sigma}\Big[\nabla^\sigma\nabla^\delta\delta g^{\alpha\lambda} - \nabla^\sigma\nabla^\alpha\delta g^{\delta\lambda} - \nabla^\lambda\nabla^\delta\delta g^{\alpha\sigma} \\ & + \nabla^\lambda\nabla^\alpha\delta g^{\delta\sigma} + R_{\beta}{}^{\delta\sigma\lambda}\delta g^{\beta\alpha} + R_{\beta}{}^{\alpha\sigma\delta}\delta g^{\delta\beta}\Big]. \end{aligned} \tag{B.29}$$

B.3.8 R^2

The variation of the square of the Ricci scalar is given by

$$\begin{aligned}\delta\left(R^2\right) &= 2RR_{\tau\nu}\delta g^{\tau\nu} - 2Rg_{\tau\nu}\Box\delta g^{\tau\nu} + 2R\nabla_\tau\nabla_\nu\delta g^{\tau\nu} \\ &= -2RR^{\tau\nu}\delta g_{\tau\nu} + 2Rg^{\tau\nu}\Box\delta g_{\tau\nu} - 2R\nabla^\tau\nabla^\nu\delta g_{\tau\nu}. \end{aligned} \tag{B.30}$$

B.3.9 Metric variation of E_4 in the gravitational action

The metric variation of the Euler density in 4D in the gravitational action is given by

$$\begin{aligned}\frac{\delta}{\delta g_{\delta\sigma}}\int \mathrm{d}^d x\sqrt{-g}E_4 = \frac{\sqrt{-g}}{2}g^{\delta\sigma}E_4 + \sqrt{-g}\Big[&4\nabla_\nu\nabla_\beta R^{\delta\nu\sigma\beta} - 2R^{\delta}{}_{\beta\mu\nu}R^{\sigma\beta\mu\nu} + 4R^{\beta\delta}R^{\sigma}{}_{\beta} \\ &+ 4\nabla_\mu\nabla^\delta R^{\mu\sigma} - 4\Box R^{\delta\sigma} - 4R^{\mu\nu}R^{\delta}{}_{\mu\nu}{}^{\sigma} - 2RR^{\delta\sigma}\Big]. \end{aligned} \tag{B.31}$$

B.4 Trace of the energy-momentum tensor of gravitational terms

$$T^{\mu}{}_{\mu} = -\frac{2}{\sqrt{-g}}g_{\mu\nu}\frac{\delta}{\delta g_{\mu\nu}}\int \mathrm{d}^d x\sqrt{-g}\left(a_0E_4 + b_0R^2 + c_0W^2\right)$$

$$= -(d-4)\,a_0 E_4 - (d-4)\,b_0 R^2 - 4\,(d-1)\,b_0 \Box R - (d-4)\,c_0 \left[W^2 - \frac{2}{3}\Box R\right]. \tag{B.32}$$

The result is obtained by assuming the Einstein Field Equations, or more precisely the relation in (B.57). Note that all terms are evanescent (i.e. proportional to $(d-4)$), except the $\Box R$ term.

Finally,

$$\frac{2}{(-g)^{\frac{1}{2}}} g^{\mu\nu} \frac{\delta}{\delta g^{\mu\nu}} \int (-g)^{\frac{1}{2}}\, \Box R\, \mathrm{d}^d x = 0, \tag{B.33}$$

which is zero since it is a surface term [42].

B.5 General Weyl Transformations

B.5.1 Basics and Definition

We define the sign convention of the general Weyl transformation to be

$$g_{\mu\nu} \to \tilde{g}_{\mu\nu} = e^{-2w} g_{\mu\nu}. \tag{B.34}$$

It then follows that

$$g^{\mu\nu} \to \tilde{g}^{\mu\nu} = e^{2w} g^{\mu\nu}, \tag{B.35}$$

such that

$$g_{\mu\nu} g^{\mu\nu} = \tilde{g}_{\mu\nu} \tilde{g}^{\mu\nu} = d. \tag{B.36}$$

In the following, the tilde notation will be used for denoting an object after a Weyl transformation.

B.5.2 $\sqrt{-\tilde{g}}$

The Weyl transformation of $\sqrt{-g} \equiv \sqrt{-\det(g_{\mu\nu})}$ is given by

$$\sqrt{-\tilde{g}} = e^{-dw} \sqrt{-g}. \tag{B.37}$$

B.5.3 $\tilde{\Gamma}^{\lambda}{}_{\mu\nu}$

The Weyl transformation of the Christoffel symbol is given by

$$\tilde{\Gamma}^{\lambda}{}_{\mu\nu} = \Gamma^{\lambda}{}_{\mu\nu} - \delta^{\lambda}{}_{\nu}\partial_{\mu}w - \delta^{\lambda}{}_{\mu}\partial_{\nu}w + g^{\lambda\sigma}g_{\mu\nu}\partial_{\sigma}w. \tag{B.38}$$

B.5.4 $\tilde{R}^{\lambda}{}_{\tau\mu\nu}$

The Weyl transformation of the Riemann tensor is given by

$$\begin{aligned}\tilde{R}^{\lambda}{}_{\tau\mu\nu} = {} & R^{\lambda}{}_{\tau\mu\nu} - \delta^{\lambda}{}_{\mu}\nabla_{\nu}\nabla_{\tau}w + \delta^{\lambda}{}_{\nu}\nabla_{\mu}\nabla_{\tau}w + g_{\mu\tau}\nabla_{\nu}\nabla^{\lambda}w - g_{\nu\tau}\nabla_{\mu}\nabla^{\lambda}w \\ & + \delta^{\lambda}{}_{\nu}\nabla_{\mu}w\nabla_{\tau}w - \delta^{\lambda}{}_{\nu}g_{\mu\tau}\left(\nabla_{\sigma}w\right)^{2} - g_{\nu\tau}\nabla_{\mu}w\nabla^{\lambda}w - \delta^{\lambda}{}_{\mu}\nabla_{\tau}w\nabla_{\nu}w \\ & + \delta^{\lambda}{}_{\mu}g_{\nu\tau}\left(\nabla_{\sigma}w\right)^{2} + g_{\mu\tau}\nabla_{\nu}w\nabla^{\lambda}w.\end{aligned} \tag{B.39}$$

B.5.5 $\tilde{R}_{\tau\nu}$

The Weyl transformation of the Ricci tensor is given by

$$\tilde{R}_{\tau\nu} = R_{\tau\nu} - (d-2)\nabla_{\nu}\nabla_{\tau}w - g_{\nu\tau}\Box w - (d-2)\nabla_{\nu}w\nabla_{\tau}w + (d-2)g_{\nu\tau}\left(\nabla_{\lambda}w\right)^{2}. \tag{B.40}$$

B.5.6 $\tilde{R}$

The Weyl transformation of the Ricci scalar is given by

$$\tilde{R} = e^{2w}\left[R - 2(d-1)\Box w + (d-2)(d-1)\left(\nabla_{\lambda}w\right)^{2}\right]. \tag{B.41}$$

B.5.7 $\tilde{C}_{\rho\sigma\mu\nu}$

The Weyl transformation of the Weyl tensor is given by

$$\tilde{C}_{\rho\sigma\mu\nu} = e^{-2w}C_{\rho\sigma\mu\nu}, \tag{B.42}$$

or equivalently,

$$\tilde{C}^{\rho}{}_{\sigma\mu\nu} = C^{\rho}{}_{\sigma\mu\nu}. \tag{B.43}$$

Thus, the tensor $C^{\rho}{}_{\sigma\mu\nu}$ is invariant under a Weyl transformation.

B.5.8 $\tilde{W}^2$

The Weyl transformation of the square of the Weyl tensor is

$$\tilde{W}^2 = e^{4w}\, W^2, \tag{B.44}$$

or equivalently,

$$\sqrt{-\tilde{g}}\, \tilde{W}^2 = e^{-(d-4)w} \sqrt{-g}\, W^2. \tag{B.45}$$

Note that in exactly four dimensions, $\sqrt{-g}\, W^2$ is invariant under a Weyl transformation.

B.5.9 $\tilde{R}^2_{\mu\nu\alpha\beta}$

The Weyl transformation of the square of the Riemann tensor is given by

$$\begin{aligned}\tilde{R}^2_{\mu\nu\alpha\beta} = e^{4w} \Bigg[& R^2_{\mu\nu\alpha\beta} - 8R_{\mu\nu}\nabla^{\mu}\nabla^{\nu}w - 8R_{\mu\nu}\nabla^{\mu}w\nabla^{\nu}w + 4R\left(\nabla_{\mu}w\right)^2 + 4\left(\Box w\right)^2 \\ & + 2\left(d-2\right)\Bigg(2\left(\nabla_{\mu}\nabla_{\nu}w\right)^2 - 4\left(\nabla_{\mu}w\right)^2\Box w + 4\nabla_{\mu}\nabla_{\nu}w\nabla^{\mu}w\nabla^{\nu}w \\ & + \left(d-1\right)\left(\nabla_{\mu}w\right)^4\Bigg)\Bigg].\end{aligned} \tag{B.46}$$

B.5.10 $\tilde{R}^2_{\mu\nu}$

The Weyl transformation of the square of the square of the Ricci tensor is given by

$$\begin{aligned}\tilde{R}^2_{\mu\nu} = e^{4w}\Big[& R^2_{\mu\nu} - 2R\Box w + (3d-4)\,(\Box w)^2 \\ & + (d-2)\Big[- 2R_{\mu\nu}\nabla^\mu\nabla^\nu w - 2R_{\mu\nu}\nabla^\mu w\nabla^\nu w + 2R\,(\nabla_\lambda w)^2 \\ & + (d-2)\,(\nabla_\mu\nabla_\nu w)^2 + 2\,(d-2)\,(\nabla_\mu\nabla_\nu w)\,(\nabla^\mu w)\,(\nabla^\nu w) \\ & - 2\,(2d-3)\,\Box w\,(\nabla_\lambda w)^2 + (d-2)\,(d-1)\,(\nabla_\lambda w)^4\Big]\Big]. \end{aligned} \tag{B.47}$$

B.5.11 $\tilde{R}^2$

The Weyl transformation of the square of the square of the Ricci scalar is given by

$$\begin{aligned}\tilde{R}^2 = e^{4w}\Big[& R^2 - 4\,(d-1)\,R\Box w + 2R\,(d-1)\,(d-2)\,(\nabla_\lambda w)^2 \\ & + (d-1)^2\left[4\,(\Box w)^2 - 4\,(d-2)\,\Box w\,(\nabla_\lambda w)^2 + (d-2)^2\,(\nabla_\lambda w)^4\right]\Big]. \end{aligned} \tag{B.48}$$

B.5.12 $\tilde{E}_4$

The Weyl transformation of the Euler density in 4D, c.f. Eq. (B.15), is given by

$$\begin{aligned}\tilde{E}_4 = e^{4w}\Big[& E_4 + (d-3)\Big(- 4R\Box w + 8R_{\mu\nu}\nabla^\mu\nabla^\nu w + 8R_{\mu\nu}\nabla^\mu w\nabla^\nu w \\ & + 2\,(d-4)\,R\,(\nabla_\mu w)^2 + 4\,(d-2)\,(\Box w)^2 - 4\,(d-2)\,(\nabla_\mu\nabla_\nu w)^2 \\ & - 4\,(d-2)\,(d-3)\,(\nabla_\mu w)^2\,\Box w - 8\,(d-2)\,\nabla_\mu\nabla_\nu w\nabla^\mu w\nabla^\nu w \\ & + (d-1)\,(d-2)\,(d-4)\,(\nabla_\mu w)^4\Big)\Big]. \end{aligned} \tag{B.49}$$

B.5.13 $\tilde{\Box}\tilde{R}$

For $\tilde{\Box}\tilde{R}$, one has to be very careful, as $\Box R$ should really be written as

$$\Box R = (-g)^{-\frac{1}{2}} \nabla_\mu \left[(-g)^{\frac{1}{2}} g^{\mu\nu} \nabla_\nu R \right]. \tag{B.50}$$

Its Weyl transformation is then given by

$$\begin{aligned}
\tilde{\Box}\tilde{R} = e^{4w} \Bigg[& \Box R - (d-6) \nabla^\mu R \nabla_\mu w + 2R\Box w - 2(d-4) R (\nabla_\lambda w)^2 \\
& + 2(d-1) \Bigg((d-6) R_{\mu\nu} \nabla^\mu w \nabla^\nu w - 2(\Box w)^2 + 2(d-4) \nabla^\mu w \Box (\nabla_\mu w) \\
& - \Box^2 w + (d-2) (\nabla_\mu \nabla_\nu w)^2 - (d-2)(d-6) \nabla_\nu \nabla_\nu w \nabla^\mu w \nabla^\nu w \\
& + (3d-10) (\nabla_\mu w)^2 \Box w - (d-4)(d-2) (\nabla_\mu w)^4 \Bigg) \Bigg].
\end{aligned} \tag{B.51}$$

The package `xTensor` in Mathematica has been used to obtain the above.

B.5.14 TEMT

Using Eq. (A.44), one can calculate the trace of the energy-momentum tensor using Weyl variations,

$$T^\mu{}_\mu = \frac{1}{\sqrt{-g}} \frac{\delta}{\delta w} \bigg|_{w=0} \int \mathrm{d}^d x \sqrt{-\tilde{g}} \left(a_0 \tilde{E}_4 + b_0 \tilde{R}^2 + c_0 \tilde{W}^2 \right) \tag{B.52}$$

$$= -(d-4) a_0 E_4 - (d-4) b_0 R^2 - 4(d-1) b_0 \Box R - (d-4) c_0 W^2. \tag{B.53}$$

The result matches Eq. (B.32), which was obtained by a variation of the metric tensor, and then traced.

B.6 Other Useful Identities involving Curved Spacetime

B.6.1 Einstein Field Equations

The Einstein field equations are given by

$$R_{\mu\nu} - \frac{1}{2}Rg_{\mu\nu} = -8\pi G\, T_{\mu\nu} - \Lambda g_{\mu\nu}. \tag{B.54}$$

Note that the equation can be understood as taking metric variations of the Einstein-Hilbert action, $\mathcal{S}_{\rm EH}$, given by

$$\mathcal{S}_{\rm EH} = \frac{1}{16\pi G}\int d^d x\,\sqrt{-g}\,(R - 2\Lambda)\,, \tag{B.55}$$

along with the matter Lagrangian (which generates the energy-momentum tensor). Taking a covariant derivative of the Einstein field equations, one arrives at

$$\nabla_\mu R^{\mu\nu} = \frac{1}{2}\nabla^\nu R, \tag{B.56}$$

which also implies

$$\nabla_\mu\nabla_\nu R^{\mu\nu} = \frac{1}{2}\Box R. \tag{B.57}$$

B.6.2 Identities relating $R^2_{\mu\nu\alpha\beta}$ and $R^2_{\mu\nu}$ to E_d and W^2

It is useful to relate $R^2_{\mu\nu\alpha\beta}$ and $R^2_{\mu\nu}$ to E_d and W^2, as the latter two play a central role in conformal anomalies. Below, for each pair of equations, the first corresponds to a general dimension d, while the second corresponds to 4D exactly.

$$\begin{aligned} R^2_{\mu\nu\alpha\beta} &= \frac{1}{d-1}R^2 + \frac{d-2}{d-3}W^2 - \frac{d-2}{2}E_d \\ &= \frac{1}{3}R^2 + 2W^2 - E_4, \end{aligned} \tag{B.58}$$

$$R^2_{\mu\nu} = \frac{d}{4\,(d-1)}R^2 + \frac{(d-2)}{4\,(d-3)}W^2 - \frac{(d-2)^2}{8}E_d$$

$$= \frac{1}{3}R^2 + \frac{1}{2}W^2 - \frac{1}{2}E_4. \tag{B.59}$$

The above identities then imply

$$\frac{(d-1)(d-2)-2}{(d-2)}R^2_{\mu\nu\alpha\beta} - \frac{4(d-3)}{(d-2)}R^2_{\mu\nu} = (d-1)W^2 - (d-3)E_d,$$

$$2R^2_{\mu\nu\alpha\beta} - 2R^2_{\mu\nu} = 3W^2 - E_4. \tag{B.60}$$

B.6.3 Integration by parts

Using the identity

$$\partial_\mu\left(\sqrt{-g}X^\mu\right) = \sqrt{-g}\nabla_\mu X^\mu, \tag{B.61}$$

one can use integration by parts, with the appropriate volume element, such that

$$\int \mathrm{d}^4x\,\sqrt{-g}X_\mu\nabla^\mu Y = -\int \mathrm{d}^4x\,\sqrt{-g}\left(\nabla_\mu X^\mu\right)Y + \text{boundary term}. \tag{B.62}$$

Appendix C

Bitensors

A bitensor is a function of 2 spacetime points which transforms according to the direct product of 2 tensor or spinor representations of the coordinate transformation and vierbein groups.

In the following, geodetic curve means 'geodesic'. Also, all bitensors will be understood to be functions of (x, x'), so the dependence will sometimes be dropped for conciseness.

Most of the results in this appendix have been obtained from [14].

C.1 Notation

C.1.1 Comma/Semicolon notation

To avoid writing many (covariant) derivatives ∇_μ, we will introduce the (semicolon) comma notation:

$$\nabla_\alpha \nabla_\beta \nabla_\mu A \equiv A_{;\mu\beta\alpha} \tag{C.1}$$

$$\partial_\alpha \partial_\beta \partial_\mu A = A_{,\mu\beta\alpha} \tag{C.2}$$

Note the order of the indices.

C.1.2 Square Bracket Notation

We use the square bracket notation to mean coincident limit of bitensors, for example,

$$[A(x,x')] \equiv \lim_{x' \to x} A(x,x'). \tag{C.3}$$

C.2 Geodetic Interval $\sigma(x,x')$

$\sigma(x,x')$ is defined as half the proper time distance between x and x'.

$\nabla_\mu \sigma$ is a vector of length equal to the distance along the geodesic between x and x', tangent to the geodesic at x and oriented in the $x' \to x$ direction.

$\nabla_{\mu'} \sigma$ is a vector of length equal to distance along geodesic between x and x', tangent to geodesic at x' and oriented in $x \to x'$ direction.

So,

$$\sigma = \frac{1}{2} \nabla_\mu \sigma \nabla^\mu \sigma \tag{C.4}$$

C.3 Van Vleck-Morette determinant $\Delta(x,x')$

We define the function $D(x,x')$, given by

$$D(x,x') = \det\left(\nabla_{\nu'} \nabla_\mu \sigma\right) \tag{C.5}$$

An important identity involving D is given by

$$\left(D\sigma^{\mu}_{;}\right)_{;\mu} = dD \tag{C.6}$$

The van Vleck-Morette determinant $\Delta(x,x')$ [52, 53] is then defined by

$$\Delta(x,x') = (-g)^{-\frac{1}{2}} D(x,x') (-g')^{-\frac{1}{2}}, \tag{C.7}$$

where $g \equiv g(x)$ and $g' \equiv g(x')$.

C.4 Geodetic Parallel Displacement

The geodetic parallel displacement bi-vector $g_{\mu\nu'}$ takes a vector $A^{\nu'}$ at x' to A^{μ} at x, parallel transporting $A^{\nu'}$ from x' to x:

$$A_{\mu} = g_{\mu\nu'} A^{\nu'} \tag{C.8}$$

$$A_{\nu'} = g_{\mu\nu'} A^{\mu} \tag{C.9}$$

A parallel transport satisfies the equation

$$A^{\mu}{}_{;\rho} \sigma_{;}{}^{\rho} = 0 \tag{C.10}$$

which leads to

$$\sigma_{;}{}^{\tau} g_{\mu\nu';\tau} = 0, \tag{C.11}$$

upon using (C.8).

Some identities involving $g_{\mu\nu'}$ are given below.

$$g_{\mu}{}^{\nu'} \sigma_{;\nu'} = -\sigma_{;\mu} \tag{C.12}$$

$$g^{\nu}{}_{\mu'} \sigma_{;\nu} = -\sigma_{;\mu'} \tag{C.13}$$

$$\sigma_{;}{}^{\tau'} g_{\mu\nu';\tau'} = 0 \tag{C.14}$$

$$g_{\mu\nu'} = g_{\nu'\mu} \tag{C.15}$$

$$[g_{\mu\nu'}] = g_{\mu\nu} \tag{C.16}$$

$$g_{\mu\sigma'} g^{\sigma'}{}_{\nu} = g_{\mu\nu} \tag{C.17}$$

$$g_{\sigma\mu'} g_{\nu'}{}^{\sigma} = g_{\mu'\nu'} \tag{C.18}$$

$$\det\left(-g_{\mu\nu'}\right) = g^{\frac{1}{2}} g'^{\frac{1}{2}} \tag{C.19}$$

C.5 Synge's Theorem

Synge's Theorem [54] is a very important result which allows us to express the coincident limits containing primed indices in terms of unprimed ones:

$$[A_{;\ldots\alpha'}] = -[A_{;\ldots\alpha}] + [A_{;\ldots}]_{;\alpha} \tag{C.20}$$

The dots represent any number of *unprimed* indices. The square brackets denote coincident limit. For example, $D = \det(\nabla_{\nu'}\nabla_{\mu}\sigma)$, which in the coincident limit goes to

$$[D] = (-g), \tag{C.21}$$

where $g = \det(g_{\mu\nu})$.

C.6 Coincident Limits

C.6.1 $\sigma(x, x')$

The starting point (see Eq. (C.4)) is

$$[\sigma] = 0 \tag{C.22}$$

$$[\sigma_{;\mu}] = 0 \tag{C.23}$$

$$\sigma = \frac{1}{2}\sigma_{;\mu}\sigma_{;}^{\ \mu} \tag{C.24}$$

Thus, we have that

$$[\sigma_{;\nu\lambda}] = g_{\lambda\nu} \tag{C.25}$$

$$[\sigma_{;\nu\sigma\tau}] = 0 \tag{C.26}$$

$$[\sigma_{;\nu\sigma\tau\rho}] = \frac{1}{3}[R_{\nu\tau\sigma\rho} + R_{\nu\rho\sigma\tau}] \tag{C.27}$$

$$\left[\sigma_{;}^{\ \nu}{}_{\nu}^{\ \tau}{}_{\tau\lambda}\right] = \nabla_{\lambda}R \tag{C.28}$$

$$\left[\sigma_{;}^{\ \nu}{}_{\nu}^{\ \tau}{}_{\tau}^{\ \lambda}{}_{\lambda}\right] = \frac{4}{15}R^2_{\mu\nu} + \frac{8}{5}\Box R - \frac{4}{15}R^2_{\mu\nu\alpha\beta} \tag{C.29}$$

We also give some results that involve primed derivatives, which are of course obtained by using Synge's theorem,

$$[\sigma_{;\mu\nu'}] = -g_{\mu\nu} \tag{C.30}$$

C.6.2 $\Delta^{\pm\frac{1}{2}}(x, x')$

The starting point is Eq. (C.6),

$$\nabla_\mu (D\nabla^\mu\sigma) = d\, D, \tag{C.31}$$

where $D = \det(\nabla_{\nu'}\nabla_\mu\sigma)$, c.f. Eq. (C.5). Defining the van Vleck-Morette determinant, $\Delta = (-g)^{-\frac{1}{2}} D\, (-g')^{-\frac{1}{2}}$, we have

$$\left[\Delta^{\pm\frac{1}{2}}\right] = 1 \tag{C.32}$$

$$\pm 2\nabla_\mu\Delta^{\pm\frac{1}{2}}\nabla^\mu\sigma + \Delta^{\pm\frac{1}{2}}\nabla^\mu\nabla_\mu\sigma = d\Delta^{\pm\frac{1}{2}} \tag{C.33}$$

Thus,

$$\left[\Delta^{\pm\frac{1}{2}}{}_{;\mu}\right] = 0 \tag{C.34}$$

$$\left[\Delta^{\pm\frac{1}{2}}{}_{;\nu\mu}\right] = \mp\frac{1}{6}R_{\mu\nu} \tag{C.35}$$

$$\left[\Delta^{\frac{1}{2}}{}_{;\ \nu\mu}^{\ \nu}\right] = -\frac{1}{6}\nabla_\mu R \tag{C.36}$$

$$\left[\Delta^{\frac{1}{2}}{}_{;\ \nu\ \mu}^{\ \nu\ \mu}\right] = -\frac{1}{30}R^2_{\mu\nu} + \frac{R^2}{36} - \frac{1}{5}\Box R + \frac{1}{30}R^2_{\mu\nu\alpha\beta} \tag{C.37}$$

$$\begin{aligned}\left[\Delta^{\frac{1}{2}}{}_{;\ \lambda}^{\ \lambda\ \mu\nu}\right] = \frac{1}{180}\Big[&- 12R^{\mu\lambda}R^{\nu}{}_{\lambda} + 5R^{\mu\nu}R + 6R^{\alpha\beta}R^{\mu\ \ \nu}_{\ \alpha\ \beta} + 6R^{\mu\alpha\beta\gamma}R^{\nu}{}_{\alpha\beta\gamma} \\ &- 9\Box R^{\mu\nu} - 27\nabla^\mu\nabla^\nu R\Big]\end{aligned} \tag{C.38}$$

In the above, wherever μ and ν exist as free indices, there is symmetry under $\mu \leftrightarrow \nu$.

We also give some results that involve primed derivatives, which are obtained by using Synge's theorem,

$$\left[\Delta^{\pm\frac{1}{2}}_{;\mu\nu'}\right] = \pm\frac{1}{6}R_{\mu\nu} \tag{C.39}$$

C.6.3 Bi-spinor $I(x, x')$

The starting point is

$$\sigma_{;\mu} I_{;}^{\ \mu} = 0 \tag{C.40}$$

$$[I] = \mathbb{1}, \tag{C.41}$$

where $\mathbb{1}$ is the identity matrix in Dirac space. Thus,

$$[I_{;\nu}] = 0 \tag{C.42}$$

$$[I_{;\sigma\nu}] = -\frac{1}{4} G_{\alpha\beta} R^{\alpha\beta}{}_{\nu\sigma} \tag{C.43}$$

$$\left[I_{;}^{\ \nu}{}_{\nu\mu}\right] = -\frac{1}{6} G_{\alpha\beta} \nabla^{\nu} R^{\alpha\beta}{}_{\mu\nu} \tag{C.44}$$

$$\left[I_{;}^{\ \nu}{}_{\nu}^{\ \mu}{}_{\mu}\right] = \frac{1}{8} G_{\alpha\beta} R^{\alpha\beta\mu\nu} G_{\gamma\delta} R^{\gamma\delta}{}_{\mu\nu} \tag{C.45}$$

In the above, $G_{\alpha\beta} = \frac{1}{4}[\gamma_\alpha, \gamma_\beta]$ is the generator of Lorentz transformations of Dirac fermions, and

$$[\nabla_\nu, \nabla_\mu]\, \Psi = \frac{1}{2} G^{\alpha\beta} R_{\alpha\beta\mu\nu} \Psi, \tag{C.46}$$

where Ψ is a Dirac spinor.

C.6.4 Bi-vector $g_{\mu\nu'}(x, x')$

The starting point is

$$\sigma_{;}^{\ \tau} g_{\mu\nu';\tau} = 0 \tag{C.47}$$

$$[g_{\mu\nu'}] = g_{\mu\nu} \tag{C.48}$$

Note also that

$$-\sigma_{;}^{\ \mu} = g^{\mu}{}_{\nu'} \sigma_{;}^{\ \nu'} \tag{C.49}$$

Thus, we have

$$[g_{\mu\nu';\alpha}] = 0 \tag{C.50}$$

$$[g_{\mu\nu'\,;\,\alpha\beta}] = \frac{1}{2}R_{\mu\nu\alpha\beta} \tag{C.51}$$

$$[g_{\mu\nu'\,;\,\alpha\beta\sigma}] = -\frac{1}{3}\left[\nabla_\sigma R_{\beta\alpha\mu\nu} + \nabla_\beta R_{\sigma\alpha\mu\nu}\right] \tag{C.52}$$

$$\left[g_{\mu\nu'\,;\,\alpha\ \beta}^{\ \ \alpha\ \ \beta}\right] = -\frac{1}{2}R_{\mu}^{\ \alpha\beta\lambda}R_{\nu\alpha\beta\lambda} \tag{C.53}$$

$$\begin{aligned}\left[g^{\mu\nu'\ \lambda\ \ \beta\alpha}_{\ \ ;\ \lambda}\right] = &-\frac{1}{6}\left(R^{\alpha}_{\ \ \sigma}R^{\mu\nu\beta\sigma} + R^{\beta}_{\ \ \sigma}R^{\mu\nu\alpha\sigma}\right) + \frac{1}{4}\Big(- R^{\mu\sigma\alpha\rho}R^{\nu\ \ \beta}_{\ \sigma\ \ \rho} - R^{\mu\sigma\beta\rho}R^{\nu\ \ \alpha}_{\ \sigma\ \ \rho} \\ &+ R^{\mu\nu\alpha\lambda}_{\ \ \ \ ;\lambda}{}^{\beta} + R^{\mu\nu\beta\lambda}_{\ \ \ \ ;\lambda}{}^{\alpha}\Big)\end{aligned} \tag{C.54}$$

$$\begin{aligned}\left[g^{\mu\nu'\ \lambda}_{\ \ ;\ \lambda\mu\nu}\right] &= -\frac{1}{8}R^2_{\mu\nu\alpha\beta} - \frac{1}{4}R^2_{\mu\nu} \\ &= \left[g^{\mu\nu'\ \lambda}_{\ \ ;\ \lambda\nu\mu}\right]\end{aligned} \tag{C.55}$$

Eq. (C.51) and Eq. (C.52) are antisymmetric in $\mu \leftrightarrow \nu$. Eq. (C.54) is symmetric in $\alpha \leftrightarrow \beta$.

In all of the above, the package `xTensor` has been used to evaluate the more complicated coincident limits. Also, in deriving some of them, the symmetries of the Riemann tensor in Sec. B.1.4 have been used.

Appendix D

Soft Integral $\mathcal{F}_{ij}^{(s)}$

D.1 IR sensitive part with photon mass and dimensional regularisation

The $\mathcal{F}_{ij}^{(s)}$ integral in Eq. (5.8) is IR-divergent and has to be regulated. We discuss dimensional regularisation and photon mass regularisation in this section. The regularised integral, denoted by an $\mathcal{R}$-subscript, is

$$\left[\mathcal{F}_{ij}^{(s)}(\omega_s)\right]_{\mathcal{R}} = \int [d\Phi_\gamma]_{\mathcal{R}} \left[\frac{-(E_\gamma^{(n)})^2\, p_i \cdot p_j}{(k\cdot p_i)(k\cdot p_j)}\right] = \frac{1}{2\pi}\int_0^{(E_\gamma^{(n)})^{\max}} \frac{dE_\gamma^{(n)}}{E_\gamma^{(n)}} \rho_{\mathcal{R}}^{E}\, I_{ij}^{(\mathcal{R},n)}(E_\gamma^{(n)}) \,, \tag{D.1}$$

where

$$I_{ij}^{\mathcal{R}}(E_\gamma^{(n)}) \equiv \int d\Omega_\gamma^{(n)}\; \rho_{\mathcal{R}}^{\Omega^{(n)}} \left[\frac{-(E_\gamma^{(n)})^2\, p_i \cdot p_j}{(k\cdot p_i)(k\cdot p_j)}\right] \,, \tag{D.2}$$

and

$$(E_\gamma^{(1,2)})^{\max} = \frac{\omega_s m_B}{2} \tag{D.3}$$

corresponds to the expression in (4.77) with $\delta_{\rm ex} \to \omega_s \ll 1$ for which the two frames become equivalent and

$$\rho^E_{\mathcal{R}} = \begin{cases} \frac{\Gamma(1-\epsilon)}{\Gamma(1-2\epsilon)} \left(\frac{E^{(n)}_\gamma}{\sqrt{\pi}\mu}\right)^{-2\epsilon} & \text{dim-reg} \\ \theta(E^{(n)}_\gamma - m_\gamma) & m_\gamma \end{cases} , \quad \rho^{\Omega^{(n)}}_{\mathcal{R}} = \begin{cases} (\sin\theta_\gamma \, \sin\phi_\gamma)^{-2\epsilon} & \text{dim-reg} \\ \frac{|\vec{k}^{(n)}_\gamma|}{E^{(n)}_\gamma} & m_\gamma \end{cases} , \tag{D.4}$$

and in addition one needs to set $m_\gamma \to 0$ in dim-reg. We will argue that the angular integral is Lorentz-invariant when the regulator is removed. We may restore Lorentz invariance of (D.1) by removing the photon energy cut-off. In a second step, we remove the regulator, $\rho^E_{\mathcal{R}}, \rho^{\Omega^{(n)}}_{\mathcal{R}} \to 1$. Then, the integral, which is frame- and scheme-independent, factorises into an energy integral K and an angular integral $I^{(0)}_{ij}$, where the superscript (0) indicates that the regulator has been removed. Since the energy integral is Lorentz invariant on its own, this implies the Lorentz-invariance of the finite $I^{(0)}_{ij}$-integral.

Focussing on the IR sensitive part, we keep $\rho^E_{\mathcal{R}}$ to regulate the divergent energy integral and remove the angular regularisation $\rho^{\Omega^{(n)}}_{\mathcal{R}} \to 1$ which is a useful limit as the integral still factorises into a doable energy integral and the Lorentz invariant $I^{(0)}_{ij}$-part,

$$\left[\mathcal{F}^{(s)}_{ij}\right]_{\mathcal{R}} = -K_{\mathcal{R}}(\omega_s)\, I^{(0)}_{ij} + \mathcal{O}(f,\mathcal{R}) \, , \tag{D.5}$$

where

$$I^{(0)}_{ij} = I^{(0,n)}_{ij} \equiv \int d\Omega^{(n)}_\gamma \left[\frac{-(E^{(n)}_\gamma)^2\, p_i \cdot p_j}{(k\cdot p_i)(k\cdot p_j)}\right] = (5.13) \, , \tag{D.6}$$

and we have used the Lorentz invariance of $I^{(0,n)}_{ij}$. We note that while $\rho^{\Omega^{(n)}}_{\mathcal{R}} \to 1$ captures all IR sensitive terms, it misses constant terms, indicated by $\mathcal{O}(f,\mathcal{R})$. These terms are determined in DR in the next section.

In DR, the $K_{\mathcal{R}}(\omega_s)$ integral evaluates to

$$K_\epsilon(\omega_s) = \int_0^{(E^{(n)}_\gamma)^{\max}} \frac{dE^{(n)}_\gamma}{E^{(n)}_\gamma} \frac{\Gamma(1-\epsilon)}{\Gamma(1-2\epsilon)} \left(\frac{E^{(n)}_\gamma}{\sqrt{\pi}\mu}\right)^{-2\epsilon} = -\frac{1}{2} r_{\rm soft} + \ln\left(\frac{\omega_s m_B}{\mu}\right) + \mathcal{O}(\epsilon), \tag{D.7}$$

whereas in photon mass regularisation the result is

$$K_{m_\gamma}(\omega_s) = \int_{m_\gamma}^{(E_\gamma^{(n)})^{\max}} \frac{dE_\gamma^{(n)}}{E_\gamma^{(n)}} = -\frac{1}{2} r_{\text{soft}} + \ln\left(\frac{\omega_s m_B}{2\mu}\right) + \mathcal{O}(m_\gamma) \,, \tag{D.8}$$

and we note the additional factor of 2 in the logarithm as compared to the DR result.

D.2 Soft integrals in dimensional regularisation

In this section, we calculate the soft integrals fully analytically up $\mathcal{O}(\epsilon^0)$ to using dimensional regularisation. We perform the integrals by introducing a soft cut-off ω_s, and the result is obtained up to $\mathcal{O}(\omega_s)$ corrections, which can be safely neglected since $\omega_s \ll 1$.

The integrals have the general form

$$\begin{aligned}\mathcal{F}_{ij}^{(s)}(\omega_s) = \frac{(\pi\mu^2)^\epsilon}{2\pi} \frac{\Gamma(1-\epsilon)}{\Gamma(1-2\epsilon)} \int_0^{(E_\gamma^{(n)})^{\max}} \frac{dE_\gamma^{(n)}}{\left(E_\gamma^{(n)}\right)^{1+2\epsilon}} \int_0^\pi \frac{d\theta_\gamma}{\sin^{2\epsilon-1}\theta_\gamma} \\ \times \int_0^\pi \frac{d\phi_\gamma}{\sin^{2\epsilon}\phi_\gamma} \left[\frac{-(E_\gamma^{(n)})^2\, p_i{\cdot}p_j}{(k{\cdot}p_i)(k{\cdot}p_j)}\right] \,.\end{aligned} \tag{D.9}$$

We have a total of 10 soft integrals to evaluate, corresponding to the different cases of i and j. Most of them can be evaluated using the results in the appendix of [139] and [112] (see also [140] for a detailed discussion on how to evaluate them). For $i = j$, we can write them as

$$\mathcal{F}_{ii}^{(s)}(\omega_s) = \left[\frac{1}{2} r_{\text{soft}} - \ln\left(\frac{\omega_s m_B}{\mu}\right)\right] + \frac{1}{2\beta_i} \ln\left(\frac{1+\beta_i}{1-\beta_i}\right) \,, \tag{D.10}$$

where r_{soft} refers to the DR version in (4.46), and all β_i are measured in the p_B-RF, with $k = 0$, since we are in the soft limit.[1] We note that in the soft limit, the (1)- and (2)-frames are the same, and thus, we will use the two interchangeably in this section. Further, we can isolate the collinear logs in the case of small lepton

[1] The reason for measuring all β_i in the p_B-RF is that it is the same frame in which we impose the cut-off on the photon energy, c.f. Eq. (4.77).

masses by considering

$$\frac{1}{2\beta_i}\ln\left(\frac{1+\beta_i}{1-\beta_i}\right)=\frac{1}{2\beta_i}\ln\left(\frac{(1+\beta_i)^2}{1-\beta_i^2}\right)\overset{m_i\to 0}{\longrightarrow}\frac{1}{2}\ln\frac{4E_i^2}{m_i^2}=-\ln m_i+\text{non-div}\ . \tag{D.11}$$

It is worth noting that if particle i were truly massless, i.e. $m_i \to 0$, the integral would simply vanish (since it is proportional to m_i^2). This can also be seen as a cancellation of the IR pole in r_{soft}, and the $\ln m_i \to \frac{1}{2}\frac{1}{\epsilon_{\text{IR}}}$. The cut-off dependent term, $\ln\left(\frac{\omega_s m_B}{\mu}\right)$, also vanishes and the same happens to its cancelling pair in Eq. (5.19), which was kept precisely because it has a $\ln\omega_s$ dependence in mass regularisation.

We now list the integrals corresponding to $i \neq j$. The simplest one is

$$\mathcal{F}^{(s)}_{i\,B}(\omega_s)=\left[\frac{1}{2}r_{\text{soft}}-\ln\left(\frac{\omega_s m_B}{\mu}\right)\right]I^{(0)}_{iB}+\frac{1}{2\beta_i}\left[\text{Li}_2\left(\frac{2\beta_i}{1+\beta_i}\right)+\frac{1}{4}\ln^2\left(\frac{1+\beta_i}{1-\beta_i}\right)\right]\ , \tag{D.12}$$

where $I^{(0)}_{iB}$ can be obtained by using $j = B$ in Eq. (5.13). The 3 other non-diagonal integrals require more work since they are not attributed to the frame in which the integral is evaluated. One can recast the remaining integrals as

$$\mathcal{F}^{(s)}_{ij}(\omega_s)=\left[\frac{1}{2}r_{\text{soft}}-\ln\left(\frac{\omega_s m_B}{\mu}\right)\right]\Omega_{ij}\ , \tag{D.13}$$

where $\Omega_{ij} = \Omega(\beta_i, \beta_j, \tau_{ij})$,

$$\begin{aligned}\Omega(\beta_i,\beta_j,\tau_{ij}) =& P_{ij}\int_0^\pi \frac{d\theta_\gamma}{\sin^{2\epsilon-1}\theta_\gamma}\int_0^\pi\frac{d\phi_\gamma}{\sin^{2\epsilon}\phi_\gamma}\times \\ &\left[\frac{1}{(1-\beta_i\cos\theta_\gamma)(1-\beta_j\cos\theta_\gamma\cos\chi_{ij}-\beta_j\sin\theta_\gamma\cos\phi_\gamma\sin\chi_{ij})}\right]\ ,\end{aligned} \tag{D.14}$$

where

$$\begin{aligned}\cos\chi_{ij} &= 2\tau_{ij}-1,\\ \sin\chi_{ij} &= \sqrt{1-\cos^2\chi_{ij}},\\ P_{ij} &= \frac{(1-\beta_i\beta_j(2\tau_{ij}-1))}{2\pi}.\end{aligned} \tag{D.15}$$

Before matching β_i, β_j and τ_{ij} to the cases we have, consider $\Omega(\beta_i, \beta_j, \tau_{ij})$. For $\beta_i \neq 1$ and $\beta_j \neq 1$, the result to $\mathcal{O}(\epsilon)$ is not known in the literature. This is needed for isolating the collinear logs, since they arise from the $\mathcal{O}(\epsilon)$ part of the angular integrals multiplied by the $1/\epsilon$ from the r_{soft}.

However, through [141], we were able to get an expression for $\Omega(\beta_i, \beta_j, \tau_{ij})$. The result is

$$\Omega_{ij} = \frac{\pi\, P_{ij}}{2\, C_{ij}} \Bigg\{ \ln\left(\frac{v_{ij}+C_{ij}}{v_{ij}-C_{ij}}\right) + \epsilon \Bigg[-\ln\left(\frac{1-C_{ii}}{1+C_{ii}}\right) \ln\left(\frac{R_{ij}+S_{ij}}{R_{ij}-S_{ij}}\right) + \left(\sum_{a,b=1}^{4} \left[-1+2\left(\delta_{a2}+\delta_{a3}\right)\right] \left[1-2\left(\delta_{b3}+\delta_{b4}\right)\right] G(r_{ij}^{(a)}, r_{ij}^{(b)}, 1) \right) \Bigg] \Bigg\} . \quad \text{(D.16)}$$

The functions $G(a, b, 1)$ are generalised polylogarithms of weight 2, and for our parameters a and b the following representation holds

$$\begin{aligned} G(a,b,1) &= \mathrm{Li}_2\left(\frac{b-1}{b-a}\right) - \mathrm{Li}_2\left(\frac{b}{b-a}\right) + \ln\left(1-\frac{1}{b}\right) \ln\left(\frac{1-a}{b-a}\right) , \\ G(a,a,1) &= \frac{1}{2} \ln^2\left(1-\frac{1}{a}\right) , \end{aligned} \quad \text{(D.17)}$$

and

$$\begin{aligned} r_{ij}^{(1)} &= \frac{f_{ij}-\sqrt{g_{ij}}}{h_{ij}} , & r_{ij}^{(2)} &= \frac{f_{ij}+\sqrt{g_{ij}}}{h_{ij}} , \\ r_{ij}^{(3)} &= r_{ij}^{(1)}|_{\beta_{i,j}\to-\beta_{i,j}} , & r_{ij}^{(4)} &= r_{ij}^{(2)}|_{\beta_{i,j}\to-\beta_{i,j}} , \\ f_{ij} &= \beta_i\left(\beta_j\left(1-2\tau_{ij}\right)+1\right) , & h_{ij} &= \beta_i\left(\beta_j+2-4\tau_{ij}\right)+\beta_j , \\ g_{ij} &= \beta_i^2\left(4\beta_j^2\tau_{ij}\left(\tau_{ij}-1\right)+1\right) + \beta_i\beta_j(2-4\tau_{ij}) + \beta_j^2 , \\ R_{ij} &= C_{ii}v_{ij}C_{jj} - 8v_{ii}v_{jj} + v_{ij} , & S_{ij} &= \left(C_{ii}+C_{jj}\right)C_{ij} , \\ C_{ii} &= \sqrt{1-4v_{ii}} , & v_{ii} &= \frac{1}{4}\left(1-\beta_i^2\right) , \\ C_{jj} &= \sqrt{1-4v_{jj}} , & v_{jj} &= \frac{1}{4}\left(1-\beta_j^2\right) , \\ C_{ij} &= \sqrt{v_{ij}^2-4v_{ii}v_{jj}} , & v_{ij} &= \frac{1}{2}\left(1-\beta_i\beta_j\left(2\tau_{ij}-1\right)\right) , \end{aligned}$$

with no summation over indices implied. For the matching, we consider the

momenta p_K, ℓ_1 and ℓ_2 in the (2)-frame. Thus, for $\mathcal{F}^{(s)}_{K\ell_{1,2}}(\omega_s)$, one has

$$\beta_K = \frac{|\vec{p}_K^{(2)}|}{E_K^{(2)}}\,, \quad \beta_{\ell_{1,2}} = \frac{|\vec{\ell}_{1,2}^{(2)}|}{E_{1,2}^{(2)}}\,, \quad \tau_{K\ell_{1,2}} = \frac{1}{2}\left(1 - \frac{\ell^{(2)}_{1,2,x}}{|\vec{\ell}^{(2)}_{1,2}|}\right)\,, \tag{D.18}$$

where $\ell^{(2)}_{1,2,x}$ corresponds to the $x-$component of $\ell^{(2)}_{1,2}$. Recall that the β_i's can be evaluated either in the (1)-RF or (2)-RF as these are equivalent in the $k \to 0$ limit assumed here.

Finally, for $\mathcal{F}^{(s)}_{\ell_1\ell_2}(\omega_s)$, before the matching can be performed, one needs to perform a 3D rotation to eliminate the y-component of one of the momenta, for which we choose ℓ_1. Thus, one has

$$\tau_{\ell_1\ell_2} = \frac{1}{2}\left(1 + \frac{\ell^{(2)}_{2,x}\cos\alpha - \ell^{(2)}_{2,y}\sin\alpha}{|\vec{\ell}^{(2)}_2|}\right)\,, \tag{D.19}$$

where, as before, the subscript on ℓ_2 denotes the corresponding component of ℓ_2. The angle of rotation α is defined via

$$\begin{aligned}\cos\alpha &= \frac{\ell^{(2)}_{1,x}}{|\vec{\ell}^{(2)}_1|}\\ \sin\alpha &= \sqrt{1-\cos^2\alpha}.\end{aligned} \tag{D.20}$$

Obviously, $\beta_{\ell_{1,2}}$ are the same after the rotation.

Taking the limit of small lepton masses, one can isolate the collinear logs and obtain

$$\begin{aligned}\mathcal{F}^{(s)}_{\ell_1\ell_2}(\omega_s) &= \left[\frac{1}{2}\Delta_\epsilon - \ln(\omega_s m_B)\right] I^{(0)}_{\ell_1\ell_2}\\ &\quad + \left(\frac{1}{2}\ln^2 m_{\ell_1} - \ln m_{\ell_1}\ln\left(2E^{(1)}_{\ell_1}\right) + \{1\leftrightarrow 2\}\right) + \text{finite}\,,\\ \mathcal{F}^{(s)}_{K\ell_1}(\omega_s) &= \left[\frac{1}{2}\Delta_\epsilon - \ln(\omega_s m_B)\right] I^{(0)}_{K\ell_{1,2}} + \frac{1}{2}\ln^2 m_{\ell_1} - \ln m_{\ell_1}\ln\left(2E^{(1)}_{\ell_1}\right) + \text{finite}\,.\end{aligned} \tag{D.21}$$

We now collect all single logs in $\mathcal{F}^{(s)}(\omega_s) \equiv \sum_{i,j}\hat{Q}_i\hat{Q}_j\mathcal{F}^{(s)}_{ij}(\omega_s)$. To this end,

consider the divergent parts of the different limits of $I_{ij}^{(0)}$.

$$I_{ij}^{(0)} \to \begin{cases} -\ln m_i & m_i \ll m_K, m_B \\ -\ln m_i - \ln m_j & m_i \simeq m_j \ll m_K, m_B \end{cases} . \tag{D.22}$$

Assembling all bits and pieces, and using charge conservation, we obtain

$$\begin{aligned} \mathcal{F}^{(s)}(\omega_s)|_{\ln m_{\ell_{1,2}}} &= \hat{Q}_{\ell_1}^2 \ln m_{\ell_1} (2 \ln 2E_{\ell_2}^{(1)} - (1 + 2 \ln (\omega_s m_B)) + \{1 \leftrightarrow 2\} \\ &= \hat{Q}_{\ell_1}^2 \ln m_{\ell_1} [-1 - 2 \ln (\bar{z}(\omega_s))] + \{1 \leftrightarrow 2\} , \end{aligned} \tag{D.23}$$

where we have used $2\hat{E}_{\ell_1}^{(1)} \equiv 1 - \hat{s}_{K\ell_2}{}^2$ to arrive at the final result, and $\bar{z}(\omega_s) \equiv 1 - z(\omega_s)$ with $z(\omega_s)$ given in Eq. (5.22).

[2]It is straight-forward to check that this is true in the soft limit.

Appendix E

Passarino-Veltman Functions

The aim of this appendix is to give a minimal self-contained discussion of the Passarino-Veltman functions appearing in our results. The integrals are defined in [142],

$$I_n \equiv \frac{(2\pi\mu)^{4-d}}{i\pi^2}\int \mathrm{d}^d l \frac{1}{(l^2-m_0^2+i0)((l+\ell_1)^2-m_1^2+i0)((l+\ell_1+\ell_2)^2-m_2^2+i0)\dots}\,, \tag{E.1}$$

where $n = 1, 2, 3, 4$ form a complete 1-loop basis and are usually referred to as A_0, B_0, C_0, D_0 respectively. For our case, $n = 1, 2, 3$ are sufficient. The A_0 and B_0 functions are given to $\mathcal{O}(\varepsilon^0)$, with $d = 4 - 2\varepsilon$,

$$A_0(m^2) = m^2\left(\frac{1}{\hat{\epsilon}_{\mathrm{UV}}} + 1 - \ln\left(\frac{m^2}{\mu^2}\right)\right) + \mathcal{O}(\varepsilon)\,, \tag{E.2}$$

$$\begin{aligned} B_0(s, m_0^2, m_1^2) = \Bigg(&\frac{1}{\hat{\epsilon}_{\mathrm{UV}}} + 2 - \ln\frac{m_0 m_1}{\mu^2} + \frac{m_0^2 - m_1^2}{s}\ln\frac{m_1}{m_0} \\ &- \frac{m_0 m_1}{s}\left(\frac{1}{r} - r\right)\ln r\Bigg) + \mathcal{O}(\varepsilon)\,, \end{aligned} \tag{E.3}$$

where $r = -\frac{1}{2}(-b+\sqrt{b^2-4})$ with $b = -\frac{s-m_0^2-m_1^2+i0}{m_0 m_1}$, and $\frac{1}{\hat{\epsilon}_{\mathrm{UV}}}$ is given in Eq. (4.45).

The C_0 function used is $C_0(s, t, u, m_0^2, m_1^2, m_2^2)$, where the cuts of the momenta $\{s, t, u\}$ start at $\{(m_0+m_1)^2, (m_0+m_2)^2, (m_1+m_2)^2\}$ respectively. This is the same convention used in FeynCalc [143, 144] and [142].

In the following, we define and use $s \equiv (\hat{p}_i+\hat{p}_j)^2$. The C_0 function can be found in the review paper [145], valid for small photon mass (up to $\mathcal{O}(m_\gamma^2)$ corrections)

in mass regularisation and to $\mathcal{O}(\epsilon^0)$ in DR,

$$C_0(m_i^2, m_j^2, s, m_i^2, m_\gamma^2, m_j^2) = \frac{x_{ij}}{m_i m_j (1-x_{ij}^2)} \Bigg\{ \left(\ln\left(\frac{m_i m_j}{\mu^2}\right) - r_{\text{soft}} \right) \ln(x_{ij}) \\ - \frac{1}{2}\ln^2(x_{ij}) + 2\ln(x_{ij})\ln(1-x_{ij}^2) + \frac{1}{2}\ln^2\left(\frac{m_i}{m_j}\right) - \frac{\pi^2}{6} \\ + \text{Li}_2(x_{ij}^2) + \text{Li}_2\left(1 - x_{ij}\frac{m_i}{m_j}\right) + \text{Li}_2\left(1 - x_{ij}\frac{m_j}{m_i}\right) \Bigg\}, \tag{E.4}$$

where r_{soft} is defined in (4.46), and

$$x_{ij} \equiv \frac{\sqrt{y_{ij}} - 1}{\sqrt{y_{ij}} + 1}, \quad y_{ij} \equiv \frac{(\hat{p}_i + \hat{p}_j)^2 - (m_i + m_j)^2 + i0}{(\hat{p}_i + \hat{p}_j)^2 - (m_i - m_j)^2 + i0}. \tag{E.5}$$

Further to this, we give the results for different limits of the C_0-function for reference.

For $s, m_j \gg m_i \gg m_\gamma$, we have

$$C_0(m_i^2, m_j^2, s, m_i^2, m_\gamma^2, m_j^2) = \frac{1}{s - m_j^2} \left\{ \ln\left(\frac{m_i(m_j^2 - \bar{s})}{m_\gamma^2 m_j}\right) \ln\left(\frac{m_j^2 - \bar{s}}{m_i m_j}\right) + \text{Li}_2\left(\frac{\bar{s}}{m_j^2}\right) \right\} \\ \to \frac{1}{s - m_j^2} \left\{ \ln\left(m_\gamma^2\right) \ln\left(\frac{m_i m_j}{m_j^2 - \bar{s}}\right) - \ln^2\left(m_i\right) \right\} + \mathcal{O}(1), \tag{E.6}$$

where $\bar{s} = s + i0$, and $\mathcal{O}(1)$ denotes finite terms and imaginary parts of the C_0 function, which is not relevant since we consider the real part when calculating the amplitude squared. One can obtain Eq. (E.6) from Eq. (E.4), using

$$x_{ij} \to -\frac{m_i m_j}{s - m_j^2}, \tag{E.7}$$

valid in the limit $m_i \ll s, m_j$.

For $s \gg m_i = m_j = m_\ell \gg m_\gamma$, we have

$$C_0(m_\ell^2, m_\ell^2, s, m_\ell^2, m_\gamma^2, m_\ell^2) = \frac{1}{s} \left\{ \ln\left(\frac{m_\gamma^2}{-\bar{s}}\right) \ln\left(\frac{m_\ell^2}{-\bar{s}}\right) - \frac{1}{2}\ln^2\left(\frac{m_\ell^2}{-\bar{s}}\right) - \frac{\pi^2}{6} \right\} \\ \to \frac{1}{s} \left\{ \ln\left(m_\gamma^2\right) \ln\left(\frac{m_\ell^2}{-\bar{s}}\right) - 2\ln^2 m_\ell \right\} + \mathcal{O}(1), \tag{E.8}$$

where, as above, $\mathcal{O}(1)$ denotes finite terms and imaginary parts of the C_0 function.

It is striking to note that, for small m_i, the C_0 function never produces single $\ln m_i$; the latter is always accompanied by either $\ln m_\gamma$, or another $\ln m_i$, producing a $\ln^2 m_i$, c.f. Eq. (E.6) and Eq. (E.8).

Appendix F

Other Useful Results

F.1 Gaussian Integrals

The 1D Gaussian integral is

$$\int dx\, e^{-ax^2} = \sqrt{\frac{\pi}{a}}. \tag{F.1}$$

Generalising this, we have that

$$\int \frac{d^dx}{(2\pi)^d}\, e^{-\lambda x^2} = \frac{1}{(4\pi\lambda)^{\frac{d}{2}}}. \tag{F.2}$$

Note that the above assumes that we have a positive definite metric for the scalar product in x^2, ie. Wick rotation has already been performed.

Differentiating Eq. (F.2), we have that

$$\int \frac{d^dx}{(2\pi)^d}(-x^2)\, e^{-\lambda x^2} = -\frac{d}{2}\,\frac{\lambda^{-1-\frac{d}{2}}}{(4\pi)^{\frac{d}{2}}}, \tag{F.3}$$

$$\int \frac{d^dx}{(2\pi)^d}x^4\, e^{-\lambda x^2} = \frac{d}{2}\left(\frac{d}{2}+1\right)\,\frac{\lambda^{-2-\frac{d}{2}}}{(4\pi)^{\frac{d}{2}}}. \tag{F.4}$$

Generalising the Gaussian integral, we have that

$$\int \frac{d^dx}{(2\pi)^d}\, e^{-\frac{1}{2}x_iA_{ij}x_j+b_ix_i} = (2\pi)^{-\frac{d}{2}}\,(\det A)^{-\frac{1}{2}}\, e^{\frac{1}{2}b_i\left(A^{-1}\right)_{ij}b_j}. \tag{F.5}$$

If the argument of the exponential is imaginary, we have that

$$\int dx\, e^{i\left(ax^2+bx\right)} = e^{-\frac{ib^2}{4a}}\, e^{i\,\mathrm{sgn}(a)\frac{\pi}{4}} \sqrt{\frac{\pi}{|a|}}, \tag{F.6}$$

with the only requirement being that a and b are real. There is thus no ambiguity for any metric used in its multi-dimensional extension.

However, there is an ambiguity when dimensional regularisation is used in Minkowski space. This is resolved by *always* adding the extra dimension in the spatial coordinates. This makes sense since the time coordinate need to be Wick rotated, and therefore, we need to treat it as a discrete dimension. One could also argue that dimensional regularisation comes into play after the Wick rotation is performed.

Bibliography

[1] G. Isidori, S. Nabeebaccus, and R. Zwicky, "QED corrections in $\overline{B} \to \overline{K}\ell^+\ell^-$ at the double-differential level," *JHEP* **12** (2020) 104, arXiv:2009.00929 [hep-ph].

[2] M. Bordone, G. Isidori, and A. Pattori, "On the Standard Model predictions for R_K and R_{K^*}," *Eur. Phys. J.* **C76** no. 8, (2016) 440, arXiv:1605.07633 [hep-ph].

[3] M. Gell-Mann, "A schematic model of baryons and mesons," *Physics Letters* **8** no. 3, (Feb., 1964) 214–215.

[4] S. Glashow, "Partial Symmetries of Weak Interactions," *Nucl. Phys.* **22** (1961) 579–588.

[5] S. Weinberg, "A Model of Leptons," *Phys. Rev. Lett.* **19** (1967) 1264–1266.

[6] A. Salam, "Weak and Electromagnetic Interactions," *Conf. Proc. C* **680519** (1968) 367–377.

[7] P. W. Higgs, "Broken Symmetries and the Masses of Gauge Bosons," *Phys. Rev. Lett.* **13** (1964) 508–509.

[8] F. Englert and R. Brout, "Broken Symmetry and the Mass of Gauge Vector Mesons," *Phys. Rev. Lett.* **13** (1964) 321–323.

[9] K. Wilson and J. B. Kogut, "The Renormalization group and the epsilon expansion," *Phys. Rept.* **12** (1974) 75–199.

[10] **LHCb** Collaboration, R. Aaij *et al.*, "Test of lepton universality using $B^+ \to K^+\ell^+\ell^-$ decays," *Phys. Rev. Lett.* **113** (2014) 151601, arXiv:1406.6482 [hep-ex].

[11] **LHCb** Collaboration, R. Aaij *et al.*, "Test of lepton universality with $B^0 \to K^{*0}\ell^+\ell^-$ decays," *JHEP* **08** (2017) 055, arXiv:1705.05802 [hep-ex].

[12] **LHCb** Collaboration, R. Aaij *et al.*, "Search for lepton-universality violation in $B^+ \to K^+\ell^+\ell^-$ decays," *Phys. Rev. Lett.* **122** no. 19, (2019) 191801, arXiv:1903.09252 [hep-ex].

[13] B. S. DeWitt, "Quantum Field Theory in Curved Space-Time," *Phys. Rept.* **19** (1975) 295–357.

[14] B. S. DeWitt, "Dynamical theory of groups and fields," *Conf. Proc.* **C630701** (1964) 585–820. [Les Houches Lect. Notes13,585(1964)].

[15] R. Ellis, D. Ross, and A. Terrano, "The Perturbative Calculation of Jet Structure in e+ e- Annihilation," *Nucl. Phys. B* **178** (1981) 421–456.

[16] C. W. Misner, K. Thorne, and J. Wheeler, *Gravitation*. W. H. Freeman, San Francisco, 1973.

[17] V. M. Braun, G. P. Korchemsky, and D. Mueller, "The Uses of conformal symmetry in QCD," *Prog. Part. Nucl. Phys.* **51** (2003) 311–398, arXiv:hep-ph/0306057 [hep-ph].

[18] J. Wess, "The conformal invariance in quantum field theory," *Il Nuovo Cimento (1955-1965)* **18** no. 6, (1960) 1086–1107. http://dx.doi.org/10.1007/BF02733168.

[19] J.-F. Fortin, B. Grinstein, and A. Stergiou, "Scale without Conformal Invariance: Theoretical Foundations," *JHEP* **07** (2012) 025, arXiv:1107.3840 [hep-th].

[20] R. Jackiw and S. Y. Pi, "Tutorial on Scale and Conformal Symmetries in Diverse Dimensions," *J. Phys. A* **44** (2011) 223001, arXiv:1101.4886 [math-ph].

[21] J. Polchinski, "Scale and conformal invariance in quantum field theory," *Nuclear Physics B* **303** no. 2, (1988) 226 – 236. http://www.sciencedirect.com/science/article/pii/0550321388901794.

[22] C. G. Callan, S. Coleman, and R. Jackiw, "A new improved energy-momentum tensor," *Annals of Physics* **59** no. 1, (1970) 42 – 73. http://www.sciencedirect.com/science/article/pii/0003491670903945.

[23] A. Dymarsky, K. Farnsworth, Z. Komargodski, M. A. Luty, and V. Prilepina, "Scale Invariance, Conformality, and Generalized Free Fields," *JHEP* **02** (2016) 099, arXiv:1402.6322 [hep-th].

[24] F. Belinfante, "On the current and the density of the electric charge, the energy, the linear momentum and the angular momentum of arbitrary fields," *Physica* **7** no. 5, (1940) 449 – 474. http://www.sciencedirect.com/science/article/pii/S003189144090091X.

[25] G. 't Hooft, "Dimensional regularization and the renormalization group," *Nucl. Phys. B* **61** (1973) 455–468.

[26] J. C. Collins, *Renormalization*, vol. 26 of *Cambridge Monographs on Mathematical Physics*. Cambridge University Press, Cambridge, 1986. http://www-spires.fnal.gov/spires/find/books/www?cl=QC174.17.R46C65::1985.

[27] C. G. Callan, "Broken scale invariance in scalar field theory," *Phys. Rev. D* **2** (Oct, 1970) 1541–1547. https://link.aps.org/doi/10.1103/PhysRevD.2.1541.

[28] K. Symanzik, "Small distance behavior in field theory and power counting," *Commun. Math. Phys.* **18** (1970) 227–246.

[29] J. Polonyi, "Lectures on the functional renormalization group method," *Central Eur. J. Phys.* **1** (2003) 1–71, arXiv:hep-th/0110026.

[30] O. J. Rosten, "Fundamentals of the exact renormalization group," *Physics Reports* **511** no. 4, (Feb, 2012) 177–272. http://dx.doi.org/10.1016/j.physrep.2011.12.003.

[31] S. L. Adler, J. C. Collins, and A. Duncan, "Energy-Momentum-Tensor Trace Anomaly in Spin 1/2 Quantum Electrodynamics," *Phys. Rev.* **D15** (1977) 1712.

[32] J. C. Ward, "An identity in quantum electrodynamics," *Phys. Rev.* **78** (Apr, 1950) 182–182. https://link.aps.org/doi/10.1103/PhysRev.78.182.

[33] Y. Takahashi, "On the generalized Ward identity," *Nuovo Cim.* **6** (1957) 371.

[34] K. Fujikawa, "Path-integral measure for gauge-invariant fermion theories," *Phys. Rev. Lett.* **42** (Apr, 1979) 1195–1198. https://link.aps.org/doi/10.1103/PhysRevLett.42.1195.

[35] K. Fujikawa, "Energy-momentum tensor in quantum field theory," *Phys. Rev. D* **23** (May, 1981) 2262–2275. https://link.aps.org/doi/10.1103/PhysRevD.23.2262.

[36] K. Fujikawa and H. Suzuki, *Path integrals and quantum anomalies*. 8, 2004.

[37] D. J. Gross and F. Wilczek, "Ultraviolet behavior of non-abelian gauge theories," *Phys. Rev. Lett.* **30** (Jun, 1973) 1343–1346. https://link.aps.org/doi/10.1103/PhysRevLett.30.1343.

[38] H. D. Politzer, "Reliable perturbative results for strong interactions?," *Phys. Rev. Lett.* **30** (Jun, 1973) 1346–1349. https://link.aps.org/doi/10.1103/PhysRevLett.30.1346.

[39] W. E. Caswell, "Asymptotic behavior of non-abelian gauge theories to two-loop order," *Phys. Rev. Lett.* **33** (Jul, 1974) 244–246. https://link.aps.org/doi/10.1103/PhysRevLett.33.244.

[40] T. Banks and A. Zaks, "On the phase structure of vector-like gauge theories with massless fermions," *Nuclear Physics B* **196** no. 2, (1982) 189 – 204. http://www.sciencedirect.com/science/article/pii/0550321382900359.

[41] L. Parker and D. Toms, *Quantum field theory in curved spacetime: quantized fields and gravity*. Cambridge university press, 2009.

[42] M. J. Duff, "Observations on Conformal Anomalies," *Nucl. Phys.* **B125** (1977) 334–348.

[43] M. Duff, "Twenty years of the Weyl anomaly," *Class. Quant. Grav.* **11** (1994) 1387–1404, arXiv:hep-th/9308075.

[44] R. A. Bertlmann, *Anomalies in quantum field theory*. 1996.

[45] L. S. Brown and J. C. Collins, "Dimensional Renormalization of Scalar Field Theory in Curved Space-time," *Annals Phys.* **130** (1980) 215.

[46] I. Jack and H. Osborn, "Analogs for the c Theorem for Four-dimensional Renormalizable Field Theories," *Nucl. Phys.* **B343** (1990) 647–688.

[47] M. D. Freeman, "The Renormalization of Nonabelian Gauge Theories in Curved Space-time," *Annals Phys.* **153** (1984) 339.

[48] W. Pauli and F. Villars, "On the Invariant regularization in relativistic quantum theory," *Rev. Mod. Phys.* **21** (1949) 434–444.

[49] J. S. Schwinger, "On gauge invariance and vacuum polarization," *Phys. Rev.* **82** (1951) 664–679. [,116(1951)].

[50] R. T. Seeley, "Singular integrals and boundary value problems," *American Journal of Mathematics* **88** no. 4, (1966) 781–809. http://www.jstor.org/stable/2373078.

[51] R. Seeley, "The resolvent of an elliptic boundary problem," *American Journal of Mathematics* **91** no. 4, (1969) 889–920. http://www.jstor.org/stable/2373309.

[52] C. Morette, "On the definition and approximation of Feynman's path integrals," *Phys. Rev.* **81** (1951) 848–852.

[53] J. Van Vleck, "The Correspondence Principle in the Statistical Interpretation of Quantum Mechanics," *Proc. Nat. Acad. Sci.* **14** (1928) 178–188.

[54] J. L. Synge, ed., *Relativity: The General theory*. 1960.

[55] A. E. M. van de Ven, "Index free heat kernel coefficients," *Class. Quant. Grav.* **15** (1998) 2311–2344, arXiv:hep-th/9708152 [hep-th].

[56] E. Kreyszig, *Introduction to differential geometry and Riemannian geometry*. University of Toronto Press, 1968.

[57] A. Z. Petrov, *Einstein spaces*. Elsevier, 2016.

[58] T. S. Bunch and L. Parker, "Feynman Propagator in Curved Space-Time: A Momentum Space Representation," *Phys. Rev.* **D20** (1979) 2499–2510.

[59] R. D. Ball, "Chiral Gauge Theory," *Phys. Rept.* **182** (1989) 1.

[60] N. Birrell and P. Davies, *Quantum Fields in Curved Space*. Cambridge Monographs on Mathematical Physics. Cambridge University Press, 1984. https://books.google.co.uk/books?id=-b4LAQAAQBAJ.

[61] S. Christensen, "Vacuum Expectation Value of the Stress Tensor in an Arbitrary Curved Background: The Covariant Point Separation Method," *Phys. Rev. D* **14** (1976) 2490–2501.

[62] L. S. Brown and J. P. Cassidy, "Stress Tensors and their Trace Anomalies in Conformally Flat Space-Times," *Phys. Rev. D* **16** (1977) 1712.

[63] L. S. Brown, "Stress Tensor Trace Anomaly in a Gravitational Metric: Scalar Fields," *Phys. Rev. D* **15** (1977) 1469.

[64] L. Casarin, H. Godazgar, and H. Nicolai, "Conformal Anomaly for Non-Conformal Scalar Fields," *Phys. Lett. B* **787** (2018) 94–99, arXiv:1809.06681 [hep-th].

[65] L. Abbott, "Introduction to the Background Field Method," *Acta Phys. Polon. B* **13** (1982) 33.

[66] C. de Rham, "Massive Gravity," *Living Rev. Rel.* **17** (2014) 7, arXiv:1401.4173 [hep-th].

[67] L. Faddeev and V. Popov, "Feynman Diagrams for the Yang-Mills Field," *Phys. Lett. B* **25** (1967) 29–30.

[68] N. K. Nielsen, "The Energy Momentum Tensor in a Nonabelian Quark Gluon Theory," *Nucl. Phys.* **B120** (1977) 212–220.

[69] S. L. Adler, J. Lieberman, and Y. J. Ng, "Regularization of the Stress Energy Tensor for Vector and Scalar Particles Propagating in a General Background Metric," *Annals Phys.* **106** (1977) 279.

[70] L. S. Brown and J. P. Cassidy, "Stress Tensor Trace Anomaly in a Gravitational Metric: General Theory, Maxwell Field," *Phys. Rev. D* **15** (1977) 2810.

[71] S. Christensen, "Regularization, Renormalization, and Covariant Geodesic Point Separation," *Phys. Rev. D* **17** (1978) 946–963.

[72] M. Asorey, E. V. Gorbar, and I. L. Shapiro, "Universality and ambiguities of the conformal anomaly," *Class. Quant. Grav.* **21** (2003) 163–178, arXiv:hep-th/0307187 [hep-th].

[73] A. R. Vieira, J. C. C. Felipe, G. Gazzola, and M. Sampaio, "One-loop conformal anomaly in an implicit momentum space regularization framework," *Eur. Phys. J.* **C75** no. 7, (2015) 338, arXiv:1505.05319 [hep-th].

[74] G. M. Shore, "Symmetry Restoration and the Background Field Method in Gauge Theories," *Annals Phys.* **137** (1981) 262.

[75] C.-S. Chu and Y. Koyama, "Adiabatic Regularization for Gauge Field and the Conformal Anomaly," *Phys. Rev.* **D95** no. 6, (2017) 065025, arXiv:1610.00464 [hep-th].

[76] A. B. Zamolodchikov, "Irreversibility of the Flux of the Renormalization Group in a 2D Field Theory," *JETP Lett.* **43** (1986) 730–732. [Pisma Zh. Eksp. Teor. Fiz.43,565(1986)].

[77] A. M. Polyakov, "Quantum Geometry of Bosonic Strings," *Phys. Lett. B* **103** (1981) 207–210.

[78] L. Bonora, A. D. Pereira, and B. Lima de Souza, "Regularization of energy-momentum tensor correlators and parity-odd terms," *JHEP* **06** (2015) 024, arXiv:1503.03326 [hep-th].

[79] J. L. Cardy, "The Central Charge and Universal Combinations of Amplitudes in Two-dimensional Theories Away From Criticality," *Phys. Rev. Lett.* **60** (1988) 2709.

[80] A. Cappelli, D. Friedan, and J. I. Latorre, "C theorem and spectral representation," *Nucl. Phys. B* **352** (1991) 616–670.

[81] J. L. Cardy, "Is There a c Theorem in Four-Dimensions?," *Phys. Lett. B* **215** (1988) 749–752.

[82] Z. Komargodski and A. Schwimmer, "On Renormalization Group Flows in Four Dimensions," *JHEP* **12** (2011) 099, arXiv:1107.3987 [hep-th].

[83] V. Prochazka and R. Zwicky, "On the Flow of $\Box R$ Weyl-Anomaly," *Phys. Rev. D* **96** no. 4, (2017) 045011, arXiv:1703.01239 [hep-th].

[84] L. Bonora, P. Cotta-Ramusino, and C. Reina, "Conformal Anomaly and Cohomology," *Phys. Lett. B* **126** (1983) 305–308.

[85] G. M. Shore, *The c and a-theorems and the Local Renormalisation Group*. SpringerBriefs in Physics. Springer, Cham, 2017. arXiv:1601.06662 [hep-th].

[86] A. Cappelli, J. I. Latorre, and X. Vilasis-Cardona, "Renormalization group patterns and C theorem in more than two-dimensions," *Nucl. Phys. B* **376** (1992) 510–538, arXiv:hep-th/9109041.

[87] D. Anselmi, "Anomalies, unitarity and quantum irreversibility," *Annals Phys.* **276** (1999) 361–390, arXiv:hep-th/9903059.

[88] V. Prochazka and R. Zwicky, "Finiteness of two- and three-point functions and the renormalization group," *Phys. Rev. D* **95** no. 6, (2017) 065027, arXiv:1611.01367 [hep-th].

[89] S. Weinberg, *The Quantum theory of fields. Vol. 1: Foundations*. Cambridge University Press, 2005.

[90] R. Zwicky, "A brief Introduction to Dispersion Relations and Analyticity," in *Quantum Field Theory at the Limits: from Strong Fields to Heavy Quarks*, pp. 93–120. 2017. arXiv:1610.06090 [hep-ph].

[91] R. J. Eden, P. V. Landshoff, D. I. Olive, and J. C. Polkinghorne, *The analytic S-matrix*. Cambridge Univ. Press, Cambridge, 1966.

[92] V. Prochazka and R. Zwicky, "On the a-theorem in the Conformal Window," *Phys. Rev. D* **99** no. 2, (2019) 025006, arXiv:1807.06915 [hep-th].

[93] Y. Nambu and G. Jona-Lasinio, "Dynamical Model of Elementary Particles Based on an Analogy with Superconductivity. 1.," *Phys. Rev.* **122** (1961) 345–358.

[94] M. A. Luty, J. Polchinski, and R. Rattazzi, "The a-theorem and the Asymptotics of 4D Quantum Field Theory," *JHEP* **01** (2013) 152, arXiv:1204.5221 [hep-th].

[95] H. Leutwyler and M. Shifman, "Goldstone bosons generate peculiar conformal anomalies," *Physics Letters B* **221** no. 3, (1989) 384 – 388. http://www.sciencedirect.com/science/article/pii/0370269389917309.

[96] J. F. Donoghue and H. Leutwyler, "Energy and momentum in chiral theories," *Z. Phys. C* **52** (1991) 343–351.

[97] M. Voloshin and A. Dolgov, "ON GRAVITATIONAL INTERACTION OF THE GOLDSTONE BOSONS," *Sov. J. Nucl. Phys.* **35** (1982) 120–121.

[98] D. Z. Freedman, K. Johnson, and J. I. Latorre, "Differential regularization and renormalization: A New method of calculation in quantum field theory," *Nucl. Phys. B* **371** (1992) 353–414.

[99] N. Davidson, T. Przedzinski, and Z. Was, "PHOTOS interface in C++: Technical and Physics Documentation," *Comput. Phys. Commun.* **199** (2016) 86–101, arXiv:1011.0937 [hep-ph].

[100] **Particle Data Group** Collaboration, M. Tanabashi *et al.*, "Review of Particle Physics," *Phys. Rev.* **D98** no. 3, (2018) 030001.

[101] M. Beneke, T. Feldmann, and D. Seidel, "Systematic approach to exclusive $B \to V l^+ l^-, V\gamma$ decays," *Nucl.Phys.* **B612** (2001) 25–58, arXiv:hep-ph/0106067 [hep-ph].

[102] M. Dimou, J. Lyon, and R. Zwicky, "Exclusive Chromomagnetism in heavy-to-light FCNCs," *Phys.Rev.* **D87** no. 7, (2013) 074008, arXiv:1212.2242 [hep-ph].

[103] J. Lyon and R. Zwicky, "Isospin asymmetries in $B \to (K^*, \rho) \to l^+ l^-$ and $B \to K l^+ l^-$ in and beyond the standard model," *Phys.Rev.* **D88** no. 9, (2013) 094004, arXiv:1305.4797 [hep-ph].

[104] A. Khodjamirian, T. Mannel, and Y. Wang, "$B \to K\ell^+\ell^-$ decay at large hadronic recoil," *JHEP* **1302** (2013) 010, arXiv:1211.0234 [hep-ph].

[105] T. Muta, *Foundations of quantum chromodynamics. Second edition*, vol. 57. 1998.

[106] G. F. Sterman, *An Introduction to quantum field theory.* Cambridge University Press, 8, 1993.

[107] E. S. Ginsberg, "Radiative corrections to the k-l-3 +- dalitz plot," *Phys. Rev.* **162** (1967) 1570. [Erratum: Phys. Rev.187,2280(1969)].

[108] S. Catani and M. Seymour, "A General algorithm for calculating jet cross-sections in NLO QCD," *Nucl. Phys. B* **485** (1997) 291–419, arXiv:hep-ph/9605323. [Erratum: Nucl.Phys.B 510, 503–504 (1998)].

[109] S. Dittmaier, "A General approach to photon radiation off fermions," *Nucl. Phys. B* **565** (2000) 69–122, arXiv:hep-ph/9904440.

[110] S. Dittmaier, A. Kabelschacht, and T. Kasprzik, "Polarized qed splittings of massive fermions and dipole subtraction for non-collinear-safe observables," *Nuclear Physics B* **800** no. 1-2, (Sep, 2008) 146–189. http://dx.doi.org/10.1016/j.nuclphysb.2008.03.010.

[111] M. Schönherr, "An automated subtraction of nlo ew infrared divergences," *The European Physical Journal C* **78** no. 2, (Feb, 2018) . http://dx.doi.org/10.1140/epjc/s10052-018-5600-z.

[112] B. W. Harris and J. F. Owens, "The Two cutoff phase space slicing method," *Phys. Rev.* **D65** (2002) 094032, arXiv:hep-ph/0102128 [hep-ph].

[113] F. Bloch and A. Nordsieck, "Note on the Radiation Field of the electron," *Phys. Rev.* **52** (1937) 54–59.

[114] P. Ball and R. Zwicky, "New results on $B \to \pi, K, \eta$ decay formfactors from light-cone sum rules," *Phys. Rev. D* **71** (2005) 014015, arXiv:hep-ph/0406232.

[115] G. S. Bali, V. M. Braun, S. Bürger, M. Göckeler, M. Gruber, F. Hutzler, P. Korcyl, A. Schäfer, A. Sternbeck, and et al., "Light-cone distribution amplitudes of pseudoscalar mesons from lattice qcd," *Journal of High Energy Physics* **2019** no. 8, (Aug, 2019) . http://dx.doi.org/10.1007/JHEP08(2019)065.

[116] V. Braun and A. Lenz, "On the SU(3) symmetry-breaking corrections to meson distribution amplitudes," *Phys. Rev. D* **70** (2004) 074020, arXiv:hep-ph/0407282.

[117] P. Ball and R. Zwicky, "SU(3) breaking of leading-twist K and K* distribution amplitudes: A Reprise," *Phys. Lett. B* **633** (2006) 289–297, arXiv:hep-ph/0510338.

[118] P. Ball and R. Zwicky, "Operator relations for SU(3) breaking contributions to K and K* distribution amplitudes," *JHEP* **02** (2006) 034, arXiv:hep-ph/0601086.

[119] K. Chetyrkin, A. Khodjamirian, and A. Pivovarov, "Towards NNLO Accuracy in the QCD Sum Rule for the Kaon Distribution Amplitude," *Phys. Lett. B* **661** (2008) 250–258, arXiv:0712.2999 [hep-ph].

[120] M. Greco, G. Pancheri-Srivastava, and Y. Srivastava, "Radiative Corrections for Colliding Beam Resonances," *Nucl. Phys. B* **101** (1975) 234–262.

[121] T. Huber, E. Lunghi, M. Misiak, and D. Wyler, "Electromagnetic logarithms in $\bar{B} \to X_s l^+ l^-$," *Nucl. Phys.* **B740** (2006) 105–137, arXiv:hep-ph/0512066 [hep-ph].

[122] M. E. Peskin and D. V. Schroeder, *An Introduction to quantum field theory*. Addison-Wesley, Reading, USA, 1995.

[123] G. Hiller and R. Zwicky, "(A)symmetries of weak decays at and near the kinematic endpoint," *JHEP* **03** (2014) 042, arXiv:1312.1923 [hep-ph].

[124] M. Bordone, A. Greljo, G. Isidori, D. Marzocca, and A. Pattori, "Higgs Pseudo Observables and Radiative Corrections," *Eur. Phys. J. C* **75** no. 8, (2015) 385, arXiv:1507.02555 [hep-ph].

[125] J. Gratrex, M. Hopfer, and R. Zwicky, "Generalised helicity formalism, higher moments and the $B \to K_{J_K}(\to K\pi)\bar{\ell}_1\ell_2$ angular distributions," *Phys. Rev.* **D93** no. 5, (2016) 054008, arXiv:1506.03970 [hep-ph].

[126] G. D'Ambrosio and G. Isidori, "K $\to$ pi pi gamma decays: A Search for novel couplings in kaon decays," *Z. Phys. C* **65** (1995) 649–656, arXiv:hep-ph/9408219.

[127] G. D'Ambrosio, G. Ecker, G. Isidori, and H. Neufeld, "K $\to$ pi pi pi gamma in chiral perturbation theory," *Z. Phys. C* **76** (1997) 301–310, arXiv:hep-ph/9612412.

[128] M. Beneke, C. Bobeth, and R. Szafron, "Enhanced electromagnetic correction to the rare B-meson decay $B_{s,d} \to \mu^+\mu^-$," arXiv:1708.09152 [hep-ph].

[129] M. Beneke, C. Bobeth, and R. Szafron, "Power-enhanced leading-logarithmic QED corrections to $B_q \to \mu^+\mu^-$," *JHEP* **10** (2019) 232, arXiv:1908.07011 [hep-ph].

[130] N. Carrasco, V. Lubicz, G. Martinelli, C. T. Sachrajda, N. Tantalo, C. Tarantino, and M. Testa, "QED Corrections to Hadronic Processes in Lattice QCD," *Phys. Rev.* **D91** no. 7, (2015) 074506, arXiv:1502.00257 [hep-lat].

[131] C. Sachrajda, M. Di Carlo, G. Martinelli, D. Giusti, V. Lubicz, F. Sanfilippo, S. Simula, and N. Tantalo, "Radiative corrections to semileptonic decay rates," in *37th International Symposium on Lattice Field Theory*. 10, 2019. arXiv:1910.07342 [hep-lat].

[132] D. Giusti, V. Lubicz, G. Martinelli, C. Sachrajda, F. Sanfilippo, S. Simula, N. Tantalo, and C. Tarantino, "First lattice calculation of the QED corrections to leptonic decay rates," *Phys. Rev. Lett.* **120** no. 7, (2018) 072001, arXiv:1711.06537 [hep-lat].

[133] M. Di Carlo, D. Giusti, V. Lubicz, G. Martinelli, C. Sachrajda, F. Sanfilippo, S. Simula, and N. Tantalo, "Light-meson leptonic decay rates in lattice QCD+QED," *Phys. Rev. D* **100** no. 3, (2019) 034514, arXiv:1904.08731 [hep-lat].

[134] A. Portelli, "Electromagnetic corrections to leptonic decays.". talk given at 37th International Symposium on Lattice Field Theory, Wuhan, China, June 2019.

[135] V. Cirigliano, M. Knecht, H. Neufeld, H. Rupertsberger, and P. Talavera, "Radiative corrections to K(l3) decays," *Eur. Phys. J.* **C23** (2002) 121–133, arXiv:hep-ph/0110153 [hep-ph].

[136] V. Cirigliano, M. Giannotti, and H. Neufeld, "Electromagnetic effects in K(l3) decays," *JHEP* **11** (2008) 006, arXiv:0807.4507 [hep-ph].

[137] S. de Boer, T. Kitahara, and I. Nisandzic, "Soft-Photon Corrections to $\bar{B} \to D\tau^-\bar{\nu}_\tau$ Relative to $\bar{B} \to D\mu^-\bar{\nu}_\mu$," *Phys. Rev. Lett.* **120** no. 26, (2018) 261804, arXiv:1803.05881 [hep-ph].

[138] C. A. Mantica and L. G. Molinari, "A second-order identity for the riemann tensor and applications," *Colloquium Mathematicum* **122** no. 1, (2011) 69–82. http://dx.doi.org/10.4064/cm122-1-7.

[139] W. Beenakker, H. Kuijf, W. L. van Neerven, and J. Smith, "QCD Corrections to Heavy Quark Production in p anti-p Collisions," *Phys. Rev.* **D40** (1989) 54–82.

[140] G. Somogyi, "Angular integrals in d dimensions," *J. Math. Phys.* **52** (2011) 083501, arXiv:1101.3557 [hep-ph].

[141] G. Somogyi, "private communication.".

[142] A. Denner, "Techniques for calculation of electroweak radiative corrections at the one loop level and results for W physics at LEP-200," *Fortsch. Phys.* **41** (1993) 307–420, arXiv:0709.1075 [hep-ph].

[143] R. Mertig, M. Bohm, and A. Denner, "FEYN CALC: Computer algebraic calculation of Feynman amplitudes," *Comput. Phys. Commun.* **64** (1991) 345–359.

[144] V. Shtabovenko, R. Mertig, and F. Orellana, "New Developments in FeynCalc 9.0," *Comput. Phys. Commun.* **207** (2016) 432–444, arXiv:1601.01167 [hep-ph].

[145] S. Dittmaier, "Separation of soft and collinear singularities from one loop N point integrals," *Nucl. Phys.* **B675** (2003) 447–466, arXiv:hep-ph/0308246 [hep-ph].